

Durham E-Theses

Lateglacial to Holocene relative sea-level changes in the Stykkishólmur area, Snæfellsnes peninsula, Iceland

BRADER, MARTIN,DAVID

How to cite:

BRADER, MARTIN,DAVID (2012) *Lateglacial to Holocene relative sea-level changes in the Stykkishólmur area, Snæfellsnes peninsula, Iceland*, Durham theses, Durham University. Available at Durham E-Theses Online: <http://etheses.dur.ac.uk/4459/>

Use policy

The full-text may be used and/or reproduced, and given to third parties in any format or medium, without prior permission or charge, for personal research or study, educational, or not-for-profit purposes provided that:

- a full bibliographic reference is made to the original source
- a [link](#) is made to the metadata record in Durham E-Theses
- the full-text is not changed in any way

The full-text must not be sold in any format or medium without the formal permission of the copyright holders.

Please consult the [full Durham E-Theses policy](#) for further details.

Martin David Brader

Lateglacial to Holocene relative sea-level changes in the Stykkishólmur area, Snæfellsnes peninsula, Iceland

Until recently, relatively little scientific research has been undertaken to increase our understanding of relative sea-level (RSL) change in NW Iceland. This study presents the results of diatom, tephra and radiocarbon analyses on five isolation basin and two coastal lowland sediment cores from the Stykkishólmur area, northern Snæfellsnes. The analyses provide an accurate reconstruction of the postglacial RSL changes for the Snæfellsnes peninsula, through the generation of a RSL curve. In addition, the marine limit elevations established for northern Snæfellsnes allow the determination of areas of similar ice thickness within NW. Tephrochronological analyses from sediment cores have allowed the establishment of a potential signature for samples from the Snæfellsnes Volcanic Belt (SVB), as well as the determination of the extent of the Saksunarvatn tephra in Snæfellsnes and internal tephrostratigraphical correlations. In Snæfellsnes, the marine limit is measured at approximately 69 m above sea level, with its formation being estimated at ~ 14000 cal. yrs BP. Following the formation of the marine limit, the rate of RSL change was -37 mm cal. yr⁻¹ until the isolation of site Saurar 3 at 16.20 m asl in 12558 - 12646 cal. yrs BP, relating to a rate of crustal rebound of $+55$ mm cal yr⁻¹ over the same period. Following the isolation of Saurar 3, the rate of RSL fall reduced. During the mid- to late Holocene, RSL fell below present in northern Snæfellsnes, although poor chronological control means that this event can only be tentatively dated to ~ 4800 cal. yrs BP. The results highlight the potential of isolation basin, coastal lowland and marine limit data in determining the RSL history for NW Iceland.

Lateglacial to Holocene relative sea-level changes in the Stykkishólmur area, Snæfellsnes peninsula, Iceland

Martin David Brader

Thesis submitted for the degree of
Master of Science (by Research)

Department of Geography
Durham University

2011

Contents

Title Page	
Contents	i
List of Tables	vii
List of Illustrations	viii
Statement of Copyright	xv
Acknowledgements	xvi
CHAPTER 1	1
1.1 Introduction	1
1.2 Study Aims and Objectives	2
1.3 Research Questions	3
1.3.1 What is the pattern of RSL change during the Holocene at Stykkishólmur, northern Snæfellsnes and what are the associated drivers?	3
1.3.2 Is this RSL history consistent with regional trends from NW Iceland?	3
1.3.3 Are isolation basin studies suitable for the determination of RSL and deglacial histories from Iceland?	4
1.4 Thesis Outline	5
1.5 Summary	5
CHAPTER 2	7
2.1 Introduction	7
2.2 The Icelandic Ice Sheet and the glaciation of Iceland	7
2.2.1 The hypotheses of the Icelandic glaciation	12
2.3 The deglaciation of Iceland	15

2.4 Relative Sea-Level Change in Iceland.....	19
2.4.1 Marine Limits in Iceland.....	21
2.4.2 Low postglacial RSL in Iceland.....	24
2.4.3 Isolation Basin Studies in Iceland.....	26
2.4.4 Saltmarsh studies in western Iceland.....	31
2.5 Tephrochronology in Iceland.....	31
2.5.1 The use of tephrochronology.....	31
2.5.2 Limitations to tephrochronology.....	34
2.6 Summary.....	35
CHAPTER 3.....	37
3.1 Introduction.....	37
3.2 Regional Background.....	37
3.3 The Snæfellsnes Peninsula.....	38
3.4 Study Sites.....	40
3.4.1 Borgarland (BO10 and BO11).....	41
3.4.2 Skjaldarvatn (SK1).....	43
3.4.3 Saurar 1 (SA1).....	47
3.4.4 Helgafellsvatn (HE1).....	50
3.4.5 Saurar 3 (SA3).....	53
3.4.6 Setbergsa.....	55
3.4.7 Barar.....	57
3.4.8 Other Isolation Basin and Tidal Inlet Sites.....	59
3.5 Summary.....	62
CHAPTER 4.....	63
4.1 Introduction.....	63
4.2 Field Methods.....	63
4.2.1 Stratigraphy Determination and Core Retrieval.....	65
4.2.2 Sill Determination.....	66

4.2.3 Marine Limit Determination.....	68
4.2.4 GPS Measurements.....	68
4.3 Laboratory Methods.....	69
4.3.1 Diatom Analysis.....	69
4.4 Chronological Methods.....	71
4.5 Analytical Methods.....	75
4.5.1 Elevation Correction.....	75
4.5.2 Radiocarbon Age Calibration.....	76
4.6 Summary.....	76
CHAPTER 5.....	77
5.1 Introduction.....	77
5.2 Borgarland 10.....	77
5.2.1 Stratigraphy.....	78
5.2.2 Diatom flora.....	79
5.2.3 Environmental Summary.....	81
5.3 Borgarland 11.....	84
5.3.1 Stratigraphy.....	84
5.3.2 Diatom flora.....	85
5.3.3 Environmental Summary.....	86
5.4 Skjaldarvatn (SK1).....	88
5.4.1 Stratigraphy.....	88
5.4.2 Diatom flora.....	89
5.3.3 Environmental Summary.....	91
5.5 Þingvallavatn (TH1).....	93
5.5.1 Stratigraphy.....	93
5.5.2 Diatom flora.....	96
5.5.3 Environmental Summary.....	97
5.6 Saurar 1 (SA1).....	99

5.6.1	Stratigraphy	99
5.6.2	Diatom flora	103
5.6.3	Environmental Summary	104
5.7	Helgafellsvatn (HE1)	106
5.7.1	Stratigraphy	106
5.7.2	Diatom flora	109
5.7.3	Environmental Summary	110
5.8	Saurar 3 (SA3)	112
5.8.1	Stratigraphy	112
5.8.2	Diatom flora	113
5.8.3	Environmental Summary	114
5.9	Marine Limit Sites	116
5.10.1	Setbergsa	116
5.10.2	Barar	117
5.10	Chronological Data	117
5.11.1	Radiocarbon analyses	118
5.11.1.1	Borgarland 10 (Core elevation: 3.08 m asl)	118
5.11.1.2	Pingvallavatn (Sill altitude: 5.34 ± 0.3 m asl)	118
5.11.1.3	Saurar 3 (Sill altitude: 16.20 ± 0.3 m asl)	118
5.11.2	Tephrochronological data	118
5.11.2.1	Tephra Standards	119
5.11.2.2	Skjaldarvatn (4.57 ± 0.3 m asl)	120
5.11.2.3	Pingvallavatn (5.34 ± 0.3 m above MSL)	121
5.11.2.4	Saurar 1 (8.97 ± 0.3 m asl)	122
5.11.2.5	Helgafellsvatn (12.77 m ± 0.3 asl)	124
5.11.2.6	Saurar 3 (16.20 ± 0.3 m asl)	125
5.11.3	Tephra Interpretation	126
5.12	Summary	132

CHAPTER 6.....	133
6.1 Introduction	133
6.2 RSL index points for the Snæfellsnes peninsula.....	133
6.3 RSL curve for the Stykkishólmur area, Snæfellsnes	136
6.3.1 Initial RSL curve for the Snæfellsnes peninsula	136
6.3.2 Estimated additional RSL points and updated RSL curve	136
6.4 Marine Limit Measurements.....	139
6.5 RSL history of the Snæfellsnes peninsula.....	146
6.6 Comparison with regional trends in RSL records within NW Iceland .	149
6.7 Chronological Data	154
6.8 Summary	156
CHAPTER 7	157
7.1 Introduction.....	157
7.2 Primary Conclusions.....	157
7.2.1 Isolation basin and coastal lowland data allow the construction of a RSL curve for the northern Snæfellsnes peninsula.	157
7.2.2 Marine limit elevations can be mapped along the northern side of the Snæfellsnes peninsula.	158
7.2.3 The analysis of tephra layers in the Snæfellsnes sediment cores show previously unrecognised and undated eruptions, which have implications for tephrochronology and for the understanding of ash dispersal patterns in Iceland.....	158
7.3 Secondary Conclusions	158
7.3.1 Marine limit elevations in northern Snæfellsnes highlight potential areas of similar ice thickness within NW Iceland.	158
7.3.2 Marine limit elevations in northern Snæfellsnes highlight the potential for thicker ice in southern Vestfirðir.	159
7.3.3 The Snæfellsnes ice cap may have had an effect on the RSL history of the Snæfellsnes peninsula, counteracting the potential influences from the proposed main ice loading centre.....	159

7.3.4 RSL fell relatively rapidly during the Lateglacial and early Holocene in Snæfellsnes.....	160
7.3.5 The RSL history of the Snæfellsnes peninsula fits well with regional trends over the course of the Lateglacial and Early Holocene.....	160
7.3.6 There is potential evidence for recent RSL rise in northern Snæfellsnes.....	161
7.3.7 Tephrochronology has highlighted both the lack of an easily identifiable Saksunarvatn tephra deposit in northern Snæfellsnes and also the potential signature of tephra from the Snæfellsnes Volcanic Belt (SVB).	161
7.4 Limitations and recommendations for further research.....	162
APPENDIX.....	164
REFERENCES	165

List of Tables

Table 3.1 <i>Summary table showing the approximate elevation and grid references for the additional sites not sampled in this study.....</i>	62
Table 5.1 <i>Tröels-Smith (1955) classifications and sediment descriptions for the BO10 sediment core.....</i>	79
Table 5.2 <i>Tröels-Smith (1955) classifications and sediment descriptions for the BO11 sediment core.....</i>	84
Table 5.3 <i>Tröels-Smith (1955) classifications and sediment descriptions for the SK1-1 sediment core.....</i>	89
Table 5.4 <i>Tröels-Smith (1955) classifications and sediment descriptions for the analysed section of the TH1-4 sediment core.....</i>	95
Table 5.5 <i>Tröels-Smith (1955) classifications and sediment descriptions for the SA1-3 sediment core.....</i>	102
Table 5.6 <i>Tröels-Smith (1955) classifications and sediment descriptions for the HE1-4 sediment core.....</i>	109
Table 5.7 <i>Summary of the sources and positions of tephra samples analysed from Skjaldarvatn, Þingvallavatn, Saurar 1, Helgafellsvatn and Saurar 3.....</i>	129
Table 6.1 <i>Summary of the sea-level index points generated within this study, showing radiocarbon dates, calibrated dates and altitudes in reference to Icelandic Datum.....</i>	135

List of Illustrations

Figure 2.1 <i>Locations in Iceland mentioned in the text, with the exception of the locations of volcanic systems, which are found in Fig. 2.9</i>	9
Figure 2.2 <i>Summary of previous research into the extent of the IIS in western Iceland. Source: Jennings et al. (2000)</i>	10
Figure 2.3 <i>Maximum vs. minimum glaciations of the Icelandic Ice Sheet</i>	13
Figure 2.4 <i>Thermohaline circulation and the major currents affecting Iceland. The diagram highlights the areas that could have been affected by the input of freshwater from the Icelandic Ice Sheet</i>	15
Figure 2.5 <i>The stages of deglaciation of the Icelandic Ice Sheet</i>	17
Figure 2.6 <i>Marine limit elevations in Iceland</i>	23
Figure 2.7 <i>The stages of the basin isolation process, showing the transition from fully marine (Stage I) to brackish (Stage III) and finally freshwater dominance (Stage V). Source: Lloyd and Evans (2002)</i>	27
Figure 2.8 <i>RSL changes in western Iceland, showing results from Norðdahl and Ásbjörnsdóttir (1995); Rundgren et al. (1997), Norðdahl and Pétursson (2005), Gehrels et al. (2006) and Lloyd et al. (2009)</i>	29
Figure 2.9 <i>Volcanic sources within Iceland, showing the locations of the various volcanic zones and systems</i>	33
Figure 3.1 <i>Map of the Snæfellsnes peninsula showing the locations of places mentioned in the text</i>	39
Figure 3.2 <i>Overview of the isolation basin and saltmarsh sites investigated on the Thorsnes peninsula. The sill height is recorded for each isolation basin site in metres above Mean Sea Level (MSL) and the core elevation is recorded for the Borgarland marsh samples (m asl.)</i>	40

Figure 3.3 Overview of the Borgarland marsh site, showing the artificial drainage channel and coring pattern. A recent spring high tide has left some areas of the site flooded with surface water.....	41
Figure 3.4 Contemporary sample collection pattern at Borgarland Marsh.....	41
Figure 3.5 Coring pattern and location of Borgarland Marsh. The figure outlines the locations of the fossil and contemporary samples taken from the site.....	42
Figure 3.6 Coring pattern and location of the Skjaldarvatn isolation basin site.....	43
Figure 3.7 Þingvallavatn looking NNE from the SW corner of the lake basin, showing the basin morphology and boat setup.....	44
Figure 3.8 Location and coring pattern at Þingvallavatn, showing the location of cores retrieved from the edge and within the isolation basin.....	45
Figure 3.9 Determination of the sill at the Þingvallavatn site.....	46
Figure 3.10 View east from the d-GPS base station of Saurar 1 basin showing the coring pattern, sill and extent of the basin.....	47
Figure 3.11 View south east from the most northwest margin of the Saurar 1 basin, showing the area cored and the forest road, as well as the coring pattern.....	48
Figure 3.12 Map showing the locations and coring patterns of the Saurar basins (Saurar 1-4).....	48
Figure 3.13 Determination of the sill location at the Saurar 1 site.....	49
Figure 3.14 View SE from the northwestern point of Helgafellsvatn, showing the proximity of the core samples to the edge of the isolation basin within the infilled section.....	50
Figure 3.15 Map showing the location of the Helgafellsvatn basin, alongside the coring pattern and sill location.....	51

Figure 3.16 <i>View of Helgafellsvatn looking south, showing the infilled section of the basin and Helgafellsvatn itself. The sill can be seen to the extreme left of the photograph, with the core locations also evident.....</i>	52
Figure 3.17 <i>Determination of the sill location at the Helgafellsvatn site.....</i>	53
Figure 3.18 <i>Determination of the sill location at the Saurar 3 site.....</i>	54
Figure 3.19 <i>View south west from the base station location at Setbergsa, showing the local marine limit and marine terraces.....</i>	55
Figure 3.20 <i>Map of the Setbergsa site showing the location of the marine limit measurement and the outline of the local marine limit within the surveyed valley.....</i>	56
Figure 3.21 <i>View north from the base station location showing the clear marine limit at Barar.....</i>	57
Figure 3.22 <i>Map of the Barar area, showing the location of the Barar marine limit measurement and the isolation basins on the peninsula, which were deemed unsuitable for use in this study.....</i>	58
Figure 3.23 <i>View of Innra-Bárvatn looking east at the lake and marine limit....</i>	60
Figure 3.24 <i>Ytra-Bárvatn looking north, showing site proximity to the local marine limit.....</i>	60
Figure 3.25 <i>Arnarstaðir tidal inlet looking east from the westernmost point of the inlet showing basin morphology and the basin sill.....</i>	61
Figure 3.26 <i>Skeid basin facing east showing the basin morphology and likely sill location.....</i>	61
Figure 4.1 <i>Schematic of the technique employed in the establishment of the sill location for each lake basin site.....</i>	67
Figure 4.2 <i>View east from the westernmost point of the tidal inlet used to provide a relative height constraint for the Saurar 1 site, showing the Mean High Water Spring Tide (MHWST; blue line).....</i>	69
Figure 5.1 <i>Core stratigraphy of the Borgarland samples showing the composition of each sediment layer.....</i>	78

Figure 5.2 <i>Diatom assemblage graph for Borgarland 10, showing the transition from brackish to freshwater conditions.....</i>	83
Figure 5.3 <i>Diatom assemblage graph for the Borgarland 11 site, showing the transitional sequence.....</i>	87
Figure 5.4 <i>Sediment stratigraphy for the section of the SK1-1 core analysed for diatom and tephra analyses, showing the composition of each sediment layer. T represents the position of the sampled tephra layer within the analysed core section.....</i>	88
Figure 5.5 <i>Diatom assemblage graph for the Skjaldarvatn site, showing the transition from marine-brackish to freshwater conditions at the site. T denotes the position of a sampled tephra layer within the analysed section of the SK1-1 sediment core.....</i>	92
Figure 5.6 <i>Sediment stratigraphy from the transect of cores taken from the infilled section of the Thingvallavatn basin.....</i>	94
Figure 5.7 <i>Sediment stratigraphy for the transect of cores taken from within the Thingvallavatn basin.....</i>	94
Figure 5.8 <i>Sediment stratigraphy of the section of the TH1-4 core analysed for diatoms showing the sediment composition between 335 cm and 535 cm. T denotes a sampled tephra.....</i>	95
Figure 5.9 <i>Diatom assemblage diagram for the Þingvallavatn site, showing the transition from marine-brackish to freshwater conditions.....</i>	98
Figure 5.10 <i>East-West transect of the Saurar 1 site, showing basin stratigraphy.....</i>	100
Figure 5.11 <i>North-South transect of the Saurar 1 site, showing basin stratigraphy.....</i>	101
Figure 5.12 <i>Sediment stratigraphy for the analysed section of the SA1-3 sediment core.....</i>	102
Figure 5.13 <i>Diatom assemblage diagram for the Saurar 1 site, showing the limited brackish influences at the base of the analysed section, with the dominance of freshwater species being apparent throughout.....</i>	105

Figure 5.14 <i>Sediment stratigraphy for the Helgafellsvatn site, showing the results for cores HE1-1 to HE1-5.</i>	107
Figure 5.15 <i>Sediment stratigraphy for the analysed portion of the HE1-4 sediment core retrieved from Helgafellsvatn., showing the transition from predominantly organic to predominantly inorganic sediments. The diagram also highlights the position of the tephra samples within the core sample.</i>	108
Figure 5.16 <i>Diatom assemblage diagram for the Helgafellsvatn site, showing the transitional sequence from marine-brackish to freshwater species dominance.</i>	111
Figure 5.17 <i>Sediment stratigraphy of the section of the SA3-1 sediment core extracted for diatom, tephra and radiocarbon analyses.</i>	112
Figure 5.18 <i>Diatom assemblage diagram for the Saurar 3 site, showing the transition from marine-brackish to brackish and subsequent freshwater dominance.</i>	115
Figure 5.19 <i>FeO percentage weight versus TiO₂ percentage weight for the SK1-T1-547 sample.</i>	120
Figure 5.20 <i>K₂O percentage weight versus P₂O₅ percentage weight for the SK1-Ti-547 sample, again highlighting the secondary cluster of points.</i>	120
Figure 5.21 <i>TiO₂ percentage weight versus FeO percentage weight for the Thingvallavatn samples.</i>	121
Figure 5.22 <i>K₂O percentage weight versus P₂O₅ percentage weight for the Thingvallavatn samples, showing the close clustering of the dataset.</i>	122
Figure 5.23 <i>TiO₂ percentage weight versus FeO percentage weight for the SA1-T1-334 sample.</i>	123
Figure 5.24 <i>P₂O₅ percentage weight versus K₂O percentage weight for the SA1-T1-334 sample showing the widespread cluster from the sample.</i>	123
Figure 5.25 <i>FeO percentage weight versus TiO₂ percentage weight for Helgafellsvatn samples.</i>	124

Figure 5.26 P_2O_5 percentage weight versus K_2O percentage weight for the Helgafellsvatn samples.....	125
Figure 5.27 FeO percentage weight versus TiO_2 percentage weight for the Saurar 3 samples.....	125
Figure 5.28 K_2O percentage weight versus P_2O_5 percentage weight for the Saurar 3 samples.....	126
Figure 5.29 FeO vs. TiO_2 graph for all tephra samples analysed in this study, alongside known tephra profiles.....	127
Figure 5.30 FeO/TiO_2 vs. SiO_2 graph for all tephra samples analysed in this study, alongside known tephra profiles.....	128
Figure 5.31 Diagram showing the tephrostratigraphical correlations between samples, alongside the positions of the radiocarbon dates in relation to the tephra samples analysed.....	130
Figure 5.32 Correlation between samples from Skjaldarvatn, Saurar 1 and Helgafellsvatn, plotted against known tephra profiles.....	131
Figure 6.1 Initial RSL curve of the Stykkishólmur area, northern Snæfellsnes, Vestfirðir using calibrated ages for the isolations.....	138
Figure 6.2 Calibrated age determination for the isolation basin and saltmarsh sites without radiocarbon dated samples.....	139
Figure 6.3 Selected marine limit measurements from NW Iceland.....	144
Figure 6.4 Diagram of the retreat of the LGM IIS to the Bolling Interstadial Ice Sheet, demonstrating the association between marine limit elevation and patterns of ice loading and retreat.....	145
Figure 6.5 RSL curves for NW Iceland, highlighting the regional trends within the datasets and RSL in relation to present.....	152
Figure 6.6 RSL changes within NW Iceland, showing trends within the current datasets.....	154

Statement of Copyright

The copyright of this thesis rests with the author. No quotation from it should be published without the prior written consent and information derived from it should be acknowledged.

Acknowledgements

There are several people whom I wish to acknowledge for their support and advice during this process. Firstly, I would like to thank Dr. Jerry Lloyd and Prof. Mike Bentley for their advice throughout the course of this Masters degree. Both have been extremely supportive throughout the process, from the fieldwork in Iceland to writing up. Thanks should also go to Matt Strzelecki, who provided valuable assistance in the field.

I would also like to acknowledge the advice provided by Dr. Chris Hayward, University of Edinburgh, during the tephra analyses, offering valuable assistance whilst using the electron microprobe. I would also like to thank Dr. Anthony Newton, Prof. Andy Dugmore and Dr Kate Taylor Smith of the University of Edinburgh, who provided valuable discussion of the tephra results.

The valuable advice provided by the laboratory staff is also greatly appreciated, with Neil Tunstall and Kathryn Melvin deserving particular recognition. Thanks should also be extended to David Sales in the Department of Earth Sciences for the preparation of the tephra resin blocks prior to analyses at the University of Edinburgh.

I would also like to show my appreciation for the funding opportunities provided by Van Mildert College and the Faculty of Social Sciences and Health, University of Durham and also for the time provided at the NERC TAU Facility. These provisions allowed me to successfully undertake this degree.

Finally, thanks should go to all of my friends, colleagues and family for all of their support whilst undertaking this degree. They all provided reassurance and support throughout, which is greatly appreciated.

CHAPTER 1

Introduction

1.1 Introduction

In comparison to the UK and Fennoscandia, there has been relatively little scientific investigation into postglacial relative sea-level (RSL) change in Iceland. Where research has been undertaken, records of RSL changes have generally been developed on the basis of the geomorphological mapping of raised marine features (e.g. Einarsson, 1968; Hansom and Briggs, 1991; Norðdahl and Pétursson, 2005; Principato, 2008). Recently, microfossil analyses of isolation basin sediments have also been undertaken in Iceland, leading to more accurate reconstructions of RSL changes (e.g. Rundgren *et al.*, 1997; Caseldine *et al.*, 2003; Lloyd *et al.*, 2009).

An accurate reconstruction of RSL change in Iceland is important in order to inform the debate surrounding the deglaciation of Iceland after the Last Glacial Maximum (LGM). An understanding of the pattern and style of deglaciation of the Icelandic Ice Sheet (IIS) is essential, as different patterns of meltwater flux to the North Atlantic would have various potential impacts and influences on global thermohaline circulation (Hubbard *et al.*, 2006) and hence global climate. The sensitivity of Iceland to oceanographic and atmospheric changes (Ingólfsson *et al.*, 1997; Eiríksson *et al.*, 2000; Norðdahl and Pétursson, 2005) means that ice sheet response would have been relatively rapid, with RSL study also providing an accurate constraint for such responses. Microfossil based studies of isolation basin sediments are particularly advantageous in this regard, as they provide an opportunity to quantify rates of rebound and record changes in RSL over time (Rundgren *et al.*, 1997).

At present, our understanding of the scale and volume of the IIS is also relatively limited. Modelling studies have calculated various volumes and area measurements for the IIS (e.g. Hubbard *et al.*, 2006) often with relatively little

ground truthing. RSL study provides an opportunity to generate data to test such geophysical models, thus leading to a check on the model predictions of ice sheet volume and scale (e.g. Hubbard *et al.*, 2006).

1.2 Study Aims and Objectives

The principal aim of this research is to provide an accurate reconstruction of the postglacial RSL changes from the Stykkishólmur area, northern Snæfellsnes, western Iceland. It is also hoped that the secondary aim of providing information about the deglaciation of the Snæfellsnes peninsula can also be achieved in this study.

In order to achieve the principal research aim, several objectives are to be met:

- 1. The identification of sedimentary sequences within the isolation basins of the Stykkishólmur area, northern Snæfellsnes.*
- 2. Palaeoenvironmental reconstruction of isolation basins to identify freshwater, brackish and marine influences in each basin.*
- 3. The establishment of a chronological framework for the Snæfellsnes peninsula, through the analysis of tephra and organic sediment deposits.*
- 4. The production of a RSL curve for the area, using isolation basin data, marine limit measurements and the chronological controls.*
- 5. The comparison of the RSL history of the Stykkishólmur area with regional datasets to investigate regional patterns of RSL change and the possible links to deglaciation.*

The research will provide valuable evidence from an area of Iceland currently lacking in research, both in terms of RSL and deglaciation histories. The location of the research, as further discussed in Chapter 3, is a key area of debate within the discussion of the differing hypotheses of the Icelandic LGM glaciations, which are outlined in full in Chapter 2.

The research will provide a RSL record from an area close to the present coastline, which when coupled with data from other similar sites, such as

Bjarkarlundur, Vestfirðir (Lloyd *et al.*, 2009) and northernmost Skagi (Rundgren *et al.*, 1997), will allow a regional overview of the changes within the LGM IIS to be established.

1.3 Research Questions

This research project aims to address three principal research questions:

1.3.1 What is the pattern of RSL change during the Holocene at Stykkishólmur, northern Snæfellsnes and what are the associated drivers?

The identification of the pattern of RSL changes during the Holocene at Stykkishólmur is of importance, as this data is currently lacking for the Snæfellsnes peninsula. As outlined, this area is however key in terms of the glacial and deglacial histories of Iceland. Previous research in Vestfirðir has highlighted the possibility of a secondary ice mass over the peninsula, as outlined by the differing RSL histories generated there (e.g. Hansom and Briggs, 1991). Snæfellsnes, lying South of Vestfirðir, provides an opportunity to determine whether a secondary ice mass over Vestfirðir is likely, as a signature of the ice mass would be present in the RSL record generated from the peninsula. In addition, Snæfellsnes would allow the differing effects of the ice masses on the RSL record to be determined, sitting at a hinge point between the two potential ice centres.

The RSL history of the peninsula will be determined through the establishment of the sedimentary, hydrological and microfossil isolation contacts within each of the sediment core samples. Tephrochronological and radiocarbon data are employed to provide accurate timings for the environmental changes determined from each of the analysed core samples. As a result, sufficient environmental and chronological data will be generated in this study to address this initial research question, allowing the establishment of a RSL record for the region.

1.3.2 Is this RSL history consistent with regional trends from NW Iceland?

Previous study on the Vestfirðir and Skagi peninsulas has provided information regarding the postglacial relative sea-level changes of NW Iceland, showing a trend of generally falling RSL with a mid-Holocene high stand (Rundgren *et al.*,

1997; Lloyd *et al.*, 2009). Differences in the RSL records from NW Iceland, particularly Vestfirðir, have been demonstrated in several studies focussing both on microfossil (e.g. Lloyd *et al.*, 2009) and geomorphological (e.g. Hansom and Briggs, 1991) records of RSL change when compared to the rest of Iceland.

This research question therefore aims to determine whether Snæfellsnes follows the regional trends of NW Iceland, which are notably different, or whether it follows the RSL trends found elsewhere within Iceland. In addition, it aims to investigate the RSL changes at a potential hinge point between assumed recent fall in NW and noted recent rise in western Iceland (Gehrels *et al.*, 2006). As such, a record from Snæfellsnes could be valuable in providing limits on the effects of a potential secondary ice cap in NW Iceland.

The microfossil and chronological analyses briefly outlined above allow the comparison of the Snæfellsnes data with sites elsewhere in NW Iceland, such as Bjarkarlundur (Lloyd *et al.*, 2009), Skagi (Rungren *et al.*, 1997) and Viðarhólmi (Gehrels *et al.*, 2006), and further afield. The comparisons made between the various records will allow regional trends to be evaluated and thus determine whether the Snæfellsnes record is consistent with previous study or whether local factors are having a great effect on the RSL record.

1.3.3 Are isolation basin studies suitable for the determination of RSL and deglacial histories from Iceland?

Although the isolation basin technique has previously been used with great effect in Iceland (e.g. Rungren *et al.*, 1997; Lloyd *et al.*, 2009) and has been used extensively elsewhere (e.g. Shennan *et al.*, 1993; Long *et al.*, 1999; Corner *et al.*, 2001), there are differences between the Icelandic isolation basin records and those generated by studies that employ different techniques or focus on other features (e.g. Hansom and Briggs, 1991; Gehrels *et al.*, 2006) such as the timing of RSL fall below present during the mid Holocene or recent RSL changes. As a result, the use of isolation basins in Iceland is investigated, principally on the grounds of whether the resolution of such studies provides sufficient accuracy of RSL reconstruction in Iceland, particularly over late Holocene timescales.

1.4 Thesis Outline

This thesis is divided into seven distinct chapters. Chapter 1 provides an outline of the key research aim, objectives and questions associated with this research, alongside providing a justification for the need to undertake research of this kind. Chapter 2 provides an overview of the key research previously undertaken in NW Iceland, alongside a synthesis of the gaps in our current understanding. In addition, Chapter 2 demonstrates the role that RSL research can play in the determination of the pattern and style of deglaciation within NW Iceland. Chapter 3 provides an overview of the location of the research, alongside discussion of the individual site locations within the Snæfellsnes peninsula. The coring pattern and isolation basin sill determination strategies are also discussed in Chapter 3. Chapter 4 provides an outline of the key laboratory, analytical and chronological methods used in this study. The chapter also provides an overview of the techniques of diatom, tephra and radiocarbon analyses. Chapter 5 presents the results of the research and is divided into two key sections: environmental results, where sedimentological and diatom assemblages are presented, and chronological results, where the results of the tephra and radiocarbon analyses are outlined. In addition to this, Chapter 5 provides an initial interpretation of the results. Chapter 6 provides a discussion of these results and aims to place them within a regional perspective through comparison with data from other locations in NW Iceland. The chapter also attempts to provide an insight into the deglaciation of the region by using the RSL data generated. Chapter 7 then aims to draw a series of conclusions from the data produced and analyses undertaken in this research. An overview of areas for future research is then provided in this final chapter.

1.5 Summary

This chapter has outlined the aims and objectives of this research, alongside the associated justifications. The principal aim of the research is to provide an accurate reconstruction of the postglacial relative sea-level changes of the Snæfellsnes peninsula. In turn, it is hoped that information regarding the deglaciation of the peninsula may be generated. The importance of the research has also been discussed, with the four key reasons behind the requirement for an accurate reconstruction being outlined. As outlined above, the next chapter

outlines the background to this research including information on the glaciation and deglaciation of Iceland, as well as the variation in previous RSL records. In addition to this, gaps in the present knowledge will be outlined thus confirming the approaches adopted in this research.

CHAPTER 2

Background and Literature Review

2.1 Introduction

This chapter aims to outline the background literature associated with the glacial, deglacial and relative sea level (RSL) histories of Iceland. Issues with and discrepancies between the reconstructions of the Icelandic Ice Sheet (IIS) will be discussed, alongside the key methods employed to determine its scale and volume. In addition, the rate and timing of deglaciation will be outlined, providing an overview of the level and gaps in our current knowledge and the links to the RSL history of Iceland. The reliability and limitations of previous RSL studies will then be highlighted, alongside a discussion of the key methods employed in previous studies. This discussion will highlight the transition from geomorphological studies of marine limit and raised shoreline features to the microfossil based approach using both saltmarsh and isolation basin deposits. A review of the variations in RSL histories from NW Iceland is then undertaken through the examination of existing marine limit, isolation basin and saltmarsh data. Through the analysis of the glacial, deglacial and RSL histories of western Iceland, the aim and objectives of this research will be justified.

2.2 The Icelandic Ice Sheet and the glaciation of Iceland

At the LGM, between 20 and 17 cal. ka BP (Van Vliet Lanoë *et al.*, 2006), it is estimated that the Icelandic Ice Sheet (IIS) covered 330000 km², was made up of 300000 km³ of ice (Hubbard *et al.*, 2006) and had a substantial marine based component (Hubbard, 2006; Hubbard *et al.*, 2006). It is estimated that the ice thickness reached a maximum of 1500 ± 500 m at the LGM (Ingólfsson *et al.*, 2010). Research has been conducted throughout Iceland to establish the extent of this ice sheet, through geomorphological investigations (e.g. Ólafsdóttir, 1975; Norðdahl and Pétursson, 2005) and glacial striation mapping (e.g. Thorodssen, 1905-1906; Keith and Jones, 1935; Einarsson, 1967; Hoppe, 1968; 1982). In addition to this, lake sediment studies have revealed detailed records of the timing

of deglaciation following the LGM (e.g. Rundgren, 1995). Several questions remain over the extent and thickness of the IIS however, with estimates of ice thickness varying between studies (e.g. Rundgren and Ingólfsson, 1999; Hubbard *et al.*, 2006) thus making it the subject of considerable, continuing debate. It is however clear that Iceland was covered by a considerable ice mass during the LGM (Ingólfsson *et al.*, 2010).

Initial scientific investigation into the extent of the IIS was conducted in Eyjafjörður (Figure 2.1), northern Iceland, where glacial striations were found running alongside the fjord, which led to the initial proposition of a single Icelandic ice mass (Thorodssen, 1905-1906). Following this, research in Grímsey highlighted glacial striations on both boulders and bedrock (Einarsson, 1967), alongside the identification of additional features that may have resulted from glacial action, such as smoothed bedrock surfaces (Keith and Jones, 1935). The aforementioned bedrock striations were noted running in a SSE to SE direction (Einarsson, 1967; Hoppe, 1968; 1982) and as such are treated as evidence that the IIS extended as far North as Grímsey during the LGM, some 40 km from the present coastline. Additional later discussed studies, including sedimentary and seismic resonance studies, have supposed this assertion (e.g. Andrews *et al.*, 2000).

In western Iceland, the extent of the LGM IIS has been constrained through the investigation of submerged marine features (e.g. Ólafsdóttir, 1975) alongside associated sedimentological analyses (e.g. Syvitski *et al.*, 1999; Andrews *et al.*, 2000). The Breiðarfjörður moraine, for example, has been dated to between 15.7 and 19.7 ¹⁴C ka BP (~ 18.8 and ~ 23.5 cal. ka BP) (Andrews *et al.*, 2000). However a maximum age of 36 ¹⁴C ka BP (~ 41.2 cal. ka BP) has also been generated (Norðdahl and Pétursson, 2005). Additional submerged moraine features have been dated throughout Iceland and as such have helped to constrain LGM ice extent (e.g. Egloff and Johnson, 1979). The investigations of the Látra or Breiðarfjörður moraine have demonstrated the maximum extent of the IIS at the LGM, with the feature being widely defined as an end moraine (Ólafsdóttir, 1975; Ingólfsson, 1991; Syvitski *et al.*, 1999).



Figure 2.1 Locations in Iceland mentioned in the text, with the exception of the locations of volcanic systems, which are found in Fig. 2.9.

In addition to such end moraine investigation, the study of seismic profiles has also been extensively employed (e.g. Egloff and Johnson, 1979; Syvitski *et al.*, 1999) to delimit the LGM IIS. This has led to the constraint of the LGM IIS at both the shelf edge and at intermediate locations between the shelf edge and the present coastline in some locations in SW Iceland (Egloff and Johnson, 1979). As a result, such studies have provided evidence for LGM IIS ice well beyond the present coastline, reaching tens of kilometres beyond the present coast location (Egloff and Johnson, 1979). The positions of such features and studies are summarised in Figure 2.2.

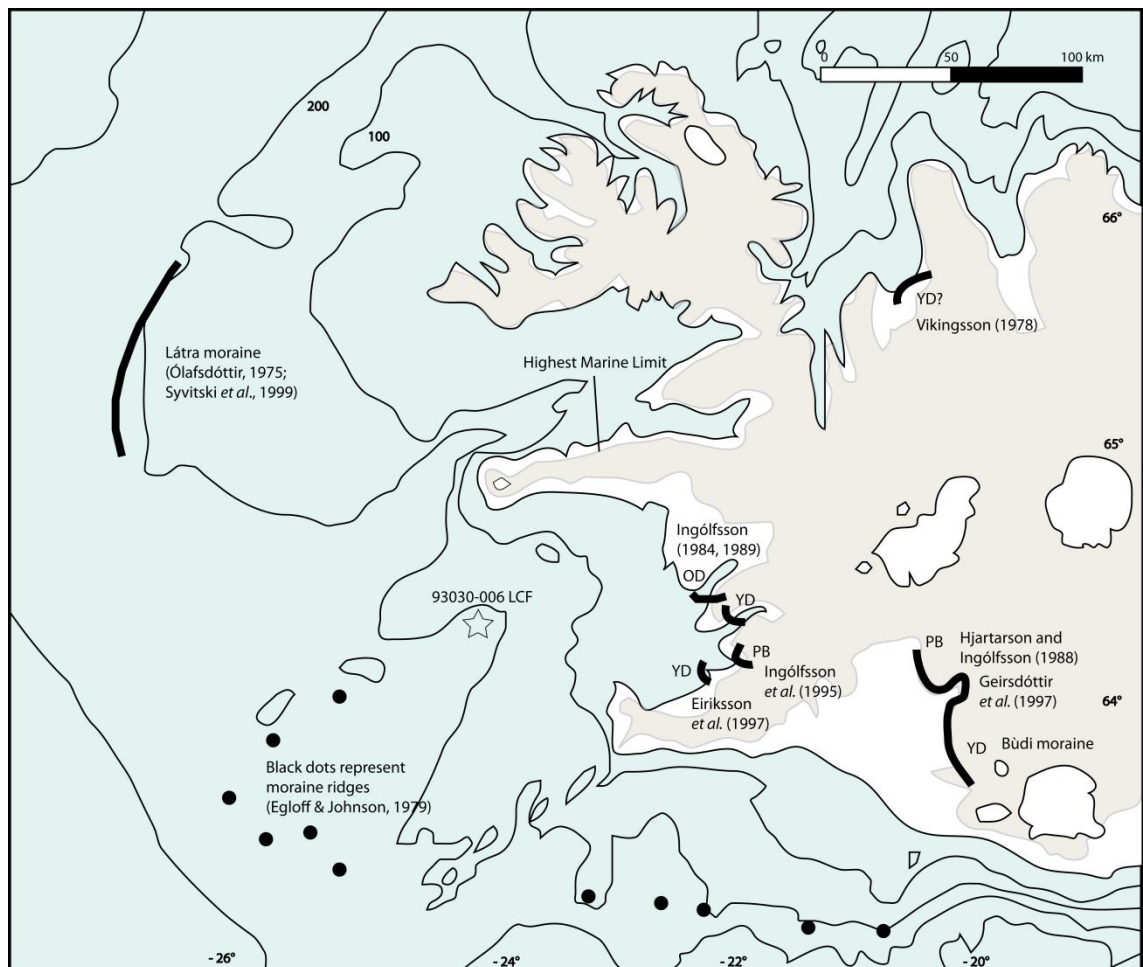


Figure 2.2: Summary of previous research into the extent of the IIS in western Iceland, including marine core data (black dots), highest elevation of the marine limit (shaded grey) and the location of moraine (thick black line). The location of present glaciers is also recorded (white areas) alongside sea floor contours. Source: Jennings *et al.* (2000).

The mapping, coring and seismic profiling of submarine features has also been used extensively in North Iceland to delimit the LGM IIS (e.g. Helgadóttir and Thors, 1998; Andrews *et al.*, 2000). Helgadóttir and Thors (1998) identified end moraines North of Vestfirðir providing a possible limit to the LGM IIS. In

addition to this, a series of cores were retrieved by Andrews *et al.* (2000) which led to the generation of 32 AMS radiocarbon dates between 64 and 67°N and 18 and 29°W. These basal peat radiocarbon dates from Reykjafjardaráll, Húnaflóadjúp, Hunaflói and Eyjafjardaráll allow the extent of the IIS on the north Iceland shelf to be determined, with five radiocarbon dates older than 16 ka BP also providing information on the deglaciation of the Iceland shelf (Andrews *et al.*, 2000). The basal dates from the Andrews *et al.* (2000) study demonstrate a peak in frequency at around 10 ka BP, with seven sites providing ages over 15 ka BP. The results generated for North Iceland highlight that glacial sediment reached the inner and mid shelf during the Bølling-Allerød period (Andrews *et al.*, 2000).

The major issue regarding the use of seismic profiling and marine feature mapping is the lack of sufficient dating analyses in some studies. In several studies, features have simply been identified and ascribed a period in which they are likely to have formed whilst bearing in mind dates generated for other features during previous studies. The results of such studies are therefore less certain than those studies which make use of Accelerator Mass Spectrometer (AMS) radiocarbon dating and other chronological techniques (e.g. Andrews *et al.*, 2000).

Although there is a considerable and growing body of evidence to suggest that ice extended beyond the present coastline, the possibility of ice free areas during and shortly after the LGM has also been explored, such as mid- to outer Djúpáll by 15 ka BP, alongside the possibility of nunataks (e.g. Andrews *et al.*, 2000). Additional studies have attempted to provide evidence for ice free coastal areas during the period (e.g. Steindórsson, 1962; 1963), yet geologically there is no evidence to support the assertion that these ice free areas existed during the LGM (Ingólfsson, 2009). Ingólfsson (2009) highlights several key errors associated with biological studies, which suggest the possibility of coastal ice free areas during the LGM in Iceland, and in doing so hypothesised the lack of such locations. Despite this, some geomorphological evidence does exist for ice free mountainous areas (e.g. Hjort *et al.*, 1985) however the likelihood of plant survival in these locations is limited (Rundgren and Ingólfsson, 1999). It is therefore likely that the whole of Iceland was covered by the LGM ice sheet, with occasional nunataks protruding thorough the ice cover (Andrews *et al.*,

2000; Norðdahl and Pétursson, 2005), although the extent of these nunataks is unknown at present (Ægisdóttir and Þórhallsdóttir, 2005).

2.2.1 *The hypotheses of the Icelandic glaciation*

Investigation into the Icelandic glaciation has led to the proposition of two contrasting theories of glaciation: extensive (e.g. Buckland and Dugmore, 1991; Hubbard *et al.*, 2006) and restricted (e.g. Hjort *et al.*, 1985). In this study, the two theories will be referred to as the maximum and minimum IIS hypotheses, representing the differences in ice sheet scale and volume presented by the two hypotheses. The hypotheses of the Icelandic glaciation were once hotly-debated (Hjort *et al.*, 1985; Hubbard *et al.*, 2006; Roberts *et al.*, 2007) with some uncertainty regarding the Icelandic glaciation and IIS extent still existing to this day (Andrews and Helgadóttir, 2003). That said, the minimum IIS hypothesis has lost some credibility following several recent studies, which have employed more accurate techniques to determine ice sheet extent than initial studies.

The minimum and maximum IIS hypotheses are associated with considerably different ice volumes, styles of glaciation and patterns of deglaciation (Figure 2.3). The maximum IIS hypothesis suggests that ice extended to the shelf edge, between 50 and 120 km from the present coastline (Andrews *et al.*, 2000; Norðdahl and Pétursson, 2005; Hubbard *et al.*, 2006). This hypothesis also suggests that the glaciation of Iceland was mono-domed, with a single ice mass covering the entire island (Hubbard *et al.*, 2006). The hypothesis is supported by the ice extent studies outlined previously, particularly the coring and seismic profiling studies carried out in western and northern Iceland (e.g. Andrews *et al.*, 2000). The minimum IIS hypothesis suggests that the ice extended to within 15 km of the present coastline (Hjort *et al.*, 1985) with the possibility of separate ice centres, with particular emphasis put on a separate ice mass over Vestfirðir (e.g. Hansom and Briggs, 1991). The separate Vestfirðir ice mass hypothesis has received particular support from RSL studies, which have highlighted the possibility of differing histories from the rest of Iceland (e.g. Hansom and Briggs, 1991).

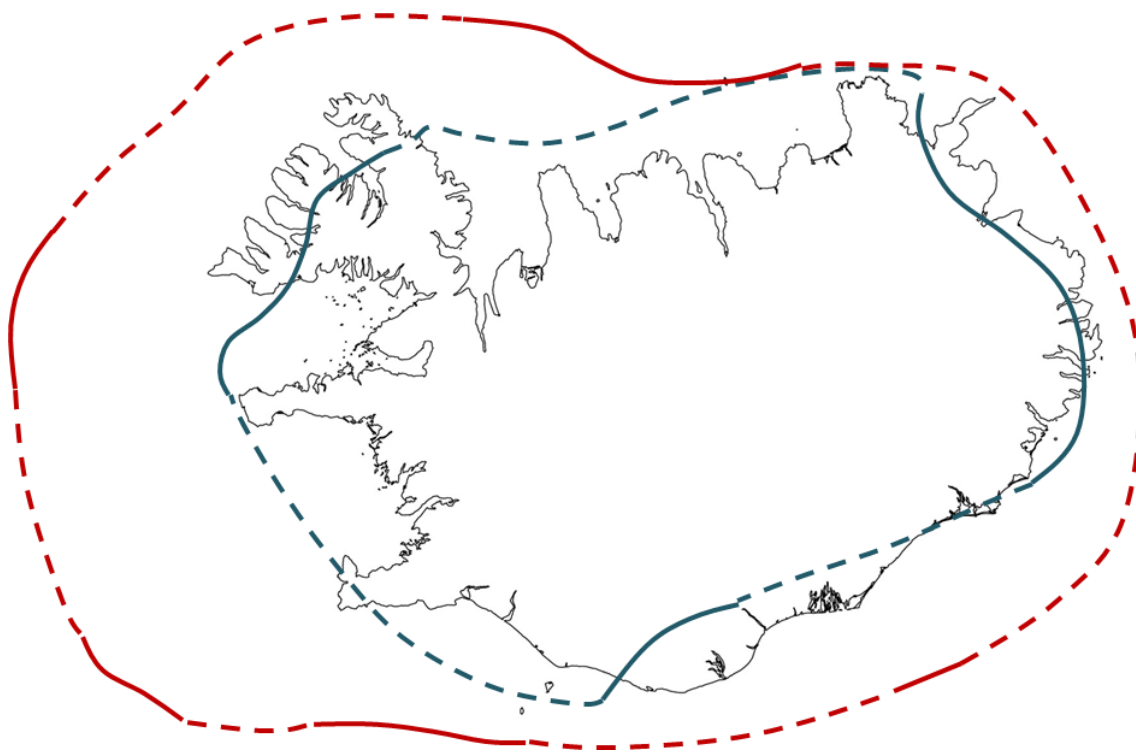


Figure 2.3: The maximum (red) vs. minimum (blue) glaciations showing ice extent estimations under the two contrasting hypotheses. Source: Hubbard *et al.* (2006).

The maximum hypothesis has received support from studies of submerged marine features (e.g. Ólafsdóttir, 1975), raised marine features (e.g. Einarsson and Albertsson, 1988), sediment analyses (e.g. Andrews *et al.*, 2000) and modelling studies (e.g. Hubbard *et al.*, 2006). However, some studies have continued to provide support for the minimum IIS hypothesis despite such a body of contradictory evidence, mainly a result of low marine limit elevations, such as in northern Vestfirðir (e.g. Hjort *et al.*, 1985) and tephra layers in lake sediments (e.g. Sigurvínsson, 1983) which, if ice covered, should not be present. In addition, the production of differing RSL records from the Vestfirðir peninsula contradicts the mono-domed maximum glaciation hypothesis.

Some of the most compelling evidence in support of the maximum IIS hypothesis has resulted from mapping studies of moraines (e.g. Andrews *et al.*, 2000) and raised shorelines (e.g. Einarsson and Albertsson, 1988). In their 1988 study, Einarsson and Albertsson noted a northerly and westerly tilt to the raised shorelines investigated resulting from the differential isostatic adjustment following the loss of the IIS. Regional tilting of raised shorelines and marine limits provide an insight into the glacial history of a locality, with marine limit elevations increasing with proximity to the centre of ice loading (Benn and

Evans, 2010). However, depending on the persistence of ice cover at the loading centre, marine limit elevations can also decrease towards the ice centre (Benn and Evans, 2010), as postglacial rebound has had a lesser opportunity to occur. As such, the pattern of marine limit elevations depends on the rapidity of deglaciation.

More recent modelling studies have also provided evidence to support the maximum IIS hypothesis (e.g. Bingham *et al.*, 2003; Hubbard *et al.*, 2006) through the modelling of the scale and volume of the IIS. Hubbard *et al.* (2006) suggest that the mean ice thickness was 940 m with a plateau elevation of 2000 m. The optimum LGM ice sheet model developed by Hubbard *et al.* (2006) produces an ice sheet which extends far beyond the present Icelandic coastline (Figure 2.3), with an area of $3.29 \times 10^5 \text{ km}^2$ made up of $3.09 \times 10^5 \text{ km}^3$ of ice. As a result, a large proportion of the base of the Hubbard *et al.* (2006) IIS is modelled below sea-level, leading to a highly dynamic ice sheet, which may have had several accumulation centres.

As a result of this dynamism and large marine component, there would have been potential for the ice sheet to influence global thermohaline circulation (Hubbard *et al.*, 2006) and hence global climate (Figure 2.4). This influence would have been greatest during deglaciation, which would have been driven by increased volcanism, RSL change, climatic adjustments or a combination thereof, when large amounts of freshwater would have entered the North Atlantic (Hubbard *et al.*, 2006). This freshwater input would have had a significant influence on the salinity of the surrounding ocean (Hubbard *et al.*, 2006) having a consequent effect on deepwater formation (Dickson *et al.*, 2002).

The model generated further demonstrates the apparent implausibility of the minimum IIS hypothesis, as the authors find little evidence to support an ice sheet within the present coastline (Hubbard *et al.*, 2006). That said, although the study provides support for the maximum IIS hypothesis, the dynamism of the modelled ice sheet is far greater than expected (Hubbard *et al.*, 2006). The Hubbard *et al.* (2006) model follows the notion that there were ice free areas and nunataks, which had the potential to act as refugia, thus supporting the

Rundgren and Ingólfsson (1999) hypothesis of limited plant survival during the LGM.

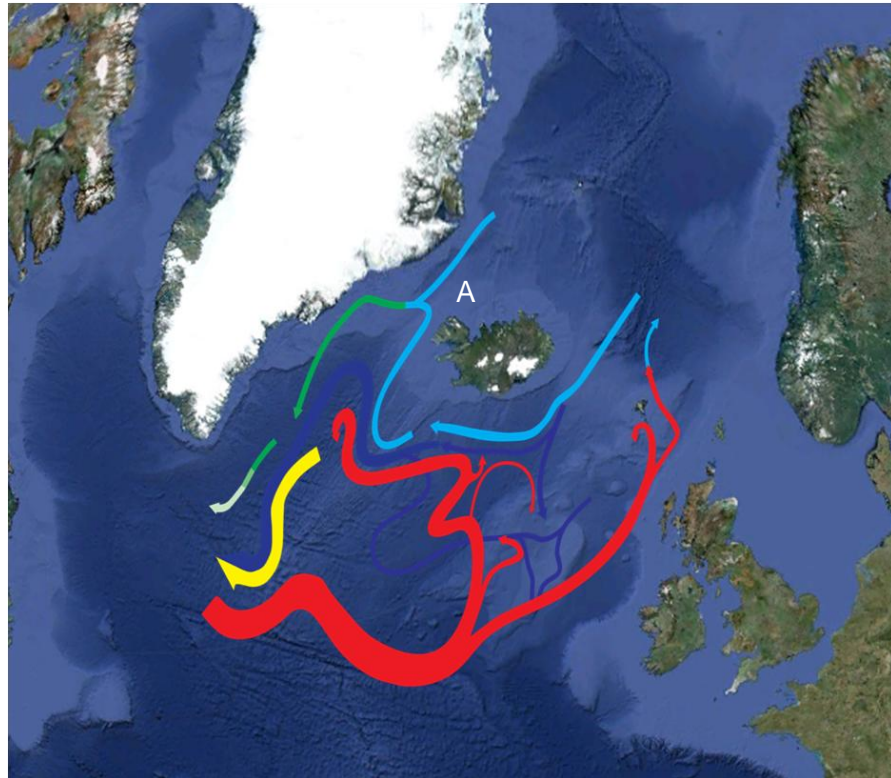


Figure 2.4: Thermohaline circulation and the major currents affecting Iceland, with red denoting warm currents and blue denoting cool currents. Meltwater input into Area A could have affected global thermohaline circulation and therefore global climate.

2.3 The deglaciation of Iceland

Following the LGM, the deglaciation of Iceland occurred relatively rapidly due to calving and subglacial heating of the IIS (Hubbard, 2006). The deglaciation of Iceland would have had a profound effect on RSL and so is discussed here using the Scandinavian glacial terminology to avoid confusion. Over recent decades, the dating of several samples has led to the reclassification of several features by age (Hjartarson, 1991) and as such the initial Icelandic stadial/interstadial terminology has been incorrectly associated with samples of different ages.

During the deglaciation, two stadials and two interstadials have been noted (Einarsson, 1973; 1979) with a third stadial also evident. Initial deglaciation occurred during the Bølling Interstadial (13 – 12 ka BP) (Ingólfsson and Norðdahl, 2001). It is thought that 81% of the IIS base was below LGM sea-

level (Hubbard, 2006) thus rising eustatic sea-level during the Bølling period (Fairbanks, 1989) led to rapid ice sheet collapse (Ingólfsson and Norðdahl, 2001; Figure 2.5).

Following the Bølling Interstadial, a brief Older Dryas stadial then led to renewed glacial advance in Iceland (Einarsson and Albertsson, 1988; Ingólfsson, 1985; 1987; 1988; Ingólfsson *et al.*, 1997; Le Breton *et al.*, 2010) following a worsening of climatic conditions at the end of the Bølling Period (Ingólfsson, 1991). Ingólfsson (1987; 1988) demonstrated such an Older Dryas readvance southwest of Borgarfjörður, western Iceland, where the ice sheet readvanced beyond the present coastline. The mapping of moraine features (e.g. Ingólfsson, 1984; 1988) has assisted in the establishment of the extent of the Older Dryas readvance however such studies and features are relatively scarce elsewhere in Iceland (Principato, 2008), with Snæfellsnes being particularly poorly constrained (Norðdahl and Pétursson, 2005).

The second glacial retreat occurred during the Allerød period (11.8 – 11 ka BP). It is thought that coastal areas were free of ice during this interstadial (Ingólfsson, 1991) and that environmental conditions were improved, as demonstrated by an increase in grass and shrubland species on Skagi (Rundgren, 1995; 1999). Other studies of Allerød sediments have revealed cooler coastal waters during this period, deposited as a result of a marine transgression during the interstadial (Ásbjörnsdóttir and Norðdahl, 1995) which resulted from eustatic sea-level change and crustal subsidence during the period (Norðdahl and Pétursson, 2005).

Following this cooling, glacial readvance led to an extensive Younger Dryas glaciation of Iceland (Norðdahl and Hjort, 1987; Hjartarson, 1991; Ingólfsson, 1991; Ingólfsson *et al.*, 2010; Figure 2.5) which was relatively rapid in its onset (Hjartarson, 1991). Investigations have revealed that the extent of the Younger Dryas glaciation has probably been previously underestimated in Iceland (Hjartarson, 1991) with glaciers expanding beyond the present coastline in some locations (Ingólfsson, 1987; Ingólfsson and Norðdahl, 2001). It is however evident that glaciers terminated onshore or close to the present coastline in western Iceland (Vikingsson, 1978; Eiriksson *et al.*, 1997;

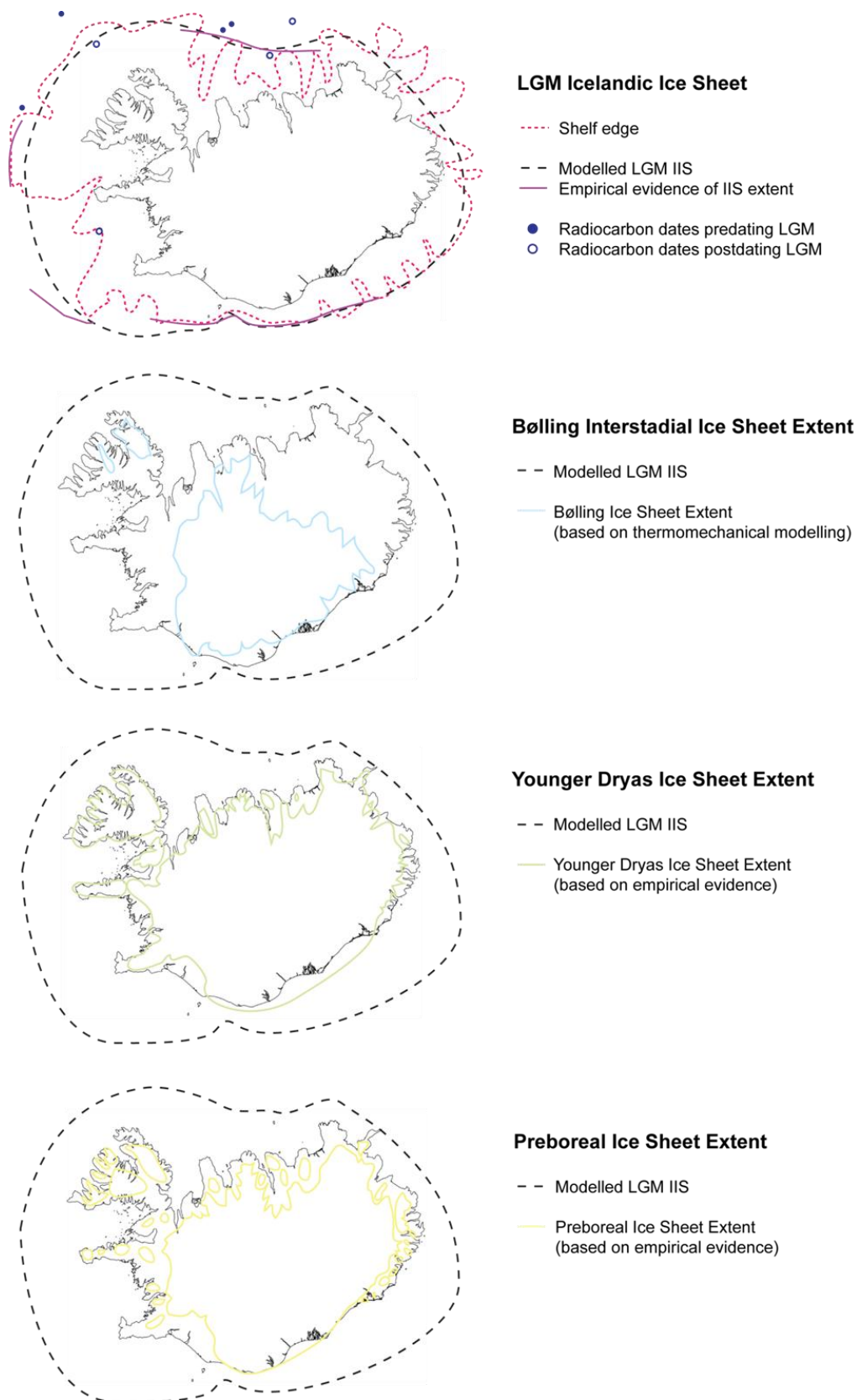


Figure 2.5: Ice extent during the LGM, Bølling Interstadial, Younger Dryas and Preboreal Readvances, highlighting the changing structure of the IIS during deglaciation. The extent of the IIS during the Allerød and Older Dryas is currently poorly constrained and so has not been included here. Adapted from Ingólfsson et al (2010).

Geirsdóttir *et al.*, 1997; Norðdahl and Pétursson, 2005) and indeed that other areas of Iceland were completely ice free (Ingólfsson *et al.*, 1997).

The extent of the Younger Dryas glaciation has been mapped through the identification of the Skógar-Vedde tephra, which was deposited c. 10600 ¹⁴C yrs BP (12.4 cal. ka BP) (Mangerud *et al.*, 1984; Grönvold *et al.*, 1995) and through the mapping of raised marine features (Norðdahl and Pétursson, 2005). The truncated nature of several such features has led to the proposition of glaciers terminating onshore in several locations (Norðdahl and Pétursson, 2005).

One final readvance has been noted in Iceland during the Preboreal (Ingólfsson *et al.*, 2010; Figure 2.5). This was particularly short-lived and the extent of the readvance is poorly constrained in western Iceland (Ingólfsson *et al.*, 2010). However, several studies have been delimited ice extent in the southwest (e.g. Hjartarson and Ingólfsson, 1988; Ingólfsson *et al.*, 1995). Previous study has also highlighted that glaciers may have occurred more extensively on Snæfellsnes than at present (Norðdahl and Pétursson, 2005) yet the actual extent is still a relative unknown. Following the short-lived Preboreal readvance, the final disintegration of the IIS and retreat to present glaciers, such as Drangajökull and Vatnajökull, occurred rapidly (Ingólfsson *et al.*, 2010).

Previous study has highlighted the many issues and complexity surrounding the Icelandic glaciation. It is clear that further research is required in order to establish an accurate record of glacial extent in Iceland. The mapping of raised features, submerged features and moraines, as well as modelling attempts, has provided valuable evidence for the glaciation and deglaciation of Iceland, with RSL research providing key data to test models of glaciation, as well as assumptions regarding the extent and size of the IIS.

In addition to the aforementioned processes associated with the deglaciation of Iceland, links between volcanism and deglaciation has also been investigated (MacLennan *et al.*, 2002), with particular attention being placed on the Reykjanes peninsula, southern Iceland (Jakobsson *et al.*, 1978). This has led to the proposition of links between increased eruption rates and glacial unloading and meltwater discharge (e.g. Gudmundsson, 1986; Jull and McKenzie, 1996). This increased volcanism would therefore have had an effect on the RSL record for the region, thus making it relevant for discussion here.

The meltwater from areas of increased volcanic activity could also have had an effect on global thermohaline circulation and hence global climate.

In addition to testing the extent of the various glaciations of Iceland, a key area for future research is both the pattern and style of the Icelandic deglaciation. The marine limit has been used extensively in North America and Scandinavia to determine such patterns and styles of deglaciation alongside the rates of rebound associated with them (e.g. Evans *et al.*, 2002). In order to establish this effectively, the density of marine limit measurements needs to be sufficiently high, thus allowing isobase maps to be generated. Furthermore, when coupled with the exploration of glacial geomorphology, principally moraines, the marine limit and raised shorelines can provide an insight into the pattern of deglaciation and glacial cover (Evans *et al.*, 2002). The use of the marine limit to determine RSL change is discussed more fully later in this chapter.

2.4 Relative Sea-Level Change in Iceland

The deglaciation of Iceland had a profound effect on the associated RSL history. The rapid withdrawal of glacial load associated with the Icelandic deglaciation led to a rapid crustal response (Le Breton *et al.*, 2010). This was due to the sensitivity of the Icelandic crust to loading (Sigmundsson, 1991; Ingólfsson *et al.*, 1995; Rundgren *et al.*, 1997; Ingólfsson *et al.*, 2010) as a result of low asthenospheric viscosity (Ingólfsson *et al.*, 1995). Recently, modelling has been used to quantify response variability; however several inaccuracies have been introduced, particularly regarding feature dating.

The amount of postglacial rebound associated with the deglaciation has been constrained through the identification and dating of raised marine features, such as the marine limit and raised shorelines (e.g. Principato, 2008; Ingólfsson *et al.*, 1995; Le Breton *et al.*, 2010), allowing the subsequent calculation of vertical displacement. The marine limit is defined as the highest elevation reached by the sea at a particular location (Andrews, 1970). Le Breton *et al.* (2010) identified two main periods of isostatic uplift: an initial period between 10 ka ¹⁴C (~ 11.4 cal. ka) BP and 8150 (~9100 cal.) BP, with an average uplift rate of $5.5 \pm 2.2 \text{ cm a}^{-1}$ and a second period between 8150 BP and present day, with uplift

rates of $0 - 1.5 \text{ cm a}^{-1}$. The study also allows the spatial variability of crustal rebound to be established, highlighting the differential effects on the RSL record in Iceland (Le Breton *et al.*, 2010).

However, the study assumes that the high marine limits in western Iceland are synchronous and were formed $10 \text{ k} \pm 300 \text{ a}$ (11155 – 12100 cal.) BP (Le Breton *et al.*, 2010), which is extremely unlikely. Despite this and the differences in the calculation results produced by Le Breton *et al.* (2010) and other studies (e.g. Norðdahl and Einarsson, 2001), the authors validate their results by stating that those of previous studies are skewed by the rapid initial rebound found immediately after the deglaciation of Iceland.

In addition, the authors note the possibility of deviation at the local scale from the values that they have calculated, stating that the method employed is not applicable in all locations around Iceland (Le Breton *et al.*, 2010). The authors defend its use in western Iceland due to the availability of features against which the modelled rebound can be compared. Although this is the case, the notion of synchronicity of the high marine limit in western Iceland is very improbable, with the variability in dates of such features being evidence in support of this. In fact, several papers have suggested that this high marine limit is likely to have formed in the Bølling Period, some two to three thousand years before the Le Breton *et al.* (2010) date. However, such studies of postglacial rebound are important, providing an insight into a major effect on the RSL record.

Until relatively recently, RSL change in Iceland was principally investigated through the geomorphological mapping of raised marine features (e.g. Hansom and Briggs, 1991; Ásbjörnsdóttir and Norðdahl, 1995; Ingólfsson and Norðdahl, 2001; Norðdahl and Pétursson, 2005; Principato, 2008). Such studies are susceptible to issues surrounding dating techniques (Fleming and Lambeck, 2004; Lloyd *et al.*, 2009), interpretation and spatial coverage (Lloyd *et al.*, 2009). A lack of dateable material can also be problematic in some locations (Fleming and Lambeck, 2004), such as eastern Vestfirðir (Principato, 2008). Although this is not a problem in North America (e.g. Andrews, 1970), sites with dateable material in Iceland have proven elusive on occasion. Furthermore, the technique tends to provide data for a single point such as a marine limit and is

often unable to provide an accurate RSL curve for a particular location (Lloyd *et al.*, 2009).

Despite these issues, such research has provided valuable information concerning the marine limits and other raised shorelines in western Iceland (e.g. Ingólfsson, 1991; Ingólfsson and Norðdahl, 2001). In some locations, raised marine features have been mapped over a long temporal and spatial scale, meaning that several areas are extensively mapped. Vestfirðir, for example, has been a focus for geomorphological surveying for over a century (e.g. Bárðarson, 1906, 1910; John, 1975; Hansom and Briggs, 1991; Norðdahl and Pétursson, 2005; Principato, 2008; Lloyd *et al.*, 2009), with raised shorelines being mapped throughout the peninsula. However, areas such as Snæfellsnes remain relatively unsurveyed. As such, the mapping of such features as part of this research could prove useful in constraining the RSL record.

2.4.1 Marine Limits in Iceland

In addition to determining patterns of deglaciation and quantifying rates of rebound, marine limits have been used extensively in a variety of locations to determine the highpoint reached by postglacial sea-level (e.g. Lloyd *et al.*, 2009). The marine limit can often be difficult to constrain, with unequivocal evidence coming from sites with marine shells present within deltaic sediments (Andrews, 1970). The effectiveness of marine limit investigation has been brought into question in previous studies, due to the difficulties in determining marine limit surface elevation, relevance and chronological constraints (Andrews, 1970).

Many raised marine features have been dated through the radiocarbon dating of driftwood and marine shells, thus providing both a timing and elevation for RSL changes. Previous studies in the Arctic and North America have had sufficient marine shell deposits to provide detailed chronologies for RSL change using marine limits (e.g. Bell, 1996). However, such deposits are less extensive in Iceland.

The marine limit in Iceland occurs at various elevations, as a result of the differences in glacial load and timing (Jennings *et al.*, 2000). The marine limit is highest in southern Iceland, occurring at c. 110 m above sea level (asl.)

(Ingólfsson, 1991; Ingólfsson *et al.*, 1995). The marine limit heights for Iceland are summarised in Figure 2.6, which demonstrates the considerable variation in local marine limit height over relatively short distances. The closest determined marine limit heights to Snæfellsnes are found at c. 80 m in Bjarkarlundur, southern Vestfirðir (Lloyd *et al.*, 2009) and in the Dalir region, at between 65 m and 70 m (Norðdahl and Ásbjörnsdóttir, 1995). Hansom and Briggs (1991) also noted a marine limit of 70 m for southeastern Vestfirðir, which will also prove beneficial for comparison in this study.

The age of the marine limit in Iceland is also varied (Hjartarson and Ingólfsson, 1988) due to the differential downwarping and divergences in deglaciation processes, patterns and styles around Iceland (Ingólfsson, 1991). Several studies have suggested a similar age for the Icelandic marine limit at c. 10000 a BP (e.g. Ingólfsson, 1988; Ingólfsson and Norðdahl, 1994; Le Breton *et al.*, 2010). However, other studies have stated that the marine limit formed during the Bølling Interstadial when RSL was at its highest (e.g. Einarsson, 1968; Rundgren *et al.*, 1997; Ingólfsson and Norðdahl, 2001; Norðdahl and Pétursson, 2005). It is however important to recognise that the dating of such features is not always accurate. The differing deglacial styles and patterns operating in Iceland are also likely to mean that this is unlikely. In fact, there is evidence to suggest that this is not the case, with a marine terrace found between 60 m and 70 m asl at Skorradalur dated to 10.3 ka ¹⁴C (12 ka cal.) BP (Ingólfsson and Norðdahl, 2001).

Lower raised shorelines have also proven beneficial in the determination of the RSL history of Iceland, particularly where several occur at various elevations at the same location. Hansom and Briggs (1991) identified several raised shorelines at Hunáflói (Figure 2.1) with the marine limit identified at 70 m asl. More recently, Principato (2008) investigated 16 raised shorelines in eastern Vestfirðir, however a lack of dateable material limited the scope of this research. The use of raised shorelines and marine limits, when in conjunction with isolation basin data, can provide accurate chronological data (Rundgren *et al.*, 1997; Lloyd *et al.*, 2009), which are particularly beneficial for determining patterns of deglaciation.

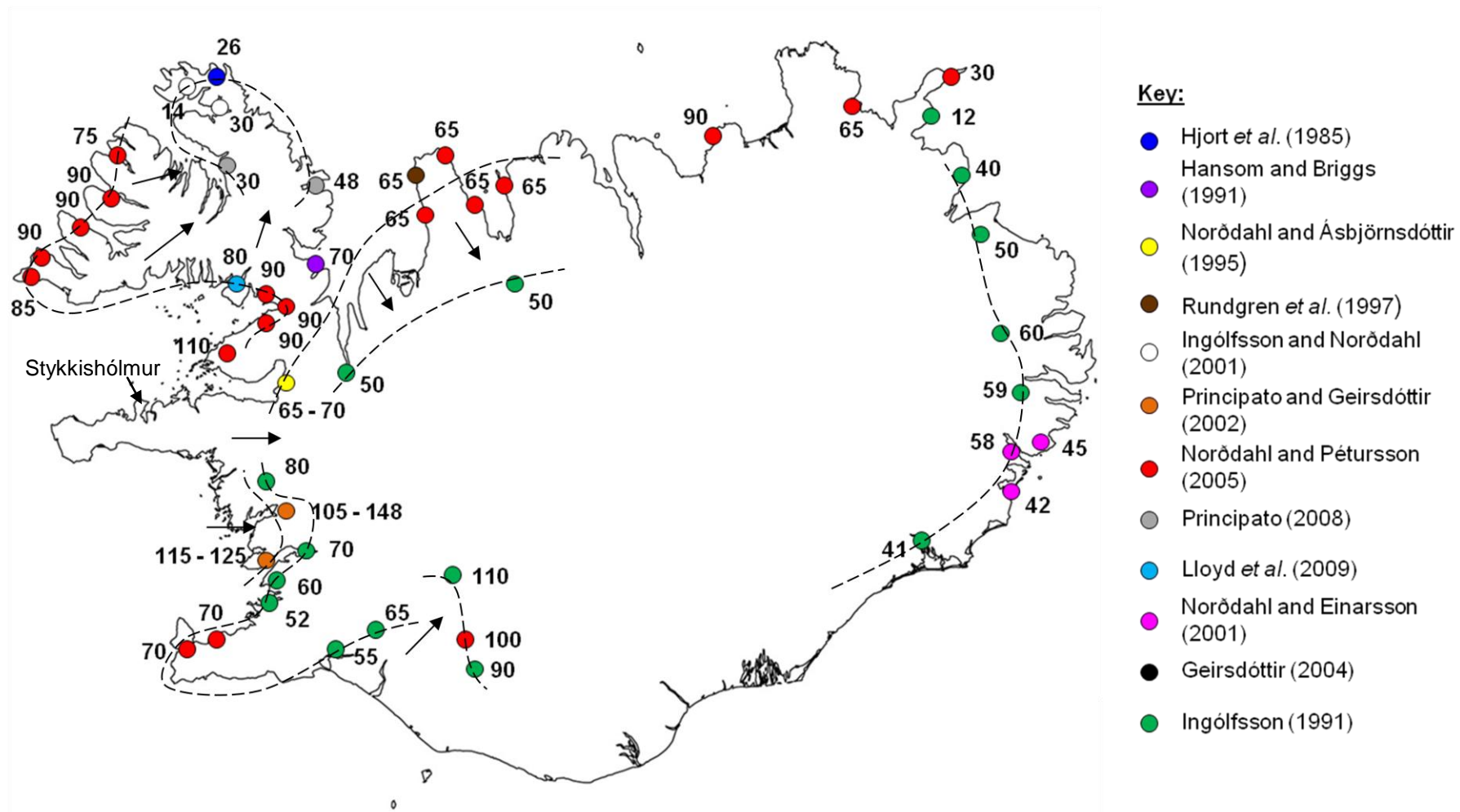


Figure 2.6: Marine limit elevations in Iceland. Elevations are given in metres asl and the data sources are shown to the right. Contours (black dashed line) denote areas of similar ice thickness and potential similar timing of deglaciation, with the arrows highlighting potential paths of glacial retreat from marine limit evidence.

It is clear that raised shorelines and marine limits can play an important role in the constraint of RSL change; however, issues regarding accuracy should not be overlooked when interpreting such data. In Canada and Fennoscandia, marine limit data has been used to great effect to determine RSL change, as well as the pattern and style of deglaciation. Evans (1990) used raised shorelines to provide a reconstruction of the deglacial and RSL history of the Canadian High Arctic, where the importance of chronological control is reported as paramount. Evans (1990) highlights the need for features to be assigned an accurate age and elevation in order to provide the most realistic reconstruction of paleo-RSL. In this research, rather than reconstructing paleo-RSL using raised shorelines, such raised marine features will be used to provide a high point for RSL in northern Snæfellsnes overcoming the issue of finding suitable material to date.

2.4.2 Low postglacial RSL in Iceland

A fall of RSL below present levels has long been proposed in Iceland (e.g. Bárðarson, 1923; Thorarinsson, 1956). Since the early proposition of this low period in Icelandic RSL, studies of submerged features and deposits have provided valuable evidence and supportive dates of such a change (e.g. Thors and Boulton, 1990; Moriwaki, 1990; Ingólfsson *et al.*, 1995). An extensive study was undertaken at Faxaflói, Kollafjörður and Hvalfjörður in western Iceland (Figure 2.1) by Thors and Helgadóttir (1991), finding RSL fall of ~ 90 m over a 700 year period at approximately 9.9 cal. ka BP. Additional studies have provided similar dates for a fall of RSL below present levels, with Thorarinsson (1956), Kjartansson *et al.* (1964) and Ingólfsson *et al.* (1995) all proposing that RSL fell below present between 10.7 cal. ka and 9.9 cal. ka BP.

Such studies are however severely limited, due to the use of radiocarbon dating from dredged peat samples, with Thors and Helgadóttir (1991) admitting that he results are circumstantial. Although these dates have provided sensible timings for such periods of low RSL, the dates should be treated with caution due to the possibility of mixing during extraction.

The uncertainty regarding this period of low RSL in SW Iceland is compounded by the results of an isolation basin investigation at Lake Hestvatn undertaken by

Geirsdóttir *et al.* (1997), demonstrating that the Southern Lowlands were submerged until 9.9 cal. ka BP. This correlates with the date of the low point in RSL from the Thors and Helgadóttir (1991) dredged peat study of between 10.3 and 9.0 ka BP. The proximity of these two study locations means that if both are correct, sea-level varied considerably over short distances in SW Iceland. It would appear that the likelihood of this occurring is however slim, particularly when the methodological limitations of the Thors and Helgadóttir (1991) study are taken into consideration.

Peat studies elsewhere in Iceland have also highlighted a period of low RSL however (e.g. Moriwaki, 1990). Studies near Blönduós, Skagi peninsula, suggest that RSL fell to or below present sea-level between 9.9 cal. ka BP (Moriwaki, 1990) and 9.5 cal. ka BP (Meyer and Venzke, 1987). This figure from northern Iceland fits well with those produced by Thors and Helgadóttir (1991) and Geirsdóttir *et al.* (1997) from SW Iceland. This period of low RSL from peat deposits also correlates well with the record produced by Rundgren *et al.* (1997).

Dredged peat studies have provided evidence for a low point in the RSL history of Iceland, alongside the rapid nature of the RSL fall to this low point, which can be valuable for testing geophysical modelling study results. The rapidity of the RSL fall highlights the high rate of postglacial isostatic rebound following the deglaciation of Iceland (Ingólfsson *et al.*, 1997). However, if the assertion that the timings of such changes are incorrect holds true, the usefulness of such studies is obviously greatly reduced.

That said, seismic profiling studies have provided evidence for a low point in RSL of a similar magnitude to those generated by the study of submerged peat samples (e.g. Thors and Boulton, 1991; Thors and Helgadóttir, 1991). Thors and Helgadóttir (1991) studied the RSL changes of southwestern Iceland, highlighting an early Holocene low point of between 30-35 m below present sea-level. In northern Iceland, Thors and Boulton (1991) have shown a similar low during the early Holocene in Eyjafjörður, with a transgression meaning sea-level reached 20 m below present. This is not the lowest point recorded during the study however, with a low point of 40 m below present during the Late Weichselian (Thors and Boulton, 1991). It is therefore clear that there is

evidence for a low point in the RSL history of Iceland. The level of certainty associated with each of these results varies with the methodology employed and therefore the results of some studies should be treated with caution.

2.4.3 Isolation Basin Studies in Iceland

Although less extensive, microfossil analyses of isolation basin sediments have also been undertaken in Iceland (e.g. Rundgren *et al.*, 1997; Lloyd *et al.*, 2009) through the employment of the Scandinavian technique. An isolation basin is defined as a basin which has become isolated from the sea and has subsequently accumulated freshwater sediments (Svendsen and Mangerud, 1987; Shennan *et al.*, 1994; Lowe and Walker, 1997). Lake basin assemblages have often been used to determine environmental changes within particular locations (e.g. Bradbury, 1975, Doner, 2003), often subsequently being used to determine changes in RSL.

The isolation basin technique relies on the impervious nature of the isolation basin sill to preserve an accurate record of RSL change (Lloyd and Evans, 2002). The impervious sill prevents the post-isolation alteration of the sediments laid down within the basin from marine influences. Figure 2.7 outlines the stages of basin isolation and the salinities associated with each stage. Figure 2.7 also highlights how the rock sill prevents alteration of the sedimentological and microfossil records following isolation. Following the initial decrease in marine influences, basin salinity during the brackish phase can vary rather than following a simple, linear transitional sequence. This variability during the brackish phase relates to the levels of influence from marine and freshwater during the isolation process.

The investigation of isolation basin sediments can provide an insight into the changes in depositional environment within the basin. In addition, subsequent microfossil analyses can then be conducted on the sediments present within the isolation basin sediment sequence to produce a record of environmental changes, based on salinity. As a result of this environmental record generation, changes in RSL can be determined.

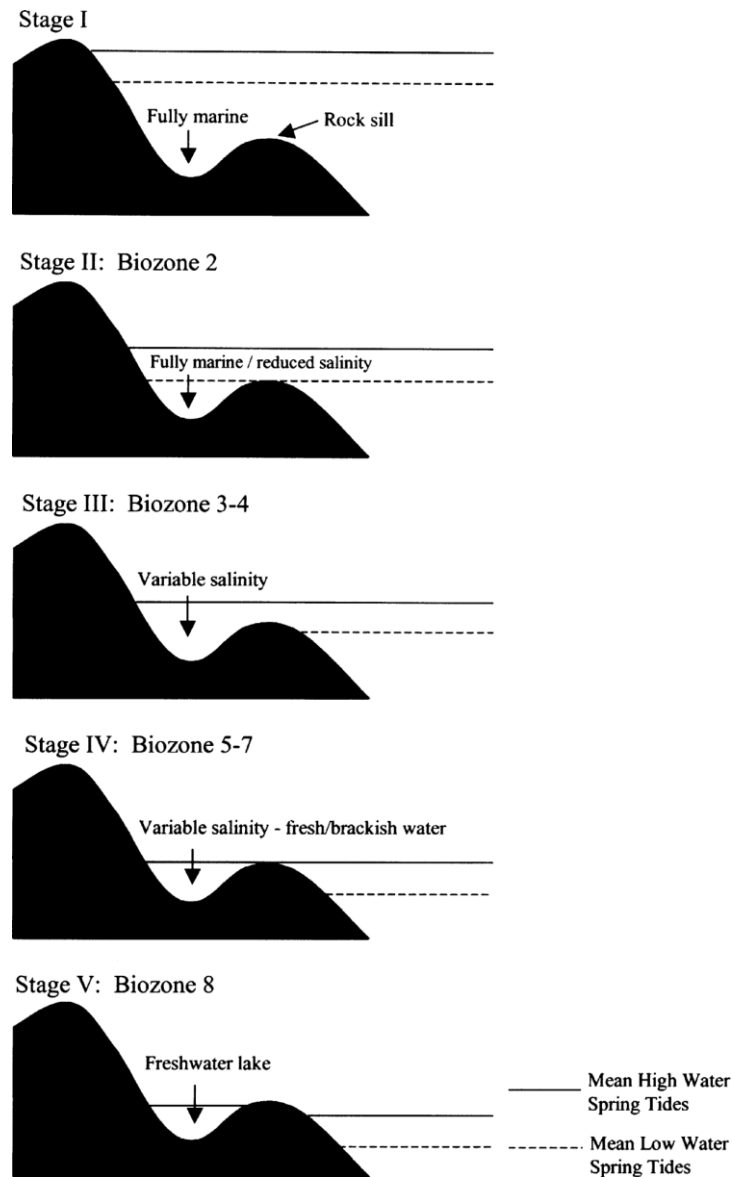


Figure 2.7: The stages of the basin isolation process, showing the transition from fully marine (Stage I) to brackish (Stage III) and finally freshwater dominance (Stage V). Source: Lloyd and Evans (2002).

In conducting the aforementioned sediment and diatom analyses, the identification of the three isolation contacts outlined by Kjemperud (1986) can be achieved:

- i) *Diatomological isolation contact:* the point at which the diatom flora supported by the basin are freshwater species.
- ii) *Sedimentological isolation contact:* the point at which the sediment within the basin changes from allochthonous clastic to autochthonous organic sediments thus denoting the change from marine to freshwater influence.

- iii) *Hydrological isolation contact*: the point at which the water column becomes entirely freshwater.

Isolation basins also offer an opportunity to determine differences in isostatic rebound and subsidence between locations (Rundgren *et al.*, 1997), thus allowing an insight into the retreat and advance of the IIS. As such, isolation basin studies allow patterns of deglaciation to be determined, which could allow variations around the IIS to be established. A series of studies within the same region could also provide the chance of determining the stages of ice retreat, thus acting as a test for geophysical models.

The first isolation basin RSL study in Iceland was undertaken by Rundgren *et al.* (1997) using a series of lakes and raised beach measurements on the Skagi peninsula, which led to the production of a RSL curve (see Figure 2.8). Rundgren *et al.* (1997) state that RSL fell 45 m between 13 cal. ka BP and 10.2 cal. ka BP, during which two transgressions also occurred, each of 5 m amplitude. Over that period, the mean uplift rate was calculated to c. 2.75 cm cal. yr⁻¹, however following the second transgression, this rose to c. 5 cm cal. yr⁻¹ (Rundgren *et al.*, 1997). The most rapid period of RSL fall occurred between the two marine transgressions (11.4 cal. ka BP – 11.25 cal. ka BP), with a fall of c. 20 m, giving to a mean absolute uplift rate of c. 15 cm cal. yr⁻¹ when eustatic changes during the period are taken into account (Rundgren *et al.*, 1997). Rundgren *et al.* (1997) correlate the two marine transgressions to ice sheet margin advances and the associated crustal loading, which is known to have occurred during the Younger Dryas and Preboreal (Ingólfsson and Norðdahl, 1994), as previously outlined.

The transgressions recorded in the Rundgren *et al.* (1997) isolation basin study also link to results from western Iceland, where Norðdahl and Ásbjörnsdóttir (1995) recorded transgressions linked to the glacial advances of the Younger Dryas and Preboreal. However, the timing of the second transgression highlighted in the Rundgren *et al.* (1997) study is brought into question, due to poor chronological control and a hiatus in the sedimentary record. That said, it appears sensible that this transgression occurs concurrently with the increased crustal loading during the Preboreal and the date of this transgression fits with results produced by Norðdahl and Ásbjörnsdóttir (1995) in western Iceland.

RSL curves for western Iceland

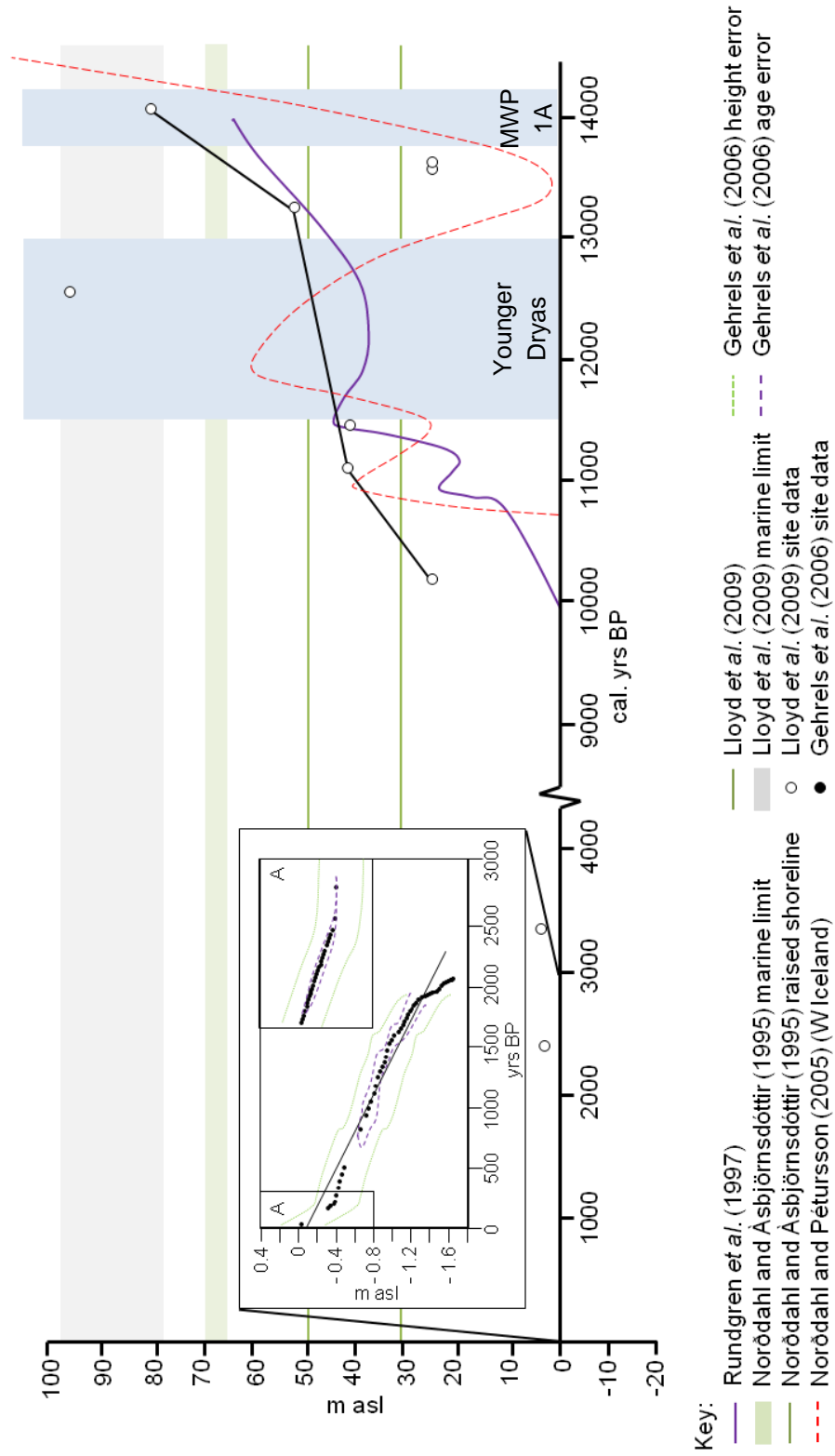


Figure 2.8: RSL change in NW and western Iceland during the Lateglacial and Holocene, including the three principal comparative records for this research. Sources: Norðdahl and Asbjörnsdóttir (1995); Rundgren et al. (1997); Norðdahl and Pétursson (2005); Gehrels et al. (2006); Lloyd et al. (2009).

More recently, the isolation basin method has been employed in the investigation of seven isolation basins in the Bjarkarlundur area of Vestfirðir (Lloyd *et al.*, 2009; Figure 2.8). Lloyd *et al.* (2009) show that the marine limit in the area is ~80 m asl. and is dated to 14 cal. ka. BP. The microfossil data suggest that RSL fall was continuous from 14 cal. ka BP to the early Holocene, with two particularly rapid periods of RSL fall before and after the Younger Dryas. In Bølling-Allerød times, RSL fell at an average rate of c. – 3.8 cm cal. yr⁻¹ and during the early Holocene, RSL was falling at an average rate of c. – 1.6 cm cal. yr⁻¹ (Lloyd *et al.*, 2009). It is clear that the Younger Dryas slowed the rate of RSL fall (to c. – 0.4 cm cal. yr⁻¹) and the possibility of RSL rise during the period is highlighted.

Interestingly, the isolation basin study conducted by Lloyd *et al.* (2009) was able to provide a constraint on the influence of the Younger Dryas readvance in the Bjarkarlundur area, stating that the fluctuation in RSL would have been in the region of 10 m. This constraint was possible due to the investigation of basins isolated before and after the Younger Dryas readvance, with the upper basin not being reinundated during the readvance (Lloyd *et al.*, 2009). This constraint is particularly valuable with used in conjunction with previous research, which has noted rapid RSL rise over the Holocene in western Iceland (Norðdahl and Pétursson, 2005). Lloyd *et al.* (2009) also provide valuable evidence of the rate of RSL fall following the Younger Dryas readvance, which is recorded as – 23 mm ¹⁴C yr⁻¹. This rate is lower than those recorded in both Skagi (Rundgren *et al.*, 1997) and south west Iceland (Ingólfsson *et al.*, 1995), which could suggest a slower rate of deglaciation in NW Iceland.

Lloyd *et al.* (2009) also suggest that RSL fell below present at c. 9 cal. ka BP, which is considerably later than seen in south west Iceland, where sea-level is thought to have fallen below present at c. 10.5 cal. ka BP (Ingólfsson *et al.*, 1995). The magnitude of this drop below present sea-level could not be constrained in the study due to the basins analysed (Lloyd *et al.*, 2009). However, Lloyd *et al.* (2009) provide evidence for a transgression above present during the Late Holocene, from which RSL is assumed to have since fallen to present from c. 3.3 cal. ka BP. .

It is therefore clear that isolation basin studies, although less numerous than other forms of RSL investigation in Iceland, have provided valuable evidence for postglacial RSL change. Whilst generating accurate evidence for RSL change in a particular location, such studies have also highlighted differences between regions, as well as generating suitable data to test geophysical models. Further isolation basin studies in Iceland have the potential to further constrain the RSL changes, glacial advances and retreats of the IIS. In addition, rates of changes can also be better constrained through the further employment of the isolation basin technique. .

2.4.4 Saltmarsh studies in western Iceland

Saltmarsh sequences have also provided important evidence of RSL changes in Iceland, particularly over the past 2000 years. Gehrels *et al.* (2006) undertook research at Viðarhólmi, southern Snæfellsnes to determine RSL changes over the last 2000 years, noting a c. 1.3 m rise in RSL since AD 100 (Figure 2.8). RSL rose at a rate of 0.65 m per 1000 yrs over the period studied (Gehrels *et al.*, 2006). Of particular significance is the rapid RSL rise over the past c. 150 – 200 years, where a c. 0.4 m increase in RSL has been recorded (Gehrels *et al.*, 2006).

The trend of rising recent RSL in southern Snæfellsnes results from a combination of isostatic subsidence and eustatic sea level rise (Gehrels *et al.*, 2006). As such, the record provides an insight into the isostatic activity of the region and therefore the potential deglacial history of the region when compared to isolation basin studies elsewhere in Iceland. Saltmarsh studies are uncommon in Iceland, but have highlighted RSL patterns which complement the isolation basin data, particularly when low elevation sites are lacking from isolation basin studies.

2.5 Tephrochronology in Iceland

2.5.1 The use of tephrochronology

Tephrochronology is a long established technique in Iceland (e.g. Thorarinsson, 1944), which has been successfully employed to determine a framework for the

timing of environmental changes (e.g. Langdon and Barber, 2005), as well as allowing sample correlation and the generation of marker horizons (Kittleman, 1979; Hafliðason *et al.*, 2000; Swindles *et al.*, 2010) and the reconstruction of eruption histories (Larsen and Eiríksson, 2008). The technique was first established in Iceland by Thorarinsson (1944) and since then, the use and importance of tephrochronology has increased and developed (Hunt and Hill, 1993; e.g. Lowe *et al.*, 2000; Lowe *et al.*, 2001), with growing numbers of tephra horizons being discovered and subsequently dated.

Tephra, described as any pyroclast exiting a volcanic system (Thorarinsson, 1944), can be analysed to determine its chemical composition, thus providing an insight both into the source area and potentially the individual eruption. The chemical composition of a sample is generally homogeneous, thus allowing the correlation of samples between sites (Westgate and Gorton, 1981). Chemical analyses of tephra layers generally correlate with the bulk geochemistry of magma samples (Barker, 1983), thus allowing further correlation. Tephra is mostly transported as fallout from eruption clouds (Larsen and Eiríksson, 2008), which can lead to a wide dispersal pattern and can be dated through the radiocarbon (^{14}C) dating of overlying or underlying peat samples (Thorarinsson, 1979). Tephrochronology has also been employed when the accuracy of other chronological methods, such as ^{14}C , have not proved sufficient (Swindles *et al.*, 2010).

The length of the available chronology is dependent on the type of sediment from which a sample is retrieved. Terrestrial soils provide tephra deposits from the past 9 – 10 ka (Larsen and Eiríksson, 2008), due to the development of such deposits since the Preboreal (Hallsdóttir and Caseldine, 2005; Larsen and Eiríksson, 2008). Through the employment of lacustrine sediment deposits, tephra deposits can be retrieved from the Lateglacial to present (e.g. Björck *et al.*, 1992), meaning that the sites employed in this research have the potential to record the environmental changes of the Snæfellsnes peninsula throughout the Holocene. The longest tephra based chronological records available have however been established through the investigation of marine deposits (e.g. Eiríksson *et al.*, 2000).

In total, approximately 30 volcanic systems have been determined in Iceland (Gudmundsson, 2000; Larsen and Eiríksson, 2008). However, since the LGM, the activity of four zones has been dominant in producing the tephra record (Sæmundsson, 1979). The various volcanic systems of Iceland are presented in Figure 2.9, which demonstrates the positioning of the principal systems within Iceland.

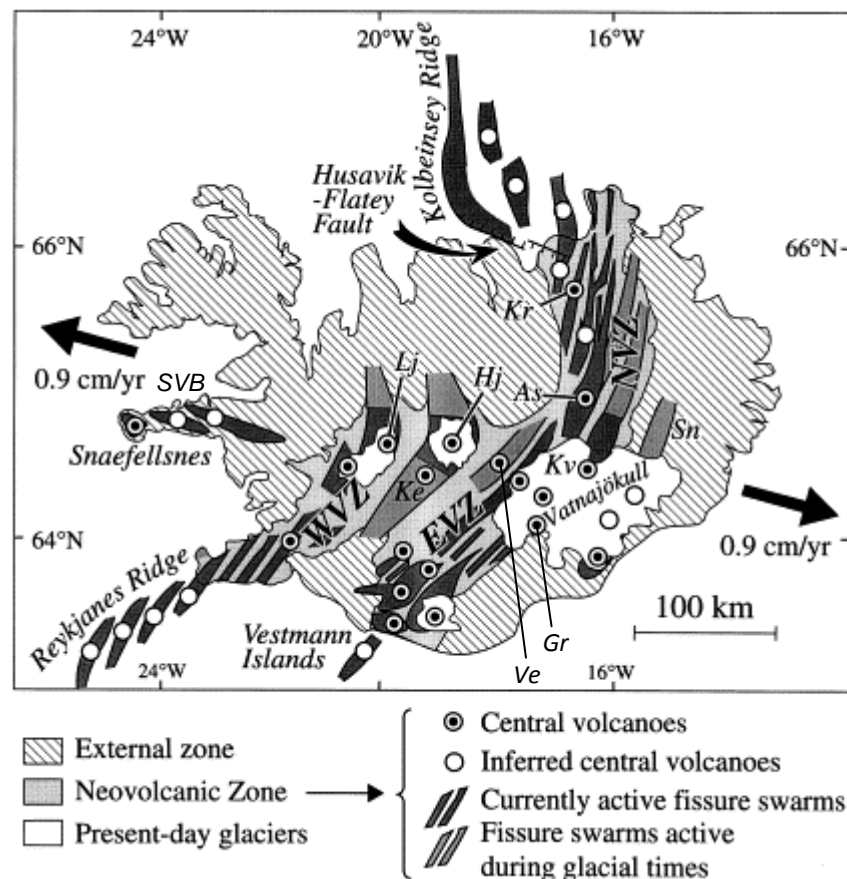


Figure 2.9: Volcanic sources within Iceland, showing the locations of the various volcanic zones and systems. As: Askja; Hj: Hofsjökull; Ke: Kerlingarfjöll; Lj: Langjökull; Sn: Snæfell (different to Snæfellsjökull); Kr: Krafla; Gr: Grímsvötn; Ve: Veidivötn; SVB: Snæfellsnes Volcanic Belt (including Ljós fjöll Volcanic System); NVZ: Northern Volcanic Zone; WVZ: Western Volcanic Zone; EVZ: Eastern Volcanic Zone. Adapted from: Bourgeois *et al.* (1998).

Over the course of the past 1100 years, approximately 200 tephra layers have been identified (Thordarson and Larsen, 2007), with the majority of samples being basaltic in nature, of least 70 of which were formed from the Grímsvötn system (e.g. Gudmundsson *et al.*, 1997). It is therefore likely that tephra deposits of a basaltic nature will be found in the Snæfellsnes sediment samples, both due to the higher numbers of basaltic eruptions and the proximity to such basaltic systems as Grímsvötn (Figure 2.9).

2.5.2 Limitations to tephrochronology

The principal issue associated with the establishment of a comprehensive tephra based chronology is the preservation of tephra layers. Good preservation has been found at several sites, with lake sediments providing valuable records in several locations (e.g. Björck *et al.*, 1992; Lloyd *et al.*, 2009). It has however been proposed that the best levels of preservation are often found outside Iceland (Larsen and Eiríksson, 2008; e.g. Wastegård *et al.*, 2001). There are however many tephra layers which are widespread and have proven particularly beneficial in establishing horizons, or isochrons, between sites.

The majority of volcanic systems have distinct chemical signatures (Larsen and Eiríksson, 2008), which as previously outlined, can be used to determine the source and in conjunction with ^{14}C dating, can provide ages for particular eruptions. However, it can be very difficult to determine differences between eruptions from the same system (Larsen *et al.*, 1999; Larsen and Eiríksson, 2008), with the differentiation of samples from systems of similar composition also being problematic on occasion. In addition, previous studies have highlighted the possibility of the alteration of the chemical composition of tephra generated during an eruption (e.g. Thorarinsson, 1950; Thorarinsson and Sigvaldason, 1972).

Chemical compositions are generally determined through the employment of electron microprobe analysis (EPMA), which quantifies the elements present in glass shards generated from an eruption (e.g. Nielsen and Sigurdsson, 1981; Dugmore and Newton, 1992; Dugmore *et al.*, 1992; 1995). The results of many chemical analyses have formed part of *TephraBase* (Newton, 1996; Newton *et al.*, 2007), which provides an online database of tephra sample compositions. Results from several key systems are published, including results from the Snæfellsjökull volcanic system, which may be of particular relevance to this study.

In addition to the limitations outlined above, levels of tephra distribution can also be problematic, as tephra layers are not deposited throughout a fallout region (Dugmore *et al.*, 1996; Swindles *et al.*, 2010), meaning that tephra

analysis often has to be used in conjunction with other chronological techniques, such as ^{14}C dating. Issues regarding the reworking of tephra samples has also been raised in previous study, particularly when the samples are being extracted from peat sections (Payne and Gehrels, 2010; Swindles *et al.*, 2010).

A more problematic issue with the employment of tephra analysis is the potential post-depositional chemical alteration of the sample (e.g. Pollard *et al.*, 2003; Swindles *et al.*, 2010). Several studies have highlighted that this is more of an issue for basaltic tephra samples (e.g. Pollard *et al.*, 2003), due to the decreased stability of basalts due to their lower silica content (Swindles *et al.*, 2010). The surrounding sediments play a key role in determining the stability and potential subsequent chemical alteration of tephra layers, with particularly acidic soils leading to decreased sample stability (Hodder *et al.*, 1991). In addition to the surrounding sediment, bacteria have the potential to alter the composition of a tephra sample (e.g. Thorseth *et al.*, 1995), although their effects are likely to be minimal in the sites studied as part of this research.

In relation to this study, the Saksunarvatn tephra will be particularly relevant, as it was deposited at ~ 10350 yrs BP (Rasmussen *et al.*, 2006) and has been found throughout Iceland and in particular in the northwest (e.g. Hjort *et al.*, 1985; Björck *et al.*, 1992; Ingólfsson *et al.*, 1995; Andrews *et al.*, 2002; Lloyd *et al.*, 2009). In addition to the Saksunarvatn tephra, deposits from the Snæfells volcanic system are also likely to be found in the sites presented within this study and there is also potential for tephra from Snæfellsjökull to be discovered.

2.6 Summary

This chapter has outlined the current state of knowledge regarding the RSL changes, glaciation and deglaciation of Iceland. Regional differences in the RSL record suggest that varying RSL histories occur around Iceland (Einarsson and Albertsson, 1988) with distinct differences between the SW (e.g. Ingólfsson *et al.*, 1995) and the NW (e.g. Hansom and Briggs, 1991; Lloyd *et al.*, 2009), as well as over relatively short distances, such as between Viðarhólmi (Gehrels *et al.*, 2006) and Bjarkarlundur (Lloyd *et al.*, 2009) in western Iceland. It is therefore apparent that further research is required in order to better constrain

the differences in the RSL records, alongside the investigation of associated causes.

The key limitation of this study is the resolution at which a RSL record can be established, which could be too low to highlight recent fluctuations in the RSL record. In order to address this issue, fossil cores from saltmarshes have been extracted to pick up these recent RSL changes. These samples can be analysed at a higher resolution than the isolation basin sediments if required thus allowing a more detailed record of more recent change to be established.

The next chapter aims to outline the location and provide descriptions of the sites studied in this research. The scale and climate of Iceland are discussed, alongside the major areas of Snæfellsnes investigated in this research, such as Thorsnes and Barar. In addition to this, the sites are outlined in terms of their location, elevation and coring patterns.

CHAPTER 3

Geographical Location and Site Descriptions

3.1 Introduction

This chapter outlines the location of this research, including an overview of Iceland, the Snæfellsnes peninsula and the locations of the isolation basin and saltmarsh sites. Section 3.2 provides information regarding the climate and setting of Iceland, including the geology and influences on the climate of the region. Section 3.3 provides an overview of the Snæfellsnes peninsula with Section 3.4 then providing detailed information on the isolation basin, saltmarsh and marine limit sites investigated in this study.

3.2 Regional Background

Iceland is situated in the mid North Atlantic between 63°23'N to 66°32'N and 13°30'W to 24°32'W (Einarsson, 1984). Iceland covers an area of 103,100 km² and its climate is greatly affected by the dominant oceanic currents. The North Atlantic and Irminger Currents bring relatively warm waters to the southern, western and northern coast of Iceland (Einarsson, 1984; Figure 2.4), meaning that the South tends to be warmer than the North. The North receives cold waters from the East Greenland and East Icelandic Currents, which leads to the establishment of temperature fronts between the warmer southern waters and cooler northern waters (Einarsson, 1984).

The climate of Iceland is also greatly affected by its position at the boundary between major air masses with warmer sub-tropical air from the South and cooler Arctic air from the North (Einarsson, 1984). This results in large pressure and weather variations around the island. This has been highlighted by the long term records from a weather station in Stykkishólmur providing data since 1845 (Einarsson, 1984). Tide gauge data is also collected in Stykkishólmur, which will be useful for use in this study. The climate of the island is described as cold oceanic, being assigned the Cfc band of the Köppen Classification System.

The warmest month in Iceland is July, with an average maximum temperature of 13.6°C and an average minimum of 8.5°C in Stykkishólmur.

3.3 The Snæfellsnes Peninsula

The Snæfellsnes peninsula is situated in western Iceland, approximately 50 km south of Vestfirðir, the focus of previous RSL research. The peninsula is dominated by the Snæfellsjökull volcanic system, which is situated to the extreme west of the peninsula. There are five main centres of population in Snæfellsnes: Rif, Hellisandur, Ólafsvik, Grundarfjörður and Stykkishólmur (Figure 3.1). In this study, the peninsula is divided into three key areas:

1. *Outer Snæfellsnes*: This part of Snæfellsnes is dominated by Snæfellsjökull, a large volcano situated to the extreme west of the Snæfellsnes peninsula, which has had a profound effect on the geology of the region, with lava flows evident throughout the surrounding area. The volcanic system has also deposited various tephras around the peninsula (Steinþórsson, 1983), which will can be used as chronological markers in palaeoenvironmental studies.
2. *Mid Snæfellsnes*: This area includes the extinct volcanic system called Setberg on the northern coast of Snæfellsnes. In this study, it will be referred to as Barar, in order to avoid confusion with the marine limit site closer to Stykkishólmur. Barar is also the location of one of the marine limit points generated by this study. In addition, two possible isolation basin sites are also located in the area, although these were not sampled for further diatomological analyses.
3. *Inner Snæfellsnes*: This is a small peninsula on the northern coast of Snæfellsnes, at the northernmost point of which Stykkishólmur is located. The Thorsnes peninsula will be the main focus of this research, as it is the location of the majority of the isolation basin sites. The Setbergsa marine limit point is also in close proximity to these isolation basin sites.

The Snæfellsnes peninsula is a key location for climate research, due to the long term temperature record from Stykkishólmur, in addition to studies regarding species growing conditions. The peninsula has not however been a site for sea-level study over the Holocene. .

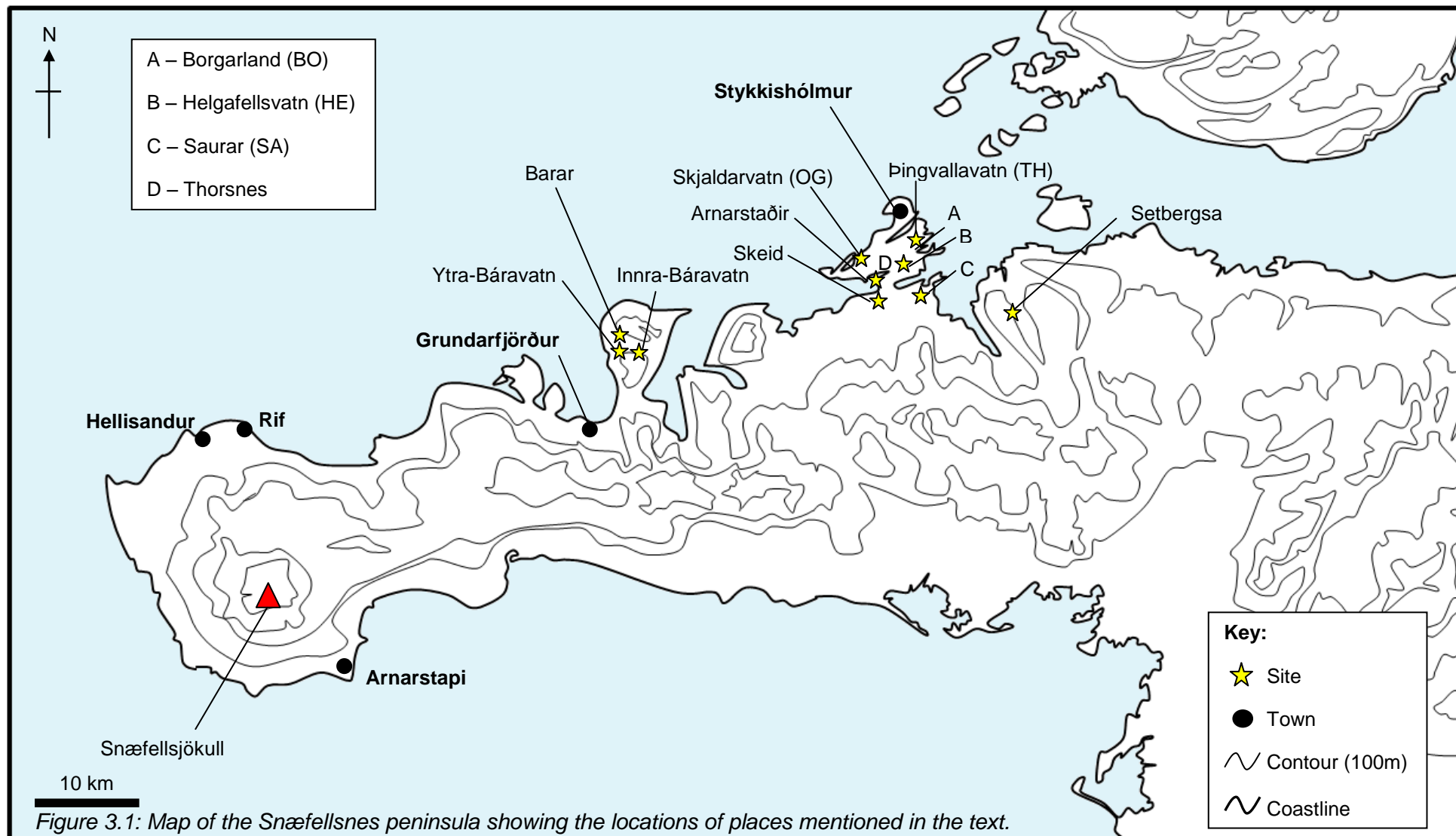


Figure 3.1: Map of the Snæfellsnes peninsula showing the locations of places mentioned in the text.

3.4 Study Sites

A total of 11 sites were investigated as part of this research, with samples for further analyses being taken from six of the investigated sites. The sites range from tidal inlet and saltmarsh to isolation basins and were chosen using the criteria outlined in the Methods Chapter and due to their relative proximity to one another. This close spacing allowed the effects of differential isostatic rebound to be minimised as much as possible. The saltmarsh and isolation basin sites were all located on the Thorsnes peninsula (Figure 3.1 and 3.2), with the marine limit sites at Barar and Setbergsa (Figure 3.1).

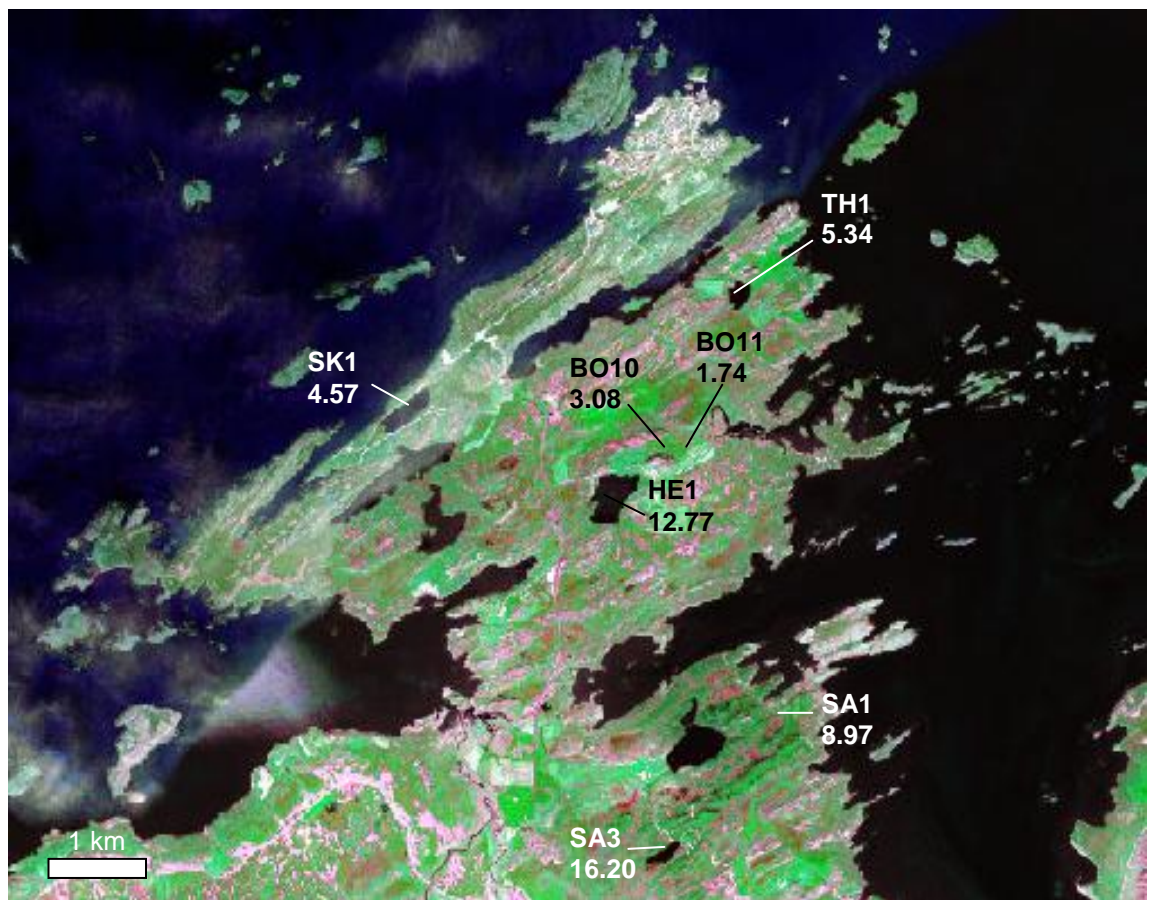


Figure 3.2: Overview of the isolation basin and saltmarsh sites investigated on the Thorsnes peninsula. The sill height is recorded for each isolation basin site in metres above Mean Sea Level (MSL) and the core elevation is recorded for the Borgarland marsh samples (m asl.).

3.4.1 Borgarland (BO10 and BO11)

Sample Elevation: BO10 3.08 m asl., BO11 1.74 m asl.

Site Grid Reference: 65°2'40.78"N 22°43'35.51"W

The Borgarland marsh sites (BO10 and BO11) are situated approximately 2.75 km south of Stykkishólmur (Figure 3.1). The site was initially cored along a transect running from Helgafell to the marsh creek using a gouge corer. Fossil samples were retrieved for analysis using a Russian corer at higher elevations, with contemporary samples being removed from the upper, mid- and lower marsh. The site had recently been artificially drained, with a fresh drainage channel being excavated (Figure 3.3 and 3.4). The site is accessed along the same road as Þingvallavatn and the former tidal creek is still evident (Figure 3.5).

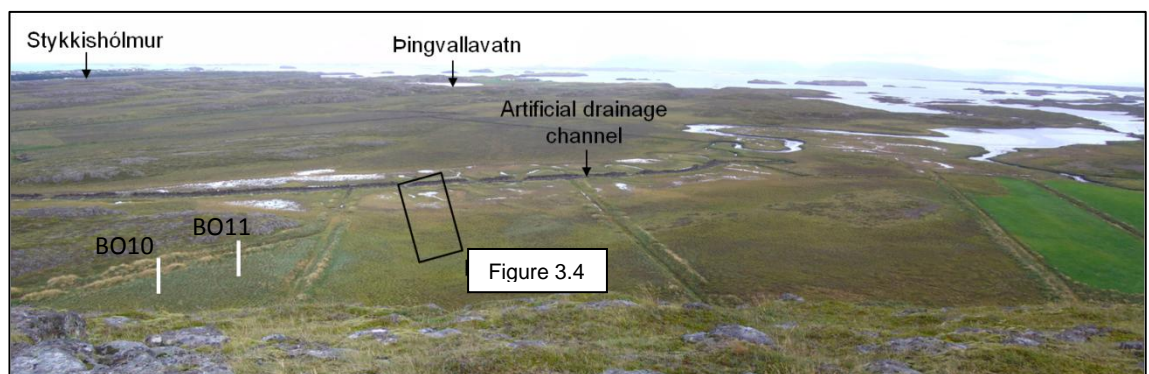


Figure 3.3: Overview of the Borgarland marsh site, showing the artificial drainage channel and coring pattern. A recent spring high tide has left some areas of the site flooded with surface water.

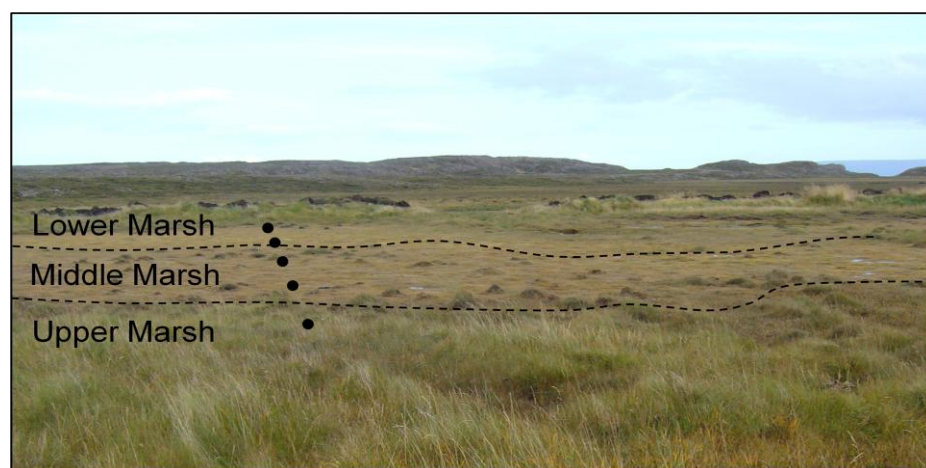


Figure 3.4: Contemporary sample collection pattern at Borgarland Marsh.

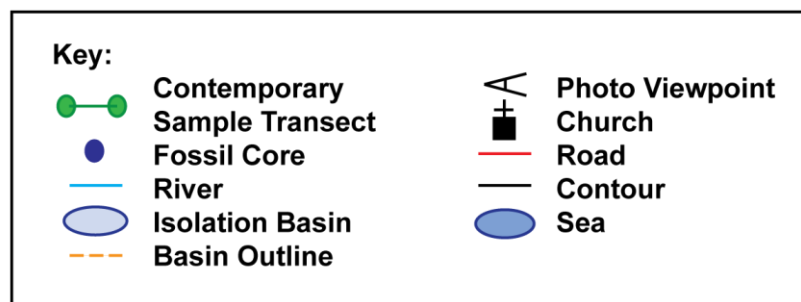
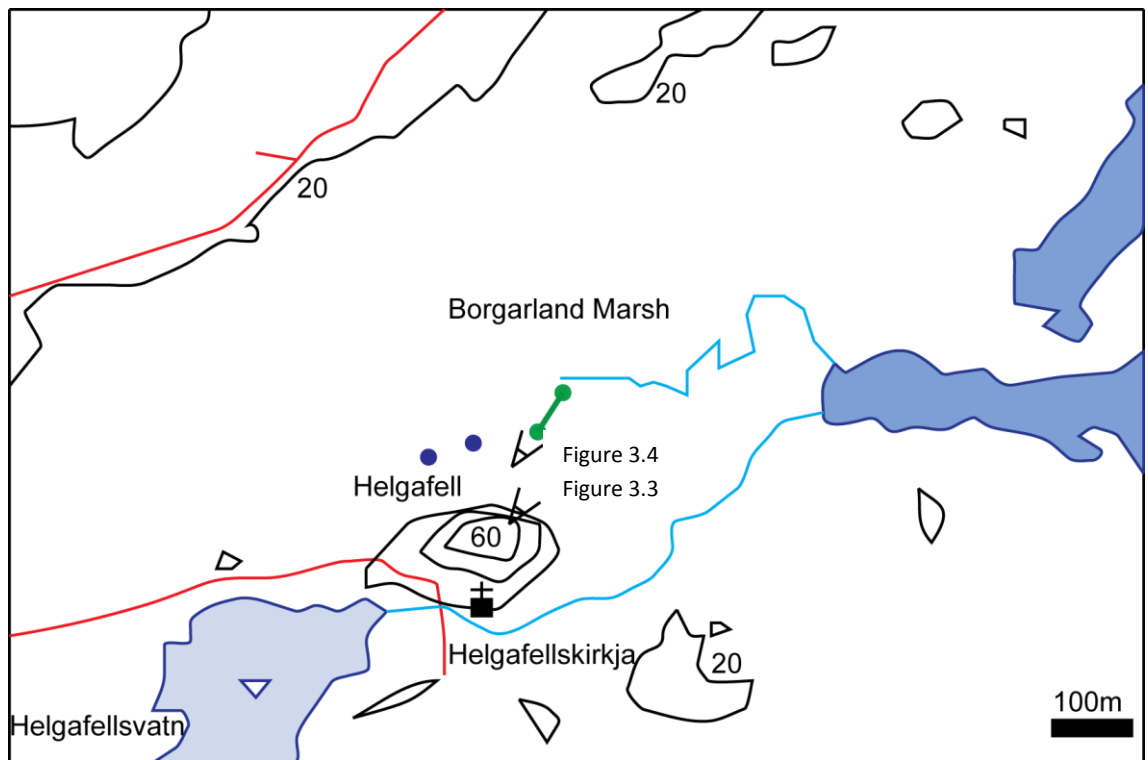


Figure 3.5: Coring pattern and location of Borgarland Marsh. The figure outlines the locations of the fossil and contemporary samples taken from the site.

3.4.2 Skjaldarvatn (SK1)

Sill Height: 4.57 ± 0.3 m asl. Grid Reference: $65^{\circ}2'50.67''N$ $22^{\circ}47'11.35''W$

The Skjaldarvatn site is situated approximately 4 km south west of Stykkishólmur on the Thorsnes peninsula (Figures 3.1 and 3.2). The site is easily accessed from the road leading to the Ögur farmstead, which crosses the drainage channel close to the basin sill. The basin is partly infilled towards the NE end of the basin (Figure 3.6). The site was cored at the centre point of the width of the lake, within the infilled section and as close to the lake edge as possible (Figure 3.6). One core sample was removed from the site for analysis (Core SK1-1). The sill location was located close to the present coastline. The sill location was easily identifiable, with a rock-floored drainage channel running from the basin to the sea (Figure 3.6). The sill height measurement was taken from the base of the exposed gravel in the bottom of the stream.

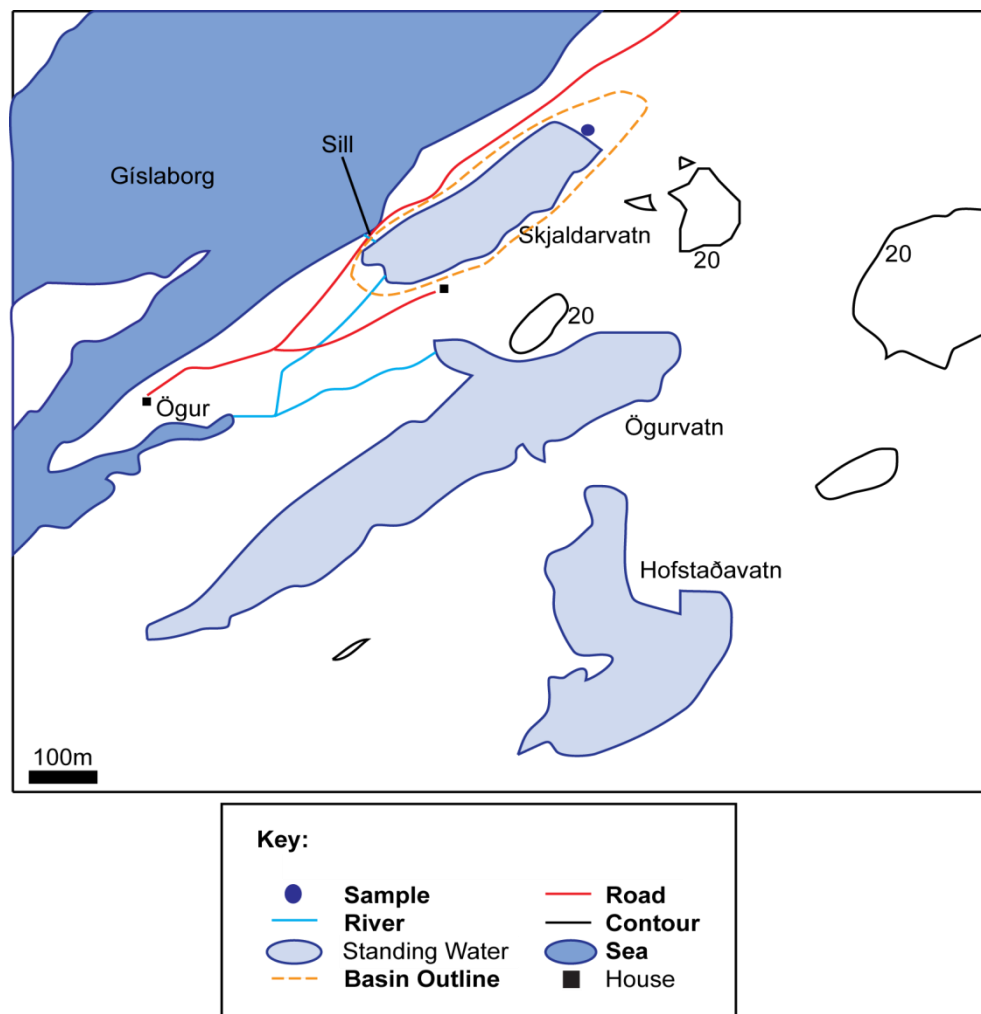


Figure 3.6: Coring pattern and location of the Skjaldarvatn isolation basin site.

3.4.3 Þingvallavatn (TH1)

Sill Height: 5.34 ± 0.3 m asl. Grid Reference: $65^{\circ}3'33.30''\text{N } 22^{\circ}42'43.16''\text{W}$

Þingvallavatn is situated approximately 1.6 km southeast of Stykkishólmur (Figure 3.1). The site is easily accessible from the road leading to the Þingvellir farmstead. The site sits in an area of low lying topography with occasional rocky outcrops, as shown in Figure 3.7. In order to establish site stratigraphy, a transect was initially cored on the southern edge of the lake basin using a Gouge Corer, with a second transect being cored within the lake itself (Figure 3.8). A core sample was retrieved from the centre of the lake for subsequent diatom analyses using the Russian Corer.

Two possible sill locations were identified through an analysis of the basin morphology, which were subsequently cored (Figure 3.9). One possible sill location was to the WNW and the other to the NE of the lake basin. Following the coring of the two possible locations, the sill was found to the WNW of the basin.



Figure 3.7: Þingvallavatn looking NNE from the SW corner of the lake basin, showing the basin morphology and boat setup.

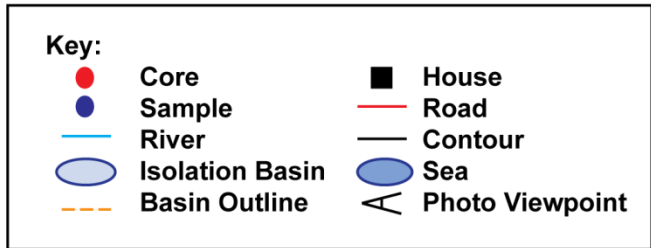
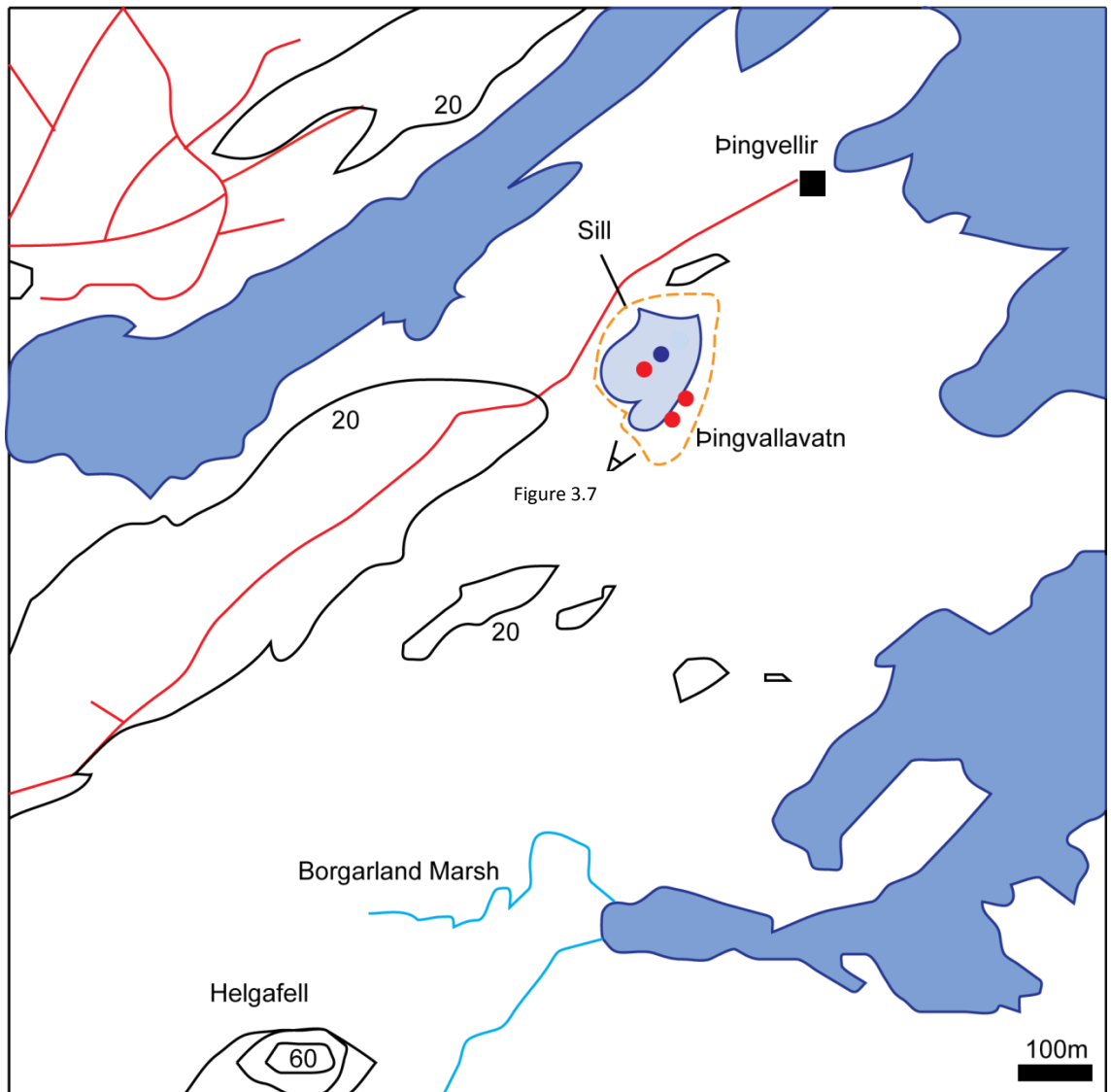


Figure 3.8: Location and coring pattern at Pingvallavatn, showing the location of cores retrieved from the edge and within the isolation basin.

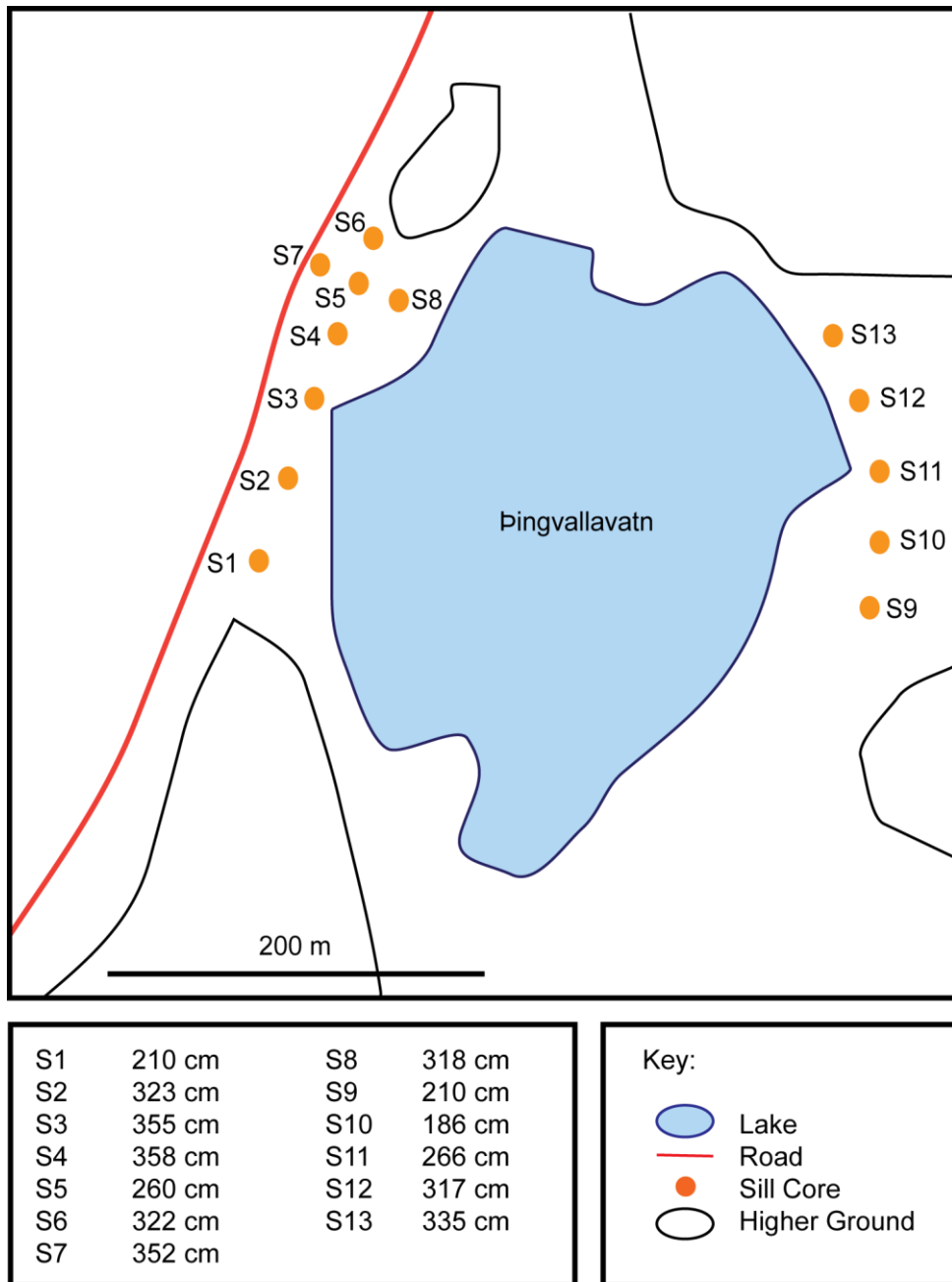


Figure 3.9: Determination of the sill at the Pingvallavatn site.

3.4.3 Saurar 1 (SA1)

Sill Height: 8.97 ± 0.3 m asl. Grid Reference: $65^{\circ}1'4.53''N$ $22^{\circ}41'47.11''W$

Saurar 1 is situated approximately 7.5 km south of Stykkishólmur in northern Snæfellsnes (Figures 3.1 and 3.2). The basin is located in an area of undulating, low lying topography, which has been planted to create an extensive birch forest. A forest road crosses the basin (Figure 3.10) and leads to Saurar 2 basin, which is discussed later. The surface of Saurar 1 gradually slopes NE towards the sea, which aided in the identification of the basin sill at its NE end. An outlet stream is visible at the ground surface close to the basin sill (Figure 3.10), although this runs underground for the majority of its course to the sea. The basin was initially cored in transects along and across the basin (Figures 3.10, 3.11 and 3.12) using a Gouge Corer, with a sample for analysis being retrieved from the centre point of the two transects using a Russian Corer (Figure 3.12). The basin sill was identified through the coring of a further set of transects using the Gouge Corer (Figure 3.13) and can be seen to the left of Figure 3.10. The d-GPS measurement for MSL control of the sill elevation point was taken from a tidal inlet approximately 200m north of the basin sill.

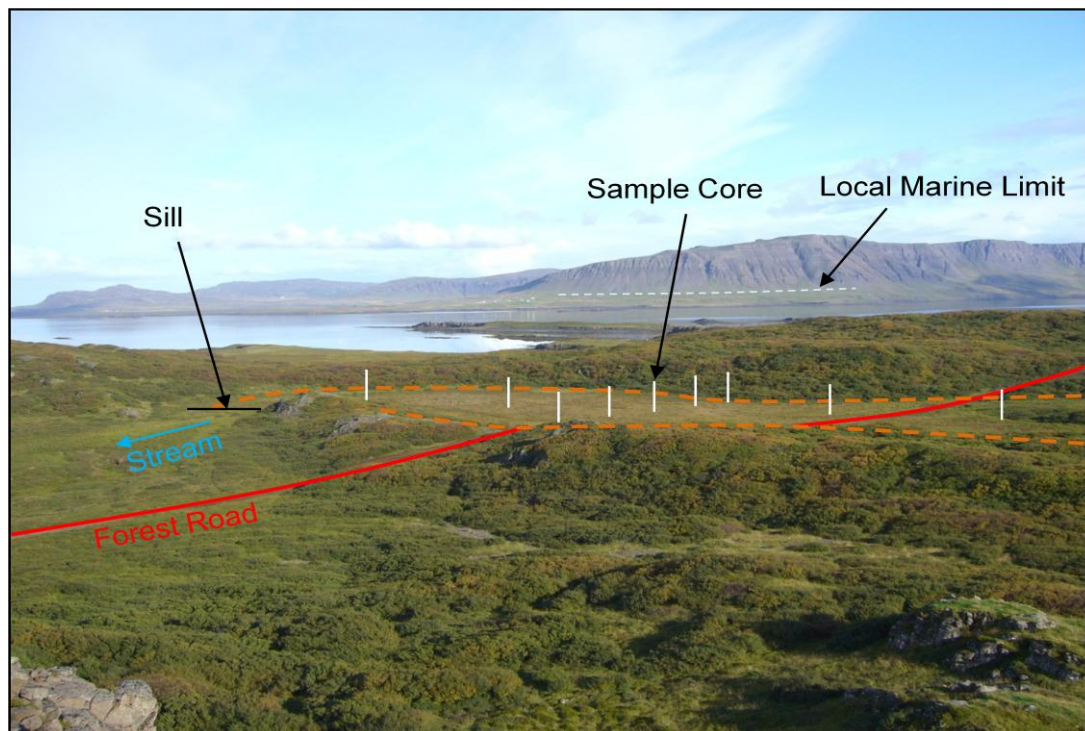


Figure 3.10: View east from the d-GPS base station of Saurar 1 basin showing the coring pattern, sill and extent of the basin.

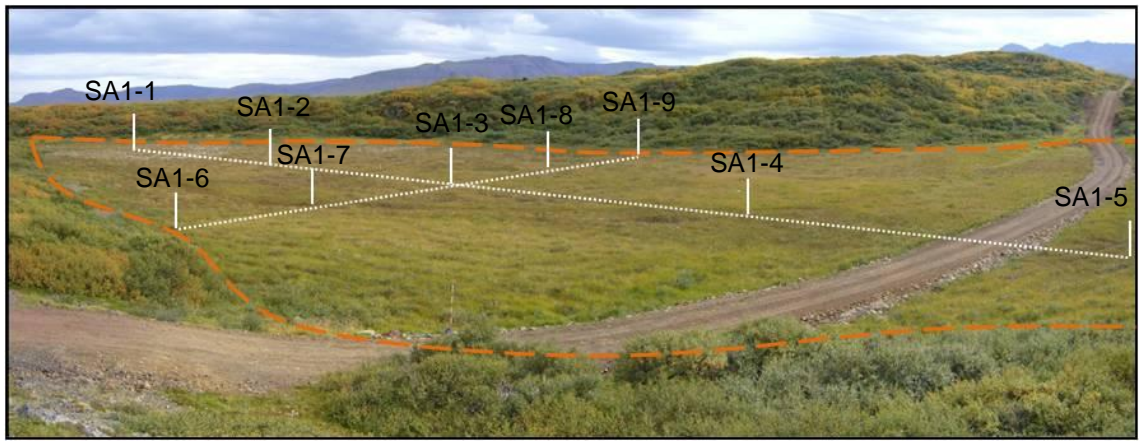


Figure 3.11: View south east from the most northwest margin of the basin, showing the area cored and the forest road, as well as the coring pattern.

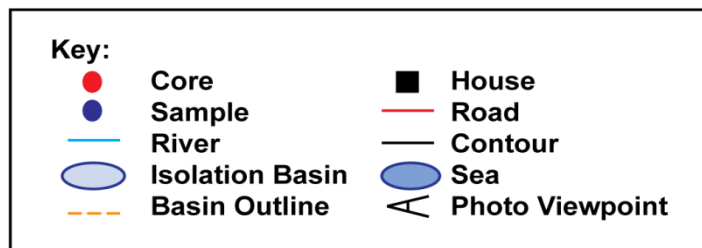
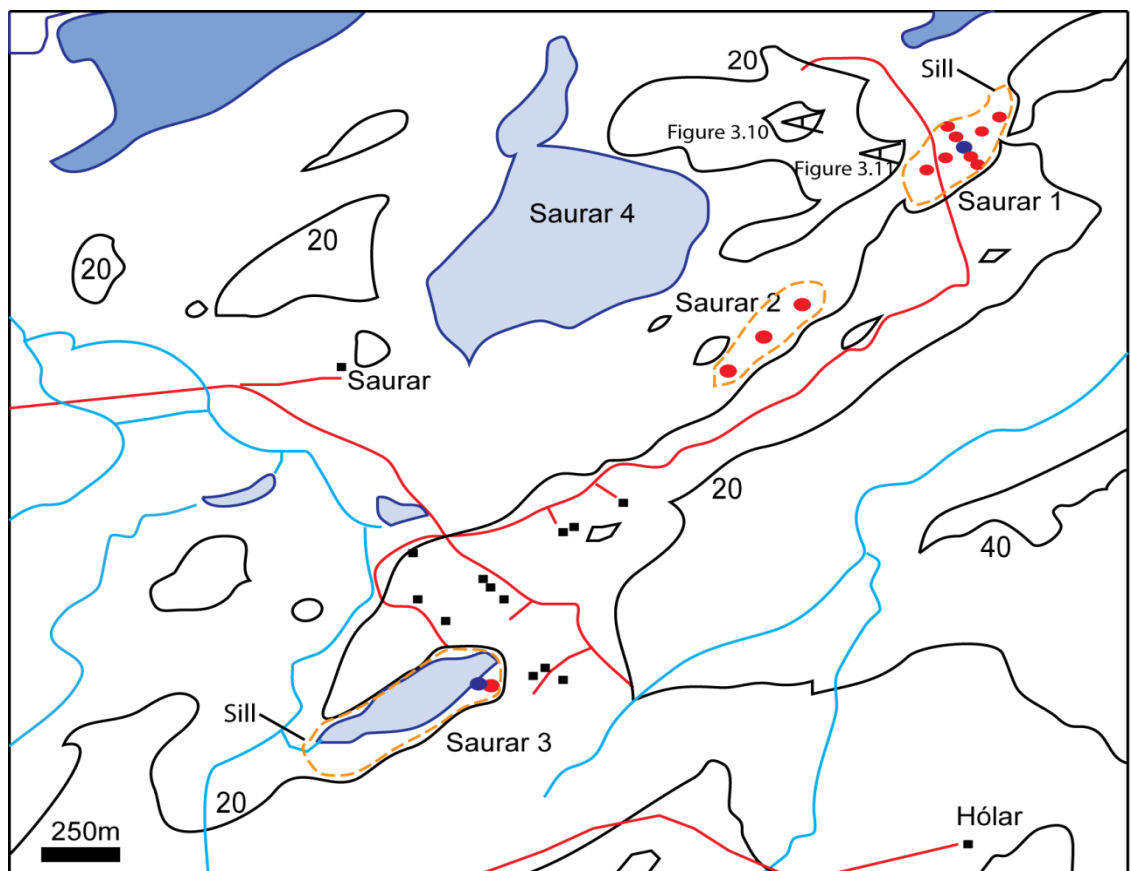
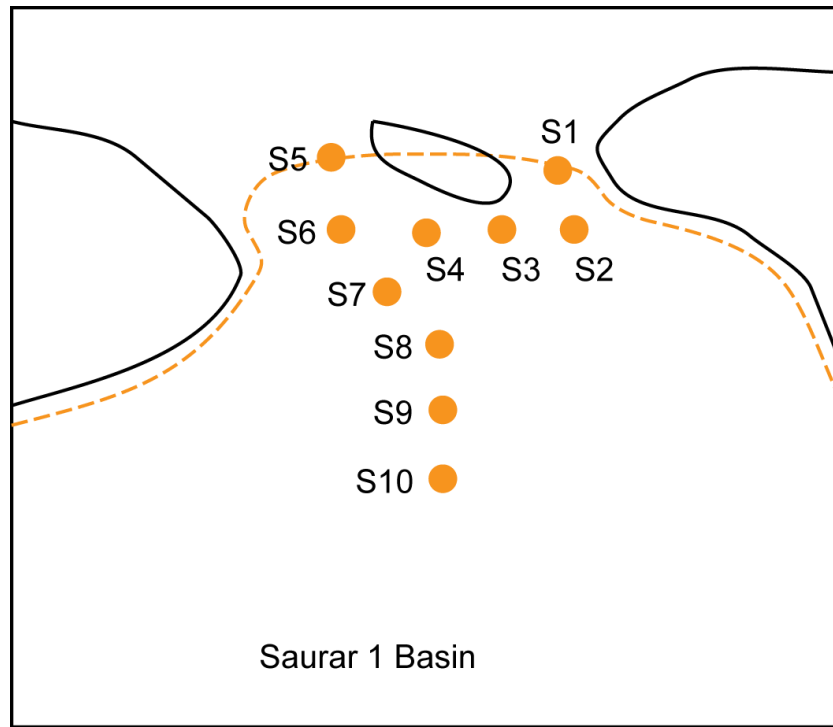


Figure 3.12: Map showing the locations and coring patterns of the Saurar basins (Saurar 1-4).



S1	272 cm	S6	67 cm
S2	288 cm	S7	229 cm
S3	282 cm	S8	257 cm
S4	170 cm	S9	264 cm
S5	0 cm	S10	290 cm

Figure 3.13: Determination of the sill location at the Saurar 1 site.

3.4.4 Helgafellsvatn (HE1)

Sill Height: 12.77 ± 0.3 m asl. Grid Reference: 65°2'18.87"N 22°44'23.25"W

Helgafellsvatn is situated 3.2 km due south of Stykkishólmur on the Thorsnes peninsula (Figure 3.1). The basin is partly infilled (Figures 3.14, 3.15 and 3.16), with the infilled section being artificially drained into a natural drainage channel which runs past the church. The area is surrounded by generally low-lying, undulating topography, with higher areas surrounding the lake, particularly to the north, such as the route of the access road (Figure 3.15). The dominant morphological feature at the site is Helgafell, which is 64 m high and is located to the northeast of the basin. The site was accessed down a steep embankment close to the Helgafell car park. The site was cored in a single transect close to the lake edge within the infilled section of the basin (Figures 3.14, 3.15 and 3.16), providing a representative depiction of site stratigraphy. A sample for analysis was extracted using the Russian Corer at Point 4 of the transect (Core HE1-4) (Figure 3.14). The basin sill was located close to the church, following the coring of a further transect (Figure 3.17). The likely location of the sill was determined through an examination of basin morphology and the location of the drainage channel. The d-GPS measurement for sill height was conducted using a base station on the summit of Helgafell itself.



Figure 3.14: View SE from the northwestern point of Helgafellsvatn, showing the proximity of the core samples to the edge of the isolation basin within the infilled section.

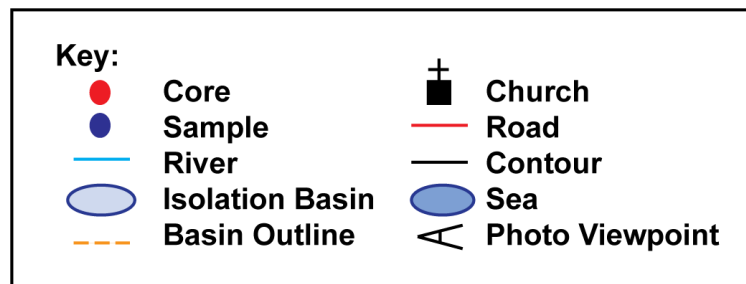
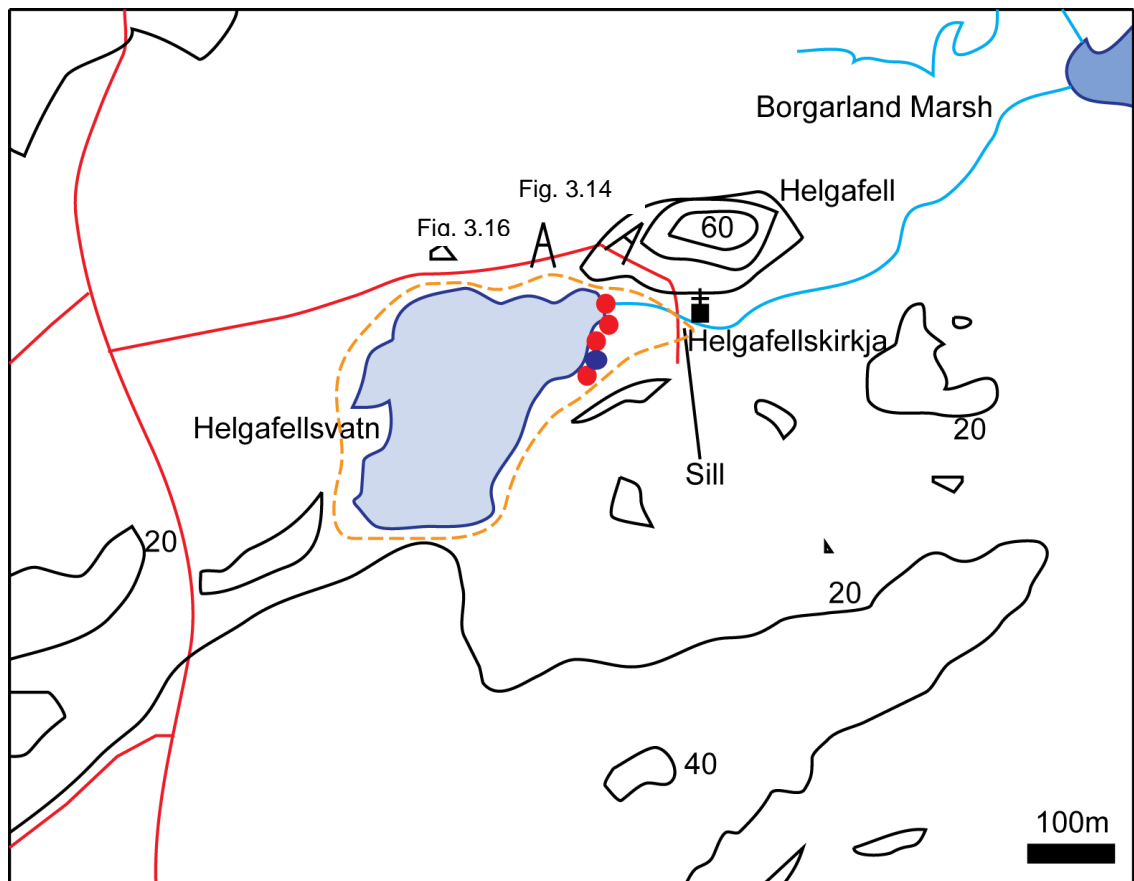


Figure 3.15: Map showing the location of the Helgafellsvatn basin, alongside the coring pattern and sill location.

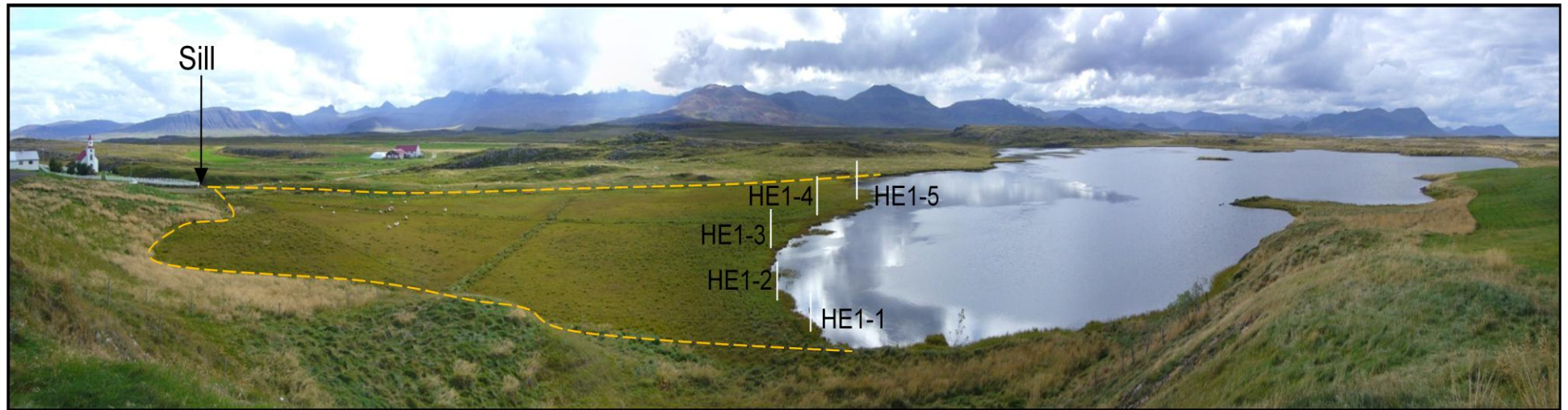


Figure 3.16: View of Helgafellsvatn looking south, showing the infilled section of the basin and Helgafellsvatn itself. The sill can be seen to the extreme left of the photograph, with the core locations also evident.

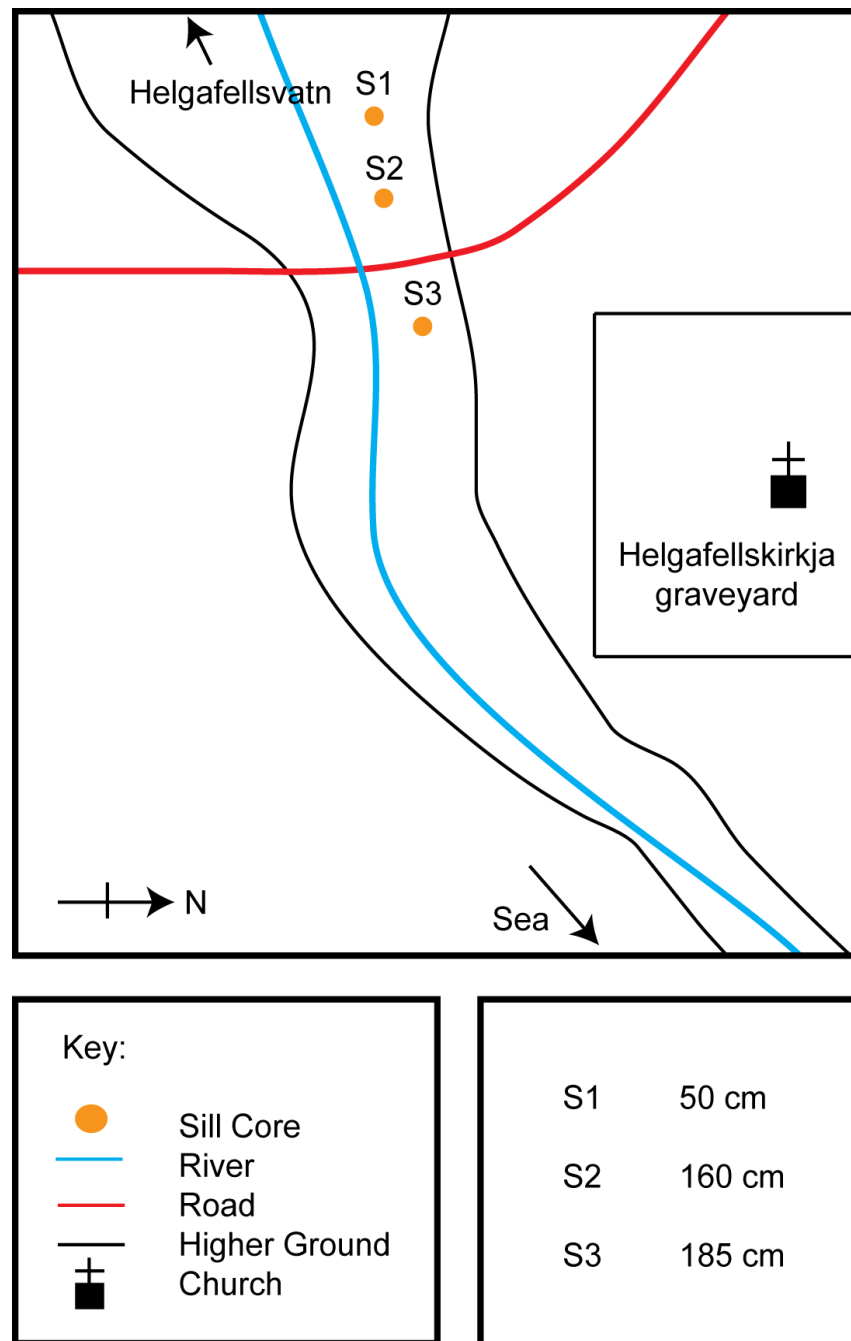


Figure 3.17: Determination of the sill location for the Helgafellsvatn site.

3.4.5 Saurar 3 (SA3)

Sill Height: 16.20 ± 0.3 m asl. Grid Reference: $65^{\circ}0'18.79''N$ $22^{\circ}43'6.19''W$

Saurar 3 is situated along a subsidiary track in the same forested area as Saurar 1, south of Stykkishólmur (Figure 3.12). The site is easily accessed along these subsidiary tracks, due to recent housing developments in the area. The area is generally low lying, with embankments surrounding the lake to the north, east and south. The basin is covered with low lying vegetation. The site

was initially cored using a Gouge Corer along a transect of two points running from the east side of the basin to the lake edge (Figure 3.12). A core sample for analysis was retrieved using the Livingstone Corer at Point 3 (Core SA3-2). The sill location was easily identified due to the nature of the basin morphology, with a relatively low area to the western side of the basin, through which an outlet stream was evident. This area was cored using a Gouge Corer along a series of transects in order to establish the exact sill location (Figure 3.18).

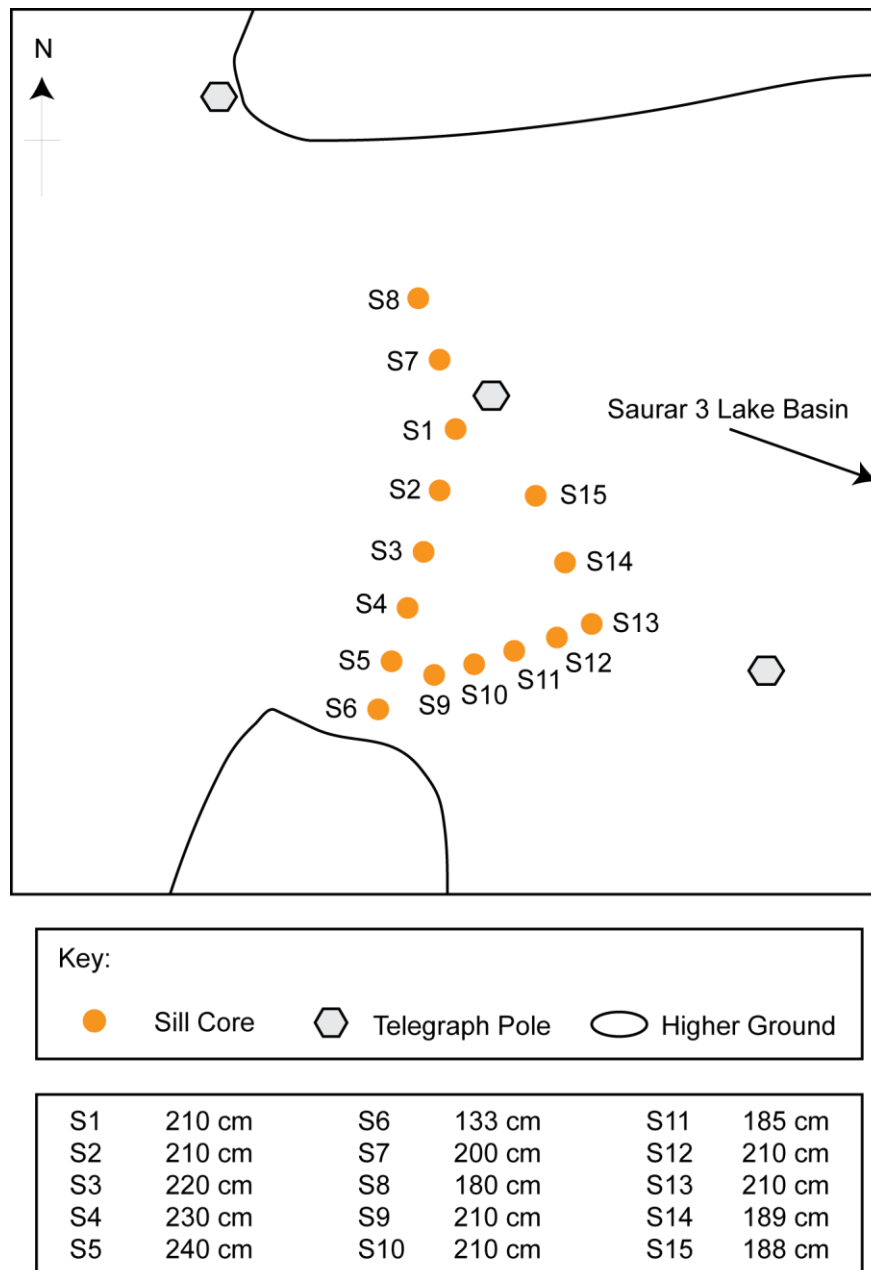


Figure 3.18: Determination of the sill location at the Saurar 3 site.

3.4.6 Setbergsa

Marine Limit Height: 62.84 ± 0.25 m asl.

Grid Reference: 65°0'6.17"N 22°33'15.85"W

The Setbergsa marine limit point was taken within the valley close to the Setbergsa farmstead (Figures 3.1, 3.19 and 3.20) approximately 11 km SE of Stykkishólmur. The marine limit point in this valley was chosen due to its proximity to the isolation basin sites investigated on the Thorsnes peninsula, thus limiting the effects of differential isostatic rebound on the RSL record. The base station was set up on a marine terrace at the mouth of the valley, with a control point taken at Ös (Figure 3.20). The marine limit is easily identifiable in the area, forming a reasonably continuous beach platform (Figure 3.19), aiding in the measurement of the marine limit.



Figure 3.19: View south west from the base station location at Setbergsa, showing the local marine limit and marine terraces.

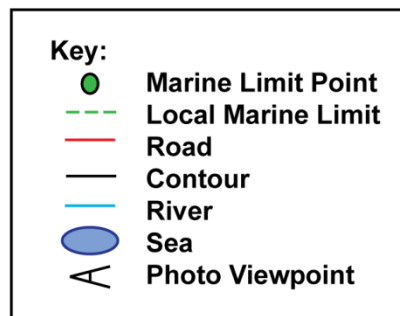
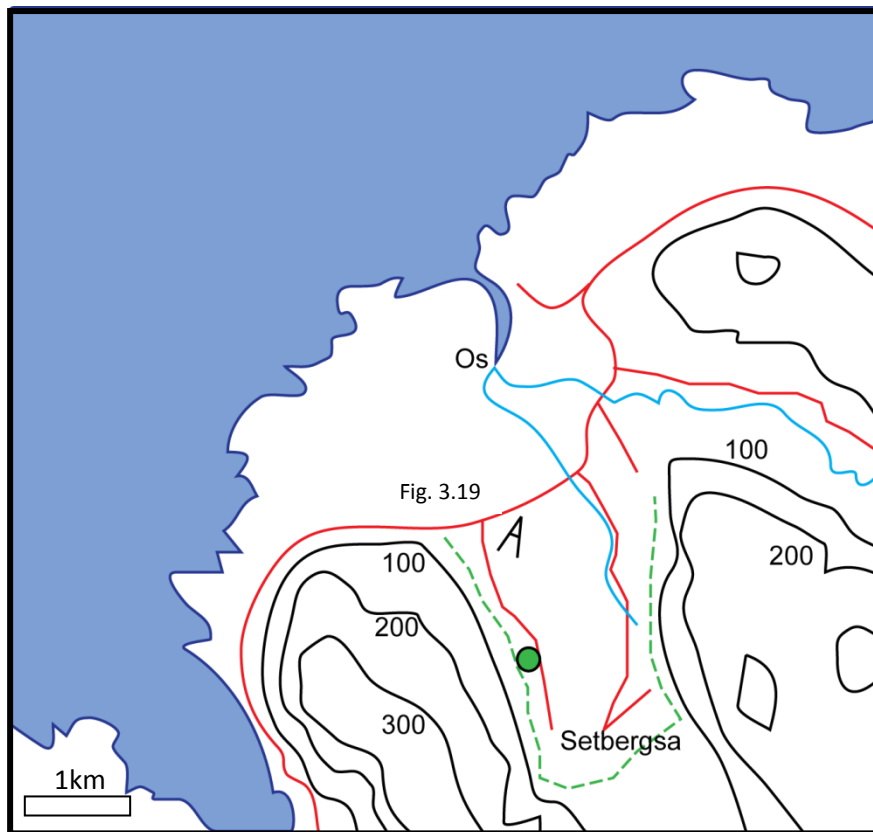


Figure 3.20: Map of the Setbergsa site showing the location of the marine limit measurement and the outline of the local marine limit within the surveyed valley.

3.4.7 Barar

Marine Limit Height: 68.87 ± 0.35 m asl.

Grid Reference: 64°59'20.25"N 23°11'39.09"W

The Barar marine limit measurement was taken close to Ytra-Báravatn (Figure 3.1 and 3.21). The site is accessed up a steep embankment of a marine terrace, with vehicular access being difficult. The marine limit measurement was taken close to the mouth of a large valley, which runs between two areas of high ground and is where the Ytra- and Innra-Báravatn lakes are situated (Figures 3.21 and 3.22). The marine limit was easily identifiable at this site (Figure 3.21), forming a continuous cobble platform. The basestation was set up at the centre point of the valley width, close to the waterfall which runs from Ytra-Báravatn (Figure 3.21). The d-GPS control point was taken at the coast close to the Barsker farmstead. The Barar site forms a high point for postglacial RSL in this study, being the highest RSL measurement recorded during the research.



Figure 3.21: View north from the base station location showing the clear marine limit at Barar.

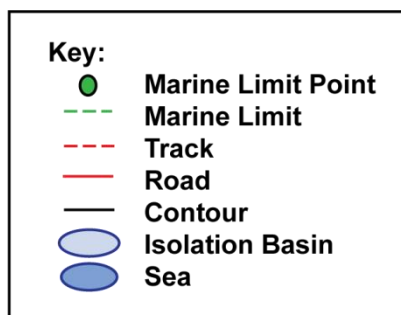
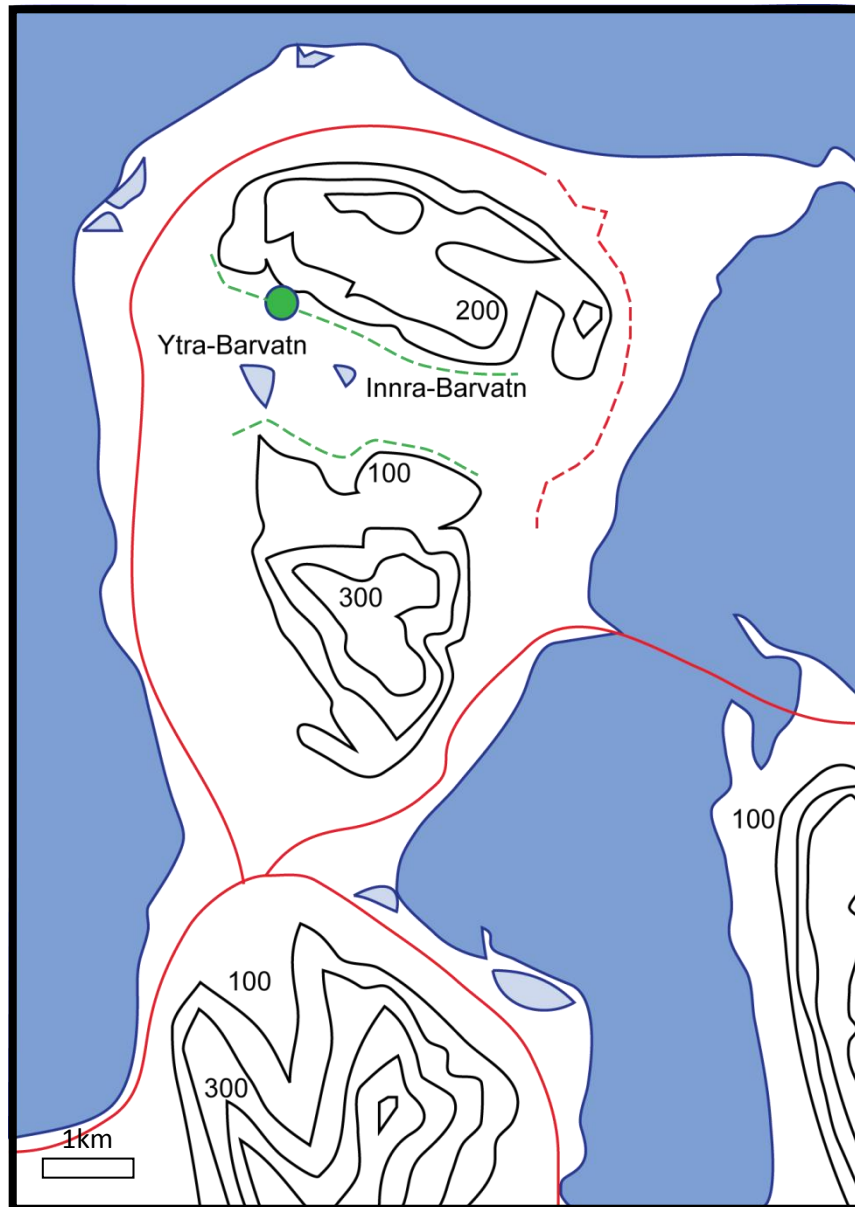


Figure 3.22: Map of the Barar area, showing the location of the Barar marine limit measurement and the isolation basins on the peninsula, which were deemed unsuitable for use in this study.

3.4.8 *Other Isolation Basin and Tidal Inlet Sites*

In addition to the aforementioned sites, several other locations were investigated during the course of the fieldwork, the approximate elevations and grid references for which can be found in Table 3.1.

Saurar 2 (Figure 3.12) was accessed along the same forest road as Saurar 1, although the transect of cores undertaken at the site did not reveal any material which would have been suitable for further analysis. Saurar 4 was also considered for investigation (Figure 3.12), although the site was rejected for use in this study due to difficulties surrounding access, the size of the lake basin and the similarity of altitudes to other nearby sites.

Ytra-Bárvatn (Figure 3.23) and Innra-Bárvatn (Figure 3.24), close to the marine limit site at Barar (Figure 3.1), were also considered for investigation. Initial investigations revealed that the bottoms of the lake basins appeared to be covered in gravel and as such it was uncertain whether suitable samples for analysis would be retrieved. In addition to this, access to the sites was relatively difficult due to steep embankments lower down the hillside. Finally, the two sites were not cored due to the distance between them and the other isolation basin sites used in this study, despite them being relatively high within our framework of sill heights. This decision was made to minimise the effects of differential isostatic rebound, which can have a great effect on the results generated by RSL studies. The sites would have provided an accurate control for RSL at a higher point within the framework of RSL, as the isolation basin sites studied here in greater detail are all at relatively low points. However, the distance between these sites and those on the Thorsnes peninsula (Figure 3.1) is too great to ensure that isostatic gradients are minimised.



Figure 3.23: View of Innra-Bárvatn looking east at the lake and marine limit.



Figure 3.24: Ytra-Bárvatn looking north, showing site proximity to the local marine limit.

In order to determine a RSL point close to present day sea level, the tidal inlet at Arnarstaðir (Figure 3.1 and 3.25) was also cored to determine basin stratigraphy. Two cores were extracted using the Russian Corer, but these failed to provide any organic sediments. The cores were comprised entirely of sands and silts, which meant that the site was deemed unsuitable for further use in this study.



Figure 3.25: Arnarstaðir tidal inlet looking east from the westernmost point of the inlet showing basin morphology and the basin sill.

The final isolation basin study site considered but then rejected was Skeid (Figures 3.1 and 3.26). This study site was rejected due to a lack of suitable material for analysis. The site was situated in a low-lying area, with a well defined sill. The three cores extracted from the site revealed organic material deposited onto the underlying gravel and failed to show a transition which would correspond with a RSL signal.



Figure 3.26: Skeid basin facing east showing the basin morphology and likely sill location.

The elevations of the additional sites not surveyed as part of this study can be found in Table 3.1 below. This table shows the possible breadth of data points from the Snæfellsnes region.

Site Name	Estimated Elevation (m asl)	Grid Reference
<i>Saurar 2</i>	11	65°0'52.28"N 22°42'27.23"W
<i>Saurar 4</i>	9	65°1'2.75"N 22°43'7.22"W
<i>Upper Bararvatn</i>	64	64°59'7.43"N 23°10'42.28"W
<i>Lower Bararvatn</i>	50	64°59'2.97"N 23°11'39.34"W
<i>Skeid</i>	39	65°0'25.99"N 22°47'30.71"W
<i>Arnarstaðir</i>	<0	65°1'47.98"N 22°46'6.59"W

Table 3.1: Summary table showing the approximate elevation and grid references for the additional sites not sampled in this study.

3.5 Summary

This chapter has provided an overview of the locations studied and investigated as part of this research. The study sites, alongside potential additional sites for future research have been outlined, in addition to those sites which were deemed unsuitable for use in this study. The next chapter aims to outline the key methods employed at these sites in order to reach the research aim.

CHAPTER 4

Methods

4.1 Introduction

This chapter outlines the principal methods employed to provide the necessary data to meet the research objectives and answer the research questions outlined in the introductory chapters of this thesis. The chapter is divided into three key areas: methods employed in the field, laboratory techniques and analytical methods. The chapter aims to provide an overview of the key techniques, outline any potential issues associated with them and to justify the approach adopted in this research. The chapter involves discussion of the methods of site selection, surveying, coring, microfossil and chronological analyses. Furthermore, discussion of radiocarbon age calibration and elevation correction is undertaken to provide an insight into the analytical techniques employed in this research.

4.2 Field Methods

Fieldwork was undertaken between the 6th and 15th September 2010, with a base initially at Arnarstapi and subsequently at Stykkishólmur, Snæfellsnes, western Iceland (Figure 3.1). Potential sites were initially identified through the analysis of satellite imagery of the study area, prior to arrival in Iceland. Potential sites were identified in several locations around the peninsula, principally in Setberg, Thorsnes and southern Snæfellsnes (Figure 3.1). These potential sites were subsequently visited in the field, at the beginning of the fieldwork period, in order to assess their suitability for use within this study. The main criteria employed in the assessment of site suitability were:

1. *Site Elevation*: In order to produce an accurate and comprehensive record of RSL change, a range of isolation basin sill elevations were sought. This spread of sill elevations allows a series of RSL points to be generated throughout the frame of potential postglacial RSL change. As

a result, rather than sampling several basins at similar elevations, sites at differing elevations were actively sought thus producing spread in the data points. This resulted in the coring of isolation basins, saltmarsh and estuary sites, which have been a beneficial combination in previous studies (e.g. Selby and Smith, 2007).

2. *Lake Depth:* The depth of the lake was also taken into consideration when selecting sites. Shallow lakes often suffer from poor sediment preservation (Smith *et al.*, 2005) or sediment infilling (Long *et al.*, 2011) producing samples unsuitable for diatom or other microfossil analyses. Poor sediment preservation has been noted in research in sub-polar environments, where lake ice can disturb underlying sediment and therefore the record of palaeoenvironmental change. Deep lakes also pose problems in terms of paleoenvironmental reconstruction, as sediments can become easily reworked (Smith *et al.*, 2005), thus disturbing the preserved record of paleoenvironmental and in turn RSL change. In addition, large basins can contain trapped layers of saline water, thus providing an inaccurate depiction of RSL changes (Long *et al.*, 2011). To minimise such issues, basins with a maximum depth of ~ 10 m are frequently used (Long *et al.*, 2011).
3. *Post-isolation alteration:* Sites which have experienced changes following their isolation, such as artificial bank creation, were avoided where possible, due to the possible effects on the RSL record.
4. *Sill identification:* The ability to identify an impervious bason sill was also taken into consideration when determining the suitability of an isolation basin for use in this study. The impervious rock sill allows an accurate record of RSL change to be preserved (Lloyd and Evans, 2002). Sites with sand and gravel sills were avoided, due to the possibility of post-depositional alteration to the lake sediments and thus to the RSL record.
5. *Practicality of sampling:* The practicality of retrieving suitable samples for analysis was also taken into consideration when selecting sites for use in this study. Saurar 4, for example, was relatively difficult to access and the size of the lake made using the boat impractical. Unfortunately, the scale of some of the lakes surveyed was simply too large to allow this to happen. As a result, the decision was taken, on the grounds of safety and practicality, not to sample these sites.

6. *Spacing of sites:* In order to minimise the effects of differential isostatic rebound on the RSL record produced in this research, the decision was taken to focus on the Thorsnes peninsula, which offered a number of potential isolation basin sites in close proximity to one another. Although the peninsula offered several isolation basin sites, the topography is not sufficiently high to allow a marine limit point to be taken from the peninsula. As a result, the Setbergsa site was chosen as it is within sufficient proximity to minimise differences in the isostatic gradient and at a sufficient altitude to record the high point in postglacial RSL.

Following the initial site visits, the Barar isolation basin sites were deemed to have lesser potential than the Thorsnes sites, with the sites in southern Snæfellsnes being rejected due to sand and gravel barriers being present and the lack of a spread of sill elevations. It was also uncertain whether these sites in southern Snæfellsnes had been altered by later action, such as road construction. In total, samples for diatom and chronological analyses were retrieved from five lake sites and one saltmarsh, as outlined in the previous chapter, which led to the analysis of 106 diatom slides.

4.2.1 Stratigraphy Determination and Core Retrieval

Following the identification of sites suitable for analysis, site stratigraphies were determined through the coring of transects, where possible, using a gouge corer. The transects cored are summarised in the site descriptions associated with each isolation basin and saltmarsh site. Where the coring of transects was not possible, samples were retrieved from the centre point of the width of the basin or saltmarsh, thus providing a sample as representative of the site as possible. Core samples extracted from the centre of the isolation basins are most likely to preserve the longest record of environmental change, as this is likely to be the deepest part of the lake basin. Upon retrieval, each core was categorised in the field using the Trøels-Smith (1955) classification scheme, as well as being photographed.

For the majority of the lake basin sites, site stratigraphies were determined through the coring of infilled sections of the lake basins. Due to the difficulties associated with retrieving samples using a boat, it was preferable to retrieve

samples from these infilled basin sections whenever possible. The boat was however used to retrieve samples from the Þingvallavatn basin, as well as in the determination of the suitability of the Arnarstaðir tidal inlet for use in this study. When using the boat, a rope was tied across the isolation basin, allowing the boat to remain steady during the extraction of the core sample, thus ensuring that the record was extracted from the same point within the basin.

Following the establishment of site stratigraphy, representative samples were retrieved for analysis using either the Russian (Jowsey, 1966) or Livingstone Corer (Livingstone, 1955). The Russian Corer was used for samples predominantly made up of peats, clays and gyttjas. The corer allows 50 cm sections of sediment to be extracted (Jowsey, 1966), with the sections overlapping by 5 cm to ensure that the entire sediment sequence be preserved. As a result, when the Russian Corer was employed, the coring took place in two separate locations in close proximity to one another.

The Livingstone Corer was used at the Saurar 3 site, where the core was predominantly made up of lake sediments. The Livingstone Corer is designed for use in such lake sediment deposits and allows the extraction of 100 cm sections (Livingstone, 1955). Following their extraction, the samples were packed in plastic tubing and wrapped in plastic film, in order to preserve the sample as well as possible during transport back to Durham for further analyses.

4.2.2 Sill Determination

After having retrieved sediment cores for microfossil and chronological analyses, the sill height at each basin was established. This was conducted following an initial observation of basin morphology, which led to the identification of possible sill locations. The prospective sill locations were easily identified at the majority of sites, with Þingvallavatn being the exception, where two sill locations were proposed. The true sill location was confined by the detailed surveying of both candidate locations.

Where the sill was covered by sediments, the anticipated sill locations were cored in a grid of cores using a gouge corer, in order to establish the exact location of the sill, as summarised in Figure 4.1. The depths reached for each

point cored were recorded for each possible sill location thus providing an insight into sill morphology. The grids cored at each site in order to determine the sill locations are summarised within the site descriptions of the relevant locations in Chapter 3. The location of the sill at each site was recorded using differential GPS (d-GPS). Where the sill was clearly constrained by the drainage stream and found at ground level, such as at the Skjaldarvatn (SK1) and Helgafell (HE1) sites, the sill elevation was determined through a d-GPS surveying transect rather than the coring of the proposed sill location. The d-GPS are also summarised within the results section of each site, where appropriate.

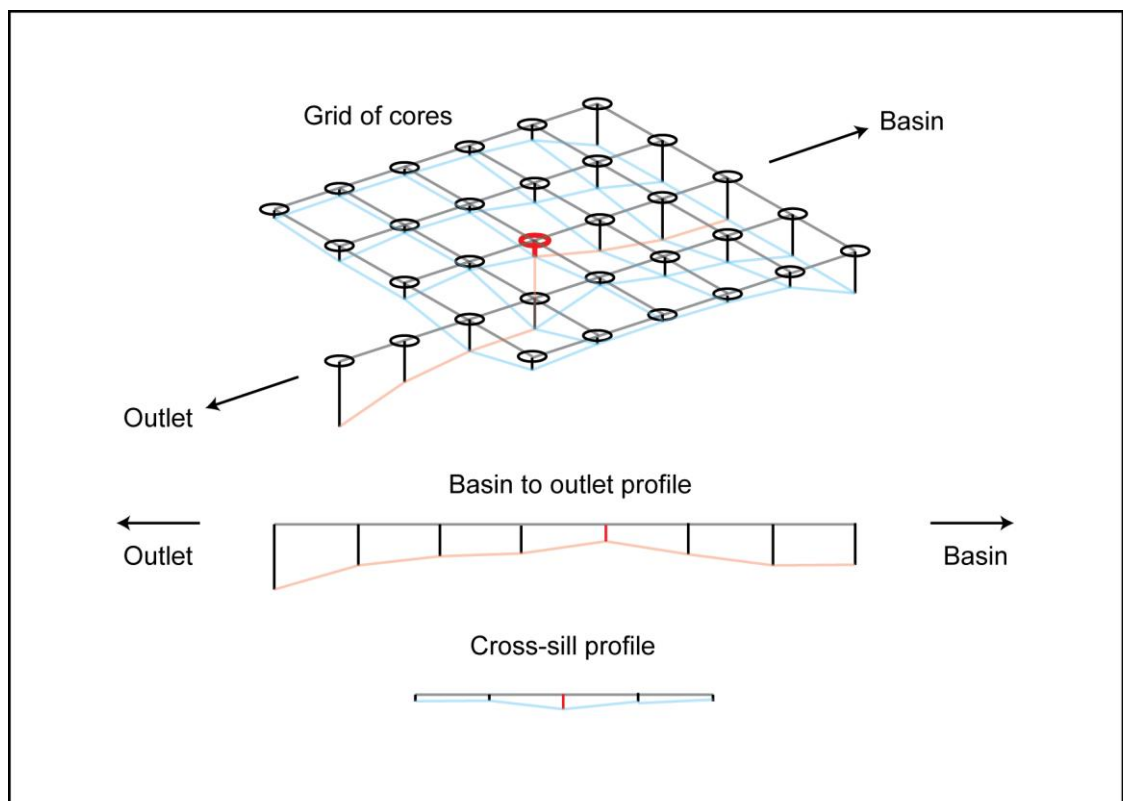


Figure 4.1: Schematic of the technique employed in the establishment of the sill location for each lake basin site. The black grid represents the ground surface, with each black circle representing a core in the grid. The blue grid represents the sill morphology, with the red core being the lowest point cored in the sill grid. The red line represents the proposed route of the former drainage channel. The cross sections demonstrate the position of the sill, being the deepest point at the highest part of the underlying bedrock.

4.2.3 Marine Limit Determination

Marine limit elevation measurements were taken at two sites in the field, which were identified whilst determining the suitability of the lake basin sites. The sites were within close proximity to the cored basin and saltmarsh locations, thus meaning that issues of differential postglacial rebound were minimised. The site at Barar is approximately 23 km to the WSW of Stykkishólmur, with the Setbergsa site approximately 11.3 km to the SE.

The marine limit was defined as the maximum elevation attained by the sea at a particular location (Andrews, 1970) and was identified using the four criteria outlined by Sim (1960):

1. The lowest elevation of ground moraine.
2. The lowest elevation of a hanging boulder.
3. The highest elevation of a beach ridge or delta.
4. The highest elevation at which marine shells or algae can be found.

In terms of the marine limits measured in Snæfellsnes, the third criterion was the most frequently used to identify the marine limit. As discussed in the previous chapter, marine ridges and terraces were apparent at both of the marine limit sites investigated in this study. Photographs of the marine limit sites can be found in Chapter 3, alongside the associated site descriptions.

4.2.4 GPS Measurements

Two sets of GPS measurements were taken in the field. Initially, core sites and sill locations were recorded using a handheld Garmin GPS. This allowed the sites to be relocated for more accurate differential GPS (d-GPS) measurements. D-GPS was used to determine accurate elevations for the retrieved cores and the sill locations using a temporary basestation on Helgafell and later on a rocky outcrop close to Saurar 1.

The elevations of cores and sill locations were recorded in relation to Mean High Water Spring Tide (MHWST) at coastal locations as near to the sample sites as possible (Figure 4.2). These elevations were then subsequently adjusted to account for sediment depth, tidal range and corrected to mean sea level, as discussed later.

For each site, there was uncertainty associated with the determination of sill elevation as a result of instrument error, incomplete stratigraphic investigations (Figure 4.1) or artificial sill lowering following isolation (Long *et al.*, 2011). As such, isolation basin sill elevations have been given an assumed error of ± 0.3 m to take these issues into consideration, even when the sill was visible at the ground surface. Marine limit measurements were given an error associated with the variability in the marine limit elevations at the two locations surveyed, which is representative following multiple measurements at the two sites.



Figure 4.2: View east from the westernmost point of the tidal inlet used to provide a relative height constraint for the Saurar 1 site, showing the Mean High Water Spring Tide (MHWST; blue line).

4.3 Laboratory Methods

4.3.1 Diatom Analysis

Previous studies have shown the effectiveness of microfossil analyses of isolation basin sediments in Iceland (e.g. Rundgren *et al.*, 1997; Lloyd *et al.*, 2009), which provide an accurate reconstruction of basin paleoenvironmental changes (Lowe and Walker, 1997). Diatom analyses provide important information concerning basin salinity, due to the rapid response of diatoms to changes in environmental conditions (Stoermer and Smol, 2001) and their strong depositional patterns (Freund *et al.*, 2004). An accurate record of basin salinity can then be related to marine inundations or isolations, thus allowing a series of former RSL changes to be reconstructed (Kjemperud, 1986) when coupled with information regarding tidal range and basin sill altitude. The impervious isolation basin sill ensures that an accurate record of RSL change is

preserved in the microfossil record (Lloyd and Evans, 2002) making it suitable for use in this study and elsewhere.

Diatom preparation followed the standard techniques outlined by Palmer and Abbott (1986) and Battarbee (1986). Initially, 0.5 cc of sample was placed into a polypropylene tube to which approximately 20 ml of hydrogen peroxide (H_2O_2) solution (20 vol.) was added to digest any organic material. It is necessary to remove as much organic material as possible at this stage in order to improve the quality of the final slide for microfossil identification purposes. These samples were covered in aluminium foil and placed in a water bath for approximately two hours to allow the digestion to take place. Using a water bath allowed a large number of samples to be prepared simultaneously (Renberg, 1990), usually in batches of 16 or 24. If the digestion was not completed after the initial two hour period, further hydrogen peroxide was added to the samples to allow further digestion over an additional one to two hour period. Following the completion of the organic digestion, distilled water was added to the sample solution until the total volume reached 35 ml. This solution was then centrifuged, decanted and again topped up with distilled water to the 35 ml mark. A second round of centrifuging was then undertaken to ensure that the majority of the hydrogen peroxide used to digest the organic material was removed from the final sample solution.

Following this initial sample preparation, microscope slides were then prepared. Distilled water was added to cover slips to which drops of sample were subsequently pipetted. These samples were then left to dry over a low heat on a hotplate for a few hours. Once these cover slips had dried, microscope slides were laid out and labelled, with drops of Naphrax pipetted onto each. The cover slips were then inverted, leading to the diatom sample on the cover slip facing the Naphrax solution on the microscope slide. These slides were then heated on a hotplate to drive off the toluene solvent from the Naphrax mounting medium. Following this, the sample slides were allowed to cool and were checked to certify that they were appropriately labelled, thus ensuring that the correct core and sample depth was assigned to the correct sample slide.

In order to ensure a valid sample for analysis, at least 250 diatoms were counted for each slide sample. Diatoms were counted systematically using

traverses across the slide, ensuring that no diatoms were counted multiple times. Diatoms were identified using several classification schemes including Lefébure (1947), Smith (1950), Brun (1965), Foged (1974) and Hartley *et al.* (1996), as well as online resources such as Algaebase. Following the enumeration of diatoms for each sample, summary diagrams were generated for each core using C2 (Juggins, 2005), a computer software program. CONISS (Grimm, 1987) was subsequently used to determine levels within the diatom assemblages for each site, thus denoting multi-species changes within the assemblages.

4.4 Chronological Methods

In order to produce a RSL curve for the Snæfellsnes peninsula, the isolation contacts identified in each core require chronological control. Two techniques were employed in this study: tephrochronology and radiocarbon dating. Tephrochronology has previously been used to great effect in Iceland (e.g. Rundgren *et al.*, 1997; Lloyd *et al.*, 2009) to provide a chronology of RSL changes, with tephra layers widely being seen as important markers or isochrons in core samples (Lowe *et al.*, 2001). The rapidity and widespread nature of tephra deposition means that an accurate date can be produced for particular isochrones (Alloway *et al.*, 2007), thus proving extremely useful for environmental, RSL and volcanic studies, as exact or limiting dates for sedimentary and microfossil changes can be generated. Radiocarbon dating was used for core samples with a lack of tephra deposits or with no tephra layers close to the isolation contact and has been used extensively in previous RSL studies (e.g. Zwartz *et al.*, 1998; Lambeck and Chappell, 2001).

Initially, a framework core chronology was produced through the geochemical analysis of tephra samples, with analyses being undertaken between 10th and 12th August 2011. Electron microprobe analysis allows the elements present in a sample to be identified and quantified, based on the X-ray spectra generated by the analysis procedure (Reed, 1975). The technique has several key benefits over other tephra analysis methodologies, in particular, its high spatial resolution, high precision and accuracy (Hayward, 2011). The geochemistry of the sample represents that of the magma produced by the eruption (Barker, 1983) and as such the tephra deposit can be correlated to a specific area or

event (Westgate and Gorton, 1981; Hayward, 2011). This correlation allows the determination of the source volcano and in turn provides information on the fallout pattern of particular eruption events.

The tephra layers present in the Snæfellsnes sediment cores were initially identified visually, as tephra rather than as particular eruptions, during extraction in the field. Upon receipt of the cores in Durham, the layers with closest proximity to the isolation contacts were sampled for geochemical analysis using an electron microprobe at the NERC TAU Facility, School of Geosciences, University of Edinburgh. Geochemical analyses are preferable when determining the mineral composition of tephra layers, as the chemical composition of the tephra does not differ with distance from the source eruption (Dugmore *et al.*, 1992). The determination of tephra geochemistry also provides an effective method of establishing correlations between sediment deposits due to the distinct sample geochemistries from single eruptions (Westgate and Gorton, 1981). The employment of the technique on several of the sediment cores from the Snæfellsnes peninsula will therefore hopefully provide an opportunity of correlations between sediment core samples.

The technique relies on two key assumptions:

- i) that the deposition of the tephra layer was instantaneous and;
- ii) that the tephra samples have specific chemical compositions, thus generating specific geochemical signals (Hunt and Hill, 1993).

Previous research has however highlighted one major issue with the technique, with the similarity of eruptions from the same volcanic system being problematic when identifying specific eruption events (Larsen *et al.*, 1999). This issue has however recently been the subject of review by Hayward (pers. comm.). It has been shown that if sufficient numbers of analyses are undertaken, separation of different eruptions from the same volcanic system is technically possible, through the analysis of ten elements (Hayward, 2011). As a result, ten elements, and their oxides, were analysed as part of this study: Sodium (Na), Magnesium (Mg), Aluminium (Al), Potassium (K), Calcium (Ca), Silicon (Si), Iron (Fe), Phosphorous (P), Titanium (Ti) and Manganese (Mn).

In order to provide a suitable sample for analysis, the tephra samples were initially subjected to an acid digestion similar to that outlined in Persson (1971). An acid digestion is essential for organic rich samples, aiding electron microprobe and microscope analyses without affecting the geochemistry of the final tephra sample (Dugmore *et al.*, 1992). Samples rich in silts were sieved using 63 and 125 μm sieves in order to remove as much silty material as possible whilst leaving sufficient tephra of a suitable size for analysis (Anthony Newton, pers. comm.). This sieving technique has been conducted extensively and with great effect in previous studies (e.g. Larsen *et al.*, 1999), reducing the range of shard sizes employed in such geochemical analyses.

Following the initial tephra sample preparation, the techniques set out by Steele and Engwell (2009) were followed to allow the electron microprobe analyses to be conducted. Steele and Engwell (2009) highlight the sample mounting and grinding techniques required to ensure that samples are suitable for use with electron microprobes. Furthermore, information surrounding sample polishing is outlined, which is important in ensuring a suitable surface for analysis. The tephra samples for electron microprobe analysis can either be mounted on slides or be set into resin blocks.

The tephra samples for analysis from Snæfellsnes were set into resin blocks of 25 mm diameter to allow them to be held within the electron microprobe sample holder. These resin blocks were then polished in the Department of Earth Sciences, Durham University and subsequently sent to the School of Geosciences, University of Edinburgh for carbon coating. The Cameca SX100 electron probe microanalyser at the NERC TAU Facility, School of Geosciences, University of Edinburgh was used for the analyses following a successful NERC application. Upon arrival at the facility, the machine was calibrated, with measurements for standards being taken to ensure that the element compositions measured by the probe were within a suitable tolerance. In this research, the BCR2G standard was used, due to the basaltic nature of the samples analysed from the Snæfellsnes sediment cores.

The Cameca SX100 electron microprobe allows samples to be scanned manually or automatically, depending on the size of the tephra surface available for scanning. Samples rich in crystallites were scanned manually, with

unaltered samples and samples low in crystallites being scanned automatically overnight. In order to gain a sufficient level of accuracy for the chronology, 20 analyses were conducted per sample. Both automatic and manual analyses were taken for each sample to ensure that the tephra shards analysed were representative of the tephra deposit as a whole. Samples results were then reviewed to ensure that any non-tephra samples were removed, such as plagioclases. At the end of each set of analyses, the standards were re-sampled to ensure that the element compositions generated by the analyses were within an acceptable tolerance.

Following the completion of the tephra analyses, the chemical compositions of each sample analysed were compared to existing records from Iceland, such as those found on Tephabase (www.tephrabase.org, Newton, 1996; Newton *et al.*, 2007) in order to obtain a specific date for each distinct tephra layer. There is currently relatively little information regarding the tephtras present in Snæfellsnes due to a lack of previous research; however Tephabase does hold information on 20 such geochemical analyses. Several additional sources on Snæfellsnes tephtras do exist (e.g. Steinþórsson, 1967) but they fail to provide the chemical compositions of the noted tephtras. Previous research in Vestfirðir has revealed the presence of the Saksunarvatn tephra, both at Reykjarfjörður (Andrews *et al.*, 2002) and Bjarkarlundur (Lloyd *et al.*, 2009), thus being an initial tephra layer for comparison with the geochemical composition of the sampled Snæfellsnes tephra deposits.

In addition to the tephrochronological analyses undertaken, samples were also taken for radiocarbon dating. The radiocarbon dates generated were aimed at providing dates for samples where insufficient coverage from tephrochronology was produced. Samples for radiocarbon analysis were therefore taken from the Þingvallavatn, Saurar 3 and Borgarland 10 sediment cores due to the lack of a tephra layer in close proximity to the microfossil isolation contact identified in the core samples. Microfossil assemblages were used to identify the isolation contact and therefore select the point at which the radiocarbon sample should be removed. The samples were taken in mid August 2011 for analysis at the Poznań Radiocarbon Laboratory, Poland, with the results of the analyses being received in early November 2011.

Radiocarbon analyses are affected by the ^{14}C offset or reservoir effect (Stuiver and Braziunas, 1993; Ascough *et al.*, 2011), which leads to the generation of sample ages which do not truly represent the age of the sample. The offset arises from the differences in ^{14}C residence times between freshwater and marine reservoirs and the atmosphere (Ascough *et al.*, 2011). There are two reservoir effects that must be taken into account when undertaking radiocarbon analyses:

- i) *marine reservoir effect*: The marine reservoir effect arises from the ageing of water masses during deep oceanic circulation (Ascough *et al.*, 2011). This can be quantified and accounted for using the correction outlined by Stuiver *et al.* (1986).
- ii) *freshwater reservoir effect*: The freshwater reservoir effect and its implications on ^{14}C ages from lacustrine sediments from Iceland has been investigated by Ascough *et al.* (2011) and will be further discussed alongside the results of the radiocarbon analyses from this study. The freshwater reservoir effect arises from several factors, such as the input of ^{14}C from geological sources (Ascough *et al.*, 2011).

4.5 Analytical Methods

4.5.1 Elevation Correction

Following the determination of the basin sill and core elevations, altitudes above Mean High Water Spring Tide (MHWST) were calculated and subsequently corrected to Mean Sea Level (m. asl.) using Icelandic tide table data. As a result, all measurements were converted from metres above Mean High Water Spring Tide (MHWST) to metres above Mean Sea Level (MSL). The Icelandic tide gauge data was sourced from the Icelandic Hydrographic Centre, a copy of which can be found below. It was decided that tide gauge data from Reykjavik be used rather than that from Stykkishólmur, as the Stykkishólmur dataset only covers a limited time period and as such the Reykjavik dataset was more robust.

Tidal Statistics for REYKJAVIK
Latitude 64°09' N Longitude 21°56' W

Port details: Reykjavík
Datum of Predictions = Chart Datum
Highest Astronomical Tide (HAT): 4.62 metres
HAT occurs at 07:14 GMT on 20/02/2015
Lowest Astronomical Tide (LAT): -0.30 metres
LAT occurs at 01:01 GMT on 18/09/1997
Maximum Tidal Range possible: 4.78 metres
Mean High Water Spring (MHWS): 4.01 metres
Mean High Water Neap (MHWN): 2.98 metres
Mean Low Water Neap (MLWN): 1.38 metres
Mean Low Water Spring (MLWS): 0.36 metres
Tide Type: 0.10 (semidiurnal)
Shallow Water Influence: 0.02

An example calculation associated with the adjustment at the marine limit sites can be found in Chapter 5.

4.5.2 Radiocarbon Age Calibration

In order to adjust the radiocarbon ages generated to account for variations in atmospheric carbon, the CALIB 6.0 program (Stuiver *et al.*, 2010) was used. The ages generated from the samples extracted from the Saurar 3, Þingvallavatn and Borgarland 10 sites were inputted into the program leading to the generation of 1-sigma and 2-sigma graphs of the data, which are presented in Chapter 6. These 1-sigma and 2-sigma plots provide a calibrated age estimation and potential range for each radiocarbon point within the dataset.

4.6 Summary

This chapter has provided an overview of the key field, laboratory, chronological and analytical methods employed in this study. This has involved the discussion of the coring and surveying of sites, extraction of core samples, the provision of chronological controls and diatom analytical techniques, as well as elevation correction and age calibration requirements. The adopted methods have been justified and alternative approaches to those undertaken have been discussed where appropriate, with the chapter also outlining potential issues regarding the methods employed. The next chapter outlines the results of the research and the associated analyses.

CHAPTER 5

Results and Interpretation

5.1 Introduction

This chapter aims to outline the results of the analyses conducted as part of this study. The results will be presented on an individual site basis, with a summary describing the general trends within the datasets alongside the RSL curve generated for the region. Each isolation basin and saltmarsh site will be split into three sections: sedimentology, diatom flora and chronology. The results of sediment surveys will be shown, alongside a detailed description of the core stratigraphy used for the analyses. Following this, the diatom assemblage from the site will be outlined, highlighting changes in environmental conditions and, where relevant, isolation contacts within from each site. The results of the marine limit surveys will be briefly outlined, thus providing the high point for postglacial RSL in the region. Finally, the chronological analyses conducted on the core samples will be discussed. This will allow the Snæfellsnes results to be placed within the regional context within Chapter 6, through the construction of a RSL curve.

5.2 Borgarland 10

Core Elevation: 3.08 m asl

Site Location: 65°2'40.78"N 22°43'35.51"W

The BO10 core was extracted from the Borgarland site using a Russian Corer, with the base of the core being at 57cm. The top section of the core was not sampled, due to the need to remove a section of the marsh surface to allow the extraction of the underlying sediments. The BO10 core is the lowest lying core analysed in this study and was sampled for both diatom and radiocarbon analyses. Radiocarbon dating was used at this site due to the lack of tephra layers within the extracted core sample.

5.2.1 Stratigraphy

The Borgarland stratigraphy (BO10 and BO11) is summarised in Figure 5.1, alongside descriptions of the sediments, which are provided in Table 5.1.

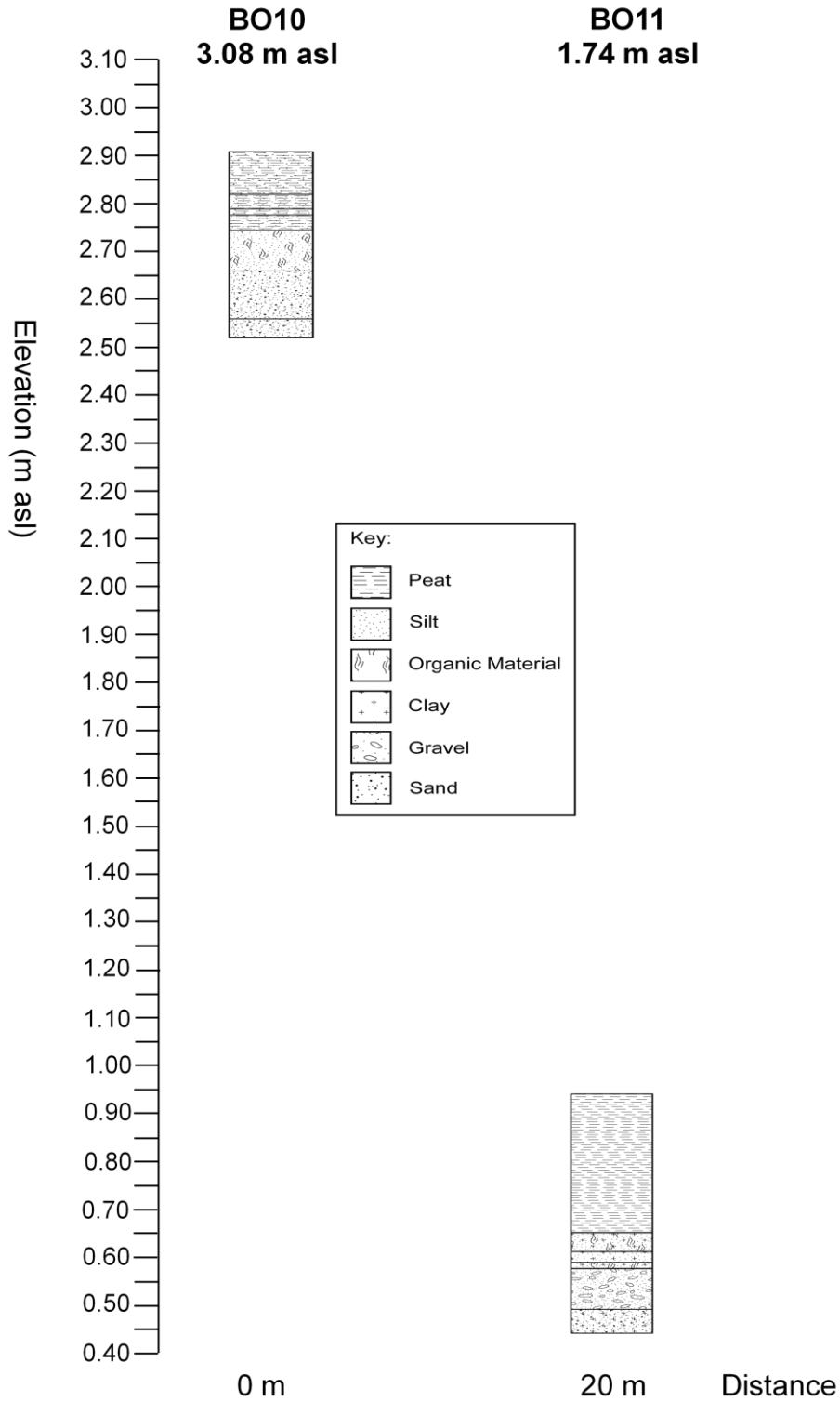


Figure 5.1 Core stratigraphy of the BO10 and BO11 core samples showing the composition of each sediment layer.

<i>Top (cm)</i>	<i>Bottom (cm)</i>	<i>Description of sediment</i>	<i>Tröels-Smith</i>
18	27	Light brown fibrous turfa peat with some silt	Th4 Ag+
27	30	Mid brown turfa peat with silt	Th3 Ag1
30	31.5	Light brown fibrous turfa peat with some silt	Th4 Ag+
31.5	34.5	Mid brown turfa peat with silt	Th3 Ag1
34.5	43	Brown organic rich silt with abundant roots	Ag3 Sh1 Th+
43	53	Dark brown/grey organic rich silty sand	As3 Gmin1 Sh+
53	57	Light brown/olive green organic rich silty sand	As3 Gmin1 Sh+

Table 5.1 Tröels-Smith (1955) classifications and sediment descriptions for the BO10 sediment core.

The BO10 core can be separated into three principal sedimentary units: lower silty sands, lower silts with abundant organic material and an upper fibrous turfa peat of various shades. Coring stopped at the site when the Russian Corer hit a basal gravel at 57 cm. The organic material outlined in Fig. 5.1 represents rootlets within the sediment rather than an organic sediment layer i.e. a mixture of clay, peat and limus.

The sedimentological results reveal a clear sequence from basal gravel to silty sand, organic rich silt and upper fibrous turfa. This sequence is indicative of an environment of decreased energy, with the gravel layer representing a high energy environment and the silty sand showing a decrease in the energy along the coastline. Following this decrease in the energy within this part of the coastal system, the introduction of organic material suggests the commencement decreased marine influence.

5.2.2 Diatom flora

In total, 18 diatom samples were removed from the core for analysis at a 2 cm resolution between 22 cm and 56 cm. The diatom assemblage from the site is summarised in Figure 5.2 and shows decreased brackish-marine influence at 50 cm. The diatom assemblage shows a transition from predominantly brackish

to mainly freshwater conditions, with a minor brackish component towards the top of the core section at 28 cm.

The BO10 diatom assemblage can be separated into four distinct zones: BO10-DZ1 (56 cm to 49 cm), BO10-DZ2 (49 cm to 43 cm), BO10-DZ3 (43 cm to 36 cm) and BO10-DZ4 (36cm to 28 cm). These four diatom zones clearly define the transition from predominantly brackish to fresh-brackish/freshwater conditions.

BO10-DZ1 is characterised by a strong brackish influence, which peaks at 52 cm. Several brackish and fresh-brackish species occur during this zone, such as *Navicula peregrina*, *Nitzschia sigma*, *Navicula cincta* and *Rhopalodia gibberula* occur throughout this lower zone. Some salt intolerant and freshwater species also occur in this zone, suggesting a mid to high marsh environment.

The beginning of BO10-DZ2 is marked by the loss of marine species and decrease in brackish species such as *Navicula peregrina*. Levels of fresh-brackish species continue at similar levels to those found in BO10-DZ1, although the levels of individual species differ from the previous zone. Levels of freshwater diatoms also increase in this zone, with increases in *Hantzschia amphioxys* and *Pinnularia borealis* being particularly noticeable.

The third diatom zone, BO10-DZ3, is characterised by an increased freshwater and salt intolerant component to the diatom assemblage. In addition to these increases, the levels of brackish and fresh-brackish species decrease during this zone. Increases in *Navicula thorodsseni* and *Pinnularia parva* var. *minuta* are particularly noticeable, which are coupled with an increased occurrence of *Eunotia praerupta* and *Pinnularia nodosa*. The relatively high levels of *Navicula cincta* and *Rhopalodia gibberula* highlighted in the previous zone are seen to decrease in BO10-DZ3. Despite this higher occurrence of freshwater and salt-intolerant forms, the significant presence of fresh-brackish taxa suggests that the environment is one of weak brackish conditions, thus suggesting a high marsh environment during this period. As such, this area would likely be inundated by the sea relatively rarely, hence the predominance of freshwater conditions.

The final and uppermost zone of the diatom assemblage, BO10-DZ4, shows high levels of freshwater and salt-intolerant forms, such as *Eunotia septentrionalis*, *Rhopalodia rupestris*, *Navicula cocconeiformis* and *Tabellaria fenestrata*. The zone also contains relatively high levels of fresh-brackish taxa however, which often make up between 10% and 15% of the assemblage and is predominantly made up of *Navicula cincta*, although other fresh-brackish species also occur throughout the zone. This combination of higher levels of fresh-brackish and minor decreases in freshwater and salt intolerant species suggests a slightly greater influence of brackish conditions at the site, although it is likely that this assemblage continues to represent a high marsh environment. There are low occurrences of brackish species during this zone although these do not reach above 5% of the total count.

It is therefore clear from the diatom assemblage at the BO10 site that there is a transition from brackish dominance to greater freshwater influence. The base of the analysed section demonstrates a strong brackish water signal and there remains a brackish signal throughout the site assemblage, as demonstrated by the presence of fresh-brackish species such as *Navicula cincta*. It is likely therefore that the assemblage represents the progression through the marsh profile, from a low marsh regularly inundated by the sea to a mid-marsh and subsequent high marsh environment, which rarely experienced tidal inundation. This environmental interpretation can be linked to changes in RSL, with the changes in the site assemblage appearing to demonstrate a lowering of RSL at the site.

5.2.3 Environmental Summary

As previously mentioned, the sedimentological data supports the diatom evidence of decreased marine influence over time at the Borgarland 10 site. This is shown by the decrease in mesohalobous species during the silty sand sediment band, with increased numbers of oligohalobous indifferent and halophobous species following the commencement of organic sediment production. When the two datasets are combined, there is clear evidence for decreased marine influence and therefore a lowering of RSL within the Borgarland 10 record. This is demonstrated by the correlation between decreased levels of clastic sediment deposition and polyhalobous and

mesohalobous prevalence in the diatom record. The diatoms suggest that the change in sediment composition signifies a decrease in marine influence at the site rather than other potential reasons for such changes.

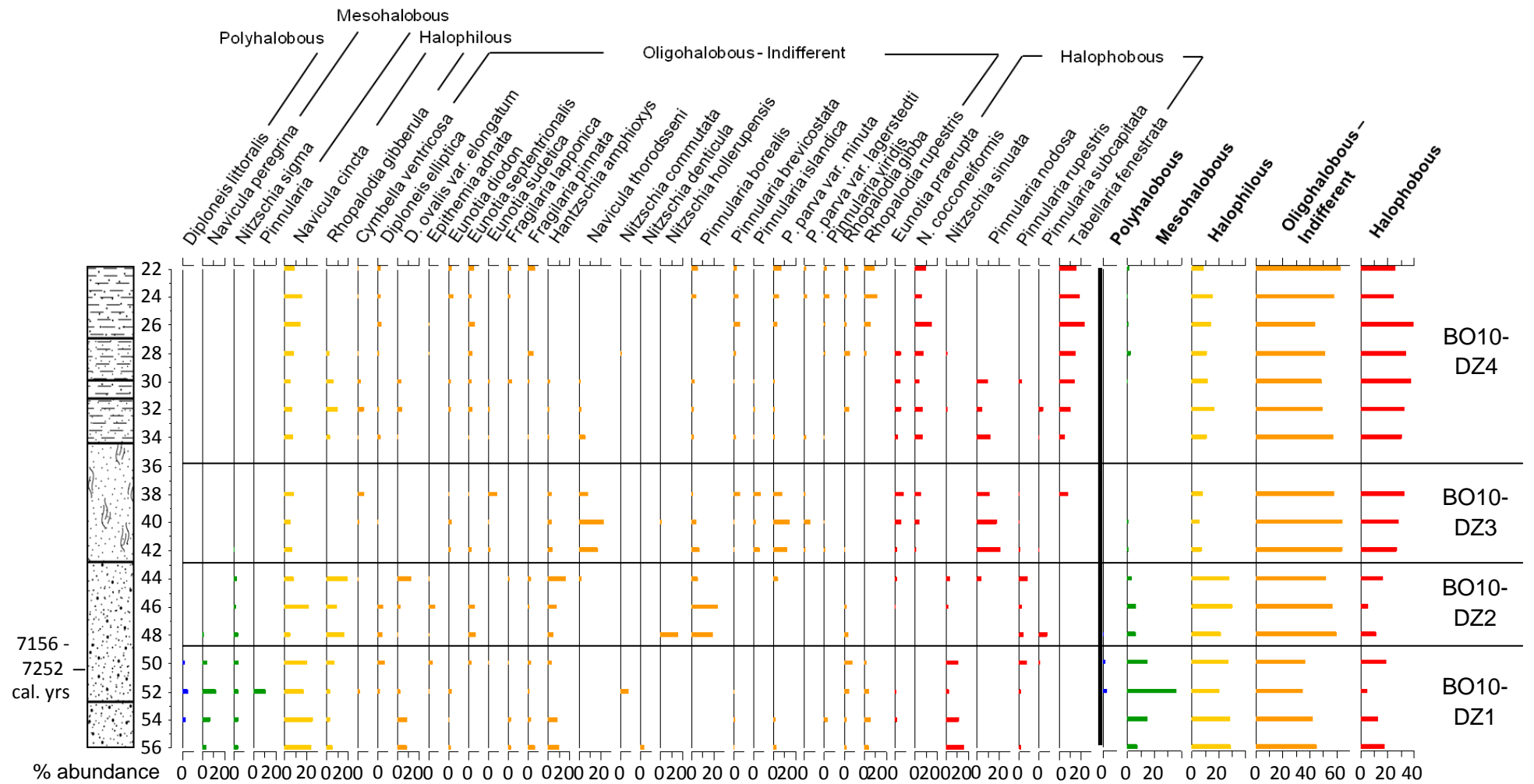


Figure 5.2: Diatom assemblage graph for Borgarland 10, showing the transition from brackish to freshwater conditions. A key to stratigraphy can be found in Figure 5.1.

5.3 Borgarland 11

Core Elevation: 1.74 m asl

Site Location: 65°2'40.78"N 22°43'35.51"W

The BO11 core was also retrieved using a Russian Corer from the Borgarland marsh site approximately 20 m ESE from the BO10 core (see Figure 3.3). The marsh surface was again removed prior to the extraction of the sediment core for analysis. The core was sampled for diatom analyses, although these were less numerous than for the other Borgarland site, due to the poor preservation of the diatoms found within the cores. As a result of this poor diatom preservation and subsequently poor sample resolution, the core was not sampled for chronological control. The results from this site may however still be of relevance for the interpretation of the RSL record of the Snæfellsnes region and thus are presented here.

5.3.1 Stratigraphy

The stratigraphy of the BO11 core is summarised in Figure 5.1 alongside that of BO10. Core BO11 sampled 50 cm of sediment. No tephra layers were present within the core sample. The sediment core has four distinct sections: a basal sandy silt, a silt layer rich in gravel, a silt layer with varying levels of organic material and a turfa peat layer. The sediment stratigraphy is summarised in Table 5.2.

<i>Top (cm)</i>	<i>Bottom (cm)</i>	<i>Description of sediment</i>	<i>Tröels-Smith</i>
80	109	Dark brown turfa peat	Th4
109	113	Dark brown organic rich silt with some clay and rootlets	Ag2 Sh2 As+
113	115.5	Grey silt with some clay	Ag3 As1
115.5	116.5	Dark brown silt with some clay and rootlets	Ag2 Sh1 As1
116.5	125	Blue-grey sandy silt with some gravel	Ag2 Gmin2 Gmaj+
125	130	Blue-green-grey sandy silt with some clay	Ag2 Gmin1 As1 Sh+

Table 5.2: Tröels-Smith (1955) classifications and sediment descriptions for BO11 core.

The sedimentary record from the Borgarland 11 site shows a similar trend to the Borgarland 10 results. The clastic sediments at the base of the sediment core

sample represent the brackish-marine influences at the site. This appears to be a relatively low energy environment, when compared to the results from the other Borgarland core; however, this may be due to the higher elevation of this core sample not recording the potential earlier stronger marine influences at the Borgarland site. The organic material highlighted in Figure 5.1 is a mixture of clay, peat and some silts, which is broadly classified as organic due to the predominance of rootlets and organic sediments. This sediment has been hypothesised as demonstrating a transitional period between potential dominant influences at the site.

5.3.2 *Diatom flora*

Four diatom samples were initially enumerated for the BO11 core, with additional samples taken to increase the sample resolution to 4cm. Diatom preservation was generally poor, with low numbers of diatoms present in the majority of samples. In order to ensure a valid sample for analysis, a minimum total of 200 diatoms were required for each sample. This was difficult to achieve for some samples, with two or three slides being enumerated to achieve the minimum diatom count level at 104 cm, 116 cm and 124 cm. The diatom assemblage for the BO11 site is summarised in Figure 5.3.

The diatom assemblage can be separated into two distinct zones: a basal zone with marine and brackish components and an upper freshwater zone with a more limited brackish component. The basal zone, BO11-DZ1, contains marine and brackish species, such as *Thalassiosira eccentric*, *Thalassiosira tenera* and *Tabularia fasciculata*, alongside high levels of fresh-brackish species, particularly *Rhopalodia gibberula*. Several freshwater species are also numerous within this BO11-DZ1 zone, with *Pinnularia parma* var. *minuta*, *Rhopalodia brebissoni* and *Rhopalodia gibba* all reaching levels over 10% of the total assemblage at some point during the zone. The upper BO11-DZ2 zone has a lesser brackish influence, with levels of *Nitzschia sigma* and *Tabularia fasciculata* decreasing through the zone. Levels of freshwater species increase, with peaks in *Eunotia curvata* var. *subarcuata* and *Eunotia exigua* found towards the top of the analysed section. Minimal marine influence is noted within the zone. The site assemblage has an increasingly freshwater

component, but there remains a minor marine and brackish component throughout.

5.3.3 *Environmental Summary*

It is clear that the environmental interpretation from the Borgarland 11 site should be treated with some caution due to the poor levels of preservation of the diatoms within the coastal lowland sediments. That said, there is still a clear transition within the diatom assemblage, showing inferred decreased marine influences at the site over time, as demonstrated by the reduction in the levels of both polyhalobous and mesohalobous species (Figure 5.3). This decrease in the polyhalobous and mesohalobous species is coupled with changes in the dominant sediment composition, with a transition from basal sandy silts to silty clays and subsequent turfa peat deposition (Figure 5.1). The transition from Zone BO11-DZ1 to BO11-DZ2 within the diatom assemblage is coupled with the shift from dark brown organic rich silt to dark brown turfa peat. This sedimentary support for the change in environmental conditions highlighted by the diatom analyses is useful in determining the dominant processes occurring at the site. Furthermore, the correlation between the diatom inferred environmental record and sedimentary data allow the changes in sediment to be explained through potential RSL changes rather than increases in productivity or temperature, for example.

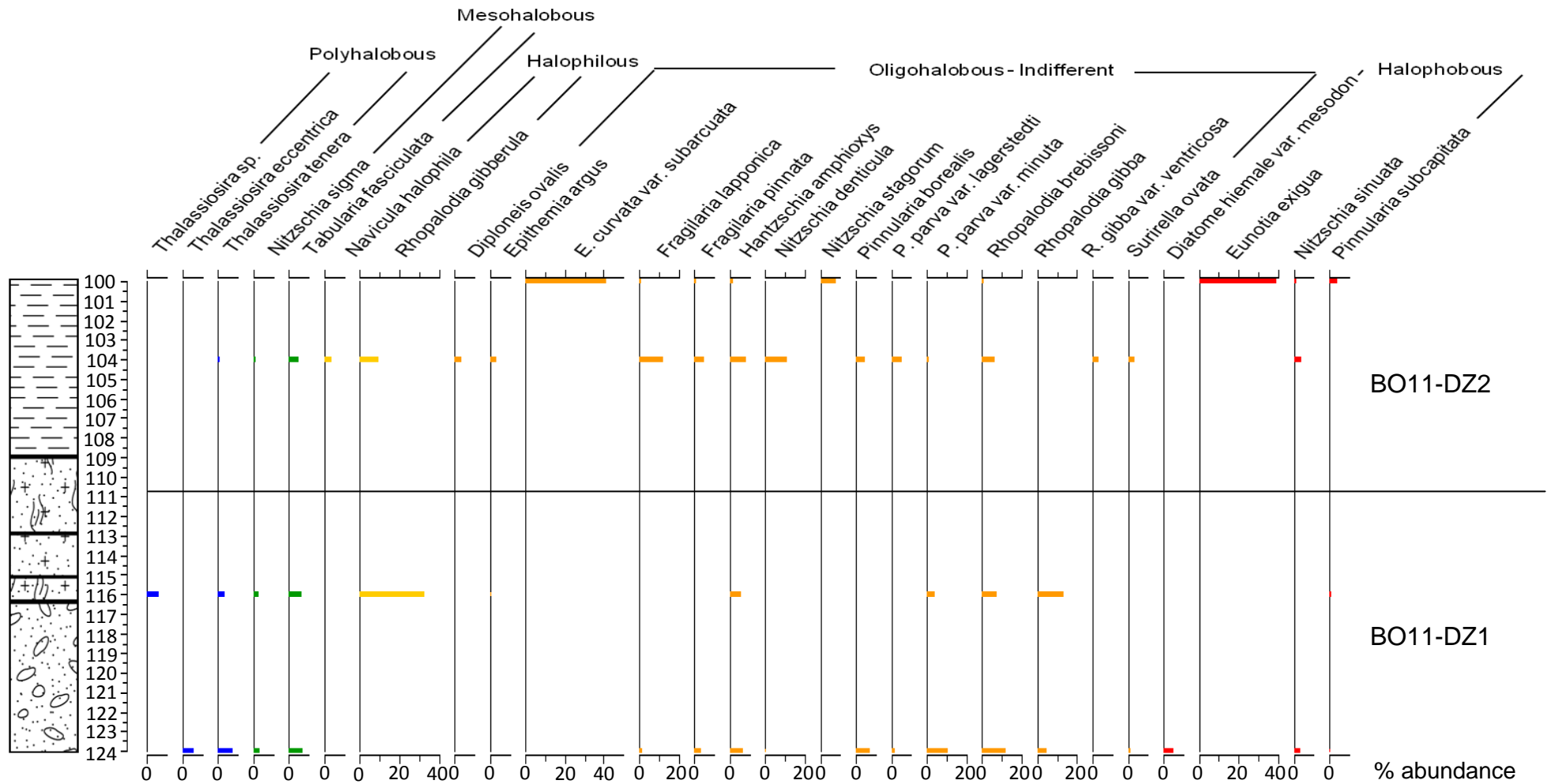


Figure 5.3: Diatom assemblage graph for the Borgarland 11 site, showing the transitional sequence. Key to sediments can be found in Fig. 5.1

5.4 Skjaldarvatn (SK1)

Sill Height: 4.57 ± 0.3 m above MSL Location: $65^{\circ}2'50.67''N$ $22^{\circ}47'11.35''W$

One core was extracted from the Skjaldarvatn site and was sampled for tephrochronological and diatom analyses. The core was extracted from the centre of the basin and is therefore seen as a representative sample for basin stratigraphy, as this is likely to be the deepest part of the basin and thus provide the longest and most complete record of environmental change at the site. The Russian corer was again used to extract this core sample due to the predominance of organic rich sediments.

5.4.1 Stratigraphy

The stratigraphy of the analysed section of the Skjaldarvatn core is summarised in Figure 5.4. The core stratigraphy demonstrated in Figure 5.4 shows the sedimentological isolation contact at 548 cm. The core sediments are described and summarised in Table 5.3, alongside the corresponding Tröels-Smith (1955) classifications.

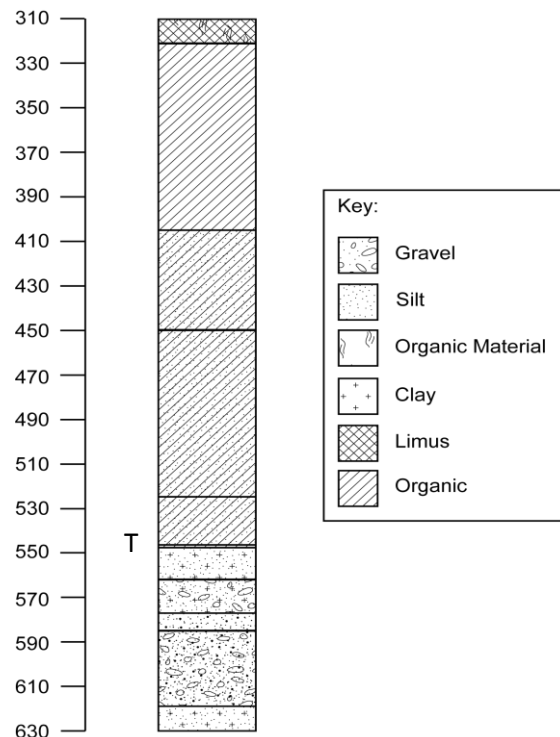


Figure 5.4: Sediment stratigraphy for the section of the SK1-1 core analysed for diatom and tephra analyses, showing the composition of each sediment layer. T represents the position of the sampled tephra layer within the analysed core section.

<i>Top (cm)</i>	<i>Bottom (cm)</i>	<i>Description of sediment</i>	<i>Tröels-Smith</i>
310	321	Olive green limus with organic material	Ld3 Sh1
321	405	Olive green-grey silty organic material	Sh3 Ag1 Th+
405	450	Olive green-grey silty organic material with some rootlets	Sh3+ Ag1- Th+
450	525	Olive green-grey silty organic material	Sh3 Ag1 Th+
525	547.5	Olive green-grey organic material with abundant silt	Sh2 Ag2
547.5	548	Dark grey tephra layer	Gmaj4
548	562	Blue grey silty clay	Ag2 As2
562	577	Blue grey silty clay with sand and gravel	As2 Ag2 Gmin+
577	585	Blue grey silty clay	As2 Ag2
585	619	Blue grey silty clay with sand and gravel	As2 Ag2 Gmin+ Gmaj+
619	630	Blue grey silty clay	Ag2 As2

Table 5.3: Tröels-Smith classifications and sediment descriptions for the SK1-1 sediment core.

The sedimentary record from the Skjaldarvatn site demonstrates a clear transition from clastic sediments to clastic rich organic sediment and subsequent organic sediment accumulation. The basal silty clays with varying amounts of sand and gravel suggest that the site was subjected to periods of differing energy input, with the larger grained mineral sands and gravels suggesting high energy coastal processes and the silts and clays suggesting periods of lower energy.

As such, the sedimentary record provides evidence of the transition from higher energy coastal processes to lower energy coastal processes. The periods of higher energy within the system towards the base of the analysed core section are likely to be interspersed with lower energy periods, as suggested by the material grain size.

5.4.2 *Diatom flora*

The SK1 core was analysed for 9 diatom samples between 520 cm and 556 cm in order to determine the microfossil isolation contact. The diatom assemblage at Skjaldarvatn is summarised in Figure 5.5, demonstrating the change from

brackish to freshwater dominance. The microfossil isolation contact is found at 540 cm.

The diatom assemblage from the Skjaldarvatn core samples clearly demonstrates the transition from marine to brackish species, followed by an increase in freshwater and subsequent salt intolerant species dominance. As such, the core has been divided into three distinct diatom zones: SK1-DZ1, SK1-DZ2 and SK1-DZ3. SK1-DZ1, found at the bottom of the analysed core section, is dominated by marine and brackish species, particularly *Cocconeis stauroneiformis*, *Nitzschia amphiplectans*, *Nitzschia sigma* and *Tabularia fasciculata*. This zone ends abruptly at 548 cm, where high and increasing levels of *Nitzschia sigma* are replaced at 546 cm by the occurrence of fresh-brackish species, such as *Diatoma tenue* var. *elongatum* and freshwater species, such as *Fragilaria construens* and *Stephanodiscus hantzschii*.

The very high levels of *Stephanodiscus hantzschii*, which mark the beginning of the SK1-DZ2 diatom zone, can be explained through the occurrence of a tephra deposit at 547 cm. Previous study has highlighted increases in the levels of *Stephanodiscus* and *Melosira* species following tephra deposition, due to increases in nutrients and silica. Despite the influence of diatom blooming following tephra deposition, the transition from marine-brackish to freshwater dominance is clear due to the shift from high levels of marine and brackish species at 548 cm to the high levels (~ 70 %) of freshwater species following the tephra induced diatom bloom at 546 cm.

The third diatom zone outlined for the Skjaldarvatn site, SK1-DZ3 begins at 538 cm. The commencement of this zone is marked by the decrease in fresh-brackish species and increase in salt intolerant species at the Skjaldarvatn site. Above 538cm, the levels of freshwater and salt intolerant species stabilise. The upper zone is dominated by species such as *Fragilaria construens*, *Fragilaria pinnata*, *Tabellaria fenestrata* and *Amphipleura pellucida*, all of which suggest basin isolation from marine influences. This is demonstrated by the increasingly freshwater nature of the diatom species present.

It is apparent therefore that the three diatom zones identified within the Skjaldarvatn core sample demonstrate the isolation process at the site. The diatom isolation contact is seen at 540 cm following the dramatic shift from an

assemblage with a large brackish component to an assemblage with a predominantly freshwater component. As discussed above, it is likely that this rapid shift in the diatom assemblage is likely to be a misrepresentation of the regional record of environmental change and in fact represents a local response in the diatom assemblage to tephra deposition within and surrounding the lake basin. As such, basin isolation is likely to have been slightly after this point, when the signal of the initial diatom bloom would have subsided.

5.3.3 Environmental Summary

It is clear that the diatom record allows an overview of the environmental and in turn RSL changes occurring at the site. The increases in levels of oligohalobous species at 547 cm also fit well with the change in sediment deposition at the site (Figures 5.4 and 5.5). Furthermore, it is clear that the increased levels of oligohalobous species thereafter correlate well with the increased organic material levels in the sedimentary record. As such, the sedimentary evidence can be seen to support the environmental interpretation proposed from the diatom analyses.

It is also apparent from the diatom evidence that the isolation process is completed at 540 cm. The increased organic sediment and oligohalobous species level after 547 cm demonstrate that freshwater diatom species are dominant after this point. As such, the sedimentary record supports the environmental interpretation of increased freshwater activity following the input of tephra at the Skjaldarvatn site. It is however the diatom record which provides the environmental interpretation, as the changes within the sedimentary record could have been generated through a series of processes unrelated to changes in RSL.

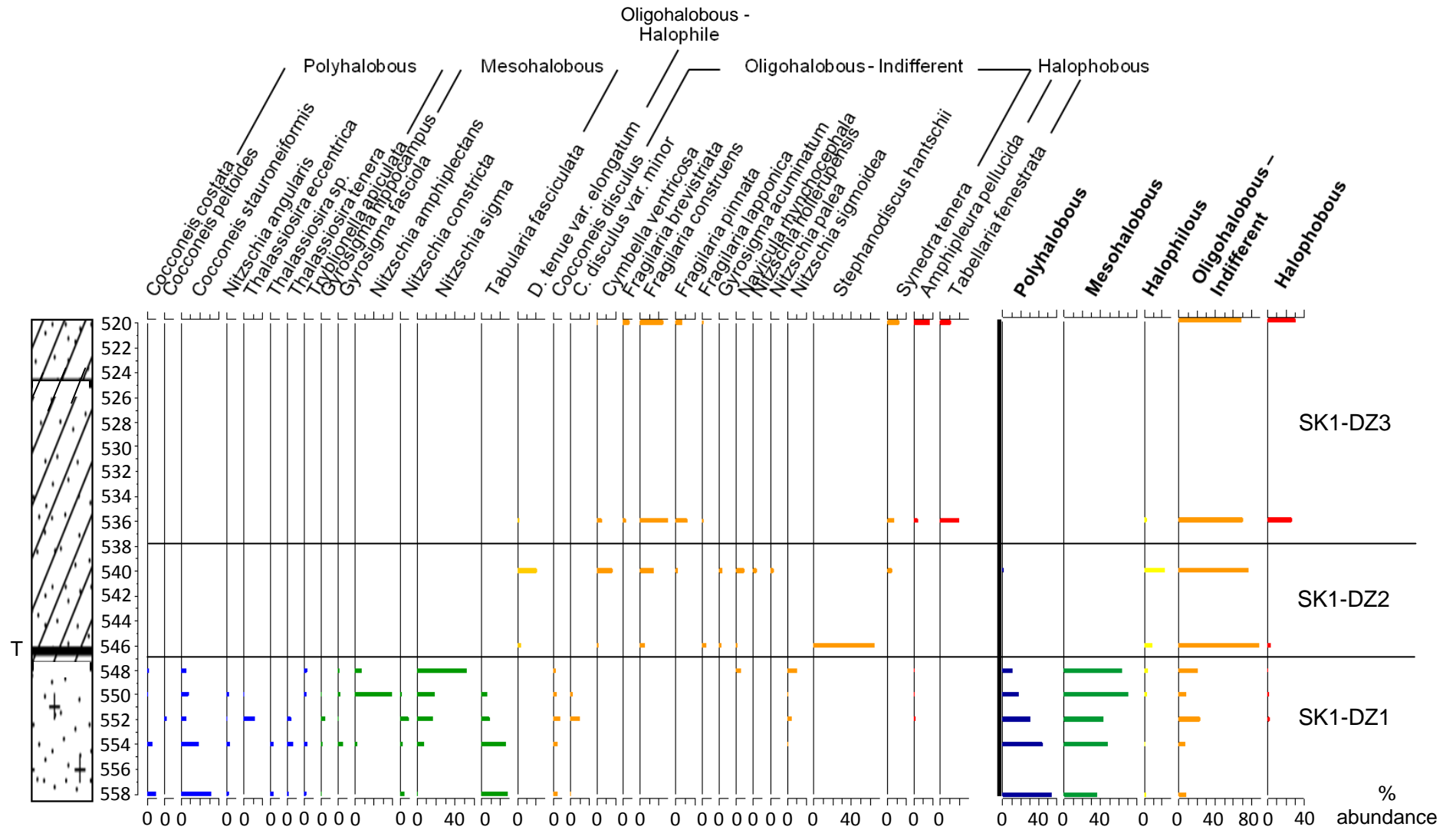


Figure 5.5: Diatom assemblage graph for the Skjaldarvatn site, showing the transition from marine-brackish to freshwater conditions at the site. T denotes the position of a sampled tephra layer within the analysed section of the SK1-1 sediment core. Stratigraphic key can be found in Figure 5.4.

5.5 Þingvallavatn (TH1)

Sill Height: 5.34 ± 0.3 m above MSL Location: 65°3'33.30"N 22°42'43.16"W

A number of cores were extracted at the Þingvallavatn site in order to establish site stratigraphy (see Fig. 3.8). Transects were cored using a gouge corer both in the infilled section of the lake basin and within Þingvallavatn itself. One sediment core was extracted for analysis using a Russian corer from the centre of the lake. This sediment core, TH1-4, was sampled for diatoms, tephra and radiocarbon analyses.

5.5.1 Stratigraphy

The transects cored at Þingvallavatn are summarised in the diagrams below, showing the cores extracted from the infilled basin section (Figure 5.6) and from Þingvallavatn itself (Figure 5.7). Core TH1-4 was re-sampled for analysis to provide a sample that was representative of the site.

The TH1-4 core sample was retrieved from the centre of the lake, which is likely to be the deepest point within the basin. As such, it is likely that this sample represents the longest possible time period and therefore presents the most complete record of environmental change at the site. The other three cores taken at the site are dominated by peat sections and as such it is unlikely that these samples record a complete record of the environmental changes. The transitional sequence seen in TH1-4 was also highlighted as having the potential to best represent these potential changes.

The analysed section of the TH1-4 core is summarised in Figure 5.8, with the associated sediment descriptions and Tröels-Smith (1955) classifications being found in Table 5.4. The sedimentological isolation contact is identified as lying at 488.5 cm, where the low levels of organic material found higher in the core are no longer present.

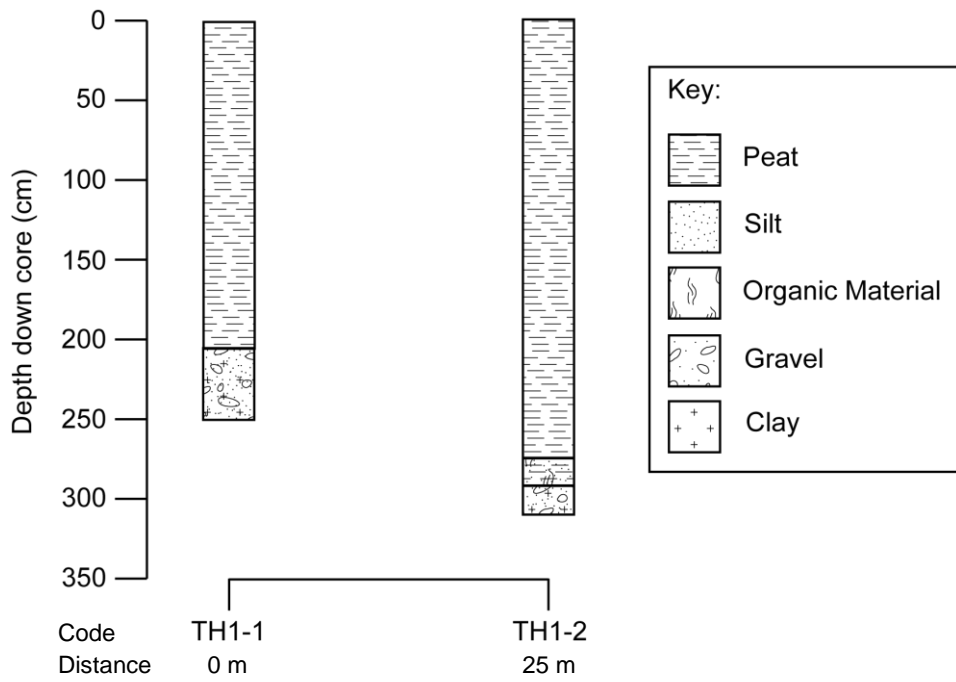


Figure 5.6 Sediment stratigraphy from the transect of cores taken from the infilled section of the Thingvallavatn basin. 'Organic material' is here defined as rootlets within a sediment layer.

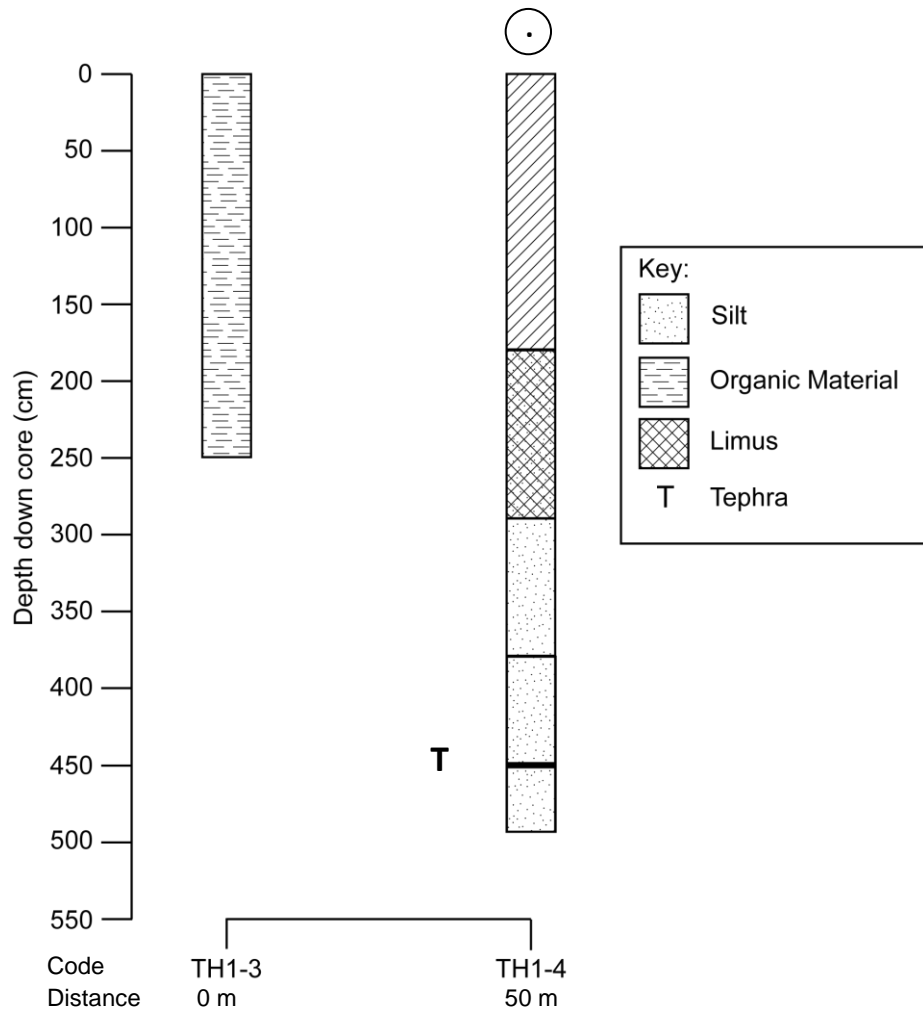


Figure 5.7 Sediment stratigraphy for cores taken from within the Thingvallavatn basin. 'Organic material' is here defined as a mixture of clay, limus and turfa. Circle denotes the sampled core.

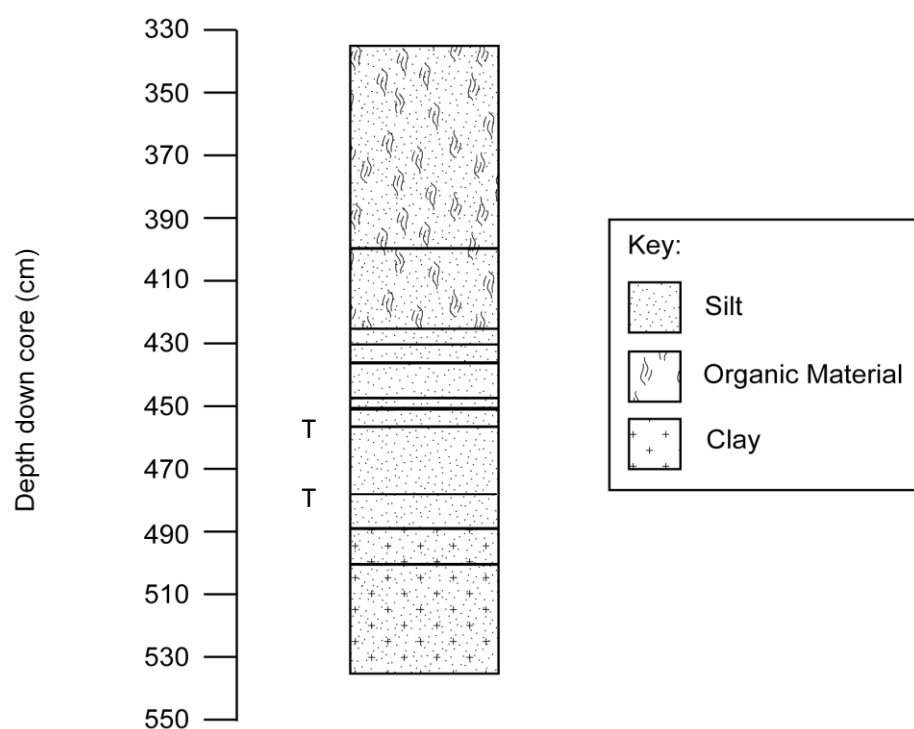


Figure 5.8 Sediment stratigraphy of the section of the TH1-4 core analysed for diatoms showing the sediment composition between 335 cm and 535 cm. T denotes a sampled tephra.

Top (cm)	Bottom (cm)	Description of sediment	Tröels-Smith
335	400	Light brown silt with abundant organic material	Ag2 Ld2
400	425	Mid brown silt with abundant organic material	Ag2 Ld2
425	430	Mid brown silt with low levels of organic material	Ag3 Ld1
430	436	Olive green silt with low levels of organic material	Ag3 Ld1
436	447.5	Dark grey silt with low levels of organic material	Ag3 Ld1
447.5	450	Grey silt with abundant organic material	Ag2 Ld2
450	456	Olive green silt with low levels of organic material	Ag3 Ld2
456.0	456.2	Dark grey tephra layer	Gmin4
456.2	479.0	Olive green silt with organic material	Ag4 Ld+
479.0	479.2	Dark grey tephra layer	Gmin4
479.2	488.5	Olive green silt with organic material	Ag4 Ld+
488.5	500	Grey silt with some clay	Ag4 As+
500	535	Blue-grey silt with some clay	Ag4 As+

Table 5.4: Tröels-Smith classifications and sediment descriptions for the analysed section of the TH1-4 sediment core.

As discussed in Chapter 3, two possible sill locations were identified at the pingvallavatn site. The sill transects cored at the NNW and NE sides of the

basin are summarised in Figure 3.9 with the sill being determined at point TH1-S5.

It is proposed that the site was subjected to lower energy coastal processes, with a lack of both gravel and sand deposits at the site. This conclusion is unsurprising, as the site is located in an area further inland of the other sites. There is also a clear transition from clastic sediments at the base of the analysed section to silts with abundant organic deposits. It is therefore clear that there is an increased freshwater influence at the site over time, thus leading to the generation of organic sediments.

5.5.2 *Diatom flora*

In total, 15 samples were extracted from the TH1-4 core in order to provide an overview in the changes in environmental conditions within the Þingvallavatn basin. The core was sampled between 460 cm and 530 cm in an attempt to establish the position of the microfossil isolation contact. The diatom assemblage is summarised in Figure 5.9. The assemblage shown in Figure 5.9 demonstrates the clear transition from marine to brackish and then freshwater dominance of the environment. The Þingvallavatn diatom assemblage shows three distinct zones: a basal marine-brackish zone (TH1-DZ1), an intermediate transitional zone (TH1-DZ2) and an upper freshwater zone (TH1-DZ3). These three zones clearly demonstrate the isolation of the Þingvallavatn basin.

The basal marine-brackish zone, TH1-DZ1, contains various species, with *Cocconeis stauroneiformis*, *Navicula digitoradiata*, *Nitzschia sigma* and *Tabularia fasciculata* all reaching 15 % of the total count at some point within the zone. During the zone, which is defined as 530 cm to 505 cm, levels of marine species, such as *Cocconeis scutellum* and *Thalassiosira tenera* decrease, with the total level of brackish species remaining relatively constant throughout, although fluctuations within individual species can clearly be noted. Towards the top of this proposed zone, which terminates at 505 cm, there is a peak in fresh-brackish species, which relates solely to a peak in *Navicula halophila*.

Following this initial marine-brackish zone, there is a transitional phase between 505 cm and 498 cm (TH1-DZ2). Levels of brackish species decrease rapidly

between the previous zone and the transitional phase, with levels of fresh-brackish species initially increasing and subsequently decreasing throughout the zone. In addition to the decreases in brackish and fresh-brackish species, freshwater species increase through this transitional zone. The initial occurrence of *Fragilaria lapponica*, *Fragilaria pinnata*, *Synedra rumpens* and *Stephanodiscus hantzschii* make up the majority of this increase in the levels of freshwater species.

Following this transitional phase of decreasing brackish and increasing freshwater influences, freshwater species become dominant in the third zone, TH1-DZ3. After 498 cm, levels of freshwater species are constantly above 65 %, with fresh-brackish species decreasing and salt intolerant species increasing through the zone. This freshwater phase is dominated by *Fragilaria* species, particularly *Fragilaria brevistriata*, *Fragilaria construens*, *Fragilaria construens* var. *binodis* and *Fragilaria pinnata*. In addition to this, peaks in *Navicula schoenfeldii* occur during this zone. At the top of this zone, salt intolerant species reach 10 % of the total count, with *Tabellaria fenestrata* and *Melosira varians* being the most numerous of the salt intolerant species.

It is therefore clear that the diatom assemblage from the Þingvallavatn site clearly demonstrates the isolation process at the site. This is evident through the decrease in the marine, brackish and fresh-brackish components and subsequent increases in the freshwater and salt intolerant components of the diatom assemblage from the site.

5.5.3 Environmental Summary

As outlined above, the diatom assemblage clearly shows the transition from marine and brackish to freshwater dominance at the Þingvallavatn site. This is supported by the sedimentary evidence from the site, which shows increases in the levels of organic material within the sediment deposits. Although the correlation between the sedimentary evidence and diatom inferred environmental interpretation are less clear at this site, there are still some similarities between the changes shown within the two datasets.

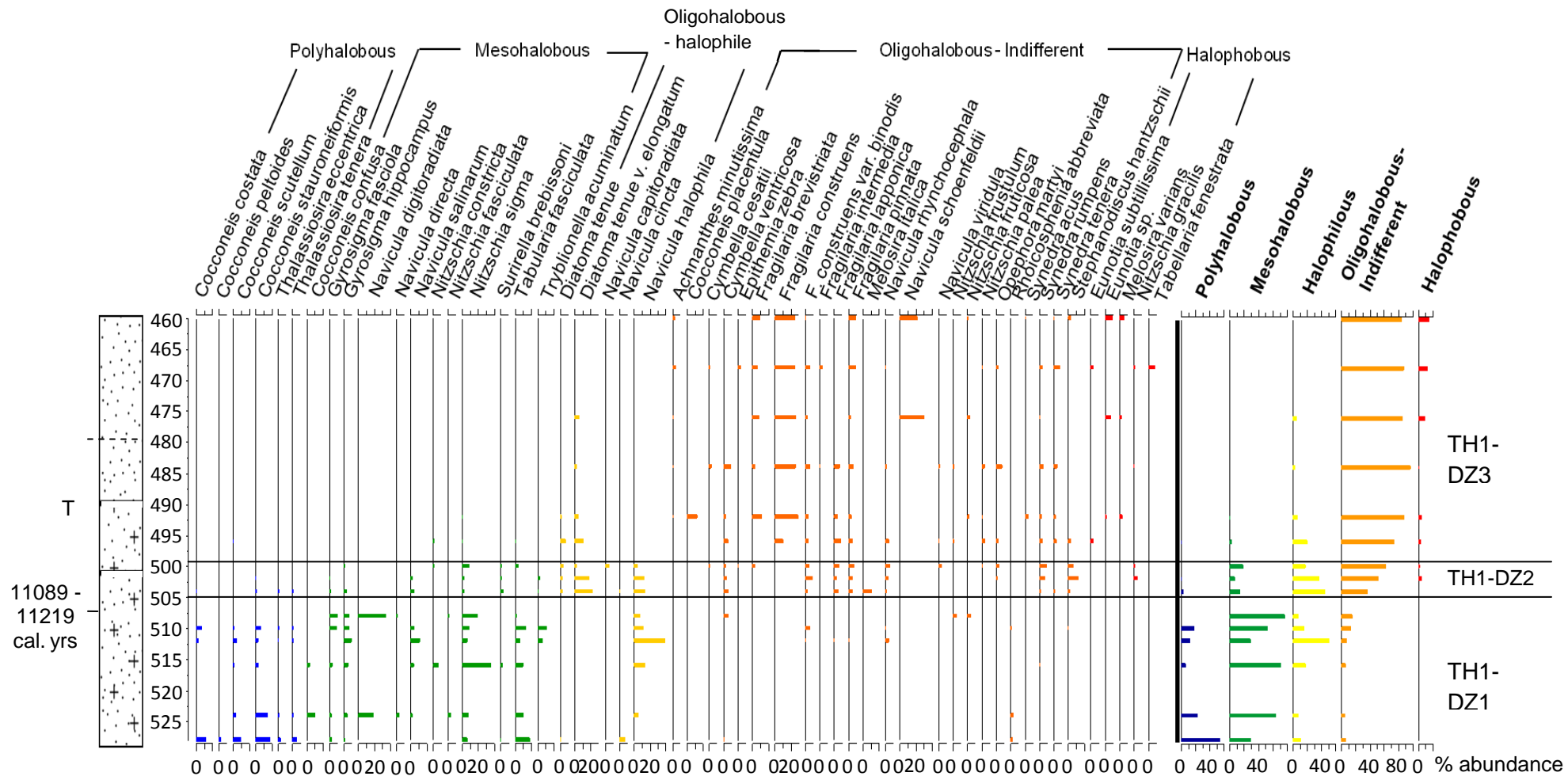


Figure 5.9: Diatom assemblage diagram for the Pingvallavatn site, showing the transition from marine-brackish to freshwater conditions. A key to stratigraphic composition can be found in Figure 5.8.

5.6 Saurar 1 (SA1)

Sill Height: 8.97 ± 0.3 m above MSL Location: 65°1'4.53"N 22°41'47.11"W

In order to establish site stratigraphy, 8 cores were retrieved from the site using a Gouge Corer (see Fig. 3.12), with the sample at SA1-3 being resampled using a Russian Corer to provide a sample representative of the site and suitable for diatom and tephra analyses. Core SA1-3 lies at the cross section of the two transects cored to determine site stratigraphy.

5.6.1 Stratigraphy

The stratigraphy of the site is summarised in Figure 5.10 and 5.11, which assumes that the ground surface is flat, due to a lack of elevation measurements for each of the gouge cores retrieved from the site. The SA1-3 core was selected for analysis due to its position within the centre of the infilled basin and the representative nature of the sediments found within the sample. The centre of the lake basin is likely to have the deepest profile and as such is likely to provide the most representative sample from the site. The section of the SA1-3 core analysed for tephra and diatoms is summarised in Figure 5.12, with the associated sediment descriptions and Tröels-Smith (1955) classifications being found in Table 5.5. The sediment cores retrieved from the site tend to have a basal gravel, overlain by a limus layer, which is in turn overlain by an upper peat layer.

The sedimentological isolation contact occurs at 330 cm in the SA1-3 sediment core. The sampled core section has a gravel layer at its base, with an overlying thin limus layer then in turn being overlaid by a second gravel. Above the upper gravel layer, a second limus layer can be found. This sedimentary unit become progressively less sandy, with sand levels decreasing after 330 cm. Above this limus layer, levels of organic material increase and the top of the core is characterised by organic sediments. The decreasing sandiness of the upper limus layer may be a result of the reworking of the underlying gravel. This is likely due to the presence of a limus layer below this upper gravel, which suggests that the basin may be in the final stages of isolation before the deposition of the upper gravel.

Saurar 1 - East-West Transect

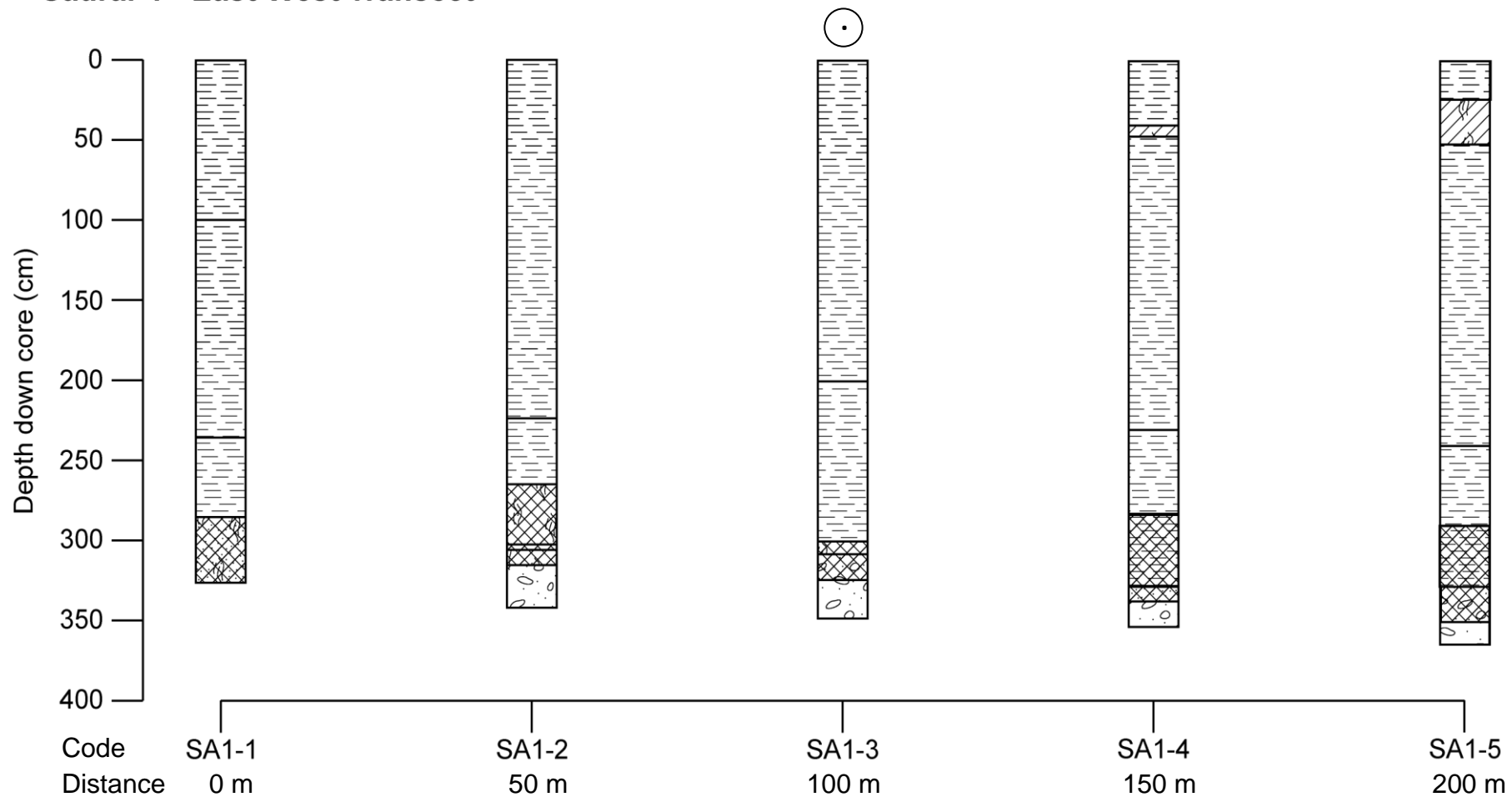


Figure 5.10: East-West transect of the Saurar 1 site, showing basin stratigraphy (see Figure 5.4 for key). Sampled core highlighted by circle. Stratigraphic key can be found in Figure 5.4

Saurar 1 - North - South Transect

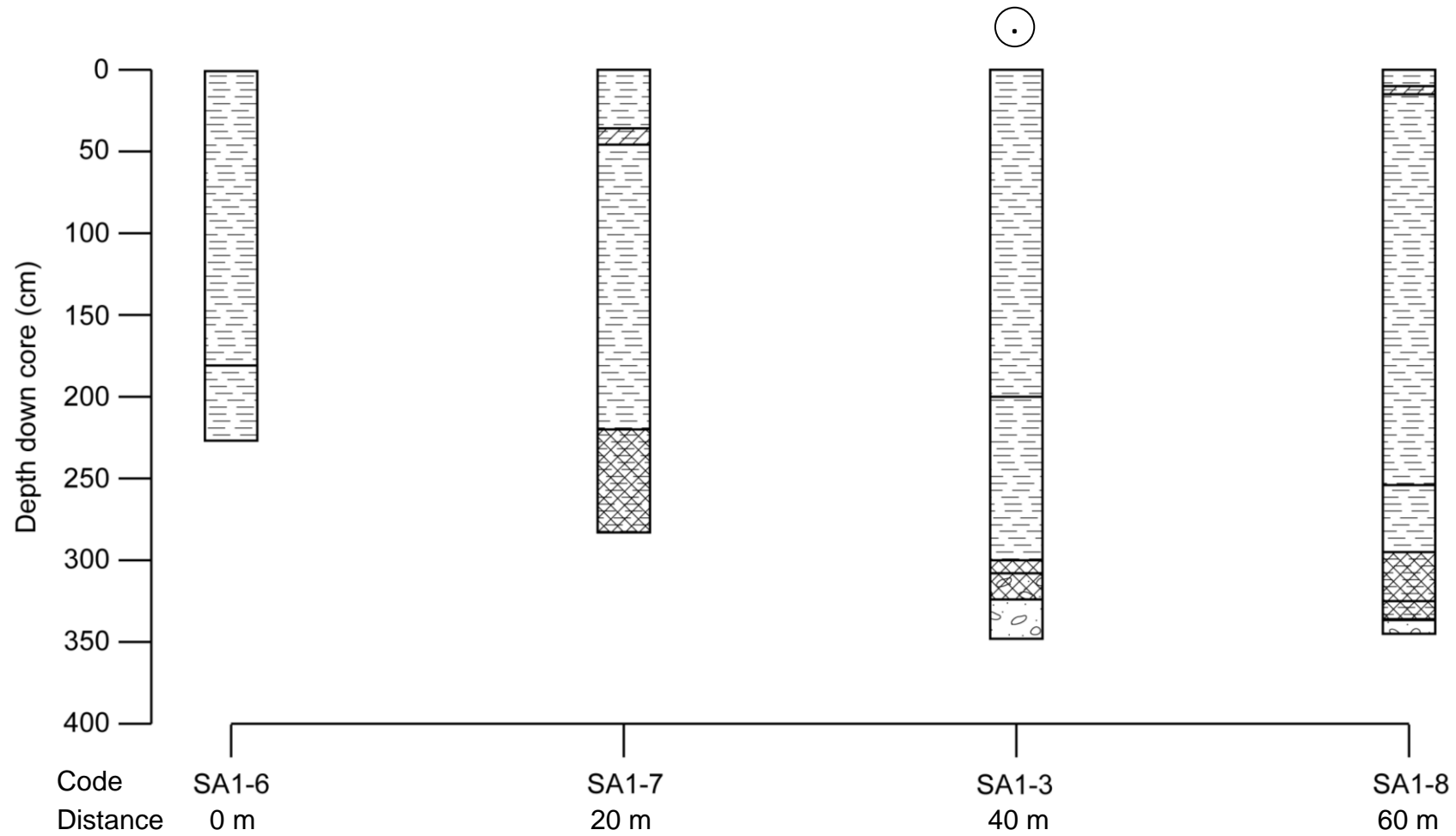


Figure 5.11: North-South transect of the Saurar 1 site, showing basin stratigraphy (see Figure 5.4 for key). Sampled core highlighted by circle.

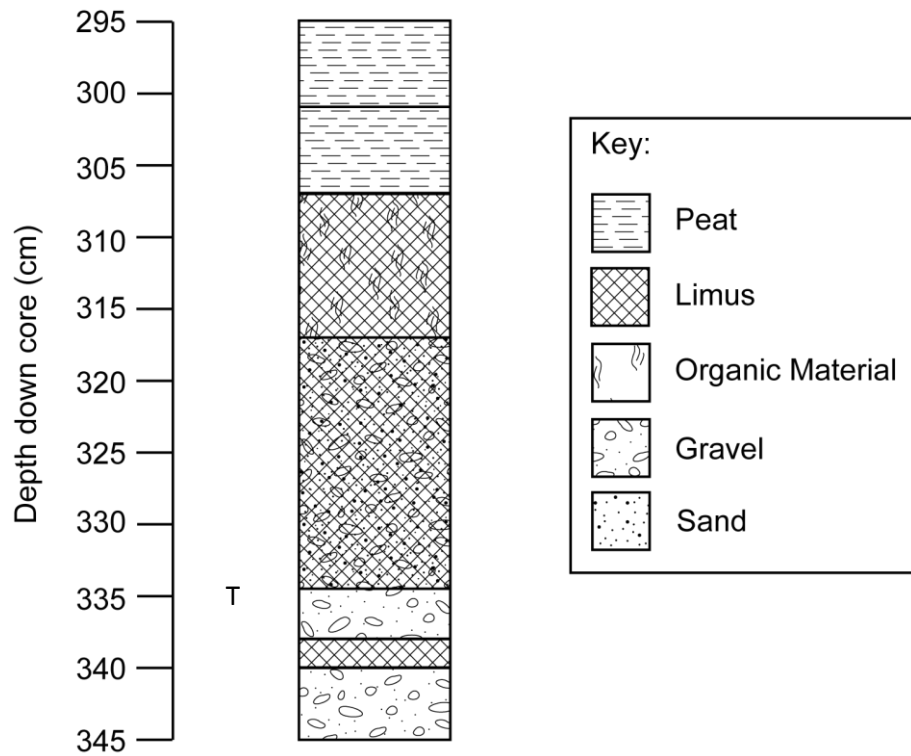


Figure 5.12: Sediment stratigraphy for the analysed section of the SA1-3 sediment core.

Top (cm)	Bottom (cm)	Description of sediment	Tröels-Smith
295	301	Dark brown turfa peat	Th4
301	307	Mid brown sphagnum peat	Th4
307	317	Mid brown-olive limus with rootlets	Ld3 Th1
317	334.5	Olive green limus with sand and gravel	Ld2 Gmin1 Gmaj1+
334.5	338	Dark grey gravel	Gmaj4
338	340	Olive green limus	Ld4
340	345	Dark grey gravel	Gmaj4

Table 5.5: Tröels-Smith classifications and sediment descriptions for the SA1-3 sediment core.

The sedimentary record from the site clearly demonstrates the dominance of freshwater influences at Saurar 1. It is also clear that during this period, there were two distinct periods of higher energy marine influence, leading to the deposition of the gravel layers noted in the sedimentary record. In addition to this, the record provides clear evidence of the transition from freshwater induced lake sediments to the generation of terrestrial organic material. This transition is further

reinforced by the change from sphagnum to turfa peat, which suggests the development of flora at the site.

Following the coring of the site for the determination of site stratigraphy and sample core extraction, it was necessary to determine the basin sill location. In order to establish the location of the basin sill, ten cores were retrieved using the gouge corer, as summarised in Figure 3.13. The sill is identified as lying at SA1-S1 close to the drainage channel with is visible at ground surface at this point of the basin.

5.6.2 *Diatom flora*

A total of 8 diatom samples were retrieved to establish the environmental changes that occurred at the site. The diatom assemblage can be found in Figure 5.13 with the raw data being presented in the Appendix. The basin shows a possible microfossil isolation contact at 335 cm, demonstrated by the disappearance of brackish and marine species within the site assemblage.

The diatom assemblage for the Saurar 1 site shows a dominance of freshwater species throughout the sequence. The diatom assemblage can be separated into three distinct zones: SA1-DZ1, which has a marine and brackish component; SA1-DZ2, which demonstrates the termination of the marine component and subsequent termination of the brackish component and SA1-DZ3, which is dominated by freshwater taxa. The base of the core has low abundances of marine and brackish diatoms, which occur throughout the gravel layer occurring between 334.5 cm and 338 cm.

Throughout SA1-DZ1, between 340 and 337 cm, the levels of these marine and brackish species are low, with *Cocconeis disculus*, *Cocconeis stauroneiformis*, *Gyrosigma hippocampus* and *Nitzschia sigma* being the only species reaching 3% or more of the total count. Despite this, there is a marine and brackish component to the diatom assemblage and this is therefore likely to represent the final stages of the isolation of the lake basin. Samples enumerated below 340 cm had no diatoms present, hence SA1-DZ1 beginning at 340 cm.

In SA1-DZ2 (337 cm to 333 cm), the brackish component of the assemblage decreases, leading to an assemblage free of brackish species above 334 cm. That said, there is remains a brackish influence until 322 cm, as demonstrated by

the very low levels of fresh-brackish taxa. The zone demonstrates the point of basin isolation, at 333 cm, with the withdrawal of the brackish species.

Above 333 cm, in SA1-DZ3, the diatom flora is dominated by almost entirely freshwater forms (~90%), indicating a freshwater environment with a small brackish component. Low levels of fresh-brackish species occur towards the bottom of this zone, with freshwater and salt intolerant species remaining relatively constant throughout. Many of the species present also remain relatively constant, such as *Fragilaria brevicostata* and *Fragilaria construens*. As with previous sites, the freshwater zone is dominated by *Fragilaria* species. Other freshwater species increase through this zone, with *Epithemia zebra* and *Navicula thorodsseni* being particularly notable. As these species increase, *Fragilaria* species decrease.

The assemblage at Saurar 1 demonstrates a brackish-marine signal at the base of the analysed section of the Saurar 1 core, with a weak fresh-brackish component existing until 322 cm. The core sequence is dominated by freshwater species throughout and therefore, as mentioned, it is likely that the diatom assemblage at the site represents the final stages of the isolation process. The transitional sequence is less clear at Saurar 1 than at other sites analysed during this study; however, this is likely to be due to the fact that the underlying sediment recording stronger brackish and marine influences was not sampled at this site. There is a sufficient marine and brackish component at the bottom of the analysed core sample to determine that the assemblage demonstrates the basin isolation at 334 cm.

5.6.3 *Environmental Summary*

It is clear from the diatom inferred environmental record that the analysed section of the SA1-3 sediment core represents the final stages of isolation. The weak brackish diatom signal at the base of the section, coupled with the gravel and sand layers present, suggests high energy coastal processes occurred at the site. The dominance of oligohalobous species throughout the upper sections of the core sample suggest that the analysed section represents the completion of isolation and subsequent freshwater dominance, which is supported by the prevalence of organic sediments within the upper sections of the analysed section. A lack of diatoms below 340 cm means that the entire isolation cannot be determined.

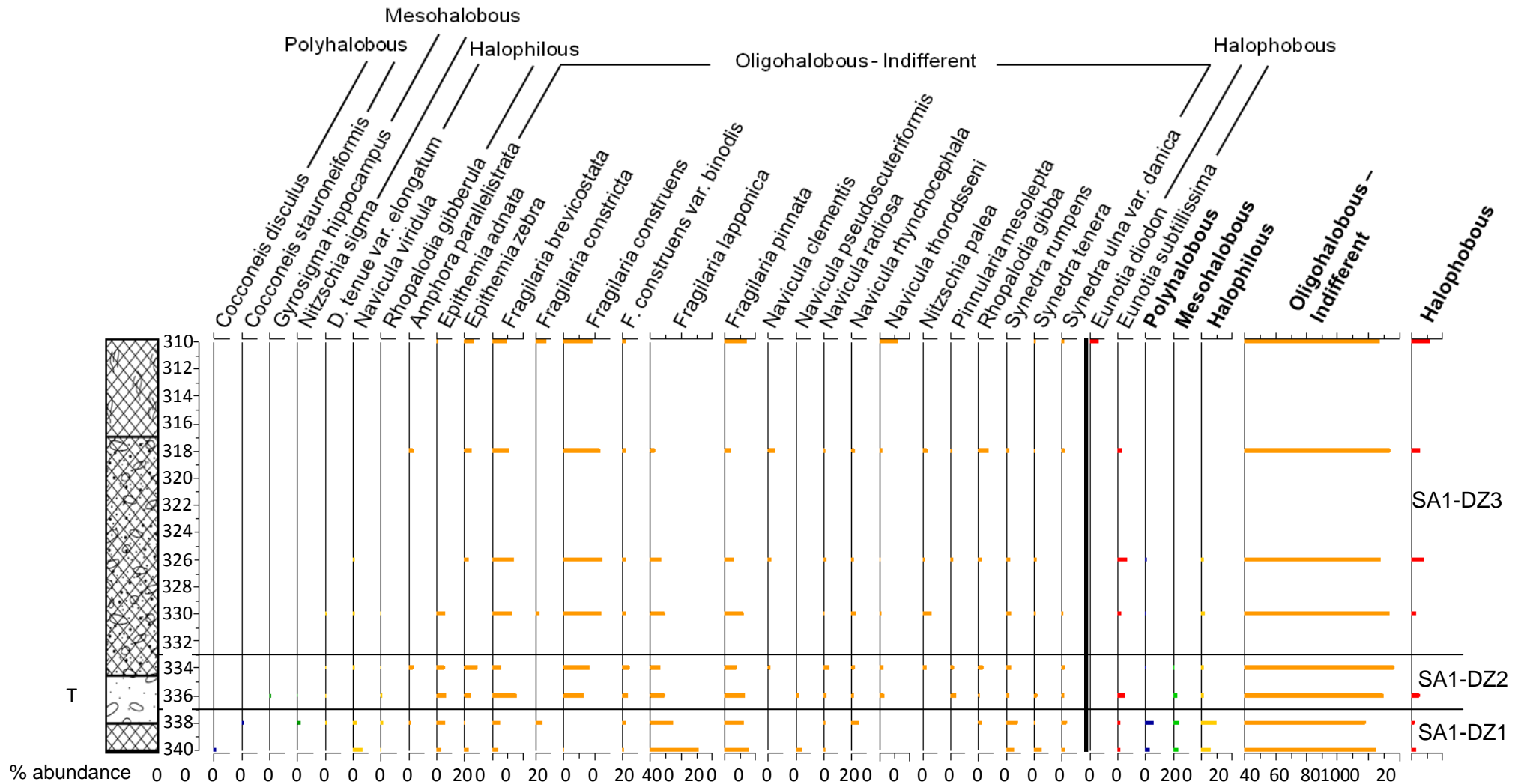


Figure 5.13: Diatom assemblage diagram for the Saurar 1 site, showing the limited brackish influences at the base of the analysed section, with the dominance of freshwater species being apparent throughout (see Figure 5.12 for the key to sediment composition).

5.7 Helgafellsvatn (HE1)

Sill Height: 12.77 ± 0.3 m above MSL Location: 65°2'18.87"N 22°44'23.25"W

The site stratigraphy was established through the coring of a single transect of five cores along the edge of the lake basin within the infilled section (Figure 3.14; 5.14). The scale of the lake made use of the boat problematic, as it would have been difficult to ensure the stability of the boat and the sampling equipment. The core extracted for analysis was HE1-4, which was sampled for both diatom and tephra analysis.

5.7.1 Stratigraphy

The site stratigraphy is summarised in Figure 5.14 with the ground surface again assumed to be level. This is likely to be the case however, due to all cores being retrieved from as close to the edge of Helgafellsvatn as possible, within a flat, low-lying section of the basin. In total, five cores were taken at the site to determine the underlying stratigraphy. One core sample was retrieved from the site for analysis at HE1-4. Core HE1-4 was chosen for the microfossil and tephra analyses as it demonstrated the most representative sample of the lake basin stratigraphy.

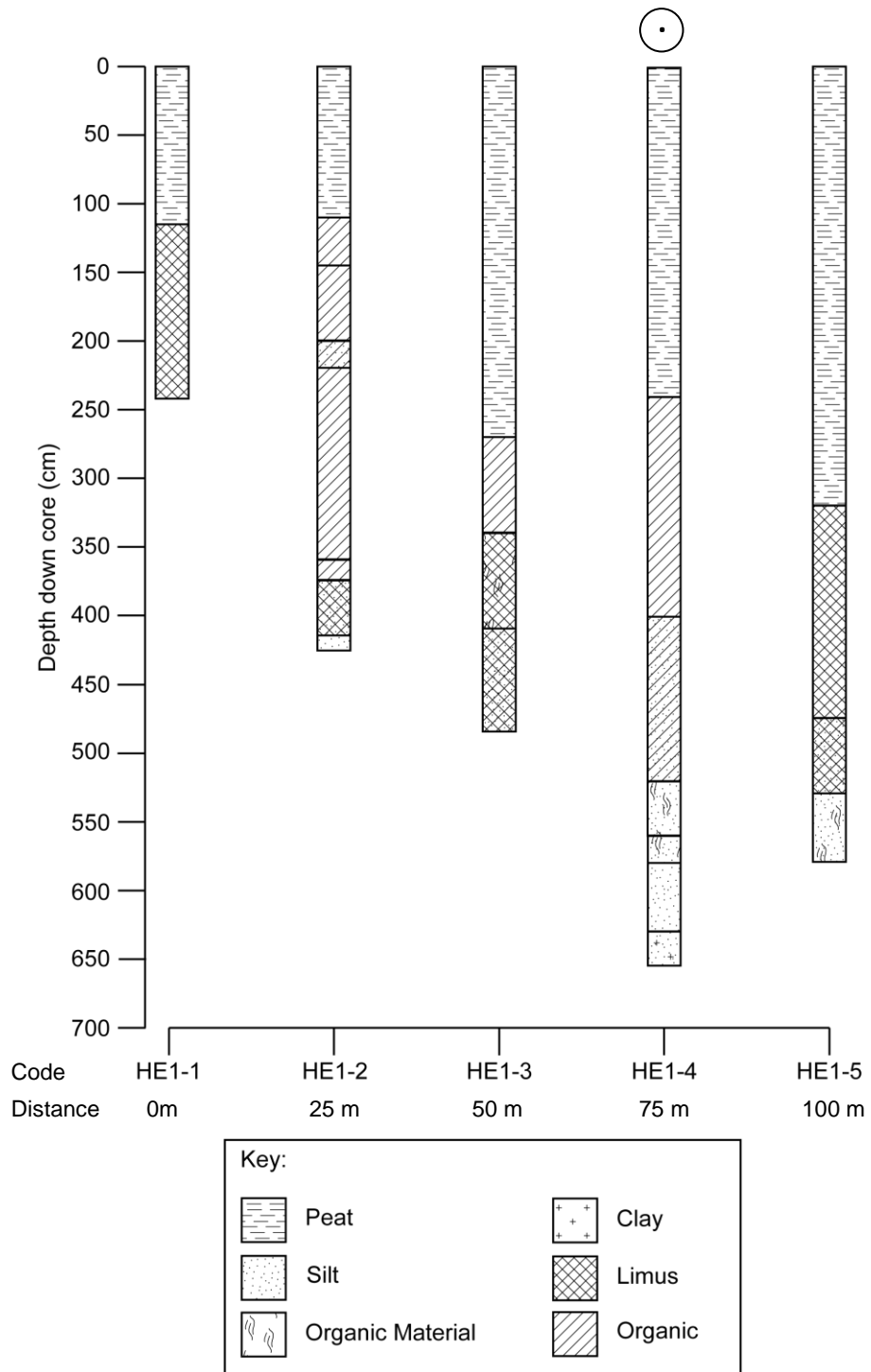


Figure 5.14: Sediment stratigraphy for the Helgafell site, showing the results for cores HE1-1 to HE1-5.

The core stratigraphy for HE1-4 is summarised in Figure 5.15, which shows the sediment composition, with Tröels-Smith (1955) classifications and sample points within the core being summarised in Table 5.6.

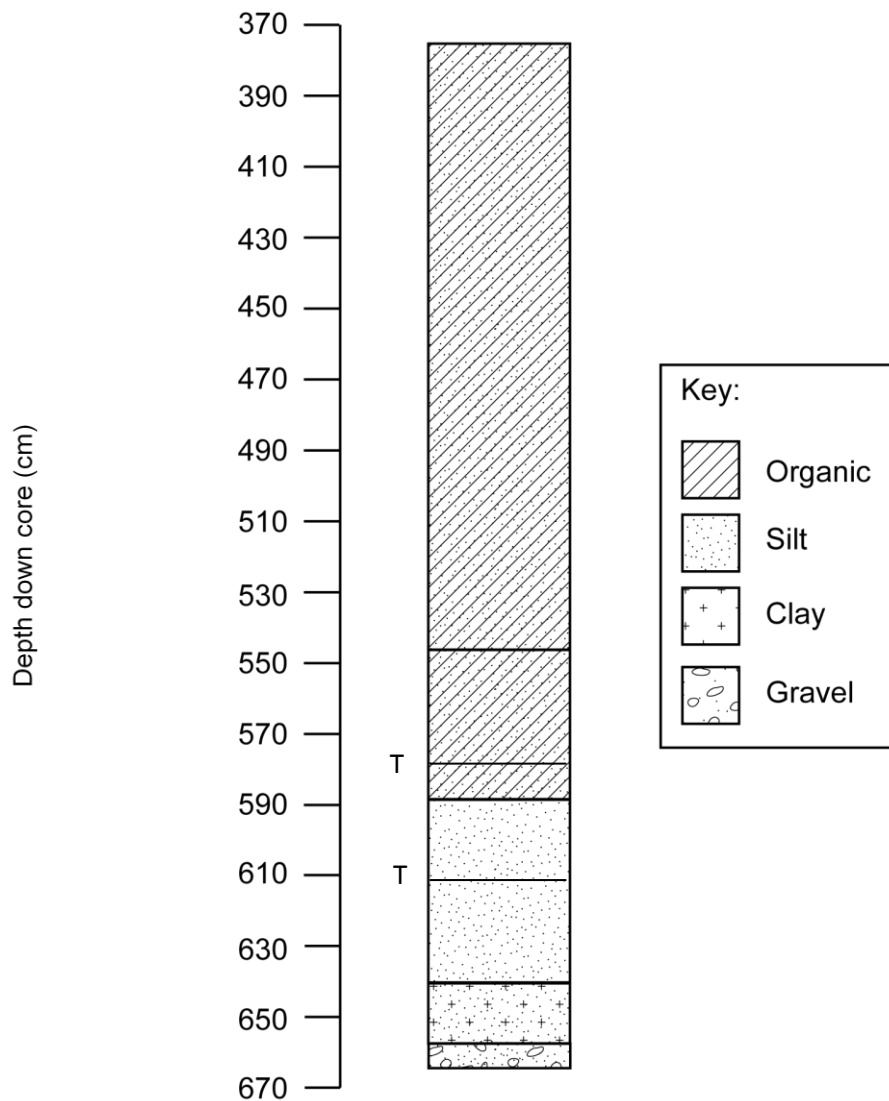


Figure 5.15: Sediment stratigraphy for the analysed portion of the HE1-4 sediment core retrieved from Helgafellsvatn., showing the transition from predominantly inorganic to predominantly organic sediments. The diagram also highlights the position of the tephra samples within the core sample.

The core stratigraphy can be divided into nine distinct layers, as outlined in Figure 5.15, with the sedimentary isolation contact being found at 590 cm.

<i>Top (cm)</i>	<i>Bottom (cm)</i>	<i>Descriptions of sediments</i>	<i>Tröels-Smith</i>
375	546	Olive green silty organic material	Ag2 Ld2
546	578	Olive green organic rich silt	Ag3 Ld1
578.30	578.2	Dark grey tephra layer	Gmin4
578.2	590	Olive green organic rich silt	Ag3 Ld1
590	615	Olive green-grey organic rich silt with	Ag3 Ld1

		some sand	As+
615.0	615.2	Dark grey tephra layer	Gmin4
615.2	640	Olive green-grey silt with some sand	Ag4 As+
640	664	Blue-grey silty clay	Ag3 As1

Table 5.6: Tröels-Smith classifications and sediment descriptions for the HE1-4 sediment core.

The propensity of silts and sands towards the bottom of the analysed section suggests that the site was dominated by low energy coastal processes, as demonstrated by the dominant grain sizes. The shift from clastic dominant to organic dominant sediments is also abundantly clear at the Helgafellsvatn site.

Following the determination of basin stratigraphy and sedimentary record, the isolation basin sill was identified. The sill coring pattern is summarised in Figure 3.18, showing the location of the sill close to Helgafellskirkja, located at point HE1-S3.

5.7.2 Diatom flora

A total of 15 samples were taken from core HE1-4 for diatom analysis. A minimum of 200 diatoms were counted per sample, ensuring a valid sample for analysis. The diatom assemblage is summarised in Figure 5.16 below, with the raw counts, for all sites, being presented in the Appendix. The microfossil isolation contact can be clearly seen at 618 cm. The microfossil isolation contact and sedimentary isolation contact are therefore in close proximity within HE1-4.

The assemblage at Helgafellsvatn can be divided into three principal zones: a lower marine-brackish zone (HE1-DZ1, 660 cm to 635 cm), an intermediate transitional zone dominated by freshwater species (HE1-DZ2, 635 cm to 616 cm) and an upper freshwater zone (HE1-DZ3, 616 cm to 560 cm).

The lower brackish-marine zone, HE1-DZ1, is dominated by *Cocconeis stauroneiformis*, *Nitzschia sigma* and *Tabularia fasciculata*, which all reach 20 % of the total count at some point during the zone. In addition to these species, several others reach at least 5 % of the total count. The marine species decrease from ~ 50 % to around 15 % of the total count within this zone, with the brackish species increasing from 40 % to 60 % of the total count.

Following this brackish marine zone, the levels of marine and brackish species decrease during the transitional phase, HE1-DZ2, between 635 cm and 622 cm. Marine species disappear entirely at the start of the zone, with brackish species falling below 10 % of the total count. During this transitional phase, the levels of freshwater species increase dramatically, with freshwater species making up over 80 % of the total count at 624 cm. This increase is primarily composed of *Fragilaria construens* and *Synedra tenera*. The 624 cm sample also sees the introduction of salt intolerant species, with the first occurrence of *Tabellaria fenestrata*.

The final zone, HE1-DZ3 (622 cm to 560 cm), is dominated by freshwater species, with *Fragilaria construens*, *Fragilaria pinnata* and *Synedra tenera* being the most populous. This zone also sees an increase in salt intolerant species, with *Tabellaria fenestrata* being present in relatively high levels throughout the zone. This three phase sequence shows the clear transition between marine-brackish and freshwater conditions at the Helgafellsvatn site, highlighting the isolation at 616 cm.

5.7.3 Environmental Summary

It is clear from the diatom induced environmental interpretation that basin isolation occurs at 632 cm. After this point, brackish-marine influences at the site decrease over time. This is supported by the increases in organic material within the sedimentary record and the commencement of oligohalobous and subsequent halophobous species dominance within the diatom record from the site. It is also apparent that the processes occurring at the site are predominantly low energy, with the dominance of silt and sand layers at the base of the analysed section suggesting a lack of high energy events at the site. As at Þingvallavatn, this site is relatively far inland of a potential early Holocene coastline, suggesting that the potential for high energy influences at the site are diminished. The transitions within the sedimentary sequence are supportive of the inferences made from the diatom species assemblage, with the isolation contact being evident at 632 cm.

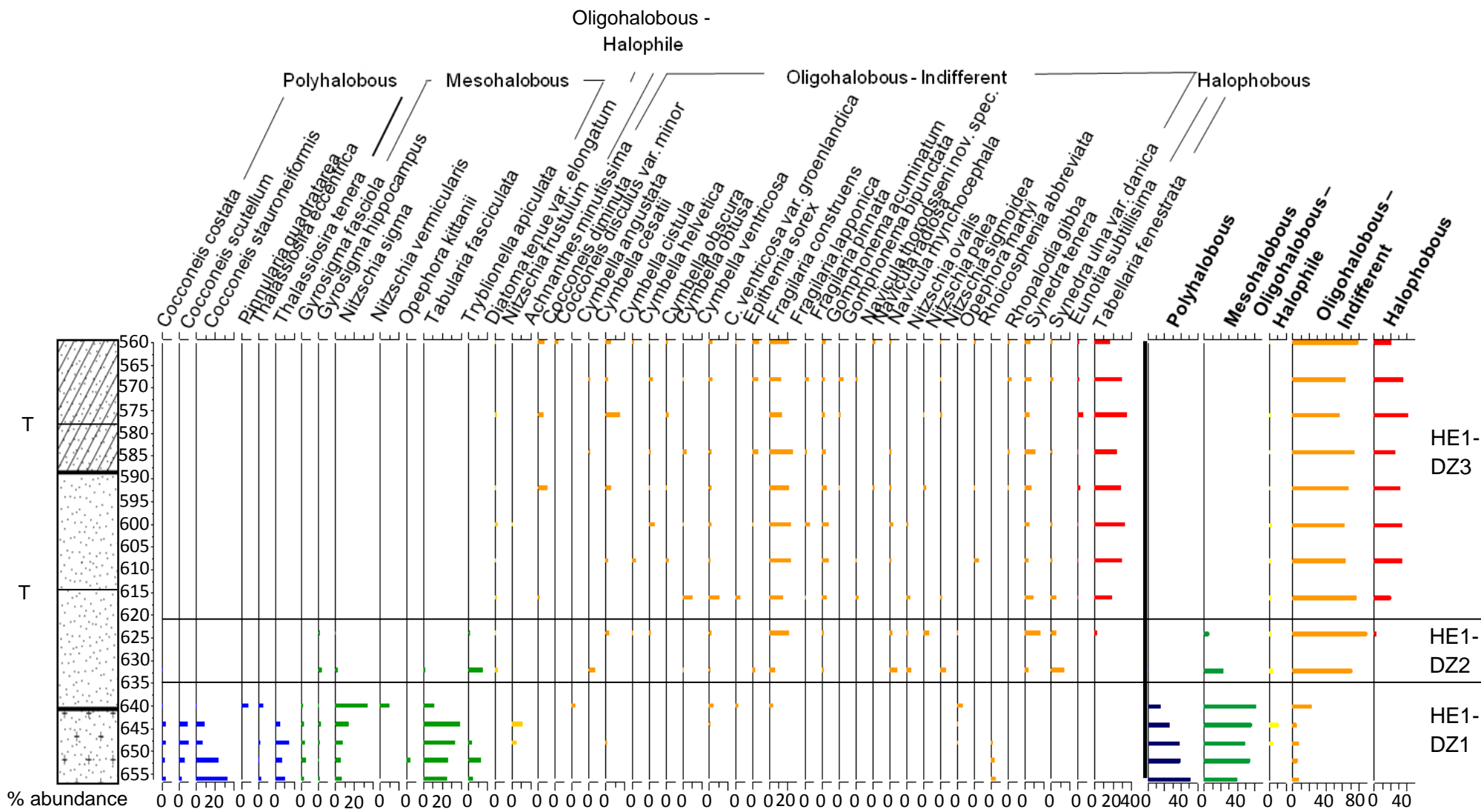


Figure 5.16: Diatom assemblage diagram for the Helgafellsvatn site, showing the shift from marine-brackish to freshwater species. See Fig. 5.15 for stratigraphic key.

5.8 Saurar 3 (SA3)

Sill Height: 16.20 ± 0.3 m above MSL Location: 65°0'18.79"N 22°43'6.19"W

Due to the limited area of infilled basin and the difficulties of using the boat at the Saurar 3 site, two cores were collected from the basin, with SA3-1 being sampled with a Livingstone corer and returned to Durham for analysis.

5.8.1 Stratigraphy

The detailed core stratigraphy for Core SA3-1 is presented in Figure 5.17. The sedimentary results from the site highlight the decrease in energy within the coastal processes operating at the site, as demonstrated by the transition from gravel to silts and clays.

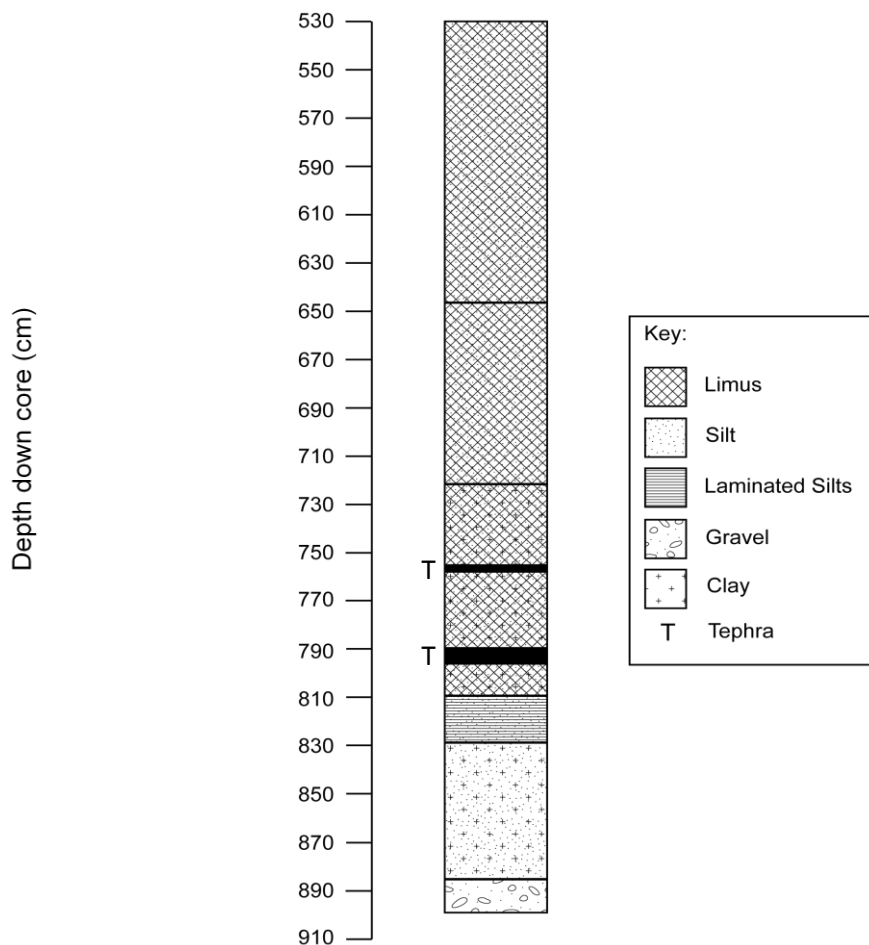


Figure 5.17: Sediment stratigraphy of the section of the SA3-1 sediment core extracted for diatom, tephra and radiocarbon analyses.

The sill at Saurar 3 was determined through the retrieval of 15 cores in the pattern summarised in Figure 3.18. The sill was identified at point SA3-S5 to the westernmost point of the basin.

5.8.2 *Diatom flora*

A total of 15 diatom samples were taken between 755 cm and 845 cm from Core SA3-1 for analysis. The diatom assemblage for the site can be seen in Figure 5.18, which demonstrates a clear microfossil isolation contact at 810 cm. The diatom assemblage shows a clear transition between marine and brackish influences and freshwater conditions. The assemblage at Saurar 3 can be divided into five clear zones: SA3-DZ1, a basal marine-brackish zone (845 cm – 825 cm); SA3-DZ2, a brackish phase (825 cm to 810 cm); SA3-DZ3, a lower freshwater zone (810 cm to 804 cm); SA3-DZ4, a middle freshwater zone (804 cm to 790 cm) and SA3-DZ5, an upper freshwater zone (790 cm to 755 cm).

The basal marine-brackish zone, SA3-DZ1, is dominated by *Cocconeis peltoides*, *Thalassiosira hyalina* and *Melosira nummuloides*. During the zone, the levels of marine species decrease, with brackish species increasing. Very low levels of freshwater species are also found during this zone. Above this basal zone, the brackish phase, SA3-DZ2, is dominated by *Melosira nummuloides*, with low levels of *Nitzschia ovalis* and *Nitzschia sigma* also being present. During this zone, levels of freshwater species increase, with *Nitzschia palaeacea* and *Fragilaria lapponica* becoming more numerous. During zone SA3-DZ3, brackish species occur only at very low levels, with freshwater species dominating the assemblage. Levels of *Cymbella ventricosa*, *Fragilaria construens*, *Fragilaria construens* var. *binodis*, *Fragilaria lapponica*, *Fragilaria pinnata* and *Melosira italica* all increase during this zone. As such, there is a dramatic increase in the levels of freshwater species, rising from ~ 40 % in the previous zone to ~ 80 % in this lower freshwater phase. The diatom assemblage in zone SA3-DZ4 demonstrates a further increase in the freshwater species, principally due to an increase in the levels of *Fragilaria construens*. Despite this, levels of *Fragilaria lapponica* and *Fragilaria pinnata* decrease. The levels of fresh-brackish species also decrease during this zone. The upper freshwater zone, SA3-DZ5, is characterised by high levels of *Fragilaria construens* and *Tabellaria fenestrata*. In relation to the previous zone, many of

the freshwater species remain at similar levels, however the introduction of *Tabellaria fenestrata* in such large quantities (10 % to over 40 % of the total count) is significant in demonstrating the freshwater nature of the basin.

As a result of the above zonation, the clear transition between marine-brackish, brackish, freshwater and subsequent high levels of salt intolerant species can be seen. This zonation also therefore demonstrates the isolation of the basin and therefore RSL fall in the area.

5.8.3 *Environmental Summary*

It is clear from the environmental interpretation of the diatom record at the Saurar 3 site that marine influences are diminishing over the course of the record (Figure 5.18), with the isolation contact occurring at 810 cm. This is supported by the sedimentary evidence presented from the site (Figure 5.17), which shows a decrease in the levels of clastic sediments at the site over time. The increases in oligohalobous and halophobous species towards the top of the analysed section highlight further the transition to freshwater dominance and decreased marine influences at the site. This is again supported by the sedimentary evidence, with increases in the levels of organic material apparent at the site towards the top of the analysed core section. As such, the environmental interpretation from the diatom results highlight the transition from polyhalobous and mesohalobous dominance to oligohalobous dominance and therefore allows the inference of decreased marine influences over time.

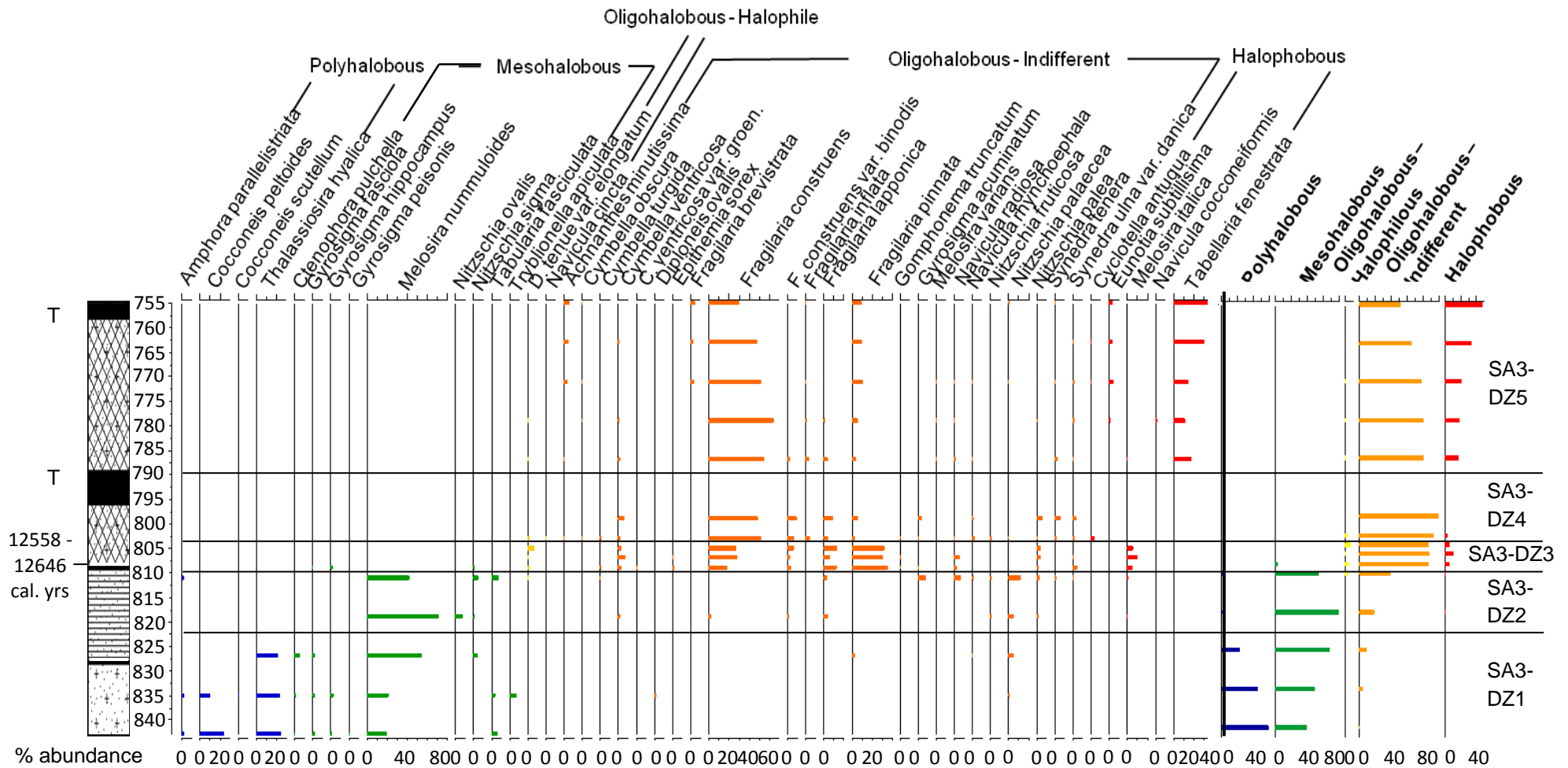


Figure 5.18: Diatom assemblage diagram for the Saurar 3 site, showing the transition from marine-brackish to brackish and subsequent freshwater dominance. See Fig. 5.17 for key to stratigraphic composition with black representing a thick tephra deposit (not present in key).

5.9 Marine Limit Sites

5.10.1 Setbergsa

The initial marine limit measurement was taken from the Setbergsa region, approximately 11 km SE of Stykkishólmur (Figure 3.1). The marine limit was measured based on the altitude of the highest raised beach found and gave a value of 61.01 m above MHWST (based on measurement using differential GPS). In order to provide a value relative to mean sea level (m asl), the elevation measurement for the Setbergsa site requires correction using tide gauge data. In this study, suitable tide gauge data has been found at the Icelandic Hydrographic Service (Icelandic Hydrographic Service, pers. comm. a), as outlined in the previous chapter. The data required to determine a value relative to m. s. l. is as follows:

Tidal Statistics for REYKJAVIK **Latitude 64°09' N Longitude 21°56' W**

Port details: Reykjavík
Datum of Predictions = Chart Datum
Highest Astronomical Tide (HAT): 4.62 metres
HAT occurs at 07:14 GMT on 20/02/2015
Lowest Astronomical Tide (LAT): -0.30 metres
LAT occurs at 01:01 GMT on 18/09/1997
Maximum Tidal Range possible: 4.78 metres
Mean High Water Spring (MHWS): 4.01 metres
Mean High Water Neap (MHWN): 2.98 metres
Mean Low Water Neap (MLWN): 1.38 metres
Mean Low Water Spring (MLWS): 0.36 metres
Tide Type: 0.10 (semidiurnal)
Shallow Water Influence: 0.02

As such, the correction to MSL can be determined as:

$$((\text{MHWS} - \text{MLWS}) / 2) + \text{MLWS} = \text{MSL (m above datum)}$$

$$((4.01 - 0.36) / 2) + 0.36 = 2.185 \text{ m above datum}$$

$$((\text{MHWN} - \text{MLWN}) / 2) + \text{MLWN} = \text{MSL (m above datum)}$$

$$((2.98 - 1.38) / 2) + 1.38 = 2.18 \text{ m above datum}$$

Therefore, MSL is 2.18 m above datum.

The elevation at Setberg was therefore determined as 62.84 ± 0.25 m above MSL, which was calculated following the addition of MHWST to the elevation, followed by the subtraction of the MSL figure.

For the Snæfellsnes sites, the marine limit is assumed to have formed between MHWST and HAT due to the nature of the formation. As such, the indicative meaning used will be MHWST-HAT. This is calculated by taking an average of the HAT and MHWST elevations and then subtracting the height of MSL to determine the required adjustment from MHWST-HAT to MSL. Therefore the correction for the data is $+ 2.13 \pm 0.33$ m for Reykjavik.

Results for Stykkishólmur do exist and were also provided by the Icelandic Hydrographic Service (Icelandic Hydrographic Service, pers. comm. B); however, the dataset only contains data for a 199 day period and thus the Reykjavik data was determined as more reliable. As such, corrections were made at all sites using the calculations made from the Reykjavik data.

5.10.2 Barar

The Barar marine limit was taken in the mid-Snæfellsnes region outlined in Chapter 3 and Figure 3.1. Differential GIS was again used at the Barar site to provide a measurement for highest postglacial RSL based on the altitude of the highest raised beach at this location. The Barar measurement returned a value of 67.04 m a MHWST. As with the elevation recorded for the Setbergsa site, a correction to ensure the site is relative to m. s. l. is required, as outlined above. The elevation of the site is calculated as 68.87 ± 0.35 m above MSL following the necessary adjustment. As above, the indicative meaning is 2.13 ± 0.33 m.

5.10 Chronological Data

In this section, the results of the chronological analyses will be presented, as well as a determination of the possible correlations between core samples. The implications of these results will then be further discussed in Chapter 7 to provide an insight into the regional context. Tephra samples were present in the majority of sediment cores, with eight samples being analysed at the NERC Tephra Facility at the University of Edinburgh. Tephra layers were therefore extracted from five of the sediment core samples, with eight tephra samples

being analysed in total for their geochemical composition. In addition to these analysed tephra layers, radiocarbon samples were extracted from three of the sediment core samples: Borgarland 10, Þingvallavatn and Saurar 3. Radiocarbon samples were extracted from these sites either due to the lack of a tephra layer or due to the distance between the microfossil isolation contact and a sampled tephra being greater than 2 cm.

5.11.1 Radiocarbon analyses

5.11.1.1 Borgarland 10 (Core elevation: 3.08 m asl)

Due to a lack of tephra layers for analysis, a radiocarbon sample was taken from the BO10 core between 50 cm and 50.5 cm, which had a mass of 2.45 g. The radiocarbon sample was removed from this point of the core due to its proximity to the decrease in marine influence identified in the microfossil records. The radiocarbon sample (BO10-50) returned a date of 6240 ± 40 ^{14}C yrs BP (7156 – 7252 cal. yrs BP).

5.11.1.2 Þingvallavatn (Sill altitude: 5.34 ± 0.3 m asl)

A radiocarbon sample was extracted from the Þingvallavatn sediment core between 496 cm and 498 cm and had a mass of 2.12g. The sample, TH1-R1-496, returned an uncorrected ^{14}C date of 9710 ± 60 ^{14}C yrs BP (11089 – 11219 cal. yrs BP). The radiocarbon sample was extracted from the sediment core due to the lack of a dated tephra close to the isolation contact. As a result, the radiocarbon sample was taken from 496 – 498 cm immediately above the isolation contact.

5.11.1.3 Saurar 3 (Sill altitude: 16.20 ± 0.3 m asl)

The final radiocarbon sample analysed was taken from the SA3-1 sediment core between 809 cm and 810 cm, having a mass of 4.04 g. The sample was analysed due to the lack of close proximity between the tephra samples and microfossil and sedimentological isolation contacts at the site. The sample returned a ^{14}C age of 10670 ± 60 ^{14}C yrs BP (12558 – 12646 cal. yrs BP).

5.11.2 Tephrochronological data

Tephra samples were extracted from the Skjaldarvatn, Þingvallavatn, Saurar 1, Helgafellsvatn and Saurar 3 sediment cores, with eight samples being analysed. Tephra layers have been noted previously in Snæfellsnes; however,

their geochemical composition has not yet been widely published (Langdon and Barber, 2001). Over the course of the Holocene, it is known that the Snæfellsjökull volcano erupted several times, depositing tephra throughout the majority of the Snæfellsnes peninsula. The principal eruptions from the Snæfellsjökull system are Sn-1, Sn-2 and Sn-3 (Jóhannesson *et al.*, 1981), which occurred at 1750 ± 150 yrs BP, 3960 ± 100 yrs BP and 7000 – 9000 yrs BP respectively (Steinthórsson, 1967). The other volcanic systems in the Snæfellsnes peninsula have received very little attention and as such, their geochemical signature is presently also poorly understood.

When analysing tephra results, a series of graphs are usually constructed in order to aid in the identification of the analysed tephra samples. In this study, FeO vs. TiO₂, K₂O vs. P₂O₅, FeO/TiO₂ vs. SiO₂ and FeO/MgO vs. TiO₂ were employed; however, the FeO vs. TiO₂ and K₂O vs. P₂O₅ graphs are presented here. Standard profiles exist for FeO vs. TiO₂ and so have been included to aid interpretation. The construction of these graphs allows comparison with previously published records of tephra geochemistry, such as *TephraBase* (Newton, 1996; Newton *et al.*, 2007). The following systems and codes have been included on the tephra graphs (Figures 5.19 to 5.30) where possible: Snæfellsjökull (Sn), Vedde (Ved), Veiðivotn (Ve), Katla (Ka), Hekla (He), Grimsvotn (Gr) and Saksunarvatn (Sak).

5.11.2.1 Tephra Standards

Prior to the analysis of the tephra samples extracted from the Snæfellsnes sediment cores, it was essential to determine the accuracy of the electron microprobe. This was achieved through the analysis of a tephra standard. For this study, the BCR-2G standard was employed due to the basaltic nature of the tephra samples to be analysed. As such, measurements of the BCR-2G sample were taken at the start and end of each analytical session. In addition to providing information regarding the accuracy of the chemical composition analyses, the measurements provided an opportunity to determine whether the electron beam had become offset during the process. Offsetting can occur when the beam is moved too quickly between analyses and can lead to false results being generated. The results can be found in the Appendix.

5.11.2.2 Skjaldarvatn (4.57 ± 0.3 m asl)

One sample was removed from 547.3 cm to 547.5 cm and was analysed for ten major elements (Figures 5.19 and 5.20).

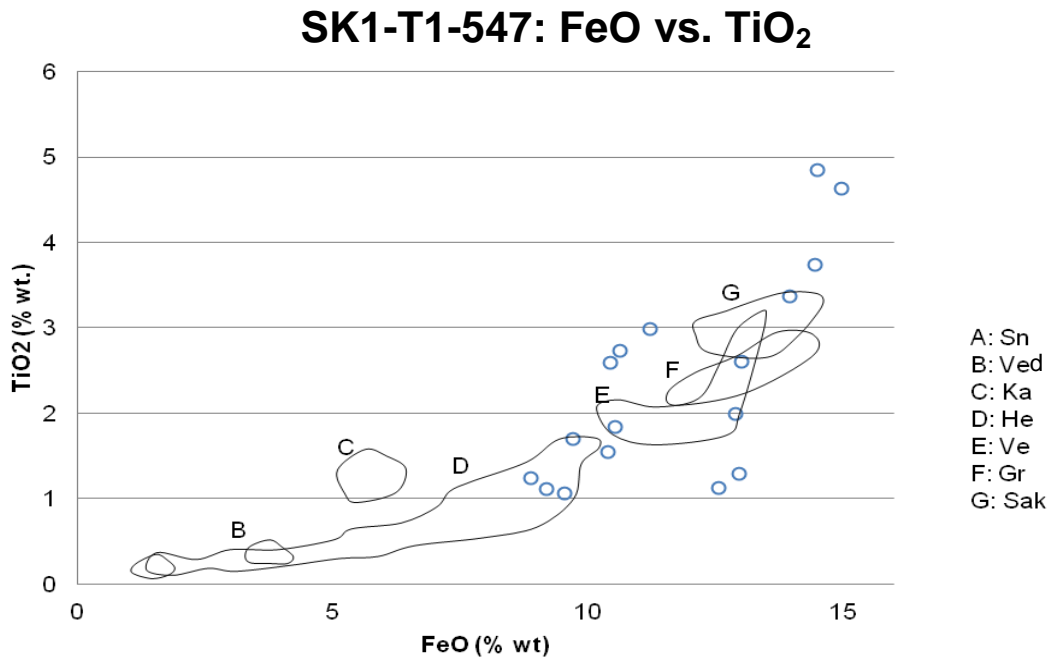


Figure 5.19: FeO percentage weight versus TiO₂ percentage weight for the SK1-T1-547 sample, showing the main cluster and a secondary higher point highlighted in other oxide combinations. Known tephra profiles are sourced from Kristjansdóttir et al. (2007) and Óladóttir et al. (2011).

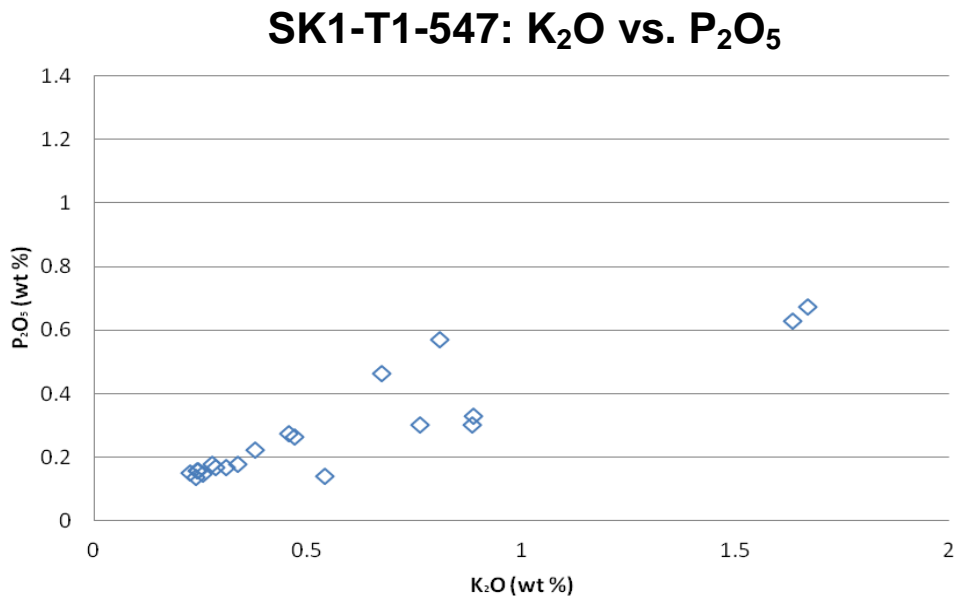


Figure 5.20: K₂O percentage weight versus P₂O₅ percentage weight for the SK1-T1-547 sample.

There is a clear cluster within the dataset, although this is not representative of the entire layer, with grains representative of several sources. This is likely due to the inwashing or reworking of previous eruption deposits within the catchment.

5.11.2.3 Þingvallavatn (5.34 ± 0.3 m above MSL)

Two samples were removed from the Þingvallavatn core: the upper tephra sample TH1-T1-456 and the lower tephra sample TH1-T2-479 (Figures 5.21 and 5.22). Figures 5.21 and 5.22 clearly demonstrate a correlation between the two samples, which both have a principal cluster with an average FeO value of 10.2% and 10.37% respectively. The small number of points outside of the principal cluster in sample TH1-T2-479 are likely sourced from inwashing of previous eruption deposits or contamination of the sample.

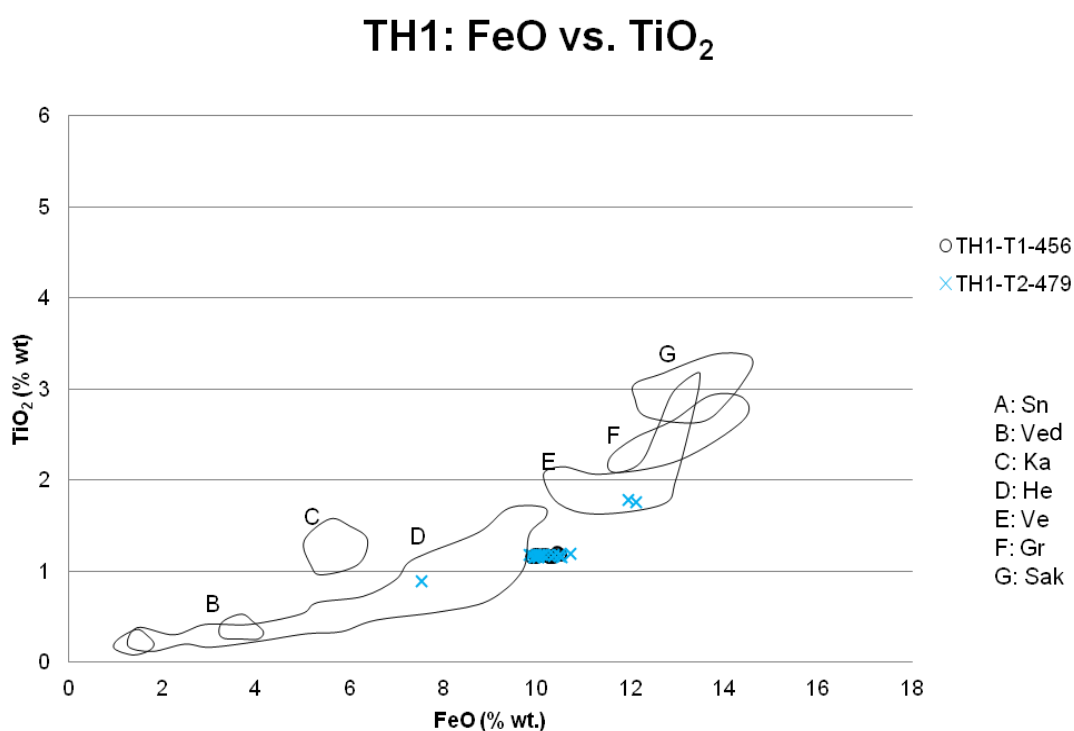


Figure 5.21: FeO vs TiO₂ for the Þingvallavatn samples, demonstrating the correlation between the two samples. Known tephra profiles are provided for comparison, being sourced from Kristjansdóttir et al. (2007) and Óladóttir et al. (2011).

TH1: K₂O vs. P₂O₅

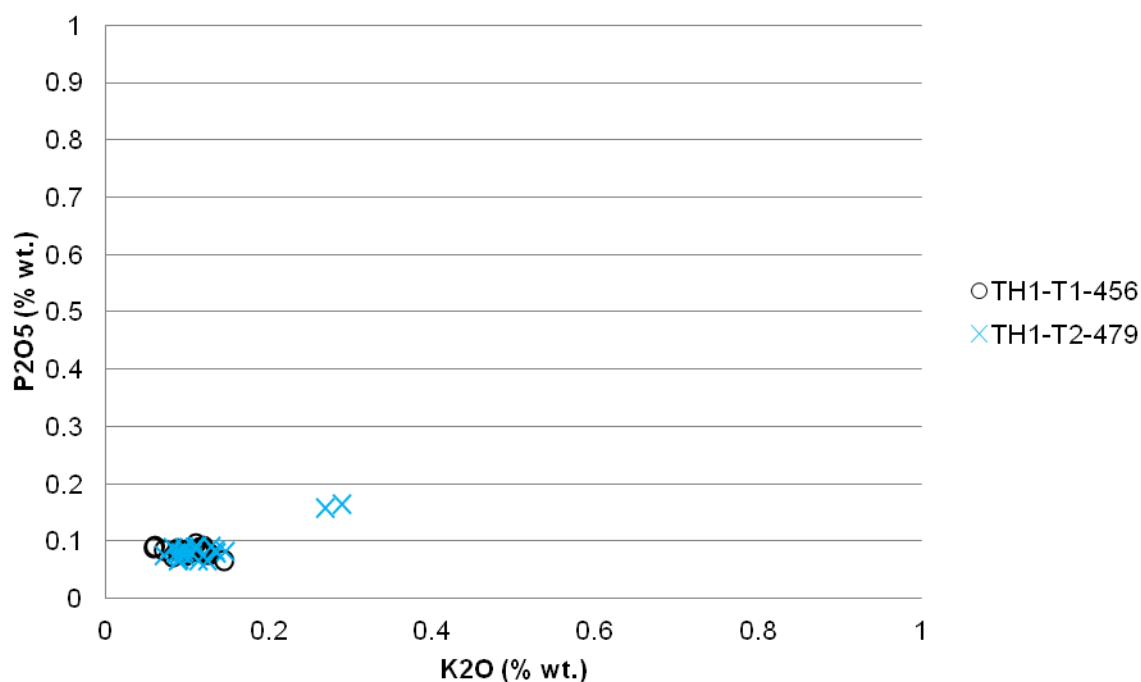


Figure 5.22: K₂O vs. P₂O₅ for the Pingvallavatn samples, showing the clustering within the sample.

It is clear that the two layers are produced by the same volcanic system and the upper layer may even represent the reworking of the lower layer. The basaltic nature of the two layers suggest that the source eruptions were from the Snæfellsnes Volcanic Belt (SVB) and are likely to originate from the Ljós fjöll Volcanic System (LVS). The geochemical composition of these systems is currently relatively poorly understood and as such, the source cannot be identified with high certainty without further research.

5.11.2.4 Saurar 1 (8.97 ± 0.3 m asl)

One sample, SA1-T1-334, was retrieved from 334.0 cm – 334.2 cm (Figures 5.23 and 5.24). The spread of the data suggests that the tephra could be sourced from three systems: Grimsvötn-type, Veiðavötn-type and the SVB. Despite not fitting the exact profile of eruptions provided, close correlation suggests that these systems may be the tephra producer. It is also worth noting here that the Saksunarvatn tephra (Sak) is derived from the Grimsvötn system.

SA1-T1-334: FeO vs. TiO₂

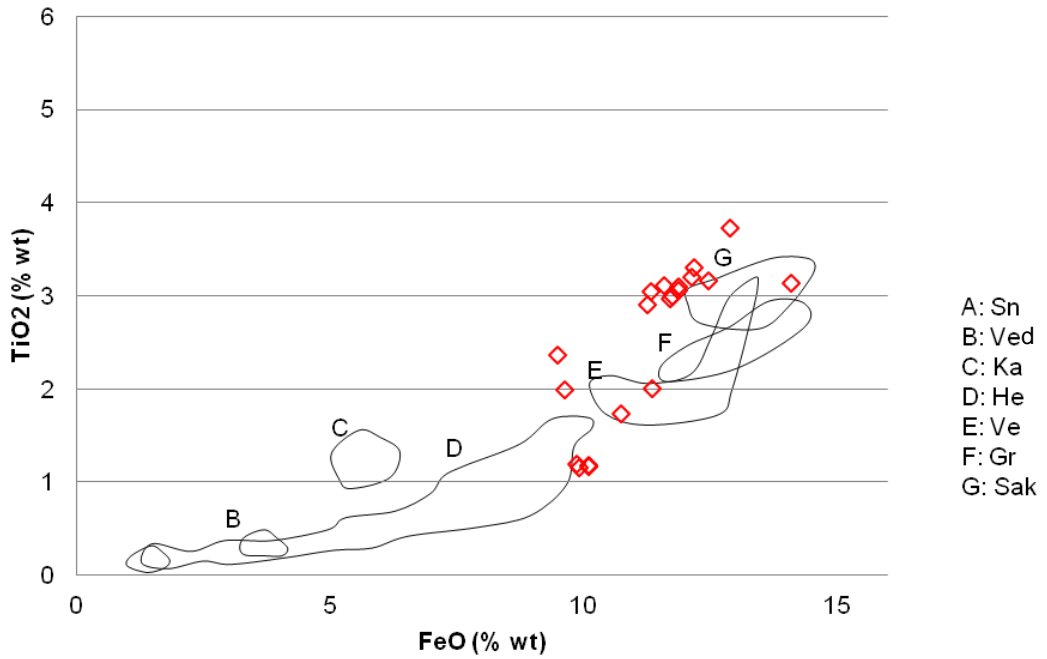


Figure 5.23 TiO₂ percentage weight versus FeO percentage weight for the SA1-T1-334 sample. Known tephra profiles are sourced from Kristjansdóttir et al. (2007) and Óladóttir et al. (2011).

SA1-T1-334: K₂O vs. P₂O₅

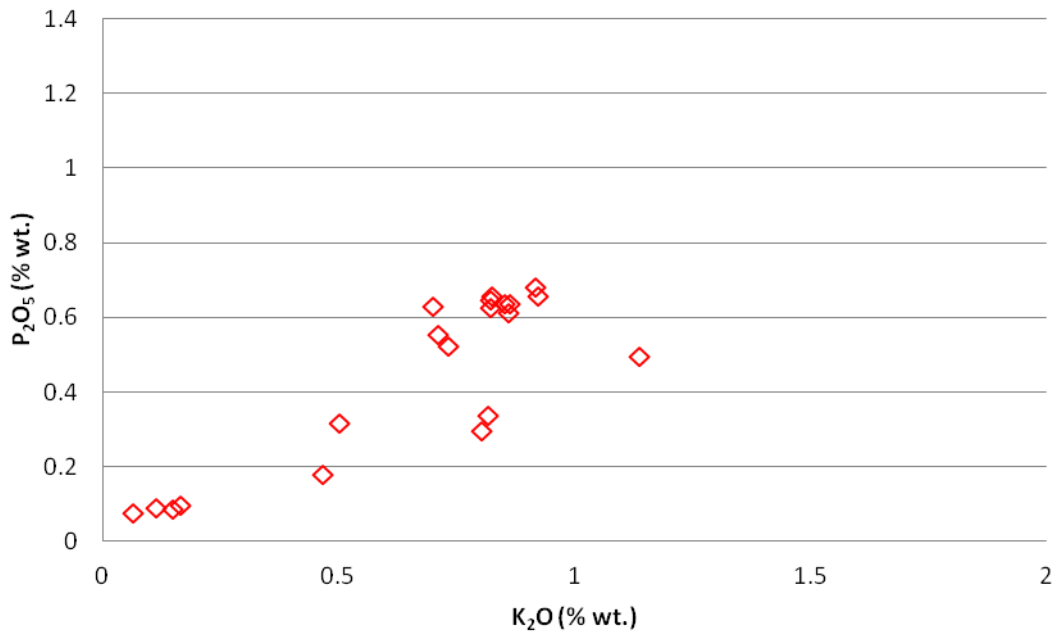


Figure 5.24: P₂O₅ percentage weight versus K₂O percentage weight for the SA1-T1-334 sample showing the widespread cluster from the sample. There appears to be some clustering at the upper and lower ends of the wider spread in the dataset.

5.11.2.5 Helgafellsvatn (12.77 m ± 0.3 asl)

Two tephra layers were sampled from the HE1-4 core, HE1-T1-578 and HE1-T2-615, which were sampled due to their proximity to the isolation contact (Figures 5.25 and 5.26). The geochemical analyses show that both samples are of mixed origin, as demonstrated by the lack of close clustering within the datasets. Both samples show a combination of Grimsvötn, Katla and Veiðavötn-type tephras, although the Veiðavötn-type is more dominant in this second tephra sample. The compositions of the tephra layers are insufficiently distinct to determine exact correlations from specific eruptions. As a result, the correlation with particular systems is all that can be achieved at present.

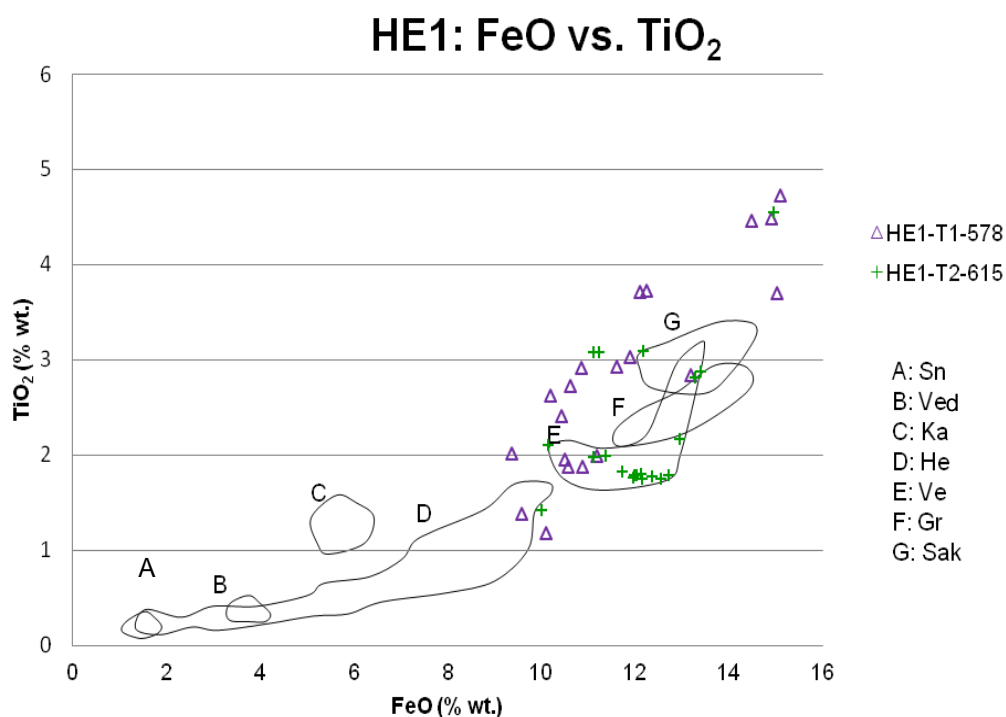


Figure 5.25 FeO percentage weight versus TiO₂ percentage weight for Helgafellsvatn. Known tephra profiles are sourced from Kristjansdóttir et al. (2007) and Óladóttir et al. (2011).

HE1: K₂O vs. P₂O₅

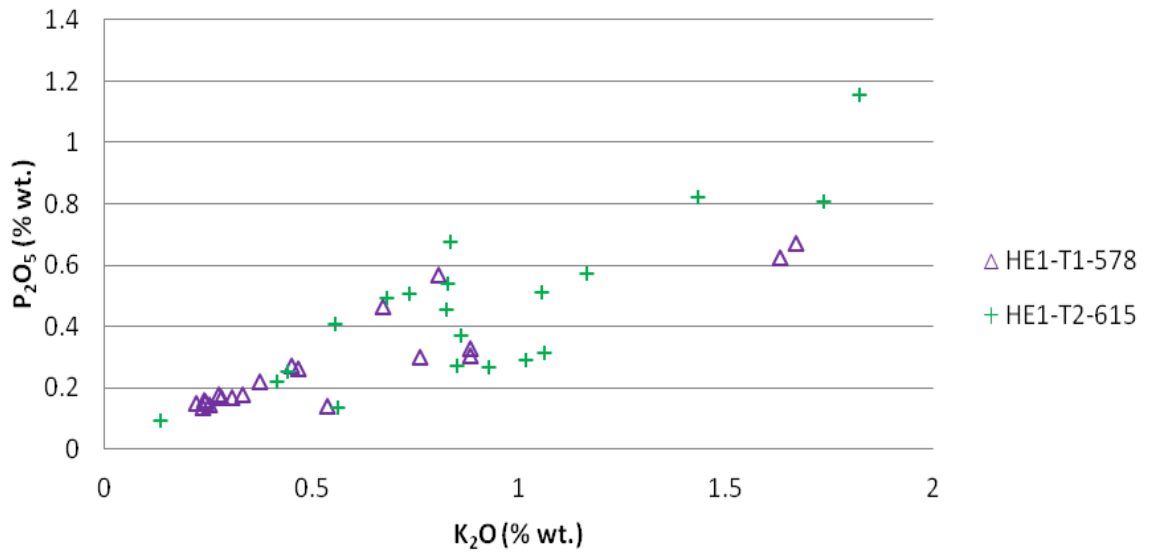


Figure 5.26: P₂O₅ percentage weight versus K₂O percentage weight for the Helgafellsvatn samples, which demonstrates two points separate from the principal cluster of results.

5.11.2.6 Saurar 3 (16.20 ± 0.3 m asl)

Two samples were retrieved for tephra analysis at 758.0 cm – 758.2 cm (SA3-T1-758) and 760.5 cm – 760.7 cm (SA3-T2-760) (Figures 5.27 and 5.28).

SA3: FeO vs. TiO₂

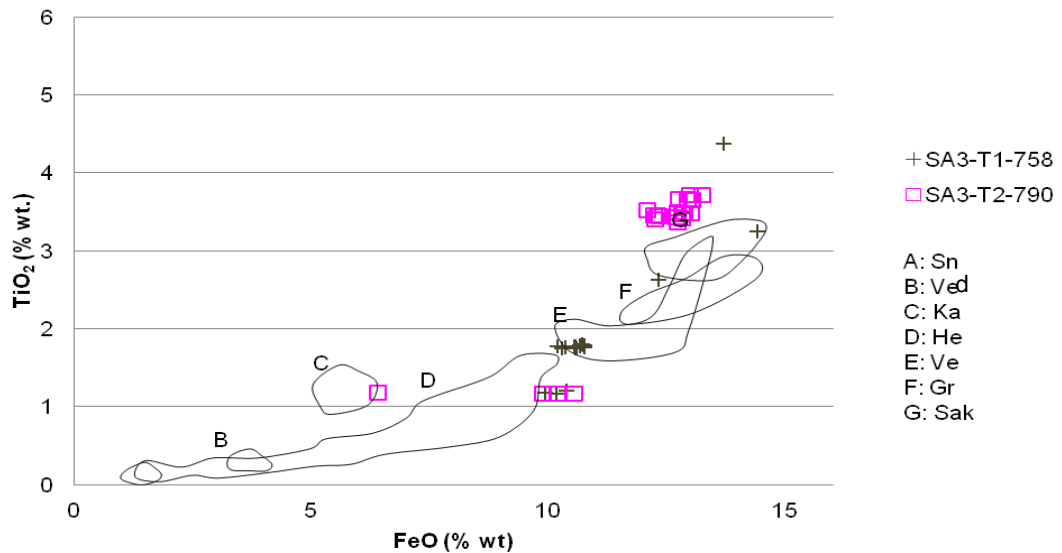


Figure 5.27: FeO percentage weight versus TiO₂ percentage weight for the Saurar 3 samples, showing two tight clusters of points alongside a more widely spread third cluster towards the top of the sample range. Known tephra profiles are sourced from Kristjansdóttir et al. (2007) and Óladóttir et al. (2011).

SA3: K₂O vs. P₂O₅

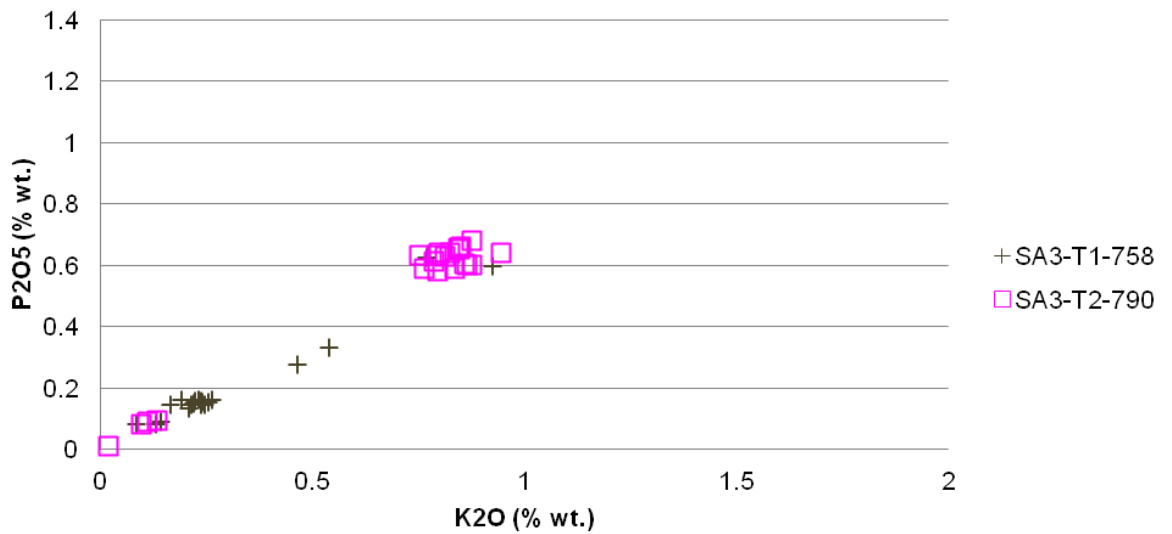


Figure 5.28: K₂O percentage weight versus P₂O₅ percentage weight for the Saurar 3 samples demonstrating the close clustering within the sample.

In both samples, there is a clearly dominant cluster. Sample SA3-T1 correlates well with Veiðavötn-type tephra, with sample SA3-T2 being representative of Grimsvötn-type. The tephra profile for Saksunarvatn (sourced from Grimsvötn) lies in close proximity to the main cluster and so it is likely that the cluster is sourced from this system but is not that particular eruption (Figure 5.27). Small numbers of grains within each sample give results which are representative of different sources and these are likely to either be inwashed from previous eruption events or contamination of the sample.

5.11.3 Tephra Interpretation

Despite difficulties with correlating with previously published records, the tephrostratigraphy and geochemical analyses suggest that some of the analysed layers are produced by the same systems (Figures 5.29 and 5.30). As stated, it is likely that the samples originate from the Ljós fjöll Volcanic System (LVS), Snæfellsnes Volcanic Belt (SVB), Grimsvötn, Veiðavötn and Katla systems, with several being of mixed origin. Internal consistencies within the dataset also allow the establishment of a robust chronology for the sites investigated. The potential sources of the tephra analysed are summarised in Table 5.7 and Figure 5.31, providing a summary of the tephrostratigraphical implications of the geochemical results.

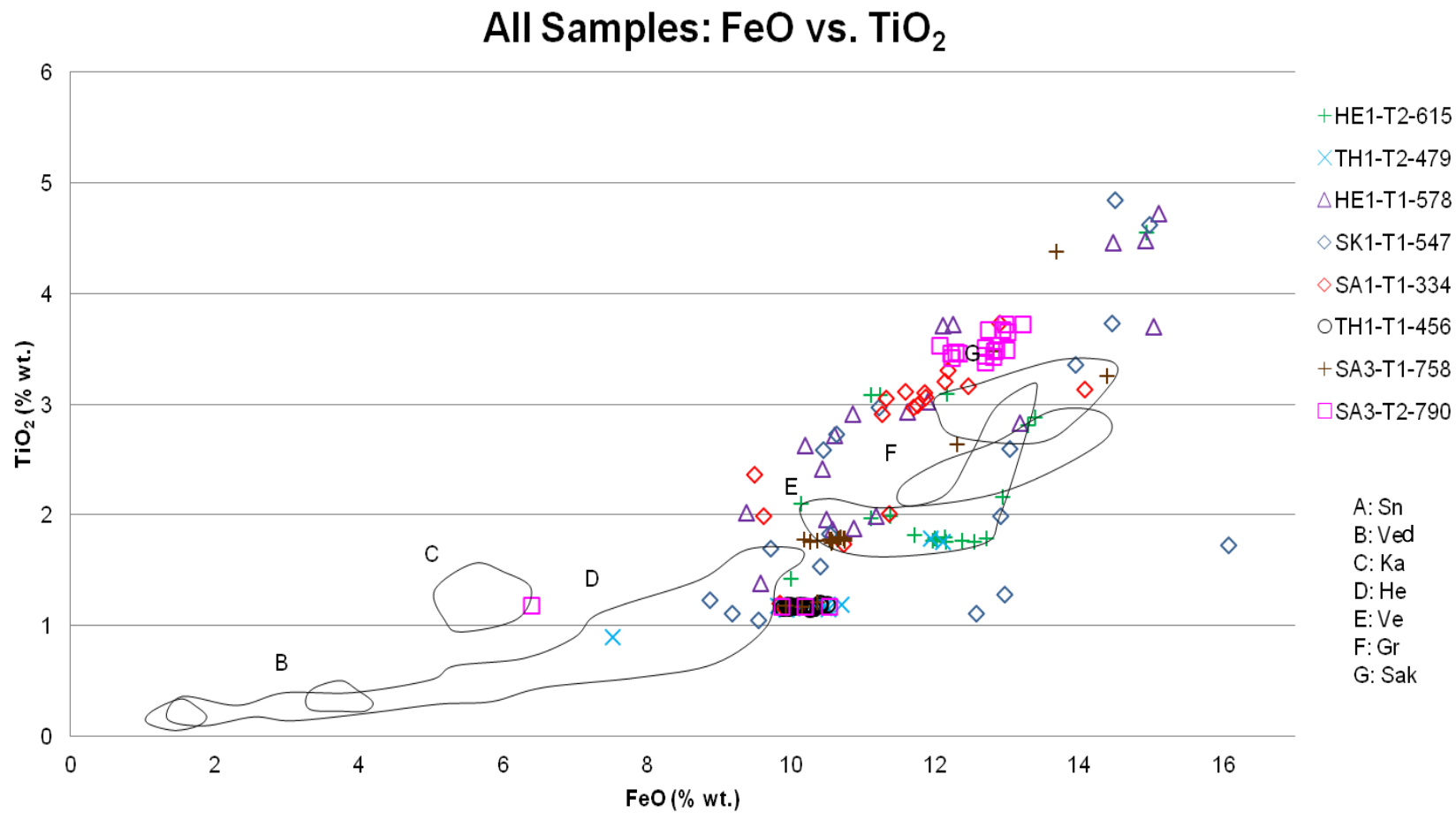


Figure 5.29: FeO vs. TiO₂ graph for all tephra samples analysed in this study. Known tephras have been plotted for comparison. Known tephra profiles are sourced from Kristjansdóttir et al. (2007) and Óladóttir et al. (2011).

All Samples: FeO/TiO₂ vs SiO₂

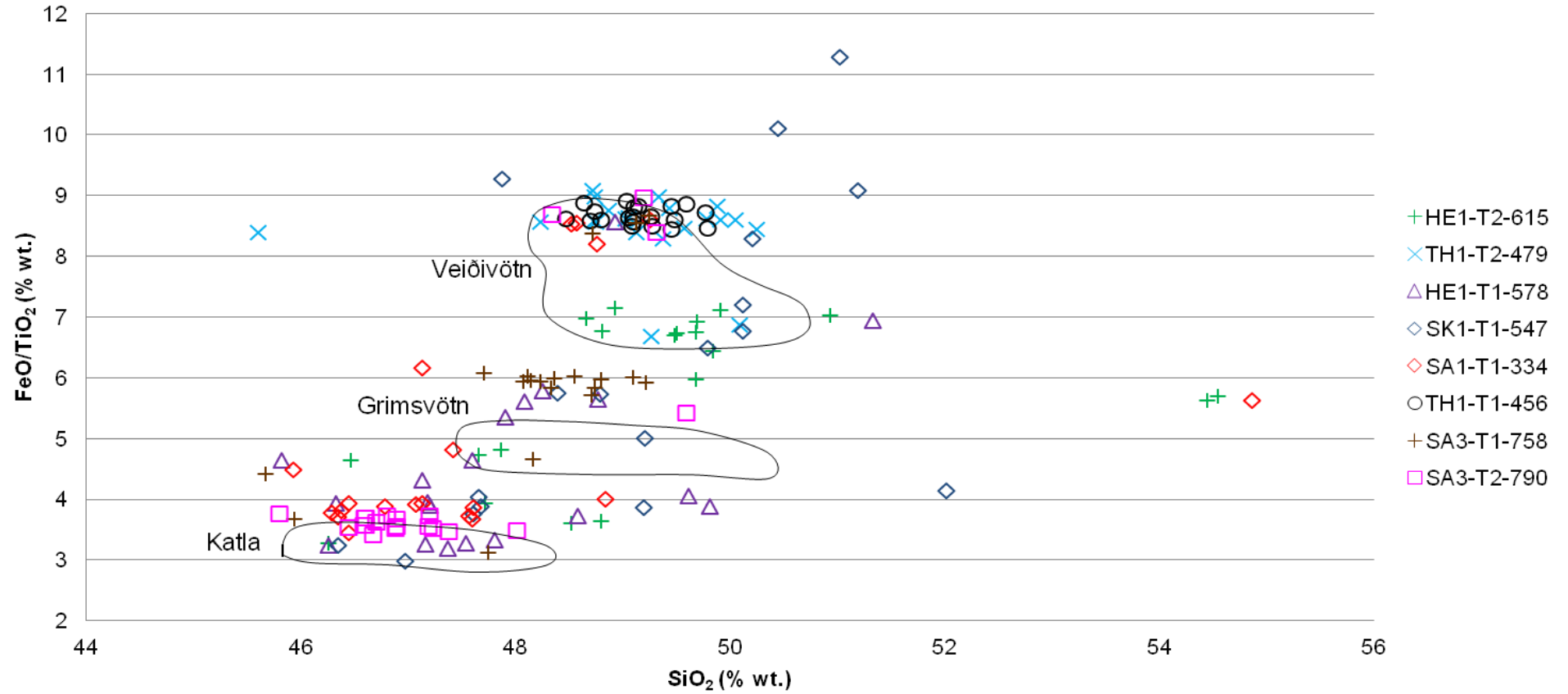


Figure 5.30: FeO/TiO₂ vs. SiO₂ graph for all tephra samples analysed in this study, alongside the known distribution for the three principal sources determined in this study. Known source profiles are taken from Jakobssen (1979).

Site	Tephra Sample	Tephra sources and composition (% of analysed grains)	Above/Below Isolation Contact
Skjaldarvatn	SK1-T1-547	Veiðavötn (50%) Grimsvötn (25%) Katla (16%) SVB (9%)	At Contact
Pingvallavatn	TH1-T1-456	SVB (100%)	Above
Pingvallavatn	TH1-T2-479	SVB (100%)	Above
Saurar 1	SA1-T1-334	Veiðavötn (22%) Grimsvötn (61%) SVB (17%)	At Contact
Helgafellsvatn	HE1-T1-578	Veiðavötn (43%) Grimsvötn (33%) Katla (14%) SVB (10%)	Above
Helgafellsvatn	HE1-T2-615	Veiðavötn (68%) Grimsvötn (26%) Katla (5%)	Above
Saurar 3	SA3-T1-758	Veiðavötn (100%)	Above
Saurar 3	SA3-T2-790	Grimsvötn (100%)	Above

Table 5.7: Summary of the sources and positions of tephra samples analysed from Skjaldarvatn, Pingvallavatn, Saurar 1, Helgafellsvatn and Saurar 3. Dominant sources are highlighted in bold.

In order to calculate the percentages in Table 5.7, individual tephra grains were assigned to a volcanic system for each set of analyses, which then allowed the percentage composition to be determined. From the results in Table 5.7, it can be hypothesised that the results from Skjaldarvatn, Saurar 1 and Helgafellsvatn represent the same point in time, due to the correlations in geochemistry between the sites, as demonstrated in Figures 5.31 and 5.32.

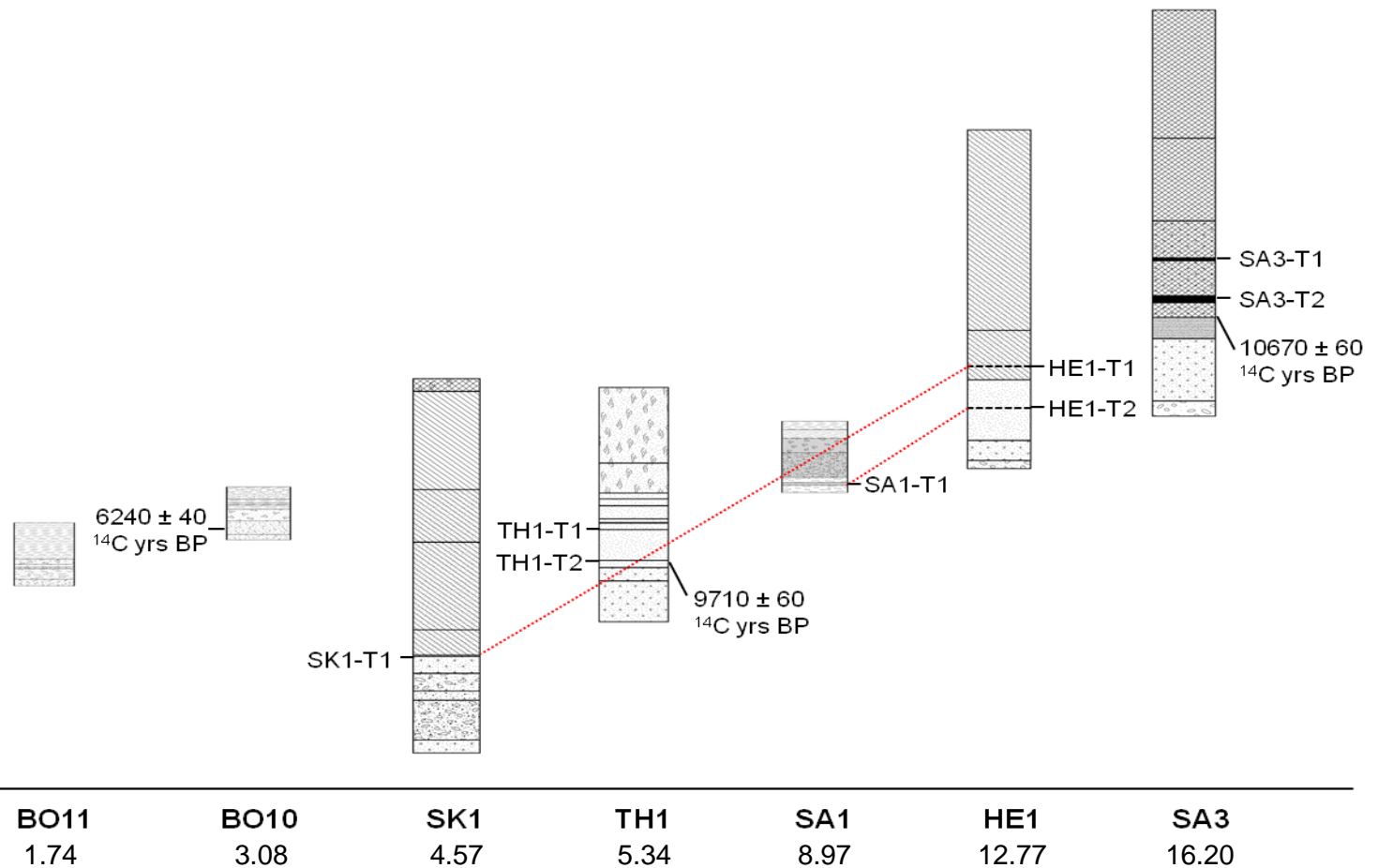


Figure 5.31: Diagram showing the tephrostratigraphical correlations between samples, alongside the positions of the radiocarbon dates in relation to the tephra samples analysed. Sediment cores are organised in elevation order, although the relative positions of these cores are for ease of understanding rather than respective elevations of the core samples.

Skjaldarvatn/Saurar 1/Helgafellsvatn Correlation: FeO vs. TiO₂

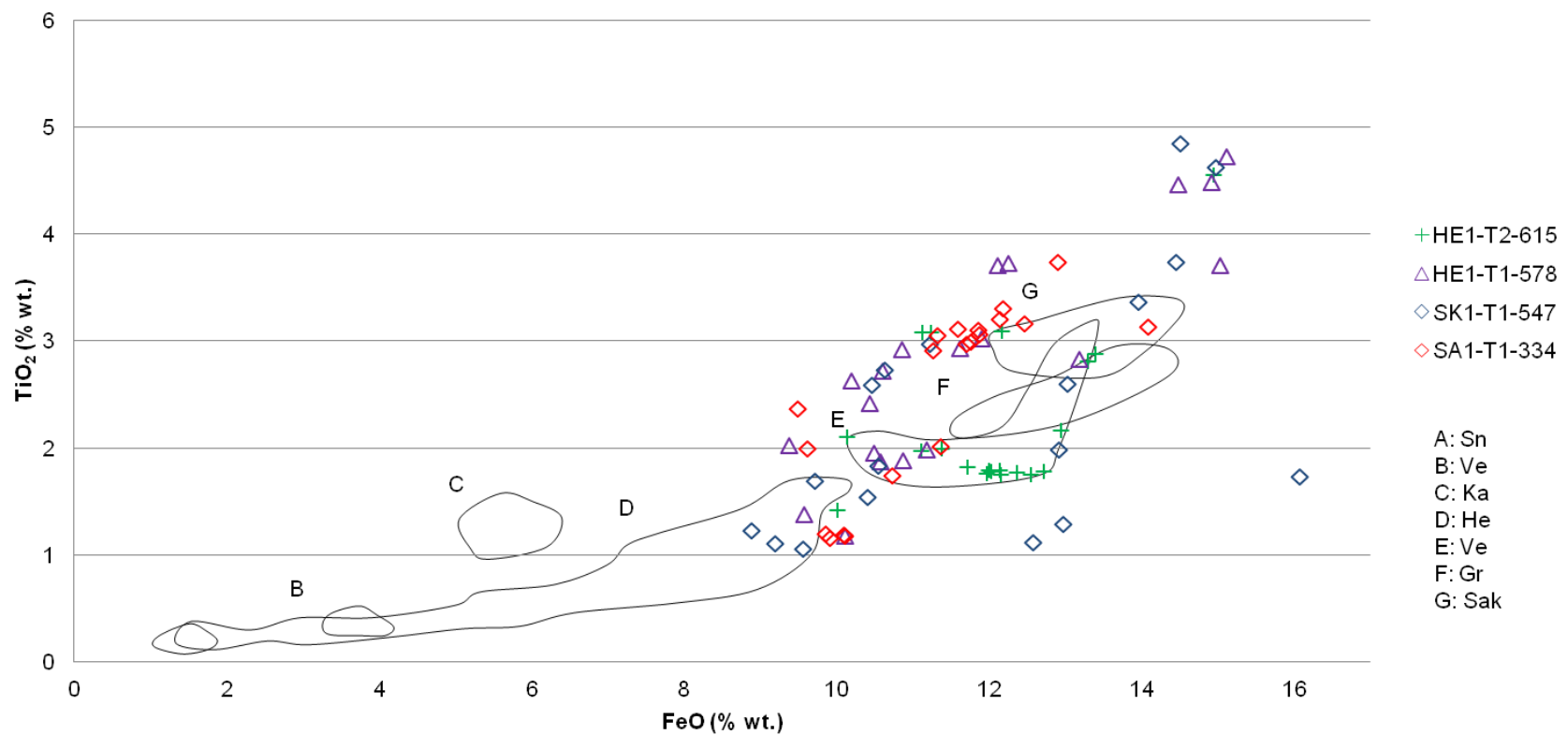


Figure 5.32: Correlation between the Skjaldarvatn, Saurar 1 and Helgafellsvatn tephra samples, plotted against known tephra profiles.

Although there are some differences between the site compositions, this may be due to the number of tephra grains analysed rather than the lack of a particular signature within the sample. Table 5.7 shows the proportions of the samples sourced from the different systems. Due to time constraints, a sample of 20 grains were analysed per sample. These grains were chosen as a representative sample of the tephra layer. It is also clear from the Helgafellsvatn site that there is potential for two different eruptive events from the same volcanic system (Table 5.7).

When coupled with the sill elevation data for each of the sites, there is evidence for two potential correlations based on the tephrostratigraphy (Figure 5.31 and 5.32). Figure 5.31 demonstrates the relationships between samples, with Figure 5.32 highlighting the correlations between geochemistries. It is hypothesised that HE1-T2-615 and SA1-T1-334 represent the same eruptive event. Although the compositions of the two layers vary, it is likely that this is due to the number of grains analysed rather than the two events being different. This correlation would suggest that Helgafellsvatn (12.77 m asl) isolated just prior to the eruption and Saurar 1 site (8.97 m asl) isolated close to the time of the eruptive event. In turn, it is suggested that HE1-T1-578 and SK1-T1-547 represent the same eruption, meaning that Helgafellsvatn had long been isolated by the time Skjaldarvatn (4.57 m asl) underwent the isolation process. These two chronological hypotheses also fit with the radiocarbon sequence and as such are taken as conclusive for the construction of the RSL curve.

5.12 Summary

This chapter has provided an overview of the results generated by this research. A description of the sediment stratigraphy, diatom assemblages and chronological controls at each site has been undertaken, providing an insight into the environmental changes at each location. In addition, the standard measurements that tested the precision of the EPMA analyses have been outlined, demonstrating the high precision of the machinery. The next chapter aims to provide a discussion of the results outlined here, thus providing an insight into the position of this investigation within previous research, as well as an overview of the trends in the current dataset.

CHAPTER 6

Discussion

6.1 Introduction

This chapter aims to provide a discussion and interpretation of the results generated as part of this research. Initially, this chapter will outline the calculation of the RSL index points for the Snæfellsnes data. Following these calculations and subsequent discussion, the determination of the RSL curve will highlight the record of RSL change generated during this research. In addition to the discussion and interpretation of the results generated, the results will be placed in the regional context, through comparison with previous study in NW Iceland.

6.2 RSL index points for the Snæfellsnes peninsula

In order to construct a RSL curve for the Snæfellsnes peninsula, it was necessary to determine a series of RSL index points for the region. This was undertaken through the employment of the radiocarbon dates and sill elevations outlined in Chapter 5, alongside tide gauge data. Here, the sea-level index point methodology summarised by Shennan (2007) have been employed. Shennan (2007) outlines that each sea level index point has four components: location, altitude, age and tendency.

The altitude of the index point was determined through the determination of indicative meaning, limiting dates and sediment consolidation rates (Shennan, 2007). In this study, the altitude of the sea-level index point is determined through the diatom analyses for the coastal lowland sites, with the sill elevation being the altitude of the sea-level index point within isolation basin samples. For coastal lowland sites, the altitude of the sea level index point was calculated through the subtraction of the sediment depth to the point within the diatom assemblage which shows decreased marine influences from the core top elevation. The age of the index point has been determined through the

employment of radiocarbon dating and tephrochronology in this study and the tendency refers to the trend within the dataset determined by the index point i.e. increasing or decreasing marine influence (Shennan, 2007).

Although radiocarbon dating provided limiting dates for the decrease in marine influences at three of the sites studied, several sites were not accurately dated, as discussed in Chapter 5. Where sufficient dating control was not achievable, the timings of isolation or reduction in marine influence were inferred from the RSL curve generated and as such are highlighted by an asterisk in Table 6.1.

In order to calculate the altitude of MSL at the sites, the indicative meaning needs to be subtracted from the altitude of the isolation basin sill or elevation of decreased marine influences identified at the coastal lowland sites (e.g. Shennan *et al.*, 1999). The indicative meaning includes two components: the reference water level and the indicative range of that reference water level (Shennan, 1986), highlighting the relationship between the sample and the tidal range (van der Plassche, 1986).

The reference water level is identified through the diatom species present within the site assemblages. MHWST has been employed extensively in previous isolation basin and coastal lowland studies as the indicative meaning for the diatom isolation contact (e.g. Shennan *et al.*, 1995; Lloyd *et al.*, 2009). However, the topic is debated in the literature, with previous study employing values between MHWST to MLWST, MHWST or MHWST-HAT (e.g. Shennan *et al.*, 1993; 1995; Long *et al.*, 2008). In this study, MHWST-HAT is employed due to the difficulties of ascertaining whether the diatom isolation contact represents HAT or MHWST. Correction is required due to the formation of particular sea-level index points at different reference water levels (Shennan *et al.*, 1995). As discussed (e.g. Shennan, 2007) and undertaken elsewhere, the indicative range is assumed to be unchanged in this study, despite the potential for this to have an effect on the results of the correction, as outlined by Gehrels *et al.* (1995). The results of these calculations can also be found within Table 6.1.

Site	Lab Code	¹⁴ C age (yrs BP)	Calibrated age (yrs BP)	Sill/Contact Elevation (m asl)	Reference Water Level	Indicative Meaning (m)	Relative Sea Level (m asl)
Borgarland 10	Poz-43545	6240 ± 40	7156 – 7252	2.58	MHWST – HAT	2.13 ± 0.33	0.45 ± 0.33
Pingvallavatn	Poz-43546	9710 ± 60	11089 – 11219	5.34	MHWST – HAT	2.13 ± 0.33	3.21 ± 0.63
Saurar 3	Poz-43548	10670 ± 60	12558 - 12646	16.20	MHWST – HAT	2.13 ± 0.33	14.07 ± 0.63
Borgarland 11*	-	-	~ 4800	0.74	MHWST – HAT	2.13 ± 0.33	- 1.39 ± 0.33
Skjalдарvatn*	-	-	~ 9800	4.57	MHWST – HAT	2.13 ± 0.33	2.44 ± 0.63
Saurar 1*	-	-	~ 11700	8.97	MHWST – HAT	2.13 ± 0.33	6.84 ± 0.63
Helgafellsvatn*	-	-	~ 12200	12.77	MHWST – HAT	2.13 ± 0.33	10.64 ± 0.63
Setbergsa*	-	-	~ 14000	62.84	MHWST – HAT	2.13 ± 0.33	60.71 ± 0.58
Barar*	-	-	~ 14000	68.87	MHWST – HAT	2.13 ± 0.33	66.74 ± 0.68

Table 6.1: Summary of the sea-level index points generated within this study, showing radiocarbon dates, calibrated dates and altitudes. Sites marked with an asterisk are extrapolated or interpolated dates from the RSL curve.

6.3 RSL curve for the Stykkishólmur area, Snæfellsnes

6.3.1 *Initial RSL curve for the Snæfellsnes peninsula*

Following the determination and attempted dating of the isolation contacts within each of the sediment cores extracted from the eight sites, an initial RSL curve was constructed. Due to the lack of correlation between the tephra samples analysed in this research and previously published values, this initial RSL curve uses the 3 sea-level index points that have an independent chronological constraint from radiocarbon dates; these are from Borgarland 10, Þingvallavatn and Saurar 3. The sea-level index points from the other 5 sites do not have independent chronological control due to lack of well dated tephra layers or radiocarbon dates from these sites. The tephrochronological results provided information regarding the sequence of basin isolation, as outlined in Chapter 5, with Helgafellsvatn being isolated prior to Saurar 3 and that Helgafellsvatn was long isolated by the time Skjaldarvatn was isolated.

The Þingvallavatn basin is well constrained by the radiocarbon date; however, the tephra layers within the sediment core are unable to be correlated with the other samples due to differences in the geochemical composition of the tephra layers. As such, it is impossible to provide a constraint on the isolation of the other sites.

Initially, the marine limit points from Setbergsa and Barar are plotted as a dashed line, thus demonstrating that postglacial RSL reached these elevations, without assigning an age to the marine limit. This initial RSL curve demonstrates the lack of data from the tephrochronological study, but does also highlight the constraint of the low point of the RSL curve following initial rapid RSL fall (Figure 6.1).

6.3.2 *Estimated additional RSL points and updated RSL curve*

Following the construction of the initial RSL curve for the Snæfellsnes peninsula shown in Figure 6.1, it is possible to include the additional sea-level index points based on the isolation contacts of the other basins from this study. Figure 6.2 demonstrates the potential timings of isolation using the calibrated ages

outlined previously. In addition, the extrapolated marine limit point is included, thus providing an estimation for the timing of the formation of the marine limit. This marine limit point fits well with the regional trends, such as those highlighted in Lloyd *et al.* (2009) and Rundgren *et al.* (1997), which provide marine limit ages of 14 cal. ka BP and 13.8 cal. ka BP respectively. Although this correlation provides valuable information about the potential timings of deglaciation for NW Iceland, the dates used within this correlation should be treated with some caution. The ages presented both in this study and the Rundgren *et al.* (1997) paper are both produced through the extrapolation of the dates generated from other sites in the respective studies. As such, the marine limit is not directly dated in either of the two studies. In contrast, Lloyd *et al.* (2009) provide an accurate timing for the formation of the marine limit through the dating of the isolation contact at Hríshóll 1, which lies at 79.1 m asl. As such, the relative reliability of the timings should be noted. The reliability of the correlation could be improved through the accurate constraint of the age of the marine limit both in Skagi and Snæfellsnes. However, the present correlation appears to show a potential pattern for deglaciation in the region, suggesting that Snæfellsnes, southern Vestfirðir and Skagi deglaciated at similar times.

The timings of isolation of the other sites in this study are predicted using the line between points generated from the radiocarbon analyses and are summarised in Table 6.1.

RSL curve for the Stykkishólmur area, northern Snæfellsnes, western Iceland

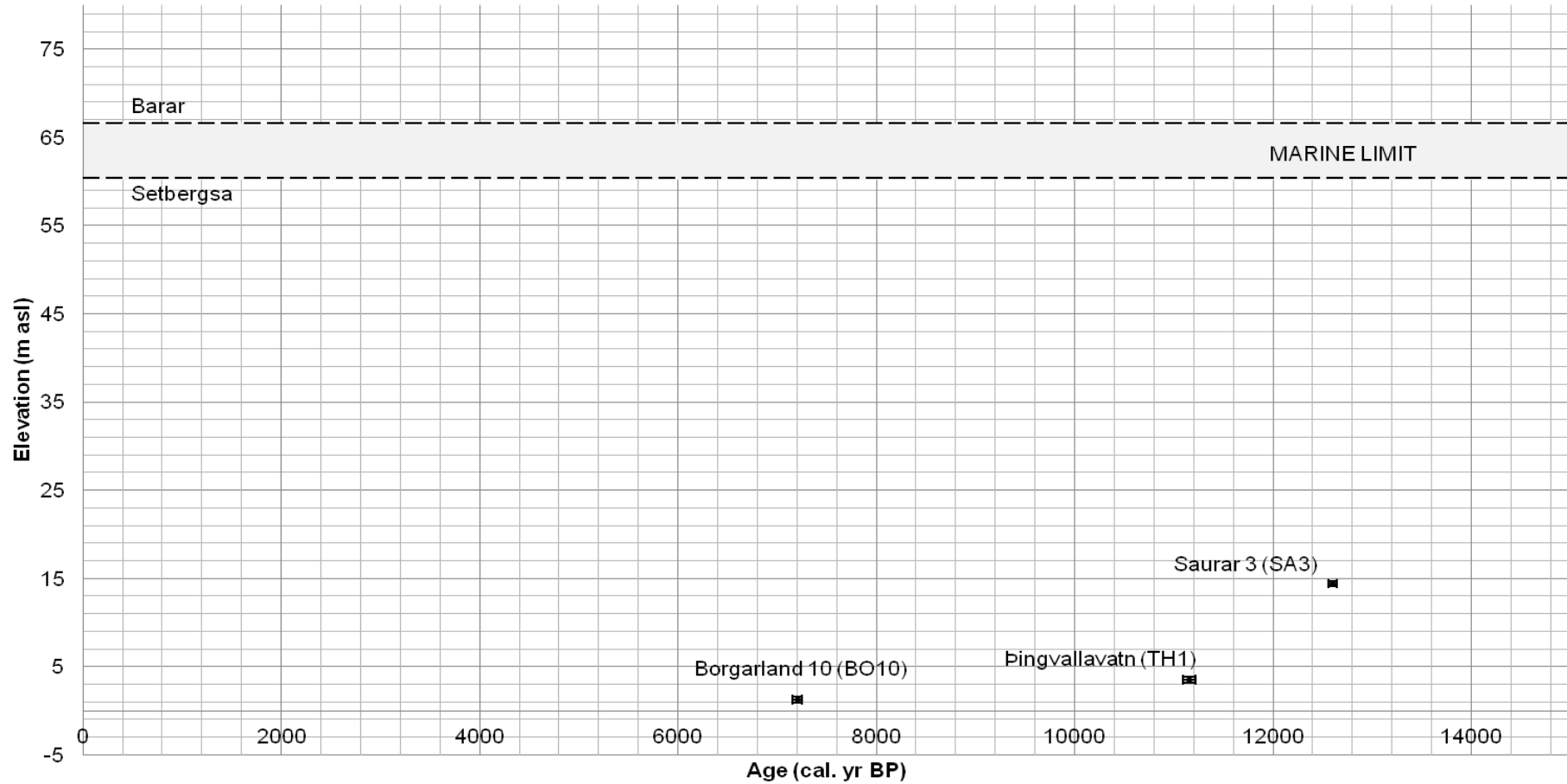


Figure 6.1: Initial RSL curve of the Stykkishólmur area, northern Snæfellsnes, using calibrated ages for the isolation of each basin.

RSL curve for the Stykkishólmur area, northern Snæfellsnes, western Iceland

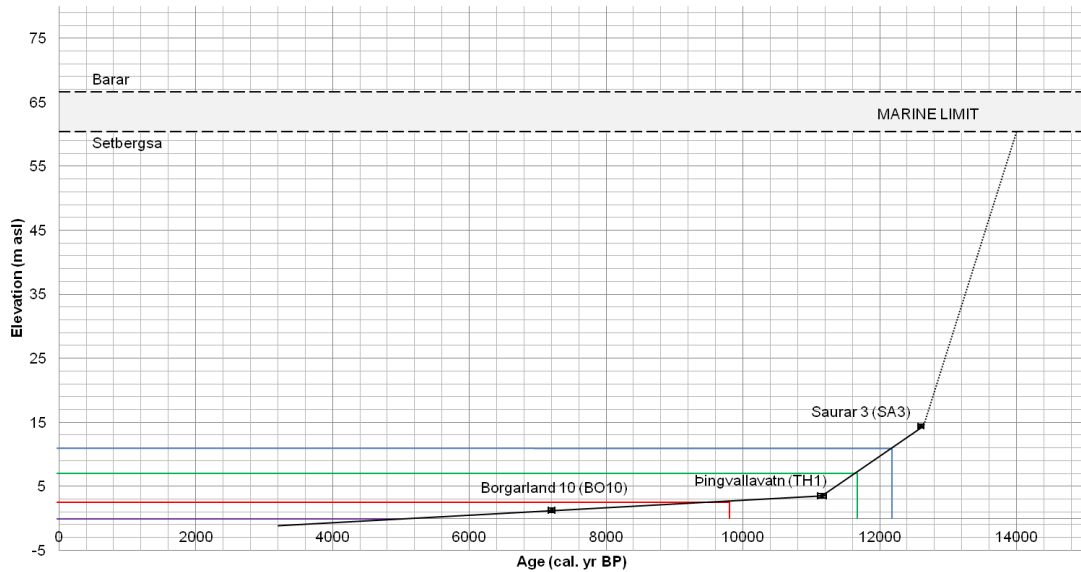


Figure 6.2: Calibrated age determination for the isolation basin and saltmarsh sites without radiocarbon dated samples (purple: BO11; red, SK1; green: SA1; blue: HE1).

6.4 Marine Limit Measurements

Two marine limit measurements were taken on the Snæfellsnes peninsula to constrain maximum postglacial RSL. Both of the elevations are plotted on the accompanying RSL curves (Figures 6.1 and 6.2). The Setbergsa value was used as the high point for postglacial RSL in the Stykkishólmur area, as the potential for differential rates of postglacial rebound were able to be minimised due to the proximity of the measurement to the isolation basin and coastal lowland sites (Figure 3.1).

The Barar marine limit measurement is also valuable however, providing an additional measurement for the determination of patterns of marine limit elevations within NW Iceland. Furthermore, the Barar marine limit provides a valuable insight into the glacial and deglacial history of the Snæfellsnes peninsula. The higher marine limit elevation at Barar suggests either:

- i) that Barar deglaciaded prior to Setbergsa and therefore has experienced greater levels of postglacial rebound, which assumes that the marine limit in Snæfellsnes formed simultaneously, or;

- ii) that ice was thicker in Barar as a result of the Snæfellsnes ice cap and as such greater rebound has occurred in Barar due to the thicker ice present during the LGM.

It appears likely that the higher marine limit elevations at Barar result from the earlier deglaciation hypothesis. This would result from the greater distance from the main ice loading centre, as outlined in Figure 6.3. Barar is situated within the mid Snæfellsnes region outlined in Figure 3.1, thus making it further from the proposed main ice loading centre in central Iceland. However the position of Barar in mid Snæfellsnes also means that it is situated closer to the Snæfellsnes ice cap, which may have led to the increased marine limit elevation through thicker ice mass. If further evidence for the influences of the Snæfellsnes ice cap could be determined, consideration of the effects of this ice cap will need to be taken in modelling the IIS. At present, ice models for Iceland do not consider large contributions to ice thickness from such small ice caps (e.g. Hubbard *et al.* (2006)).

As outlined in Chapter 2, several studies have provided elevation measurements for the marine limit in NW Iceland. The local marine limit varies throughout the region, with large differences in elevation over relatively short distances. A summary of the marine limit elevations for NW Iceland is provided in Figure 6.3, which demonstrates the variability in both the elevation and spatial coverage of measurement of the marine limit in NW Iceland.

The marine limit in Snæfellsnes seems to fit well with the regional patterns of marine limit elevations, as outlined in Figure 6.3. Norðdahl and Ásbjörnsdóttir (1995) recorded an elevation of 65 m for the Dalir region, East of Snæfellsnes and similar elevations have been measured in Skagi (Rundgren *et al.*, 1997). As such, it would appear that there are a series of marine limit measurements of similar elevation occurring at similar distances from the potential ice mass loading centre. This fits well with the extensive glaciation hypothesis outlined in Chapter 2.

Interestingly, the Snæfellsnes measurements do not fit as well with the results from southern Vestfirðir, which range from 75 m to 110 m asl (Figure 6.3) (Norðdahl and Pétursson, 2005; Lloyd *et al.*, 2009). There appears to be large variation in the marine limit elevation over relatively short distances, even within

the Vestfirðir peninsula. These southern Vestfirðir marine limit heights appear relatively high when put into this regional context and suggest that southern Vestfirðir deglaciated relatively early (e.g. Norðdahl and Pétursson, 2005) or that the region was covered by thicker ice.

The higher marine limits in southern Vestfirðir are not mirrored in northern Snæfellsnes and as such it is possible that southern Vestfirðir deglaciated earlier than Snæfellsnes when considering marine limit elevation alone, yet the dates of isolation generated from ^{14}C dating suggest that basins at relatively low altitudes were isolated relatively early during the Holocene in Snæfellsnes. When coupled, the marine limit and radiocarbon data suggest that the two regions deglaciated at a similar time, but that southern Vestfirðir experienced greater and therefore more rapid rebound following deglaciation as a result of potential thicker ice in southern Vestfirðir. Based on the evidence available, the case for thicker ice is more likely than differing timings of deglaciation due to the reliability of the dating employed in the two studies. An alternative explanation for the differential marine limit elevations would be differing lithospheric viscosity in the two locations; however it would appear more likely that this variation in marine limit height is due to differential ice loading.

The case for thicker ice in southern Vestfirðir is interesting. If ice had been thicker in southern Vestfirðir, it would be expected that evidence for thicker ice would be found in northern Snæfellsnes, as it would be likely that such thicker ice would extend into Breiðarfjörður. However, the marine limit elevations in northern Snæfellsnes suggest similar ice thickness to Skagi and Dalir, leading to a contradiction in evidence concerning ice thickness. The potential for thicker ice in southern Vestfirðir is also interesting in terms of the present models of the IIS. Currently, ice sheet models suggest that ice was thicker in northern Vestfirðir, with ice remaining for a longer period following initial deglaciation, resulting in the lower marine limit values recorded for the region (e.g. Hubbard *et al.*, 2006). However, the higher marine limit elevations in southern Vestfirðir may suggest that thicker ice could be found there.

It would appear, bearing in mind that the marine limit in Snæfellsnes is similar to that of Skagi (Rundgren *et al.*, 1997) that this potential thicker ice in southern Vestfirðir had little effect on Snæfellsnes. If the thicker ice had extended as far

as Snæfellsnes, the effects of the rebound from that ice would be seen both in the geomorphological and RSL records. The marine limit elevations in northern Snæfellsnes suggest that the potential thicker ice did not extend this far south. Furthermore, the elevations of the measured points in northern Snæfellsnes suggest that the Snæfellsnes ice cap was thinner than the ice over southern Vestfirðir, if simultaneous deglaciation throughout the region is assumed.

In order to determine whether the marine limit elevations in southern Vestfirðir relate to earlier deglaciation or thicker ice, additional accurate age constraints for the marine limits in NW Iceland are required, particularly for the higher marine limit measurements in SW Vestfirðir (e.g. Norðdahl and Pétursson, 2005). Although Lloyd *et al.* (2009) provide an accurate timing for the formation of the marine limit in Bjarkarlundur, there are several sites in SW Vestfirðir which required dating. These marine limits are all relatively high for the peninsula, particularly those presented by Norðdahl and Pétursson (2005). These additional constraints would lead to the establishment of the age of the marine limit, limiting date for the deglaciation of the region and potential inference of ice thicknesses within NW Iceland.

At present, there is insufficient evidence to unequivocally state the reasons for the differences in marine limit elevation between southern Vestfirðir and northern Snæfellsnes. The case for earlier deglaciation of southern Vestfirðir seems sensible bearing in mind the results of modelling studies (e.g. Hubbard *et al.*, 2006) which consistently suggest early deglaciation of the southern Vestfirðir region, yet there is also potential for thicker ice. This thicker ice may have been situated within northern Breiðafjörður, which may have since also rebounded, leading to the relatively shallow waters in the region.

As such, it is necessary to assume that the marine limits throughout NW Iceland have a similar age. In doing so, it is possible to determine patterns of ice mass distribution within NW Iceland. Areas of higher marine limit would have had greater masses of ice than areas of lower marine limit, as the areas of thicker ice cover experience greater crustal rebound once ice has retreated compared to areas of lower marine limit. As such, the potential for a second ice mass centre over NW Iceland can be investigated. A marine limit elevation measurement for the Snæfellsnes peninsula offers the opportunity to determine

the possible extent of such an ice mass over southern Vestfirðir, as earlier discussed.

The marine limit elevations for the Snæfellsnes peninsula do therefore demonstrate that the marine limit is lower than the majority of measurements taken from southern Vestfirðir (Figure 6.3; e.g. Norðdahl and Pétursson, 2005; Lloyd *et al.*, 2009). There are however clear correlations to the Dalir area (Norðdahl and Ásbjörnsdóttir, 1995), approximately 40 km East of Stykkishólmur, and the Skagi peninsula (Rundgren *et al.*, 1997). This has been highlighted in Figure 6.3, showing hypothesised concurrent ice thickness locations, which are likely to have deglaciated at a similar time. This has been determined using a universal marine limit age for NW Iceland and therefore assuming at the marine limit elevation map changes in ice thickness rather than the timing of deglaciation. It is therefore clear that potential ice mass centres can be further determined and used to support ice extent models (e.g. Hubbard *et al.*, 2006) through the employment of additional marine limit elevation measurements.

Consultation between Figure 6.3 and IIS ice extent (Figure 6.4) lead to some correlations between the two sets of data. Both datasets suggest similar ice thicknesses in similar locations during the retreat of the IIS, as demonstrated by the blue dashed lines in both figures, which link areas of similar ice thickness in the two diagrams. This proposal of similarities in ice thicknesses across the arc outlined is suggested through the linking of areas of similar marine limit in Figure 6.3 and modelled ice thicknesses in Figure 6.4.

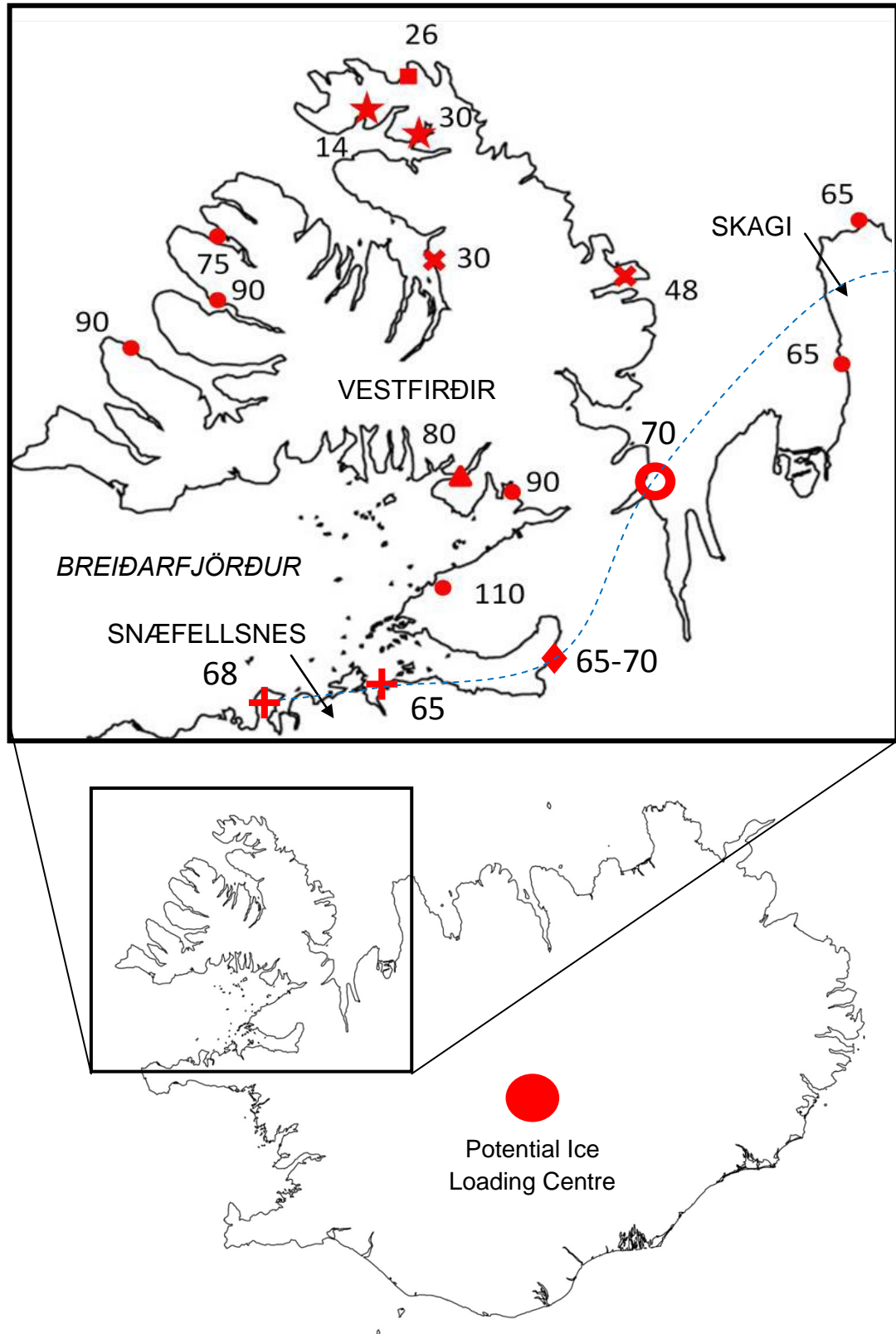


Figure 6.3: Selected marine limit measurements from NW Iceland (circle: Norðdahl and Pétursson (2005); triangle: Lloyd et al. (2009); star: Principato and Geirsdóttir (2002); square: Hjort et al (1985); cross: Principato (2008); diamond: Norðdahl and Ásbjörnsdóttir (1995); unfilled circle: Hansom and Briggs, 1991; plus: this study) and areas of similar marine limit elevation (blue dashed line).

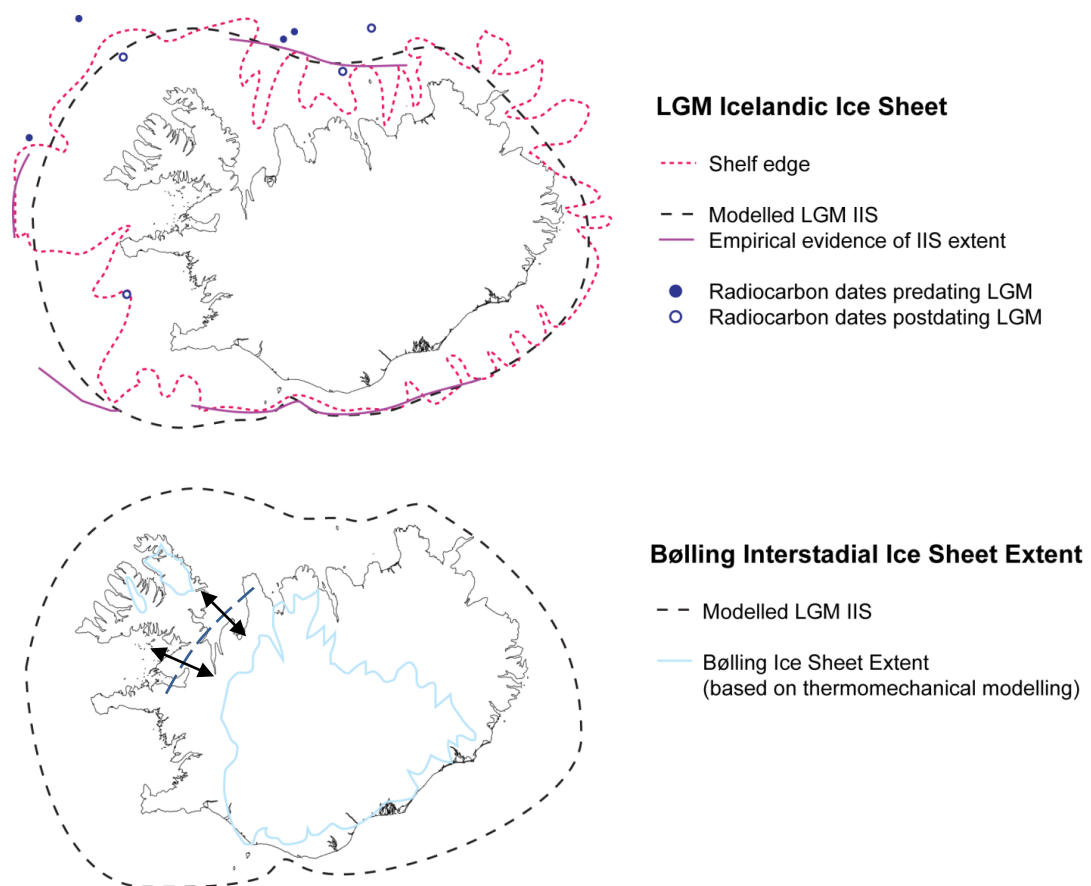


Figure 6.4: Model of IIS ice extent at the LGM and during the Bølling Interstadial. Blue dashed line represents areas of similar marine limit elevation, and therefore potentially similar ice thickness values, as outlined in Figure 6.3. Arrows denote potential ice retreat patterns. Adapted from Ingólfsson *et al.* (2010).

Although this correlation can be made between the two sets of data, the conclusion is perhaps unsurprising due to the use of marine limit data in the production of the model by Hubbard *et al.* (2006). If the timing of deglaciation is assumed to be concurrent throughout the peninsula, the addition of the Snæfellsnes data points allows similar ice thicknesses to be discussed. This discussion is limited by the lack of accurate dating of the marine limit both within this study and that undertaken by Rundgren *et al.* (1997), which both extrapolate an age for the marine limit from the respective RSL curves. The Hubbard *et al.* (2006) predictions of ice sheet extent show that separate ice caps existed on the Snæfellsnes peninsula; however, the marine limit elevations determined in this study may suggest similar ice thickness in Snæfellsnes as in Skagi.

In terms of an estimated age for the marine limit on the Snæfellsnes peninsula, the RSL curve presented earlier provides an estimated date of 14 cal. ka BP.

This date also provides a minimum date for the timing of the deglaciation of the peninsula. The date of marine limit formation fits well with dates proposed in previous studies in NW Iceland, particularly at Skagi (Rundgren *et al.*, 1997) and Lloyd *et al.* (2009). It is clear that deglaciation will have started before this time and as such, the marine limit data provide a minimum age for the completion of deglaciation.

It is therefore clear that the marine limit data generated in this study provide valuable information regarding the relative ice thickness on the Snæfellsnes peninsula. When viewed in the regional context, the Snæfellsnes marine limit data are similar in altitude to those produced in Dalir (Norðdahl and Ásbjörnsdóttir, 1995), Skagi (Rundgren *et al.*, 1997) and southeastern Vestfirðir (Hansom and Briggs, 1991). This similarity in marine limit elevation could also be a result of similar timing of deglaciation at the sites.

6.5 RSL history of the Snæfellsnes peninsula

As a result of the calibration of the radiocarbon dates, estimation of the timings of isolation at the other five sites and determination by extrapolation of a potential timing for the formation of the marine limit, it is possible to provide a RSL history for the Snæfellsnes peninsula, western Iceland. It is clear from the RSL curve generated, that deglaciation must have occurred relatively rapidly in the Snæfellsnes peninsula leading to rapid RSL change.

The well constrained radiocarbon age of the isolation of Saurar 3 provides an opportunity for the extrapolation of the RSL curve to establish an approximate age for the formation of the marine limit in the region. The extrapolation of the RSL curve from the ¹⁴C dated isolation contacts suggests that the region is likely to have deglaciated before 14000 cal. yrs BP, as demonstrated by the formation of the marine limit after this time (Figure 6.1). Previous study has provided similar ages for the deglaciation of NW Iceland: Lloyd *et al.* (2009) provide a date of 14 cal. ka BP for the deglaciation of Bjarkarlundur, southern Vestfirðir and Rundgren *et al.* (1997) give a date of 13.85 cal. ka BP for the Skagi peninsula. As previously outlined, the relative reliability of these two ages should be brought into consideration here, with the Rundgren *et al.* (1997) age estimation being from extrapolation of the RSL curve and the Lloyd *et al.* (2009)

timing being sourced from the radiocarbon dating of the isolation contact within an isolation basin close to the marine limit. The estimate for the formation of the marine limit from the extrapolated Snæfellsnes RSL curve at 14 cal. ka BP also fits well with a period of high RSL noted in Iceland, which has been dated to 12 ¹⁴C ka BP (~ 13.8 cal. ka BP) (Ingólfsson, 1988; Ingólfsson and Norðdahl, 1994). As such, the estimate of the marine limit seems sensible for the Snæfellsnes peninsula, both in relation to previous study and known events in the RSL history of the region.

Following the formation of the marine limit, RSL appears to have fallen rapidly, with Saurar 3, the highest basin surveyed in this study at 16.20 m asl, being isolated at 12558 - 12646 cal. yrs BP. This falling trend in RSL continues through the isolation of Þingvallavatn at 11089 – 11219 cal. yrs BP and subsequent decrease in marine influences at Borgarland 10 in 7156 – 7252 cal. yrs BP.

Following the isolation of Þingvallavatn at 11089 - 11219 cal. yrs BP and prior to the timing of the reduction in marine influence at Borgarland 10 at 7156 - 7252 cal. yrs BP, it is clear that there are two possible trends in the potential RSL history. Either:

- i) RSL fell below present between 11089 - 11219 cal. yrs BP and 7156 - 7252 cal. yrs BP or;
- ii) RSL fell at a relatively slow rate from 5.34 ± 0.63 m asl. to 2.58 ± 0.33 m asl over that same period.

Although the sedimentary evidence would suggest that RSL fell slowly over this period, due to the lack of a second period of marine influence in the Skjaldarvatn sediment core, it is possible that RSL fell below present and returned to a highstand of ~ 2.5 m asl. around 7156 - 7252 cal. yrs BP. If this is the case, the fall and subsequent rise can be well constrained based on the stratigraphical evidence from Skjaldarvatn. If this fall and rise were to have happened, the process would have had to have occurred relatively rapidly. In this case, the gravel layer at the base of the Borgarland 10 sediment core could in fact represent a highstand within the sedimentary record.

If this fall and rise between 11089 - 11219 cal. yrs BP and 7156 - 7252 cal. yrs BP were the case, the estimated age for the Skjaldarvatn isolation provided in Table 6.1 would be incorrect, as the trend of RSL between the Þingvallavatn and Borgarland 10 sites would not be linear. A RSL history containing a mid Holocene highstand during this period would fit well with previously published records generated for sites on the Vestfirðir peninsula (e.g. Lloyd *et al.*, 2009).

However, without sufficient dating, the only certain conclusion that can be drawn concerning this period is that RSL did not reach higher than 5.34 m asl, as there is no sedimentary evidence for re-inundation at the Þingvallavatn site. Following the decrease in marine influence at the Borgarland 10 site at 7156 - 7252 cal. yrs BP, RSL may have fallen below present, as shown by the index point from Borgarland 11.

The Borgarland 11 index point demonstrates that RSL fell below present, although there is not a chronological control or sufficiently well constrained diatom evidence to provide evidence for the timing or extent of this fall. The diatom evidence presented for the Borgarland 11 site, which shows the reduction in marine influences over time, is insufficiently detailed and is likely to show a single period of reduction in marine influence rather than the complete record of RSL change at the site. It is likely that the gravel layer within the record from Borgarland 11 represents a highstand and subsequent reduction in marine influence and that the missing upper section of the core would provide evidence for subsequent RSL changes over the late Holocene.

It is clear therefore that the Snæfellsnes peninsula experienced a relatively rapid RSL fall following deglaciation (Figure 6.1). After this, the rate of RSL fall decreased, following the isolation of Saurar 3 at 12602 ± 44 cal. yrs BP. Although there is clear evidence for RSL fall over the early Holocene, the mid Holocene RSL history of the area remains unclear. The internal correlations within the dataset do however confirm the order of isolation, which coincides with the sill and core altitudes from each site. If more certain chronological control were to be gained for these sites, the record of RSL change for the region would be greatly strengthened. In particular, the existence of a mid-Holocene highstand for the region could be tested for Snæfellsnes.

At present, it is clear that the two possible conclusions for the period between 11089 - 11219 cal. yrs BP and 7156 - 7252 cal. yrs BP require further investigation. It is also apparent that RSL did fall below present during the late Holocene, although insufficient chronological control means that the timing of this fall below present is not currently well constrained. An extrapolation of the curve produces an estimated calibrated age of 4800 cal yrs BP for Borgarland 11, although this should be taken with extreme caution, as it is unlikely that RSL would have taken a linear trend over this period.

The potential fluctuations in the record over this period can be limited to around 2.5 m asl, as demonstrated by the sedimentary and diatom record, which provide little evidence of marine inundation above the proposed sea-level index point in Borgarland 10. The short lived reintroduction of low numbers of brackish species in Borgarland 10 is likely to be due to storm activity or sea spray rather than a rise in RSL. The analysis of additional core samples from Borgarland would lead to a more definite conclusion regarding the occurrence of low numbers of brackish species in Borgarland.

6.6 Comparison with regional trends in RSL records within NW Iceland

The RSL curve generated in this research provides an insight into the timings and extent of RSL changes in the Snæfellsnes peninsula, western Iceland. In order to place this within the regional context, it is necessary to compare and contrast these results to those generated in previous study within NW Iceland (e.g. Rundgren *et al.*, 1997; Lloyd *et al.*, 2009; Figure 2.8).

The close proximity of the Lloyd *et al.* (2009) study site to this research means that trends and differences between records over a relatively short distance can be determined. As a result, potential differences in glacial load, timing of deglaciation and rates of rebound can be determined for the two study areas. In addition to this, the RSL curve presented from the Skagi peninsula, northern Iceland (Figure 2.8; Rundgren *et al.*, 1997) provides an opportunity for comparison with sites from further afield within NW Iceland. Finally, the recent RSL changes experienced are best compared to the results generated by Gehrels *et al.* (2006) from Viðarhólmi, southern Snæfellsnes, western Iceland (Figure 2.8), despite the differences in study resolution.

It is apparent from the two previously published Holocene RSL records (Figure 2.8) that the formation of the marine limit in Snæfellsnes appears to have occurred concurrently with sites elsewhere in NW Iceland. This suggests that Snæfellsnes also deglaciated at a similar time to the sites at Bjarkarlundur, southern Vestfirðir (Lloyd *et al.*, 2009) and northernmost Skagi (Rundgren *et al.*, 1997). Lloyd *et al.* (2009) provide a timing of deglaciation for southern Vestfirðir of 14 cal.ka BP, with Rundgren *et al.* (1997) providing a corresponding age for Skagi of 13.85 cal. ka BP.

Although caution should be exercised when employing dates for the marine limit, it is clear that RSL fell relatively rapidly following the deglaciation of the peninsula. Both the Lloyd *et al.* (2009) and Rundgren *et al.* (1997) curves also demonstrate relatively rapid fall following the formation of the marine limit. Rundgren *et al.* (1997) note that RSL fell around 45 m between 13 cal. ka BP and 10.2 cal. ka BP, which correlates well with the results of the Snæfellsnes analyses.

The Lloyd *et al.* (2009) paper provides discussion of the rates of both RSL fall and crustal rebound following initial deglaciation, as outlined in Chapter 2. For this section of the discussion, the dates have been converted from original radiocarbon years presented in the papers to calibrated years, using the CALIB 6.0 software. . Lloyd *et al.* (2009) note a rate of RSL fall of $-32.5 \text{ mm cal. yr}^{-1}$ during Bølling-Allerød times, which decreased to $-16.6 \text{ mm cal. yr}^{-1}$ during the early Holocene. This relates to a rate of crustal rebound of $+56 \text{ mm cal. yr}^{-1}$ between $14048 \pm 90 \text{ cal. yrs BP}$ and $13268 \pm 66 \text{ cal. yrs BP}$ and $+32 \text{ mm cal. yr}^{-1}$ during the early Holocene (Lloyd *et al.*, 2009). These values differ from the values generated by Rundgren *et al.* (1997) for the Skagi peninsula, which provide a rate of RSL fall of $-15.5 \text{ mm cal. yr}^{-1}$ and a rate of crustal rebound of $+26.5 \text{ mm cal yr}^{-1}$ between 13093 - 13314 cal. yr BP and 10183 - 10411 cal. yrs BP. The results from the Snæfellsnes peninsula demonstrate a RSL fall from 65 m asl at approximately 14000 cal. yrs BP to 16.20 m asl at 12558 - 12646 cal. yrs BP, thus highlighting a rate of RSL fall of $-37 \text{ mm cal. yr}^{-1}$ over the period. This relates to a rate of crustal rebound of $+55 \text{ mm cal. yr}^{-1}$ between 14000 cal. yrs BP and 12558 - 12646 cal. yrs BP, taking into account the rise in eustatic sea level of $\sim 25 \text{ m}$ over the same period (Fairbanks, 1989).

The rates of both RSL fall and crustal rebound seem to fit well with the regional trends seen in NW Iceland, with the figure for RSL fall fitting particularly well with the Lloyd *et al.* (2009) data. This does not seem surprising however, due to the proximity of the two sites, with a distance of ~ 60 km between them. Although the Skagi peninsula also appears to have experienced relatively rapid initial RSL fall following deglaciation (Figure 2.8), this does not appear to have occurred as rapidly as in Snæfellsnes or southern Vestfirðir. The higher values from the Snæfellsnes data and Lloyd *et al.* (2009) study suggest that ice was thicker in southern Vestfirðir, leading to more rapid and greater levels of crustal rebound. However, it should be noted that the values presented for the Skagi peninsula represent a period later in the rebound process, during which rates of crustal rebound lower in southern Vestfirðir and as such direct comparison should be treated with caution.

The rapidity of early Holocene RSL fall in Snæfellsnes is further demonstrated by the ages of isolation for the samples dated from Saurar 3 and Þingvallavatn, which are 12558 - 12646 cal. yrs BP and 11089 – 11219 cal. yrs BP respectively. Both of these basins, which occur at relatively low elevations, appear to have isolated from the sea relatively early during the Lateglacial-Holocene transition. This correlation between rates and timings of RSL fall between Snæfellsnes and southern Vestfirðir can therefore be used to hypothesise that the two regions underwent similar RSL histories immediately following deglaciation, as demonstrated in Figure 6.5.

Following this point in the RSL history of the Snæfellsnes peninsula, differences between the Snæfellsnes and other NW Iceland records can be determined. The principal differences can be seen between the Skagi (Rundgren *et al.*, 1997) and Snæfellsnes records, as the Snæfellsnes record does not provide any evidence for marine transgressions during this period of RSL fall during the Lateglacial and early Holocene. This is demonstrated by the lack of evidence for a reversal in the trend of RSL fall in the two intermediate basins, Helgafellsvatn and Saurar 1. Neither of the basins records a transgression within the sedimentary or diatom records; however, the lack of an age constraint

RSL curves from NW Iceland (Rundgren *et al.*, 1997; Lloyd *et al.*, 2009; present study)

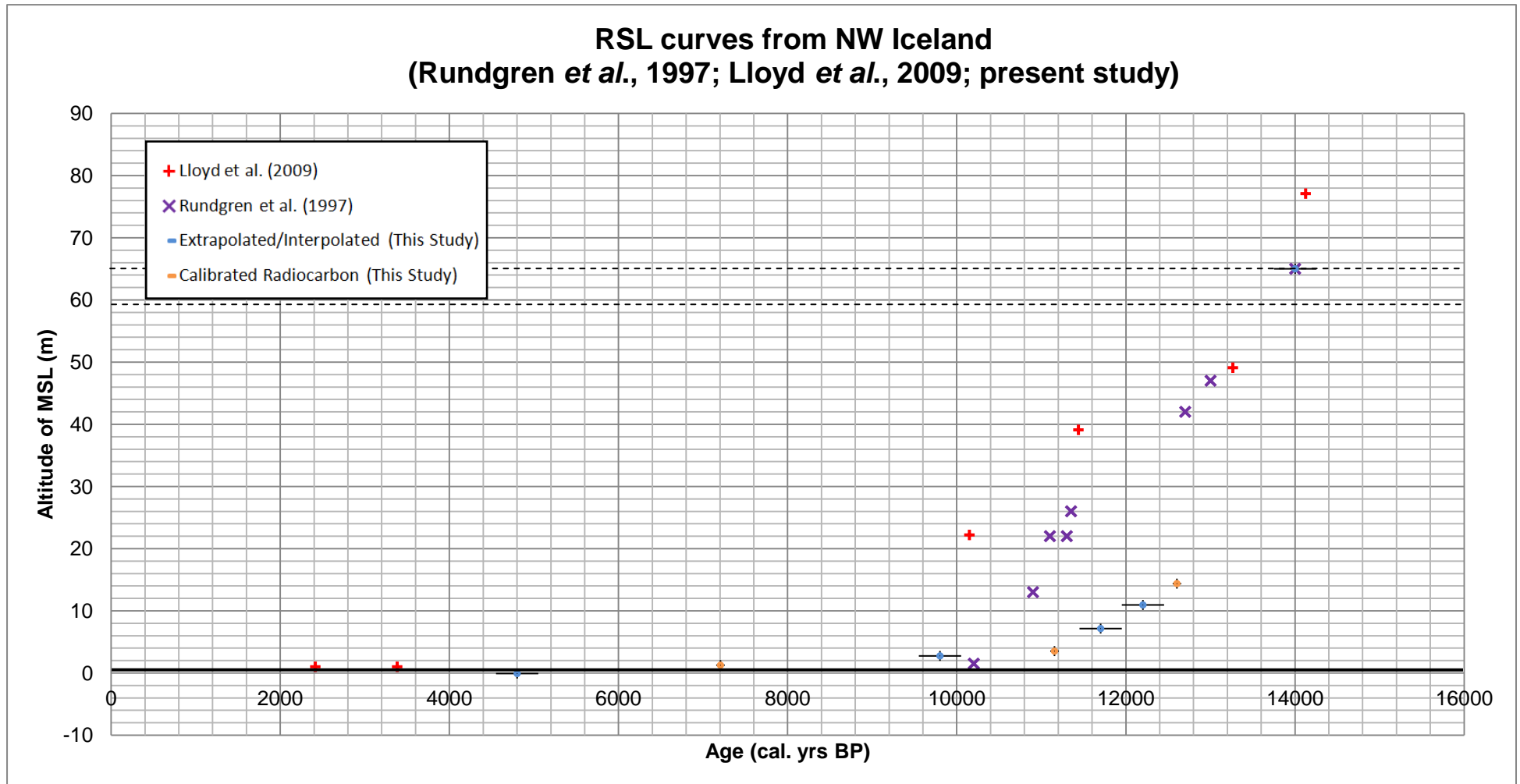


Figure 6.5: RSL curves for NW Iceland, highlighting the regional trends within the datasets and RSL in relation to present. Dashed black lines represent the marine limit elevations in the area.

at these sites means that it is difficult to establish whether the rate of RSL fall varied over this period. It is therefore possible that the rate of RSL fall slowed over this period, but without the chronological control, it is impossible to determine whether this occurred.

It is clear that there is potential for RSL to have fallen below present over the course of the Holocene in Snæfellsnes, particularly during the Late Holocene. As outlined previously, there is also potential for a lowstand in the RSL record followed by a mid Holocene highstand, as demonstrated in southern Vestfirðir by Lloyd *et al.* (2009) after 10 cal. ka BP. Further chronological constraints for both the Skjaldarvatn and Borgarland 11 cores would allow a more accurate depiction of RSL change to be provided, however the proposed fall below present sea level at Borgarland 11 confirms the possibility of recent rising RSL as outlined further south by Gehrels *et al.* (2006). Unfortunately, through the loss of these upper sections of the coastal lowland sediments, there is an incomplete record for changes at this site and so the extent and timing of subsequent transgressions and regressions cannot be achieved. Furthermore, the poor preservation of diatoms at the site means that the results from Borgarland 11 should be approached with some caution.

One would, however, expect sites in relatively close proximity to demonstrate similar trends in their RSL histories and thus the comparison of the two RSL records further highlights the potential for a RSL fall below present following the isolation of Þingvallavatn with a highstand not reaching higher than the isolation contact at Borgarland 10 of 2.54 m asl. This hypothesised RSL fall and subsequent highstand would bring the Snæfellsnes data in line with that from Vestfirðir; however, as stated above, without further chronological control, it is not possible to identify such a pattern of RSL change for this period.

The diatom evidence suggests that RSL fell just below present at ~ 4800 cal. yrs BP. Due to the lack of the upper sections of both the Borgarland 10 and Borgarland 11 sediment cores, it is impossible to determine the patterns of RSL change over the recent past. However, it is likely that the pattern of RSL change in northern Snæfellsnes lies mid way between the Lloyd *et al.* (2009) and Gehrels *et al.* (2006) studies. RSL may have risen above present in the late Holocene, but there is insufficient evidence to test this hypothesis. It is

therefore suggested from the data available that RSL rose slowly to present levels from ~ 4800 cal. yrs BP, lying at a hinge point between potential recent RSL fall in Vestfirðir and recent RSL rise in southern Snæfellsnes (Figure. 6.6).

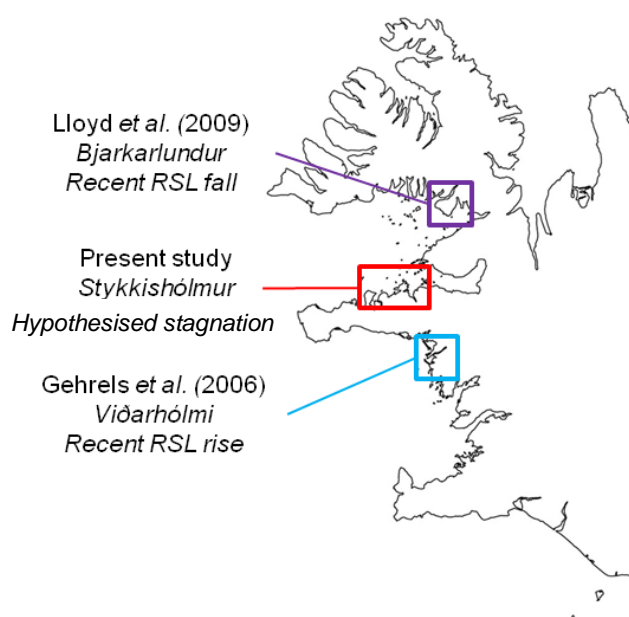


Figure 6.6: Recent RSL patterns for western Iceland, showing trends and site proximity over the last 2000 yrs.

It is worth noting here that any evidence for recent RSL rise or fall would likely have been determined through the diatom evidence from the missing sections of the Borgarland site records. RSL changes would have been better recorded in the Borgarland 11 sample, if diatom preservation levels had been sufficiently high.

It is therefore possible that the results from the Snæfellsnes peninsula demonstrate a hinge point between the hypothesised recent RSL fall in Vestfirðir and recent rise in southern Snæfellsnes. However, in order to determine the records over the recent timescale, additional analyses of saltmarsh sites, such as that at Borgarland are required.

6.7 Chronological Data

Alongside the provision of a chronology for the RSL curve, the chronological data also provides valuable information concerning the extent of tephra deposits in Snæfellsnes. As briefly outlined in the previous chapter, the results

generated as part of this study failed to correlate with well known and well constrained layers previously discovered in Iceland. This result is of particular interest, bearing in mind the distribution of tephra layers within NW Iceland.

In addition to the absence of tephra deposits from the Snæfellsjökull volcano, the Saksunarvatn tephra was also not found within the Snæfellsnes sediment cores. The potential lack of the Saksunarvatn tephra is highlighted by the radiocarbon dates generated during the research. The dates generated for the isolation contacts in the Þingvallavatn and Saurar 3 sediment cores are both older than the Saksunarvatn eruption, which has been dated to 9050 ± 50 yrs BP (Andrews *et al.*, 2002), so the Saksunarvatn tephra would be expected to be present in the sediment sequences just after the isolation contacts of these basins.

The Saksunarvatn tephra was first found by Mangerud *et al.* (1986) in the Faroe Islands and has been discovered throughout NW Iceland (e.g. Björck *et al.*, 1992; Principato, 2000; Andrews *et al.*, 2002, Lloyd *et al.*, 2009). The distribution of the Saksunarvatn throughout the region means that it has frequently been used as a marker horizon in both limnological and marine based studies (e.g. Wastl *et al.*, 1999; Eiríksson *et al.*, 2000).

As a result of the widespread nature of the Saksunarvatn tephra, it is somewhat surprising that the tephra layer was not found within the Snæfellsnes sediment cores. The absence of the Saksunarvatn within the study area may help to constrain the fallout of the eruption, which has been assigned to the Grimsvötn volcano (Grönvold *et al.*, 1995). Following the lack of the deposit near Stykkishólmur, it can now be hypothesised that the deposition of the Saksunarvatn tephra in Snæfellsnes peninsula is more limited than previously thought.

The discovery of the Saksunarvatn tephra in Bjarkarlundur, Vestfirðir (Lloyd *et al.*, 2009) does however suggest that the point at which the tephra layer can be found lies close to Stykkishólmur. Further investigation in the region would lead to an improved knowledge of the deposition pattern of the Saksunarvatn tephra within NW Iceland. It is possible that the Saksunarvatn tephra does exist within Snæfellsnes, but as a microtephra, although this would mean that the deposits are considerably less extensive in the region than elsewhere in NW Iceland.

Despite being unable to correlate the tephra layers in the sediment cores to other dated deposits, the tephrostratigraphy in the sediment cores can be correlated and the geochemical analyses suggest that most are likely to have been produced from similar sources (Figure 5.31). Due to the location of this research, it is likely that some of the tephra layers were deposited following eruptions from the Snæfellsnes Volcanic Belt (SVB). Other basaltic tephra analysed during this research demonstrate compositions similar to Grimsvötn and Katla, suggesting that the tephra samples may be sourced from a variety of volcanic systems. This result is in itself interesting, as little previous research has been undertaken on the basaltic eruptions of the SVB and as such, the tephra deposits provide a valuable insight into the eruption history of the Snæfellsnes peninsula. Furthermore, the tephra results found in the appendices may provide a potential tephra signature from the SVB.

6.8 Summary

This chapter has provided a discussion of the results generated during this study. This has included the calculation and presentation of the sea-level index points generated as part of this research and also the presentation and discussion of the RSL curve for Snæfellsnes. This RSL curve has then been used to infer the ice history for the Snæfellsnes peninsula, alongside providing an insight into the timing and rapidity of RSL changes over the course of the Holocene. These interpretations of the RSL record have then been placed in the regional context through comparison with previously published records from Vestfirðir (Lloyd *et al.*, 2009) and Skagi (Rundgren *et al.*, 1997). The reliability of the data has been discussed, as well as the potential alterations required to current models of deglaciation for Iceland. Furthermore, the tephra results have been discussed, highlighting the potential for a limited Saksunarvatn tephra in Snæfellsnes, alongside the potential signatures for tephra deposits from the SVB.

CHAPTER 7

Conclusions

7.1 Introduction

This chapter provides an overview of the key conclusions generated as part of this research project. The primary conclusions will be outlined, with the consequences of these conclusions being provided alongside. These primary conclusions then allow additional conclusions to be drawn. The secondary conclusions, which are derived from the primary conclusions, will then be presented. Following the presentation of the conclusions, the limitations and recommendations for further research will be outlined.

7.2 Primary Conclusions

7.2.1 Isolation basin and coastal lowland data allow the construction of a RSL curve for the northern Snæfellsnes peninsula.

As demonstrated by the evidence discussed in Chapters 5 and 6, there is clear support for the use of isolation basin and coastal lowland data in the determination of RSL changes in NW Iceland. The diatom data produced a reliable environmental reconstruction, which when coupled with support from the sedimentary record, allowed the reconstruction of RSL changes over the course of the Holocene. In doing so, the construction of a RSL curve was possible for northern Snæfellsnes, allowing the trends with other NW Iceland records. In the majority of locations, the diatom record was sufficiently well preserved to provide an overview of the decrease in marine influences, with the Borgarland 11 sediment core being the only exception due to poor levels of preservation.

7.2.2 Marine limit elevations can be mapped along the northern side of the Snæfellsnes peninsula.

There are several locations within northern Snæfellsnes where the elevation of the marine limit can be accurately measured. Through the determination of elevations at two distinct points within the northern Snæfellsnes area, changes in elevation could be determined.

7.2.3 The analysis of tephra layers in the Snæfellsnes sediment cores show previously unrecognised and undated eruptions, which have implications for tephrochronology and for the understanding of ash dispersal patterns in Iceland.

Tephra analyses have revealed important findings for the Snæfellsnes peninsula, through the determination of local eruptive events and the potential signature of tephra from the Snæfellsnes Volcanic Belt (SVB). In doing so, the results provide an insight into the eruptive history of the SVB and the potential for correlation with samples from elsewhere within the peninsula. Further investigation of these tephra deposits could lead to the determination of a series of chronological markers for the Snæfellsnes peninsula, which if accurately dated, could be linked to the wider Icelandic tephra chronology. Furthermore, the tephra analyses and subsequent identification of samples at particular sites have assisted in the determination of ash dispersal patterns, both from the SVB and other volcanic systems.

7.3 Secondary Conclusions

7.3.1 Marine limit elevations in northern Snæfellsnes highlight potential areas of similar ice thickness within NW Iceland.

As discussed in Chapter 6, if the marine limit is assumed to have formed concurrently throughout NW Iceland, there is a clear correlation between the potential ice thickness over the Snæfellsnes and Skagi (Rundgren *et al.*, 1997) peninsula. This assumption is further confirmed by the similarity in the extrapolated marine limit elevations between the two studies, both producing values ~ 65 m asl. This similarity of timings of deglaciation and ice thicknesses

support the predictions of the current ice models, with Hubbard *et al.* (2006) showing that ice retreated at similar times from the two locations.

7.3.2 Marine limit elevations in northern Snæfellsnes highlight the potential for thicker ice in southern Vestfirðir.

Lower marine limit elevations recorded in northern Snæfellsnes than southern Vestfirðir suggest that thicker ice was present in southern Vestfirðir, if simultaneous deglaciation is assumed. Again, the extrapolated marine limit formation age in Snæfellsnes fits well with the isolation basin-sourced marine limit age in southern Vestfirðir (Lloyd *et al.*, 2009). The lower marine limit elevations in northern Snæfellsnes suggest that the ice in this location was thinner than further north. The rebound rates for the two locations are broadly similar; however, those from southern Vestfirðir (Lloyd *et al.*, 2009) are slightly higher than in Snæfellsnes. This potential for thicker ice in southern Vestfirðir is not supported in the current models of ice thickness in Iceland, with greater ice being modelled further North near present day Drangajökull (e.g. Hubbard *et al.*, 2006). This ice is modelled as having a longer duration, thus resulting in the lower marine limit elevations in northern and central Vestfirðir (Hubbard *et al.*, 2006).

7.3.3 The Snæfellsnes ice cap may have had an effect on the RSL history of the Snæfellsnes peninsula, counteracting the potential influences from the proposed main ice loading centre.

The two marine limit elevation measurements highlight a rising marine limit with distance from the proposed main ice loading centre. This could result from either earlier deglaciation of the outer Snæfellsnes region (Figure 3.1) or through the increased influence of the Snæfellsnes ice cap on measurements taken in outer Snæfellsnes. This proposed greater influence of the Snæfellsnes ice cap should be considered when modelling ice thickness. At present, the influence of such ice caps is taken into consideration (e.g. Hubbard *et al.*, 2006); however, greater emphasis on this may be required.

7.3.4 RSL fell relatively rapidly during the Lateglacial and early Holocene in Snæfellsnes.

There is abundant evidence from the records of environmental change and subsequent generation of sea-level index points that RSL fell relatively rapidly over the course of the Lateglacial and early Holocene. The results generated in this research provide a rate of RSL fall of $-37 \text{ mm cal. yr}^{-1}$ between 14000 cal. ka BP and $12602 \pm 44 \text{ cal. yrs BP}$, which corresponds to a crustal rebound rate of $+55 \text{ mm cal. yr}^{-1}$ over the same period. As demonstrated by the RSL curve for the region (Figures 6.1 and 6.5) the rate of this RSL fall reduced dramatically after the isolation of Saurar 3.

7.3.5 The RSL history of the Snæfellsnes peninsula fits well with regional trends over the course of the Lateglacial and Early Holocene.

As demonstrated through the discussion of the marine limit and environmental datasets, there are clear correlations between the RSL history produced in this study and in those generated in Rundgren *et al.* (1997), Lloyd *et al.* (2009) and, to some extent, Gehrels *et al.* (2006). The positioning of the Snæfellsnes data within the regional datasets (Figure 6.5) demonstrates the close correlation between the records from the region.

It is apparent that RSL has fallen over the course of the Lateglacial and early Holocene periods throughout NW Iceland from a high point at $\sim 14000 \text{ cal. yrs BP}$. The rates of this fall vary throughout the region, although there is a strong correlation between the results generated from northern Snæfellsnes and southern Vestfirðir. In the late Holocene, the RSL record from northern Snæfellsnes appears to demonstrate that the area sits at the proposed hinge point between rising RSL further South, as demonstrated by Gehrels *et al.* (2006) and the proposed falling RSL further North, as demonstrated by Lloyd *et al.* (2009). This suggests that RSL rose slowly after $\sim 4800 \text{ cal. yrs BP}$ and has then remained around present levels.

It is likely that the differences between the datasets are generated through differences in ice thickness and deglacial patterns. The variation over the

recent timescale may be a result of the residual rebound rates in the various study areas. In southern Vestfirðir, the rate of RSL rise may be outpacing the rate of RSL rise due to the thicker ice present there during the LGM, for example.

7.3.6 There is potential evidence for recent RSL rise in northern Snæfellsnes.

Evidence of RSL fall below present has been presented from the Borgarland 11 site, although an accurate age constraint on this is required in order to provide a more reliable pattern of RSL change. Through the extrapolation of the Snæfellsnes RSL curve generated in this study, the tentative date of 4800 cal. yrs BP has been assigned to this period of RSL below present. Although this timing should be treated with some caution, the case for RSL fall below present seems compelling. At present, due to the time assigned to this fall, it is proposed that RSL has risen recently within northern Snæfellsnes. Further investigation is required to determine the extent of these changes and potential fluctuations, although it is certain that RSL did not rise above the sill of Skjaldarvatn, as there is no evidence of reinundation within the diatom record from the site.

7.3.7 Tephrochronology has highlighted both the lack of an easily identifiable Saksunarvatn tephra deposit in northern Snæfellsnes and also the potential signature of tephra from the Snæfellsnes Volcanic Belt (SVB).

Despite being unable to correlate the tephra analysis results with previously published records, the tephra results have provided an opportunity to make internal correlations using tephrostratigraphy and also an insight into the potential composition of the SVB tephras. There are clear correlations within the dataset, thus allowing confirmation of the relative timing of decrease in marine influence in the isolation basins and coastal lowland samples investigated in this study. This has allowed a greater certainty to be associated with the RSL record, as timings have been related to sample elevations.

The tephra analyses have also provided an insight into the extent of the Saksunarvatn tephra within the Snæfellsnes region. Extensive Saksunarvatn deposits have been found elsewhere in NW Iceland (e.g. Andrews *et al.*, 2002; Lloyd *et al.*, 2009), yet there is little evidence of its existence within the

Snæfellsnes records. The Saksunarvatn may be present as a thin layer however, which may mean that it is not visible to the naked eye.

7.4 Limitations and recommendations for further research

There are limitations which should be considered when evaluating this research. In addition, there are various recommendations which could be employed when undertaking further research in this area.

The principal limitation to this research is the lack of chronological control for several of the sites studied. An accurate timing of the decrease in marine influences at Borgarland 11, Skjaldarvatn, Saurar 1 and Helgafellsvatn would allow more reliable sea-level index points to be generated for each of the sites, rather than interpolating values from the RSL curve produced. Furthermore, an accurate timing for the formation of the marine limit would be greatly beneficial, as the current value is based on an extrapolation of the RSL curve rather than an accurately dated deposit. Despite the value correlating well with values published elsewhere, the marine limit formation timing would be more reliable if based on a dated deposit or isolation basin contact. Further investigation of the isolation basins identified in Barar (Innra-Baravatn and Ytra-Baravatn) could potentially provide this data.

The timing of the decreases in marine influence at the non-radiocarbon dated sites could be established through additional radiocarbon sampling; however, resources did not permit this in the present study. In addition, the further analysis of tephra deposits within the sediment core samples may generate further data for tephrostratigraphic correlation between the core samples. This would involve the analysis of tephra deposits at greater distance from the isolation contact within the isolation basin sediments. However, this may in turn correlate with the tephra deposits analysed close to isolation contacts in other sediment cores and as such would allow the determination and confirmation of relative isolation at the various sites.

In future study, it would be greatly beneficial to further investigate the isolation basins at higher elevations within the region, such as those found near the Barar marine limit site, as well as to further investigate the tephra deposits within the region. If an accurate composition and timing of the SVB tephra

deposits can be established, the use of tephrochronology in the region would be greatly strengthened. This would allow the correlation of samples within the peninsula and relative to well known tephra layers elsewhere in Iceland and further afield. In addition, the tephra deposits within the lake sediments could be related to tephra samples within open sections on the peninsula, thus allowing a correlation between the lake and terrestrial sediment deposits and providing the potential to further extend the available chronology. If a sample within the lake sediments can be linked to deposits within an open section, the lake deposit can then in turn be related to other tephra deposits not present within the lake sequence. As such, the chronology for the isolation basin and coastal lowland sites would become more robust.

APPENDIX

The raw diatom counts and results of the geochemical analyses can be found on the CD which accompanies this thesis.

REFERENCES

Ægisdóttir, H. H. and Þórhallsdóttir, Þ. E. (2005) Theories on migration and history of the North Atlantic flora: a review *Jökull Vol. 54 Pg. 1-16*.

Alloway, B. V.; Larsen, G.; Lowe, D. J.; Shane, P. A. R. and Westgate, J. A. (2007) Tephrochronology In, Elias, S. A. (edit.) *Encyclopedia of Quaternary Science Amsterdam: Elsevier Pg. 2869-2898*

Andrews, J. T (1970) A geomorphological study of postglacial uplift: with particular reference to Arctic Canada *London: Institute of British Geographers 156pp*.

Andrews, J. T. and Helgadóttir, G. (2003) Late Quaternary ice extent and deglaciation of Hunafloaall, north Iceland: evidence from marine cores. *Arctic, Antarctic, and Alpine Research Vol. 35 Pg. 218–232*

Andrews, J. T.; Hardardóttir, J.; Helgadóttir, G.; Jennings, A. E.; Geirsdóttir, Á.; Sveinbjörnsdóttir, Á. E.; Schoolfield, S.; Kristjánisdóttir, G. B.; Smith, L. M., Thors, K. and Syvitski, J. P. M. (2000) The N and W Iceland Shelf: insights into Last Glacial Maximum ice extent and deglaciation based on acoustic stratigraphy and basal radiocarbon AMS dates *Quaternary Science Reviews Vol. 19 Pg. 619-631*

Andrews, J. T.; Kihl, R.; Kristjánisdóttir, G. B.; Smith, L. M.; Helgadóttir, G.; Geirsdóttir, A. and Jennings, A. E. (2002) Holocene sediment properties of the East Greenland and Iceland continental shelves bordering the Denmark Strait (64-68N), North Atlantic *Sedimentology Vol. 49 Pg. 5-24*.

Ásbjörnsdóttir, L. and Norðdahl, H. (1995) Götungar í sjávarsetlögum við Mela á Skarðsströnd. In, Hróarsson, B.; Jónsson, D.; Jónsson, S. S. (eds.) *Eyjar í Eldhafi Reykjavík: Gott mál Pg. 179-188*

Ascough, P. L.; Cook, G. T.; Hastie, H.; Dunbar, E.; Church, M. J.; Einarsson, Á.; McGovern, T. H. and Dugmore, A. J. (2011) An Icelandic freshwater

radiocarbon reservoir effect: implications for lacustrine ^{14}C chronologies *The Holocene Vol. 21 No. 7 pg. 1073-1080*

Bárðarson, G. G. (1906) *Purpura lapillus* L. i haevede Lag paa Nordkysten af Island. *Videnskabelige Meddelelser fra dansk naturhistorisk Forening Vol. 58 Pg. 177-85.*

Bárðarson, G. G. (1910) Maerker efter Klima- og Niveauforandringer ved Húnaflói i Nord-Island. *Videnskabelige Meddelelser fra dansk naturhistorisk Forening Vol. 62 Pg. 35-79.*

Bárðarson, G. G. (1923) Fornar Sjávarminjar vid Borgarfjörd og Hvalfjörd. *Rit Visinda-felags Islendinga Vol. 1 Akureyri, Iceland.*

Barker, D. S. (1983) *Igneous Rocks Prentice-Hall: Englewood Cliffs, New Jersey, USA.*

Battarbee, R.W. (1986) Diatom Analysis In, Berglund, B.E. (ed.) *Handbook of Holocene palaeoecology and palaeohydrology Chichester: Wiley p. 527-570*

Bell, T. (1996) the last glaciation and sea-level history of Fosheim Peninsula, Ellesmere Island, Canadian High Arctic *Canadian Journal of Earth Sciences Vol. 33 No. 7 Pg. 1075-1086*

Benn, D. I. and Evans, D. J. A. (2010) *Glaciers and Glaciation Second Edition Abingdon: Hodder Education.*

Bingham, R.; Hulton, N. and Dugmore, A. J. (2003) Modelling the southern extent of the last Icelandic Ice Sheet *Journal of Quaternary Science Vol. 18 No. 2 Pg. 169-181.*

Björck, S.; Ingólfsson, Ó.; Hafliðason, H.; Hallsdóttir, M. and Anderson, N. J. (1992) Lake Torfadalsvatn: a high resolution record of the North Atlantic Ash Zone 1 and the last glacial-interglacial environmental changes in Iceland *Boreas Vol. 21 Pg. 15-22.*

Bourgeois, O.; Dauteuil, O. and Van Vliet-Lanoe, B. (1998) Pleistocene subglacial volcanism in Iceland: tectonic implications *Earth and Planetary Science Letters Vol. 164 Pg. 165-178*

Bradbury, J. P. (1975) Diatom stratigraphy and human settlement in Minnesota
Geological Society of America Special Paper No 171 Pg. 1-74

Brun, J. (1965) Diatomées des Alpes et du Jura *Amsterdam: Asher and Co.*

Buckland, P. and Dugmore, A. (1991) 'If this is a Refugium, why are my feet so bloody cold?' The origins of the Icelandic biota in the light of recent research In, Caseldine, C. and Maizels, J. K. (edits.) *Environmental Change in Iceland: Past and Present Dordrecht: Kluwer Pg. 107-125*

Caseldine, C.; Geirsdottir, A. and Langdon, P. (2003) Efstadalsvatn – a multi-proxy study of a Holocene lacustrine sequence in NW Iceland *Journal of Paleolimnology Vol. 30 No. 1 Pg. 55-73*

Corner, G. D.; Kolka, V. V.; Yevzerov, V. Y. and Møller, J. J. (2001) Postglacial relative sea-level change and stratigraphy of raised coastal basins on Kola Peninsula, northwest Russia *Global and Planetary Change Vol. 31 No 1-4 Pg. 155-177.*

Dickson, B.; Yashayaev, I.; Meincke, J.; Turrell, B.; Dye, S.; Holfort, J.(2002) Rapid freshening of the deep North Atlantic Ocean over the past four decades. *Nature Vol. 416 Pg. 832*

Doner, L. (2003) Late Holocene palaeoenvironments of northwest Iceland from lake sediments *Palaeogeography, Palaeoclimatology, Palaeoclimatology Vol. 193 Pg. 535-560.*

Dugmore, A. J. and Newton, A. J. (1992) Thin tephra layers in peat revealed by X-radiography. *Journal of Archaeological Science Vol. 19 Pg. 163–170.*

Dugmore, A. J.; Newton, A. J.; Sugden, D. E. and Larsen, G. (1992) Geochemical stability of fine grained silicic Holocene tephra in Iceland and Scotland *Journal of Quaternary Science Vol. 7 Pg. 173-183*

Dugmore, A. J.; Larsen, G. And Newton, A. J. (1995) Seven tephra isochrones in Scotland *The Holocene Vol. 5 Pg. 257-266*

Dugmore, A. J.; Newton, A. J.; Edwards, K. J.; Larsen, G. Blackford, J. J. and Cook, G. T. (1996) Long-distance marker horizons from small-scale eruptions:

british tephra deposits from the AD 1510 eruption of Hekla, Iceland *Journal of Quaternary Science Vol. 11 Pg. 511-516*

Egloff, J. and Johnson, G. L. (1979) Erosional and depositional structures of the Southwest Iceland insular margin: thirteen geophysical profiles In, Watkins, J. S.; Montadert, L. and Dickerson, P. W. (edits.) Geological and geophysical investigations of continental margins *Tulsa, OK: AAPG Pg. 43-63*

Einarsson, Th. (1967) Zu der Ausdehnung der weichselzeitlichen Verseiung Nordislands Sonderoffentlichungen des Geologischen Institutes der Universitat Koln 13 Pg. 167-173

Einarsson, Th. (1968) Jarðfræði. Saga bergs og lands *Reykjavik: Mál og Menning*

Einarsson, Th. (1973) Geology of Iceland In, Pitcher, M. G. (edit.) *Arctic Geology: Memoirs of the American Association of Petroleum Geologists Vol. 19 Pg. 171-175*

Einarsson, Th. (1979) The deglaciation of Iceland *Norsk Geologisk Förening Medlemsblad 13 Pg. 18*

Einarsson, M. A. (1984) Climate of Iceland In, van Loon, H. (edit.) *World Survey of climatology No. 15 Climates of the Oceans Amsterdam: Elsevier Pg. 673-697.*

Einarsson, T. and Albertsson, K. J. (1988) The glacial history of Iceland during the past three million years *Philosophical Transactions of the Royal Society of London Series B Vol. 318 Pg. 637-644*

Eiriksson, J.; Simonarson, L. A.; Knudsen, K. L. and Kristensen, P. (1997) Fluctuations of the Weichselian ice sheet in SW Iceland: a glaciomarine sequence in Sudurnes, Seltjarnes *Quaternary Science Reviews Vol. 16 Pg. 221-240*

Eiríksson, J.; Knudsen, K. L.; Hafliðason, H. and Henriksen, P. (2000) Late-glacial and Holocene palaeoceanography of the North Icelandic Shelf *Journal of Quaternary Science Vol. 15 No. 1 Pg. 23-42*

Evans, D. J. A. (1990) The last glaciation and relative sea-level history of northwest Ellesmere Island, Canadian High Arctic *Journal of Quaternary Science Vol. 5 Pg. 67-82*

Evans, D. J. A.; Rea, B. R.; Hansom, J. D. and Whalley, W. B. (2002) geomorphology and style of plateau icefield deglaciation in fjord terrains: the example of troms-Finnmark, north Norway. *Journal of Quaternary Science Vol. 17 No. 3 Pg. 221-239*

Fairbanks, R. G. (1989) A 17000 year glacio-sea-level record: influence of glacial melting rates on the Younger Dryas event and deep-ocean circulation *Nature Vol. 342 Pg. 637-642*

Fleming, K. and Lambeck, K. (2004) Constraints on the Greenland Ice Sheet since the Last Glacial Maximum from sea-level observations and glacial-rebound models *Quaternary Science Reviews Vol. 23 Pg. 1053-1077*

Foged, N. (1974) Freshwater diatoms in Iceland *Bibliotheca Phycologica No. 15 118pp.*

Freund, H.; Gerdes, G.; Streif, H.; Dellwig, O. and Watermann, F. (2004) The indicative meaning of diatoms, pollen and botanical macro fossils for the reconstruction of palaeoenvironments and sea-level fluctuations along the coast of Lower Saxony; Germany *Quaternary International Vol. 112 No. 1 Pg. 71-87*

Gehrels, W. R.; Bellenap, D. F.; Pearce, B. R. and Gong, B. (1995) Modelling the contribution of M2 tidal amplification to the Holocene rise of mean high water in the Gulf of Maine and the Bay of Fundy *Marine geology Vol. 124 Pg. 71-85.*

Gehrels, W. R.; Marshall, W. A.; Gehrels, M. J.; Larsen, G.; Kriby, J. R.; Eiriksson, J.; Heinemeier, J. and Shimmiel, T. (2006) Rapid sea-level rise in the North Atlantic Ocean since the first half of the nineteenth century *The Holocene Vol. 16 No. 7 Pg. 949-965*

Geirsdóttir, Á.; Hardardóttir, J. and Eiriksson, J. (1997) The depositional history of the Younger Dryas-Preboreal Búði moraines in south-sentral Iceland *Arctic and Alpine Research Vol. 29 Pg. 13-23*

Grimm, E. C. (1987) CONISS: A FORTRAN 77 program for stratigraphically constrained cluster analysis by the method of incremental sum of squares *Computers and Geosciences Vol. 13 pg. 13-35*

Grönvold, K.; Óskarsson, N.; Johnsen, S. J.; Clausen, H. B.; Hammer, C. U.; Bond, G. And Bard, E. (1995) Ash layers from Iceland in the Greenland GRIP ice core correlated with oceanic and land sediments *Earth and Planetary Science Letters Vol. 135 Pg. 149-155*

Gudmundsson, A. (1986) Mechanical aspects of postglacial volcanism and tectonics of the Reykjanes peninsula, southwest Iceland *Journal of Geophysical Research Vol. 91 No. 12 Pg. 711-721*

Gudmundsson, A. (2000) Dynamics of volcanic systems in Iceland: example of tectonism and volcanism at juxtaposed hotspots and midocean ridge system *Annual Reviews of Earth and Planetary Sciences Vol. 28 pg. 107-140.*

Gudmundsson, M. T.; Sigmundsson, F.; Björnsson, H. (1997) Ice-volcano interaction of the 1996 Gjalp eruption, Vatnajökull, Iceland *Nature Vol. 389 Pg. 954-957.*

Hafliðason, H.; Eiriksson, J. and van Kreveld, S. (2000) The tephrochronology of Iceland and the North Atlantic region during the Middle and Late Quaternary: a review *Journal of Quaternary Science Vol. 15 No. 1 Pg. 3-22*

Hallsdóttir, M. and Caseldine, C. (2005) The Holocene vegetation history of Iceland, state-of-the-art and future research In, Caseldine, C.; Russell, A.; Hardardóttir, J. and Knudsen, Ó. (eds.) Iceland – Modern Processes and Past Environments *Developments in Quaternary Science 5 Elsevire:Amsterdam Pg. 319-334.*

Hansom, J. D. and Briggs, D. J. (1991) Sea-level change in Vestfirðir, North West Iceland In, Maizels, J. L. and Caseldine, C. J. (edits.) *Environmental Change in Iceland: Past and Present Dordrecht: Kluwer Pg. 79-91*

Hartley, B.; Barber, H. G.; Carter, J. R. and Sims, P. A. (1996) An Atlas of British Diatoms *Bristol: Biopress*

Hayward, C. (pers. comm.) Email concerning the ability to separate individual eruptions from the same volcanic system

Hayward, C. (2011) High spatial resolution electron probe microanalysis of tephra and melt inclusions without beam-induced chemical modification *The Holocene [online]* DOI: 10.1177/0959683611409777

Helgadóttir, G. and Thors, K. (1998) Setlög í Ísafjarðardjúpi, Jökulfjörðum og Djúpál (In Icelandic). Geoscience Society of Iceland, Spring Meeting 1998, p. 12

Hjartarson, A. (1991) A revised model of Weichselian deglaciation in south and southwest Iceland, In, Maizels, J.K. and Caseldine, C. (eds.) Environmental Change in Iceland, Past and Present *Dordrecht: Kluwer Academic Pg. 67-77*

Hjartarson, A. and Ingólfsson, Ó. (1988) Preboreal glaciation of Southern Iceland *Jökull Vol. 38 Pg. 1-16*

Hjort, C.; Ingólfsson, Ó. and Norðdahl, H. (1985) Late Quaternary geology and glacial history of Hornstrandir, Northwest Iceland: a reconnaissance study *Jökull Vol. 35 Pg. 9-29*

Hodder, A. P. W.; de Lange, P. J. and Lowe, D. J. (1991) Dissolution and depletion of ferromagnetism minerals from Holocene tephra layers in an acid bog, New Zealand, and implications for tephra correlation *Journal of Quaternary Science Vol. 6 No. 3 Pg. 195-208*

Hoppe, G. (1968) Grimsey and the maximum extent of the last glaciation of Iceland *Geografiska Annaler Vol 50 Pg. 16-24*

Hoppe, G. (1982) The extent of the last inland ice sheet of Iceland *Jökull Vol. 35 Pg. 3-11*

Hubbard, A. (2006) The validation and sensitivity of a model of the Icelandic Ice Sheet *Quaternary Science Reviews Vol. 25 Pg. 2297-2313*

Hubbard, A.; Sugden, S.; Dugmore, A.; Norðdahl, H. and Pétursson, H. G. (2006) A modelling insight into the Icelandic Last Glacial Maximum ice sheet *Quaternary Science Reviews Vol. 25 Pg. 2283-2296*

Hunt, J. B. and Hill, P. G. (1993) Tephra geochemistry: a discussion of some persistent analytical problems *The Holocene Vol. 3 No. 3 Pg. 271-278*

Icelandic Hydrographic centre (pers comm. A) Email detailing the tide gauge data from Reykjavik, Iceland.

Icelandic Hydrographic Centre (pers. Comm. B) Email detailing the tide gauge data from Stykkishólmur, Iceland.

Ingólfsson, Ó. (1984) A review of late Weichselian studies in the lower part of the Borgarfjörður region, western Iceland *Jökull Vol. 34 pg. 117-130*

Ingólfsson, Ó. (1985) Weichselian Glacial Geology of the Lower Borgarfjörður, Western Iceland: a preliminary report *Arctic Vol. 38 No. 3 Pg. 210-213*

Ingólfsson, Ó. (1987) The late Weichselian glacial geology of the Melabakkar-Asbakkar coastal cliffs, Borgarfjörður, W-Iceland *Jökull Vol. 37 Pg. 57-80*

Ingólfsson, Ó. (1988) Glacial history of the lower Borgarfjörður area, western Iceland *Geologiska Föreningens i Stockholm Förhandlingar Vol. 110 Pg. 293-309*.

Ingólfsson, Ó. (1991) A review of the Late Weichselian and early Holocene glacial and environmental history of Iceland In, Caseldine, C. and Maizels, J. K. (edits.) *Environmental Change in Iceland: Past and Present Dordrecht: Kluwer Pg. 13-29*

Ingólfsson, A. (2009) A marine refugium in Iceland during the last glacial maximum: fact or fiction? *Zoologica Scripta Vol. 38 Pg. 663-665*.

Ingólfsson, Ó. and Norðdahl, H. (1994) A review of the environmental history of Iceland, 13000-9000 yr BP *Journal of Quaternary Science Vol. 9 No. 2 Pg. 147-150*

Ingólfsson, Ó. and Norðdahl, H. (2001) High relative sea level during the Bølling Interstadial in Western Iceland: a reflection of ice-sheet and extremely rapid glacial unloading *Arctic, Antarctic and Alpine Research Vol. 33 No. 2 Pg. 231-243*

Ingólfsson, Ó.; Norðdahl, H. and Hafliðason, H. (1995) Rapid isostatic rebound in southwestern Iceland at the end of the last deglaciation *Boreas* Vol. 24 Pg. 245-259

Ingólfsson, Ó.; Björck, S.; Hafliðason, H. and Rundgren, M. (1997) *Glacial and climatic events in Iceland reflecting regional North Atlantic climatic shifts during the Pleistocene-Holocene transition* Quaternary Science Reviews Vol. 16 Pg. 1135-1144

Ingólfsson, Ó.; Norðdahl, H. and Schomacker, A. (2010) Deglaciation and Holocene Glacial History of Iceland In, Schomacker, A.; Krüger, J. and Kjær, K. H. (edits.) *The Mýrdalsjökull Ice Cap, Iceland: Glacial Processes, Sediments and Landforms on an active volcano* *Developments in Quaternary Science* 13 Pg. 51-68

Jakobsson, S.P.; Honsson, J. and Shido, F. (1978) Petrology of the western Reykjanes Peninsula, Iceland. *Journal of Petrology* Vol. 19 Pg. 669-705.

Jakobsson, S. P. (1979) Petrology of recent basalts of the Eastern Volcanic Zone, Iceland *Acta Naturalia Islandica* Vol. 26 Pg. 1-103.

Jennings, A.; Syvitski, J.; Gerson, L.; Grönvold, K.; Geirsdóttir, Á.; Hardardóttir, J.; Andrews, J. and Hagen, S. (2000) Chronology and palaeoenvironments during the late Weichselian deglaciation of the south west Iceland shelf *Boreas* Vol. 29 Pg. 167-183

Jóhannesson, H.; Flores, R. M. and Jónsson, J. (1981) A short account of the Holocene tephrochronology of the Snæfellsjökull central volcano, western Iceland *Jökull* Vol. 31 Pg. 23-30

John, B. (1975) Marine mollusca from Vestfirðir strandlines. *Durham University Vestfirðir Project 1975 Fieldwork Report and Research Notes* Pg. 41-45.

Jowsey, P. C. (1966) An Improved Peat Sampler *New Phytologist* Vol. 65 No. 2 Pg. 245-248.

Juggins, S. (2005) C2 Release 1.4 *University of Newcastle, United Kingdom*

- Jull, M. and McKenzie, D. (1996) The effect of deglaciation on mantle melting beneath Iceland *Journal of Geophysical Research* Vol. 101 No. 21 Pg. 815-828
- Keith, D. B. and Jones, E. W. (1935) Grimsey, North Iceland *Geographical Journal* Vol. 86 Pg. 143-152
- Kittleman, L. R. (1979) Geologic methods in studies of Quaternary tephra In, Sheets, P. D. and Grayson, D. K. (eds.) *Volcanic Activity and Human Ecology Academic Press: New York* Pg. 49-82
- Kjartansson, G.; Thorarinnsson, S. and Einarsson, T. (1964) ¹⁴C aldursákvarðanir á synishornum varðandi islenzka kvarterjarðfræði [English summary: ¹⁴C datings of Quaternary deposits in Iceland] *Náttúrufræðingurinn* Vol. 34 Pg. 97-145
- Kjemperud, A. (1986) Late Weichselian and Holocene shoreline displacement in the Trondheimsfjord area, central Norway *Boreas* Vol. 15 no. 1 Pg. 61-82.
- Kristjansdóttir, G. B.; Stoner, J. S.; Jennings, A. E.; Andrews, J. T. and Grönvold, K. (2007) Geochemistry of Holocene cryptotephra from the North Iceland Shelf (MD99-2269): intercalibration with radiocarbon and palaeomagnetic chronostratigraphies *The Holocene* Vol. 17 No. 2 Pg. 155-176.
- Lambeck, K. and Chappell, J. (2001) Sea Level Change through the Last Glacial Cycle *Vol. 292 No. 5517* Pg. 679-686.
- Langdon, P. G. and Barber, K. E. (2001) Rapid Communication; New Holocene tephra and a proxy climate record from a blanket mire in northern Skye, Scotland *Journal of Quaternary Science* Vol. 16 No. 8 Pg. 753-759
- Langdon, P. G. and Barber, K. E. (2005) The climate of Scotland over the last 5000 years inferred from multiproxy peatland records: inter-site correlations and regional variability *Journal of Quaternary Science* Vol. 20 pg. 549-566.
- Larsen, G. and Eiriksson, J. (2008) Late Quaternary terrestrial tephrochronology of Iceland – frequency of explosive eruptions, type and volume of tephra deposits *Journal of Quaternary Science* Vol. 23 No. 109-120
- Larsen, G.; Dugmore, A. J. and Newton, A. J. (1999) Geochemistry of historical-age silicic tephra in Iceland *The Holocene* Vol. 9 Pg. 463-471

- Le Breton, E.; Dauteuil, O. and Biessy, G. (2010) Post-glacial rebound of Iceland during the Holocene *Journal of the Geological Society of London Vol. 167 Pg. 417-432*
- Lefébure, P. (1947) Atlas pour la détermination des Diatomées *Paris: Laboratoire de Micrographie*
- Livingstone, D. A. (1955) A lightweight piston sampler for lake deposits *Ecology Vol. 36 Pg. 137-139.*
- Lloyd, J. M. and Evans, J. R. (2002) Contemporary and fossil foraminifera from isolation basins in northwest Scotland *Journal of Quaternary Science Vol. 17 No. 5-6 Pg. 431-443*
- Lloyd, J. M.; Norðdahl, H.; Bentley, M. J.; Newton, A. J.; Tucker, O. and Zong, Y. (2009) Lateglacial to Holocene relative sea-level changes in the Bjarkarlundur area near Reykhólar, North West Iceland *Journal of Quaternary Science Vol. 24 No. 7 Pg. 816-831*
- Long, A. J.; Roberts, D. H. and Wright, M. R. (1999) Isolation basin stratigraphy and Holocene relative sea-level change on Arveprinsenn Eiland, Disko Bugt, West Greenland *Journal of Quaternary Science Vol. 14 Pg. 323-345.*
- Long, A. J.; Roberts, D. H.; Simpson, M. J. R.; Dawson, S.; Milne, G. A. and Huybrechts, P. (2008) Late Weichselian relative sea-level changes and ice sheet history in southeast Greenland *Earth and Planetary Science Letters Vo. 272 Pg. 8-18.*
- Long, A. J.; Woodroffe, S. A.; Roberts, D. H. and Dawson, S. (2011) Isolation basins, sea-level changes and the Holocene history of the Greenland Ice Sheet *Quaternary Science Reviews Vol. 30 Pg. 3748-3768.*
- Lowe, J. J. and Walker, M. J. C. (1997) Reconstructing Quaternary Environments *Pearson Prentice Hall: Harlow, UK*
- Lowe, D. J.; Newnham, R. M.; McFadgen, B. G. and Higham, T. F. G. (2000) Tephra and New Zealand archaeology *Journal of Archaeological Science Vol. 27 Pg. 859-870*

Lowe, J. J.; Hoek, W. Z. and INTIMATE Group (2001) Inter-regional correlation of paleoclimatic records for the last Glacial-Interglacial transition; a protocol for improved precision recommended by the INTIMATE project group *Quaternary Science Reviews Vol. 20 Pg. 1175-1189*

MacLennan, J.; Jull, M.; McKenzie, D.; Slater, L. and Grönvold, K. (2002) The link between volcanism and deglaciation in Iceland *Geochemistry, Geophysics, Geosystems Vol. 3 No. 11 1062 doi: 10.1029/2001GC000282*

Mangerud, J.; Lie, S. E.; Furnes, H.; Kristianssen, I. L. and Lomo, L. (1984) A Younger Dryas ash bed in western Norway and its possible correlation with tephra in cores from the Norwegian Sea and the North Atlantic. *Quaternary Research Vol. 21 Pg. 85–104.*

Mangerud, J.; Furnes, H. J. and Johannessen, J. (1986) A 9000 year old ash bed on the Faroe Islands *Quaternary Research Vol. 26 Pg. 262-265.*

Menzies, J. (1995) The dynamics of ice flow In, Menzies, J. (ed.) *Modern Glacial Environments Oxford: Butterworth-Heinemann Pg. 139-196*

Meyer, H. H. and Venzke, J.-F. (1987) Deglaciation and sea-level changes in the vicinity of Blönduós, northern Iceland, in late glacial and early Holocene times: a preliminary report *Norden Vol. 4 pg. 47-64.*

Moriwaki, H. (1990) Late and postglacial shoreline displacement and glaciation in and around the Skagi peninsula, northern Iceland *Geographical Reports of Tokyo Metropolitan University Vol. 25 Pg. 81-97*

Newton, A. J. (pers. comm.) Email regarding tephra preparation

Newton, A.J. (1996) Tephabase: A Tephrochronological Database. *Quaternary Newsletter Vol. 78 Pg. 8-13.*

Newton, A.J., Dugmore, A.J. and Gittings, B.M. (2007) Tephabase: tephrochronology and the development of a centralised European database. *Journal of Quaternary Science Vol. 22 Pg. 737-743*

- Nielsen, C. H. and Sigurdsson, H. (1981) Quantitative methods for electron microprobe analysis of sodium in natural and synthetic glasses *American Mineralogist Vol. 66 Pg. 547-552*
- Norðdahl, H. and Ásbjörnsdóttir, L. (1995) Ísaldarlok í Hvammsfirði In, Hróarsson, B.; Jónsson, D.; Jónsson, S. S. (edits.) *Eyjar í Eldhafi Reykjavík: Gott mál Pg. 117-131*
- Norðdahl, H. and Einarsson, T. (2001) Concurrent changes of relative sea-level and glacier extent at the Weichselian-Holocene boundary in Berufjörður, eastern Iceland *Quaternary Science Reviews Vol. 20 Pg. 1607-1622*
- Norðdahl, H. and Hjort, C. (1987) Aldur jökulhörfunar í Vopnafirði, Abstract Volume, *Reykjavík: Jarðfræðafélag Íslands Pg. 18-19*
- Norðdahl, H. and Pétursson, H. G. (2005) Relative sea-level changes in Iceland: new aspects of the Weichselian deglaciation of Iceland In, Caseldine, C.; Russell, A.; Harðardóttir, J. and Knudsen, O. (eds.) *Iceland: Modern Processes and Past Environments Amsterdam: Elsevier Pg. 25-78*
- Óladóttir, B. A.; Sigmarsson, O.; Larsen, G. and Devidal, J-L. (2011) Provenance of basaltic tephra from Vatnajökull subglacial volcanoes, Iceland, as determined by major and trace element analyses *The Holocene Vol. 21 No. 7 Pg. 1037-1048.*
- Ólafsdóttir, T. (1975) A moraine ridge on the Iceland shelf, west of Breiðafjörður *Natturufredinggurin Vol. 45 Pg. 31-37*
- Palmer, A. J. M. and Abbott, W. H. (1986) Diatoms as indicators of sea-level change In, van der Plassche, O. (edit.) *Sea-Level Research: a Manual for the Collection and Evaluation of Data Norwich: Geo Books Pg. 457-488*
- Paterson, W. S. B. (1980) Ice sheets and ice shelves In, Colbeck, S. C. (ed.) *Dynamics of Snow and Ice Masses New York: Academic Press Pg. 1-78*
- Payne, R. and Gehrels, M. J. (2010) The formation of tephra layers in peatlands: an experimental approach *Catena Vol. 81 Pg. 12-23*

- Persson, C. (1971) Tephrochronological investigations of peat deposits in Scandinavia and on the Faroe Islands. *Sveriges Geologiska Undersökning Arbok Vol. 65 No. 2 Pg. 1-34*
- Pollard, A. M.; Blockley, S. P. E. and Ward, K. R. (2003) Chemical alteration of tephra in the depositional environment: theoretical stability modelling *Journal of Quaternary Science Vol. 18 Pg. 385-394*
- Principato, S. M. (2000) Glacial geology of Rejkjarfjörður, N. Iceland *Programs with Abstracts 32 Geological Society of America 7 Reno.*
- Principato, S. M. (2008) Geomorphic evidence for Holocene glacial advances and sea level fluctuations on eastern Vestfirðir, northwest Iceland *Boreas Vol. 37 Pg. 132-145*
- Principato, S. and Geirsdóttir, A. (2002) Glacial erosion patterns and moraine sequences on the Northwest Peninsula of Iceland *Programs with Abstracts Vol. 34 Geological Society of America 34 Denver.*
- Rasmussen, S. O.; Andersen, K. K.; Svensen, A. M.; Steffensen, J. P.; Vinther, B. M.; Clausen, H. B.; Siggaard-Andersen, M.-L.; Andersen, S. J.; Johnsen, S. J.; Larsen, L. B.; Dahl-Jensen, D.; Bigler, M.; Röthlisberger, R.; Fisher, H.; Goto-Azuma, K.; Hansson, M. E. and Ruth, U. (2006) A new Greenland ice core chronology for the last glacial termination *Journal of Geophysical Research Vol. 111*
- Reed, S. J. B. (1975) *Electron Microprobe Analysis Cambridge: Cambridge University Press*
- Renberg, I. (1990) A procedure for preparing large sets of diatom slides from sediment cores *Journal of Paleolimnology Vol. 4 Pg. 87-90*
- Roberts, S. J.; Sigurvinsson, J. R.; Westgate, J. A. and Sandhu, A. (2007) Late Pliocene glaciation and landscape evolution of Vestfirðir, Northwest Iceland *Quaternary Science Reviews Vol. 26 No. 1-2 Pg. 243-263*
- Rundgren, M. (1995) Biostratigraphic evidence of the Allerød-Younger Dryas-Preboreal Oscillation in Northern Iceland *Quaternary Research Vol. 44 Pg. 405-416*

- Rundgren, M. (1999) A summary of the environmental history of the Skagi peninsula, northern Iceland, 11300 – 7800 BP *Jökull Vol. 47 Pg. 1-19*
- Rundgren, M. and Ingólfsson, Ó. (1999) Plant survival in Iceland during periods of glaciation? *Journal of Biogeography Vol. 26 Pg. 387-396*
- Rundgren, M.; Ingólfsson, Ó.; Björck, S.; Jiang, H. and Hafliðason, H. (1997) Dynamic sea-level change during the last deglaciation of northern Iceland *Boreas Vol. 26 Pg. 201-215*
- Sæmundsson, K. (1979) Outline of the geology of Iceland *Jökull Vol. 29 Pg. 7-28*
- Selby, K. A. and Smith, D. E. (2007) Late Devensian and Holocene relative sea-level changes on the Isle of Skye, Scotland, UK *Journal of Quaternary Science Vol. 22 No. 2 Pg. 119-139.*
- Shennan, I. (1986) Flandrian sea-level changes in the Fenland. II: Tendencies of sea-level movements, altitudinal changes and local and regional factors *Journal of Quaternary Science Vol. 1 Pg. 155-179*
- Shennan, I. (2007) Sea Level Studies In *Encyclopedia of Quaternary Science Elsevier: Oxford Pg. 3006 – 3095.*
- Shennan, I.; Innes, J. B.; Long, A. J. and Zong, Y. (1993) Late Devensian and Holocene relative sea-level changes at Rumach, near Arisaig, northwest Scotland *Norsk Geologisk Tidsskrift Vol. 73 Pg. 161-174.*
- Shennan, I.; Innes, J.B.; Long, A.J. and Zong, Y. (1994) Late Devensian and Holocene relative sea-level changes at Loch nan Eala, near Arisaig, Northwest Scotland. *Journal of Quaternary Science Vol. 9 Pg. 261-283.*
- Shennan, I.; Innes, J. B.; Long, A. J. and Zong, Y. (1995) Late Devensian and Holocene relative sea-level changes in northwest Scotland: new data to test existing models *Quaternary International Vol. 26 Pg. 97-123.*
- Shennan, I.; Tooley, M. J.; Green, F.; Innes, J. B.; Kennington, K.; Lloyd, J. M. and Rutherford, M. M. (1999) Sea level, climate change and coastal evolution in Morar, northwest Scotland *Geologie en Mijnbouw Vol. 77 Pg. 247-262*

- Sigmundsson, F. (1991) Post-glacial rebound and asthenospheric viscosity in Iceland *Geophysical Research Letters* Vol. 18 No. 6 Pg. 1131-1134
- Sigurvinsson, J. R. (1983) Weichselian glacial lake deposits in the highlands of Northwestern Iceland *Jökull* Vol. 33 Pg. 99-109
- Sim, V. W. (1960) Maximum postglacial marine submergence in northern Melville Peninsula *Arctic* Vol. 13 Pg. 178-193.
- Smith, G. M. (1950) Freshwater algae of the United States *McGraw-Hill*
- Smith, I. R.; Bell, T. and Renouf, M. A. P. (2005) Testing a proposed Late Holocene Sea-Level Oscillation using the isolation basin approach, Great Northern Peninsula, Newfoundland *Newfoundland and Labrador Studies* Vol. 20 No. 1 Pg. 33-55.
- Steele, D. and Engwell, S. (2009) Preparation of tephra samples for Electron Microprobe Analysis *available online:* <http://www.geos.ed.ac.uk/facilities/ionprobe/EpoxyResins/Tephra-Prep3.pdf> accessed: 03/03/11.
- Steinþórsson, H. (1967) Tvær nýjar C14-aldursákvarðanir á öskulögum úr Snæfellsjökli. *Náttúrufröedingurinn* Vol. 37 Pg. 236–238.
- Steindórsson, S. (1962) On the age and immigration of the Icelandic flora. *Rit Vísindafélags Íslendinga* Vol. 35 Pg. 1-157
- Steindórsson, S. (1963) Ice age refugia in Iceland as indicated by the present distribution of plant species In, Love, A. and Love D. *North Atlantic biota and their history Pergamon:Oxford* Pg 303-320.
- Steinþórsson, S. (1983) Tvær nýjar C14-aldursákvarðanir á öskulögum úr Snæfellsjökli. *Náttúrufræðingurinn* Vol. 37 Pg. 236-238
- Stoermer, F. and Smol, J. P. (eds.) (2001) The Diatoms: Applications for the Environmental and Earth Sciences Paperback Edition *Cambridge: Cambridge University Press*

- Stuiver, M. and Braziunas, T. F. (1993) Modelling atmospheric ^{14}C influences and ^{14}C ages of marine samples to 10000 BC *Radiocarbon Vol. 35 Pg. 137-189*
- Stuiver, M. Pearson, G. W. and Braziunas, T. (1986) Radiocarbon age calibration of marine samples back to 9000 cal. yr BP *Radiocarbon Vol. 28 No. 2B Pg. 980-1021.*
- Stuiver, M.; Reimer, P. J. and Reimer, R. W. (2010) CALIB 6.0 (www program and documentation, <http://calib.qub.ac.uk/calib/>)
- Svendsen, J. J. and Mangerud, J. (1987) Late Weichselian and Holocene sea-level history for a cross-section of western Norway *Journal of Quaternary Science Vol. 2 pg. 113-132*
- Swindles, G. T.; De Vleeschouwer, F. and Plunkett, G. (2010) dating peat profiles using tephra: stratigraphy, geochemistry and chronology *Mires and Peat Vol. 7 Article 5 Pg. 1-9*
- Syvitski, J. P.; Jennings, A. E. and Andrews, J. T. (1999) High resolution seismic evidence for multiple glaciation across the southwest Iceland shelf *Arctic and Alpine Research Vol. 31 Pg. 50-57*
- Thorarinsson, S. (1944) Tefrokronologiska studier på Island *Geografiska Annaler Vol. 26 Pg. 1-217*
- Thorarinsson, S. (1950) Jökulhaup og eldgos á jökulvatnsvæði Jökulsár á Fjöllum *Náttúrufræðingurinn Vol. 20 Pg. 113-133.*
- Thorarinsson, S. (1956) Mórinn i Seltjörn [English summary: The submerged peat in Seltjörn] *Náttúrufræðingurinn Vol. 26 Pg. 179-193*
- Thorarinsson, S. (1979) Tephrochronology and its application in Iceland *Jökull Vol. 29 pg. 33-36.*
- Thorarinsson, S. and Sigvaldason, G. (1972) The Tröllagiger eruption 1862-1864 *Jökull Vol. 22 Pg. 12-26*
- Thordarson, T. and Larsen, G. (2007) Volcanism in Iceland in historical time: volcano types, eruption styles and eruptive history *Journal of Geodynamics Vol. 43 Pg. 118-152.*

Thorodssen, Th. (1905-1906) Island: Grundriss der geographie und geologie
Justus Perthes: Gotha Pg.358

Thorseth, I. H.; Furnes, H. and Tumyr, O. (1995) Textural and chemical effects of bacterial activity on basaltic glass: an experimental approach *Chemical Geology Vol. 119 pg. 139-160*

Thors, K. and Boulton, G. S. (1990) Deltas, spits and littoral terraces associated with rising sea level: Late Quaternary examples from northern Iceland *Marine Geology Vol. 98 Pg. 99-112*

Thors, K. and Helgadóttir, G. (1991) Evidence from south west Iceland of low sea-level in Flandrian times In, Maizels, J. K. and Caseldine, C (eds.) Environmental Change in Iceland: Past and Present Pg. 93-104 *Kluwer Academic: Dordrecht*

Tröels-Smith, K. (1955) Characterisation of unconsolidated sediments *Danm. Geol. Unders. Ser. IV No. 3 (10)*.

Van der Plassche, O. (1986) Sea Level Research: a manual for the collection and evaluation of data. *Geo Books: Norwich*

Van Vliet-Lanoë, B.; Guðmundsson, A.; Guillou, H.; Duncan, R.A.; Genty, D.; Ghaleb, B.; Gouy, S.; Récourt, P. and Scaillet, S. (2006) Limited glaciation and very early deglaciation in central Iceland: Implications for climate change. *Comptes Rendus Geoscience Vol. 229 Pg. 1-12*

Vikingsson, S. (1978) The deglaciation of the southern part of the Skagafjörður district, Northern Iceland. *Jökull Vol. 28 Pg. 1–17*

Wastl, M., Stotter, J. and Caseldine, C. (1999) Tephrochronology – a tool for correlating records of Holocene environmental and climatic change in the North Atlantic region *Geological Society of America Abstract Vol. 31 A315*.

Wastegård, S.; Björck, S.; Grauert, M. and Hannon, G. E. (2001) The Mjáuvötn tephra and other Holocene tephra horizons in the Faroe Islands, a link between the Icelandic source region, the Nordic Seas and the European continent *The Holocene vol. 11 Pg. 101-109*.

Westgate, J. A. and Gorton, M. P. (1981) Correlation techniques in tephra studies In, Self, S. and Sparks, S. R. J. (edits.) *Tephra Studies* Pg. 73-94
Dordrecht: Reidel.

Zwartz, D.; Bird, M.; Stone, J. and Lambeck, K. (1998) Holocene ice-sheet history in the Vestfold Hills, East Antarctica *Earth and Planetary Science Letters*
Vol. 155 Pg. 131-145.